UNIVERSIDAD NACIONAL AUTÓNOMA DE MÉXICO

DOCTORADO EN CIENCIAS BIOMÉDICAS

INSTITUTO DE ECOLOGÍA

EFECTO DE LOS MODOS DE DISPERSIÓN DE LA ROYA (*Hemileia vastatrix*) EN SU INCIDENCIA EN CAFETALES CON DIFERENTES FORMAS DE MANEJO

TESIS

QUE PARA OPTAR POR EL GRADO DE:

DOCTOR EN CIENCIAS

PRESENTA:

EMILIO MORA VAN CAUWELAERT

DIRECTORA DE TESIS:

DRA. MARIANA BENÍTEZ KEINRAD

LANCIS, INSTITUTO DE ECOLOGÍA, UNAM

COMITÉ TUTOR:

DR. DENIS BOYER

INSTITUTO DE FÍSICA, UNAM

DR. ALFONSO VALIENTE BANUET

INSTITUTO DE ECOLOGÍA, UNAM,

AGRADECIMIENTOS

Institucionales

Agradezco al Programa de Doctorado en Ciencias Biomédicas, al Instituto de Ecología y a la Universidad Nacional Autónoma de México por hacer posible esta tesis.

Al Consejo Nacional de Ciencia y Tecnología (CONACyT) por brindarme la beca que me permitió realizar el doctorado (CVU: 686776).

Al proyecto UNAM-DGAPA-PAPIIT (IN207819) y al Programa de Apoyo a los Estudios de Posgrado para una estancia de investigación en el laboratorio del Dr. John Vandermeer y la Dra. Ivette Perfecto, en la Universidad de Michigan, EEUU.

A mi tutora y a los miembros del comité tutor: Dra. Mariana Benítez Keinrad, Dr. Denis Pierre Boyer y Dr. Alfonso Valiente Banuet, por su apoyo a lo largo de este proceso. Les agradezco su constante disposición para discutir las nuevas avenidas del proyecto.

A los técnicos Gustavo Bautista y Gabriel Domínguez por su inmensa ayuda y tiempo durante el trabajo de campo.

A los miembros del jurado: Dra. Mariana Benítez Keinrad, Dr. Eugenio Martín Azpeitia Espinosa, Dra. Julieta Benítez Malvido, Dr. Mario Alberto Serrano Ortega y Dr. Daniel Ignacio Piñero Dalmau, por sus comentarios y correcciones y por su apoyo durante el proceso de titulación

Personales

El doctorado es un proceso muy largo, y como cualquier otra cosa de la vida, está atravesado por situaciones y conflictos personales y sociales, por alegrías y frustraciones, e incluso por pandemias y guerras internas o externas.

En este proceso de formación e investigación, muchas veces uno se siente solo. Existe un montón de micro y macro dudas que a veces se pueden compartir, y a veces no. Desde cómo resolver scripts en Python o en R, hasta pensar siquiera si tiene sentido tu pregunta de investigación. Desde sentirse un impostor por no entender el cómo de tu pregunta, hasta caer en crisis existenciales al darte cuenta de que el para qué es más importante. Se va construyendo. Desde decidir si dedicar mucho tiempo para poder terminar o no tanto para poder nutrir los otros proyectos de tu vida. A veces un poco más, a veces un poco menos.

En cualquier caso, en esta sección quiero decir dos cosas.

La primera es que estoy muy orgulloso de haber podido terminar este proyecto. Siempre van a faltar cosas, pero me costó un chingo de trabajo realizarlo y poder cerrarlo bien, por muchas circunstancias. Como me han dicho últimamente y creo que es muy cierto: hay que celebrar más lo que logramos. Y pues eso.

La segunda es que la sensación de soledad es totalmente relativa. A lo largo de este proceso demasiadas personas me han ayudado directa o indirectamente. Desde toda la clase obrera y campesina sin cuyo fruto de trabajo nadie podría comer y vivir –deja tú investigar–, hasta todas las personas que han sido cercanas y me han apoyado física y mentalmente. Por eso, tienen sentido estos agradecimientos. Son un ejercicio de memoria y de reconocimiento. Es una de las múltiples maneras que hay para recordar a todas las personas que encontramos y reencontramos a lo largo de este recorrido. También sirve para hacer presentes a todas aquellas que perdimos. Para decirles que estuvieron presentes aunque no lo supieran. Nombrarlas aquí

deja registro de la permanencia que han tenido en mi mente, en todo lo que pienso, siento y hago. Aviso que me van a faltar personas: recordar cinco años está canijo. Les pido disculpas y espero que no sean muchas. Así que ahí va.

A *Mariana*. Quiero empezar agradeciéndote toda la ayuda y dirección, por tu paciencia y por tu habilidad para adaptarte a los cambios que fueron surgiendo a lo largo del proyecto. En un proceso atravesado por una pandemia que hizo más complicado todo, lograr llevar a buen puerto este trabajo no fue tarea fácil. Además y sobre todo, quiero agradecerte por tu incondicional amistad y cariño ante las múltiples adversidades y tristezas que tuvimos que vivir. Saberlos a ti, a Alejandro y a Camilo fue muy importante para mí.

A *Denis*. Te agradezco toda la paciencia y tiempo que dedicaste para explicarme las bases de los modelos matemáticos. Gracias por aportar rigurosidad a la aproximación de cada nuevo problema y sobre todo por volver a reafirmar lo bonito que son las matemáticas para abstraer y entender la realidad.

A *La Parcela*. A lo largo del trabajo fue central tener un grupo tan bonito y cercano como ustedes. En particular agradecerles el apoyo durante la pandemia y la disposición a buscar alternativas para cuidarnos. Hablando como viejito, recuerdo cuando éramos un puñado de alumnos. Me sorprende ver que ahora es un grupo de veinte personas que se junta para pensar, exponer ideas y compartir deliciosuras culinarias. Gracias a todos (salvo a Nat) por dejarme la segunda o la tercera porción en las comidas.

A *Cecilia*, muchas gracias por estar siempre ahí. Compartir frustraciones, nuevas ideas y chismes, en la Finca y en labo, fue muy bonito y necesario. En esta espiral infernal de la modelación me sirvió demasiado. Algún día lograremos hacer bien nuestros trámites. Además, te quiero agradecer por abrirnos la puerta de tu casa cuando lo necesitamos.

A *Cristina*, después de tantos años acercándonos y alejándonos, quiero agradecerte profundamente tu constante y valiente disposición para seguir construyendo nuestra amistad; pero también tu paciencia para discutir horas, cosas académicas y personales. Todavía tenemos muchas cosas buenas por delante.

A *Natsuko*, por cerrar el círculo de los fósiles del grupo. Qué chido conocerte y compartir tantos años. Valoro mucho las discusiones en los viajes y las comparticiones de dudas existenciales. También decirte que eres para mí un ejemplo de científica chida, a pesar de todo lo que hemos platicado.

A *Adri*, miembro honorario de La Parcela. Estoy profundamente contento de que, a pesar de todos los cambios que da la vida, sigas siendo parte de la mía. Gracias por decirme las cosas claras y con cariño. Que bueno tenerte cerca, a pesar de lo lejos.

Al resto de miembros de *La Parcela*, viejas y nuevas adquisiciones que aportan mucha frescura e ideas nuevas para reunirnos y encontrarnos. A su vez, agradecer a la gente del Lancis, con quienes empecé a compartir al inicio y al final del doctorado y me motivan a venir todos los días hasta el Instituto.

Al igual, quiero mencionar al grupo de *Perfectomeer* en Michigan, California y Chiapas. Hicieron que la adaptación en esos lares fuera mucho más sencilla y divertida. Gracias por los múltiples aprendizajes académicos, por las cervezas y la música, por las discusiones de OOTB, por el viaje a las dunas y al lago helado, por sus enseñanzas de lucha en GEO. Cada viaje es una nueva vida, qué bueno conocerles en esta.

Hablando de viajes, quiero agradecer primero a *Lupe* y *Alex* por recibirme, de nuevo, en su hogar. Del calor de Oaxaca al frío de Montréal, estar con ustedes siempre redirecciona la brújula y se siente bien. Aprovecho para mencionar a *Luis Guillermo*, porque fue muy bueno pasar el tiempo contigo allá y compartir la poutine. Hablar contigo siempre me motiva a aprender más cosas de programación. También mencionar a *Ana*: gracias por recibirme en tu linda casa en Chiapas, qué chingón reconectar amistad.

Al buen *Alonso*. Obvio ibas a estar aquí. Por más que siempre sea reacio a empezar nuevas cosas porque no da la vida (no sé cómo te da la vida), estoy profundamente agradecido por haberlo hecho y por todo lo que aprendí a tu lado en estos años. Eres alguien que me ha dado mucha energía para seguir en la agroecología, en la militancia y en la vida en general.

A mis *camaradas de TOR*. Por mostrar con el ejemplo que, a pesar de lo caótico y lo complicado que resulta organizarse, siempre va a ser mejor que avanzar solo. Por enseñarme que la lucha por un mundo nuevo se construye todos los días y que la indignación es el motor para seguir. Por las personas que perdimos en el camino y que nos obligan a comprometernos, en cualquier parte del mundo, con la lucha por la vida.

A la *casita*. Durante años construimos una comunidad muy bonita y solidaria, cocinamos chingo de cosas, aprendimos colombiano parcero, gritamos con luchito y linda, y pudimos discutir todos los temas controversiales que quisimos. A pesar de que las cosas no siempre terminan como uno quiere y decide, no hubiera podido hacer este doctorado sin su constante apoyo.

A Fabián, Mauricio y Eto. Lo saben, se los digo, y es muy en serio: viven en mí y han sido y seguirán siendo mi referente. A pesar de las múltiples veces en que la hemos cagado, o quizás gracias a eso, me siento más cerca de ustedes que nunca ("separémonos en uno"). Porque las tristezas y las alegrías, compartidas siempre valen más la pena. Por lo que falta.

Al *Sebastián* y al *Eduardo*. Su amistad me ha balanceado muchos aspectos de la vida sin los cuales uno no investiga ni hace nada. Grandes la Tavla, las chelas y las largas discusiones sobre "lo real". A *Sebastián*, porque siempre hemos sido grandes amigos aunque no nos habláramos.

A la banda del *milpalabras*, por animarnos a sacar una nueva revista a la distancia para sobrepasar la soledad. Aunque las cosas no acabaron como planeamos, no me arrepiento de haberlo intentado. Porque al final, todos ustedes siempre me dan calorcito en el pecho. A *Santico*. Sobran las palabras.

A *Dayan*, por todo lo que he aprendido contigo en estos ya casi dos años, por volver a poner en el centro lo que importa.

A mi *familia,* cada vez más grande y extendida. *San, Oli, Zo, Natoush y Marluca*: siempre serán la razón de por qué soy cómo soy. Y del porqué quiero, añoro y busco. *Mamá, Vic*: gracias por el cuidado constante, por la disposición a siempre escuchar y por tener el corazón en el buen lugar.

Flor, *Santiago y Elodie*: gracias por todo, tenerlos cerca durante la pandemia fue importantísimo, para mí y para Elisa. A mi *papá*, por intentar estar más presentes, y por recordarme siempre de dónde venimos.

A la *familia Arcos-Alcaraz*. Gracias por cuidar a la familia, que es su familia también, y por ser solidaria en estos últimos meses que no han sido fáciles. En particular a *Lu* por los años de amistad y a *Re* por la chida y tan natural convivencia y por la ayuda en la encerrona final de la tesis.

A *Juan*. Estuviste desde antes, durante y después de que terminara este trabajo. En mi cabeza suenan tu voz, tus consejos y tus chistes. Como me habría gustado contarte lo que estuve haciendo. Cada que puedo me compro un mazapán, para abrazarte en donde sea que estés.

A *Elisa*. Sabes mejor que nadie todo lo que implicaron estos años. El estrés, la frustración y el cansancio; pero también la alegría y las risas. Desde mis hermosas presentaciones y el trabajo en campo, hasta mis pequeñas certezas para tomar decisiones, tengo demasiado que agradecerte. Gracias por adoptar a una gata tan cool y enseñarme de anfibios y reptiles aunque todo lo olvide. Gracias por abrirme las puertas a gente bonita como el *gonchis*, la *fer* y la *chiquis*. Gracias por ser tan chida, y no claudicar nunca a lo que crees. Te agradezco también que lográramos cerrar los ciclos como quisimos y pudimos.

Y obvio, gracias a la *Selva*, la gatita más hermosa de todo el planeta, sin la cual no me despertaría todos los días a las 6:30 am.

DEDICATORIA

[...] *Is anyone out there?*

Will anyone listen? […]

"We teach life sir"

(Rafeef Ziadah – Periodista, poeta y activista palestina)-

INDICE

RESUMEN GENERAL

La roya anaranjada del café (ocasionada por el hongo *Hemileia vastatrix)* se ha convertido en una de las principales plagas que afectan a los cultivos cafetaleros en el mundo. Descrita originalmente en Sri Lanka en 1869, se dispersó al resto del mundo hasta alcanzar el continente americano a finales del siglo XX. Entre el 2008 y el 2015 generó pérdidas de más del 30% de la producción en México, llevando a cientos de campesinos a abandonar sus cultivos. Para controlarla se han implementado métodos que pasan por la bioprospección de variedades resistentes a lo largo del mundo, el uso de fungicidas o la generación de nuevas variedades genéticas. Se han desarrollado también enfoques más sistémicos como el estudio epidemiológico de los ciclos de vida de los hongos o de las comunidades bióticas de los cafetales y el papel del manejo de la parcela en estos procesos. Sin embargo, ninguno de los métodos ha resultado ser completamente efectivo y en muchos casos se han centrado solo en el proceso de infección del hongo. Otros grupos han empezado a estudiar el papel de la dispersión de la roya y su relación con los arreglos espaciales de siembra de las plantas. En ese sentido buscan evitar que un foco de infección tenga repercusiones a nivel de parcela o incluso regional. La dispersión de la roya es realizada a través del viento y de gotas de agua (*splash*), pero también por el movimiento humano, de artrópodos y por el propio contacto entre plantas. El alcance de cada uno de los mecanismos depende de la escala y de la región, pero hoy en día su importancia relativa en el crecimiento de la epidemia a nivel de parcela no es clara. Muchos de los estudios son correlativos y toman en cuenta únicamente una escala, o cierto método de dispersión y no pueden poner a prueba mecanismos generales, ni su relación con los arreglos de siembra. A su vez, algunos modos de dispersión como el movimiento de las personas durante la cosecha no han sido descritos ni tampoco su papel en la epidemia de la roya en las plantaciones.

En esta tesis nos preguntamos cómo impactan algunos de los modos de dispersión de la roya del café sobre su incidencia a nivel de parcela y cómo este efecto puede estar mediado por el manejo agrícola. Para ello primero hicimos una revisión general de lo reportado en la literatura sobre los mecanismos de dispersión de la roya, sus escalas espaciales y temporales y las controversias o lagunas suscitadas en torno a su efecto en la epidemia general (**antecedentes- sección 3 y apéndice 1)**. A partir de esto exploramos en el **primer capítulo de la tesis** el efecto de un mecanismo de dispersión de roya entre plantas vecinas (el *splash*) sobre la dinámica de la epidemia a nivel de parcela. Para ello estimamos a partir de una revisión bibliográfica los tiempos generales de las fases de crecimiento de la epidemia anual de roya y su relación con la estacionalidad de las lluvias. Después construimos y parametrizamos un modelo epidemiológico compartimentalizado. Este modelo nos permitió estudiar el impacto de la dispersión por *splash* sobre los tiempos de infección y la incidencia a nivel de parcela pero también su relación con la densidad y los arreglos de siembra. El arreglo espacial de plantas agregadas resultó ser central para que la roya alcanzara a infectar la parcela durante la temporada de lluvias, cuando las condiciones climáticas son aptas para la infección y para la dispersión por *splash*. **En el segundo y tercer capítulo,** estudiamos el papel de las personas durante la cosecha en la dispersión de la roya, y su impacto sobre la incidencia del hongo en los cafetales. Para ello realizamos una caracterización estadística del movimiento espacial de los cosechadores de dos fincas cafetaleras de gran escala en la región del Soconusco, Chiapas. Además, por medio de entrevistas y observación participante, exploramos los factores a nivel de planta, ambientales y de manejo que moldean dicho movimiento y su relación con el síndrome general de producción cafetalera en estas fincas (**capítulo II -artículo 2**). Obtuvimos que el movimiento de los trabajadores durante la cosecha fue variable entre las dos fincas, con la presencia o no de grandes desplazamientos durante el mismo día. Esta trayectoria dependió de la interacción de las características de los cafetos (e.g. asincronía de la maduración, carga de café) con la forma de manejo (e.g. horas trabajadas, fechas de inicio y final de la temporada), ambos determinados dentro de un síndrome capitalista de producción de café. Finalmente, estudiamos por medio de un modelo computacional los factores suficientes para generar diferentes tipos de trayectorias durante el movimiento de cosecha y el efecto de estas sobre la incidencia de roya en parcelas con diferentes densidades de siembra (**capítulo III – artículo 3**). Como resultado, vimos que los desplazamientos o "saltos" largos durante la cosecha diaria

podían ser reproducidos por cambios en la asincronía de la maduración del café en un escenario de manejo intensivo y escasez de plantas con frutos. A su vez, la cosecha, en particular con los saltos largos y en parcelas con densidades medias de siembra, aumenta significativamente la incidencia de roya. En **las conclusiones** resaltamos los resultados principales generados en cada artículo y modelo **y** dejamos algunas propuestas de manejo relacionadas con los diferentes modos de dispersión de la roya. Esperamos que los resultados se puedan seguir ampliando y discutiendo tanto por agricultores como por científicos y se puedan poner a prueba en diferentes sistemas cafetaleros.

Esta tesis fue realizada en el Laboratorio LaParcela, en el Laboratorio Nacional de Ciencias de la Sostenibilidad (LANCIS), del Instituto de Ecología de la UNAM, bajo la dirección de la Dra. Mariana Benítez Keinrad y con apoyo del comité tutoral conformado por el Dr. Denis Boyer y el Dr. Alfonso Valiente Banuet. Fue financiada por una beca doctoral CONACyT (CVU 686776), el proyecto UNAM-DGAPA-PAPIIT (IN207819) y por el Programa de Apoyo a los Estudios de Posgrado para una estancia de investigación en el laboratorio del Dr. John Vandermeer y la Dra. Ivette Perfecto en la Universidad de Michigan, en Estados Unidos.

INTRODUCCIÓN




1. Una plaga histórica: la roya anaranjada del café

1.1. El surgimiento de plagas y patógenos en cultivos agrícolas

Uno de los ejes centrales en el estudio de los agroecosistemas es el manejo de las plagas (Altieri et al., 1999; Hilje et al., 2003; Levins y Wilson, 1980). Desde el punto de vista agroecológico, los organismos no son plagas en sí. Más bien, se convierten en plaga cuando, dadas ciertas condiciones climáticas, ecológicas o de manejo agrícola, alcanzan un nivel poblacional tal que afecta de manera significativa a algún cultivo de interés (Hilje et al., 2003; H. Morales y Perfecto, 2000).

Los organismos que se vuelven plaga y los cultivos que afectan pueden ser ambos de origen exógeno (Kim y McPheron, 1993). En este caso, al no tener enemigos naturales en las nuevas regiones, los herbívoros o patógenos crecen de manera descontrolada y afectan severamente al cultivo. Un ejemplo de esto es la cochinilla acanalada (*Icerya purchasi*) de origen australiano que afectó severamente a los cítricos de origen asiático en la región de California (Quezada y DeBach, 1973). El que un organismo externo logre establecerse exitosamente en la comunidad local dependerá también de la presencia de otras especies u hospederos alternativos, de la velocidad de su ciclo de vida y del manejo humano del agroecosistema. En otros casos, el organismo que se vuelve plaga existe previamente en un ecosistema y el cultivo infectado es de origen externo. En Sudáfrica por ejemplo, el 68% de los artrópodos que se considera plaga de 14 cultivos importados, son especies nativas (Dennill y Moran, 1989). Al llegar una nueva fuente de alimentación, los organismos locales pueden migrar a estos cultivos y afectar significativamente la producción. Finalmente, puede pasar que los organismos que se alimentan del cultivo y el cultivo mismo sean ambos endógenos y en ese caso el desarrollo de la plaga dependerá sobre todo del manejo del cultivo afectado (Van Driesche y Bellows, 1996). Ciertos manejos, como el uso desmedido de plaguicidas o la siembra extensiva de monocultivos, pueden eliminar a los enemigos naturales del organismo en cuestión, al tiempo que reducen la diversidad y la resistencia genética de los cultivos afectados (Andow, 1983; Van Den Bosch, 1979). En Nicaragua por ejemplo, el uso incrementado de insecticidas para la remoción del

picudo (*Anthonomus grandii*) en el algodón (*Gossypium sp*) promovió el surgimiento de otras 23 especies plaga (Hilje et al., 2003).

1.2. El surgimiento y la dispersión de la roya del café

El cafeto arábigo (*Coffea arabica L.* Rubiaceae) es una planta nativa del bosque lluvioso de las montañas de Etiopía (Sylvain, 1958). Por su alto valor comercial y su larga historia colonial se ha sembrado a lo largo de los trópicos y zonas templadas, en regiones con comunidades bióticas muy variadas y, en muchos casos, en grandes extensiones de monocultivos (McCook y Vandermeer, 2015). Se volvió así el escenario de surgimiento de decenas de plagas y en particular de la roya del café.

La roya del café se registró y describió por primera vez en 1869 en Sri Lanka (antes Ceilán; Talhinhas et al., 2017). Ante la devastación regional del cultivo en esta excolonia británica, los británicos decidieron eliminar el cultivo en su totalidad y plantar té en su lugar (Talhinhas et al., 2017). Hacia mediados del siglo XX, la roya ya se había dispersado al resto del continente asiático y a algunos países africanos, presuntamente por las corrientes de viento y el movimiento de trabajadores en las nuevas rutas abiertas por los barcos de vapor (McCook y Vandermeer, 2015; Waller, 1981). La roya apareció en el continente americano en 1970, específicamente en Brasil (Waller, 1972), pero por condiciones climáticas y ecológicas y algunas medidas preventivas del entonces Instituto Brasileiro do Café (IBC), los cultivos no sufrieron mayor daño (Schieber, 1972). Años más tarde la roya alcanzó a los cultivos de Centroamérica y, entre el 2008 y el 2015, creció desmedidamente en una región que comprende desde Perú hasta México, llevando a pérdidas de más del 30% de la producción en la región (Fig. 1; (Avelino et al., 2015; McCook y Vandermeer, 2015)). Este evento se denominó como “La Gran Roya” y regresó el foco de cientos de investigaciones en el mundo sobre el desarrollo de esta plaga. Hoy en día, la roya se ha registrado en casi todas las zonas cafetaleras del mundo siendo más o menos relevante según la región y los años (Hawaï-Deparment of Agriculture, 2020; Talhinhas et al., 2017; Urbina y Aime, 2023).

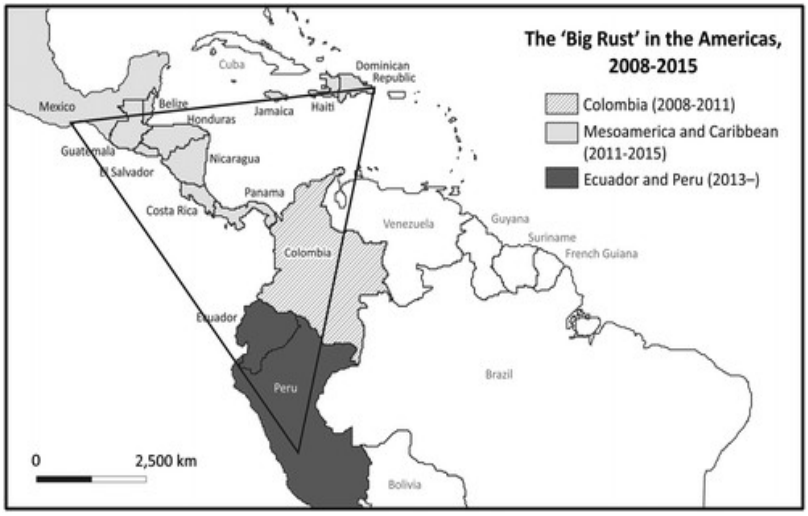

Figura 1. Países de América afectados por la Gran Roya entre 2008 y 2015. Tomado de McCook y Vandermeer (2015).

1.3. La roya del café: biología y efectos agrícolas

La roya anaranjada del café es causada por el hongo *Hemileia vastatrix (*Berk y Broome, 1869) del orden Pucciniales, de la división Basidiomycota. Este patógeno es exclusivo de las plantas de café, particularmente de las variedades arábicas (Avelino and Rivas, 2013), y se reconoce en campo por la presencia de lesiones en el envés de la hoja con esporas de color anaranjado, conocidas como uredosporas (Talhinhas et al., 2017; Fig.2B). Además de las uredosporas, el hongo produce teliosporas y basidiosporas (Carvalho et al., 2011). Hasta donde se ha reportado, ninguna de estas dos pueden infectar los cafetos (Carvalho et al., 2011). La roya tiene dos fases principales en su ciclo de vida: la invasión del hospedero (o infección *per se*) y la dispersión a nuevas plantas (Avelino et al., 2004; Fig. 2A). Durante la infección, las uredosporas entran en contacto con la hoja del café en donde germinan, penetran por los estomas y colonizan la hoja. Posteriormente, forman estructuras arbusculares conocidas como uridios que vuelven a salir por los estomas y desarrollan nuevas esporas infecciosas (Talhinhas et al., 2017). Cada una de estas fases está condicionada por factores microclimáticos, biológicos y de manejo agrícola (ver apéndice 1A y 1B; Avelino & Rivas, 2013). Durante la dispersión, las esporas son liberadas del uridio y son transportadas de una planta a la otra o de una región a otra por medio de vectores bióticos (insectos o transporte humano) o abióticos (viento y splash) (Fig. 2A; Becker y Kranz, 1977). Es importante mencionar que la epidemia de roya es policíclica: ocurren varios ciclos de infección y dispersión en cada temporada de lluvias. Por lo mismo, la intensidad de la epidemia

está muy relacionada con la velocidad a la que ocurren ambas fases (Kushalappa y Eskes, 1989). El efecto de la roya en campo es un incremento de la defoliación de las plantas de café, lo que hace caer la producción de cerezas de café en la siguiente temporada por la disminución de la capacidad fotosintética de las plantas (Fig. 2B; Talhinhas et al., 2017). En algunos casos específicos, la infección por roya puede afectar la producción de la misma temporada o incluso matar a la planta (Avelino et al., 2015). La incidencia por roya (medida como el número de hojas o plantas infectadas por unidad de tiempo) sigue un patrón no lineal anual que arranca con la temporada de lluvias y la maduración de los frutos de café (Bock, 1962c; Boudrot et al., 2016) (Fig.2C). Al inicio de la epidemia, la roya aumenta y el número de hojas sanas de los cafetos disminuye. Semanas más tarde, por la reducción de la población del hospedero, la tasa de reproducción de la roya disminuye, lo que lleva su población a un pico máximo y eventualmente a su descenso (Fig.2C). Durante la época seca, las hojas se recuperan y cuando las condiciones son óptimas reinicia el ciclo de infección (Mulinge y Griffiths, 1974).

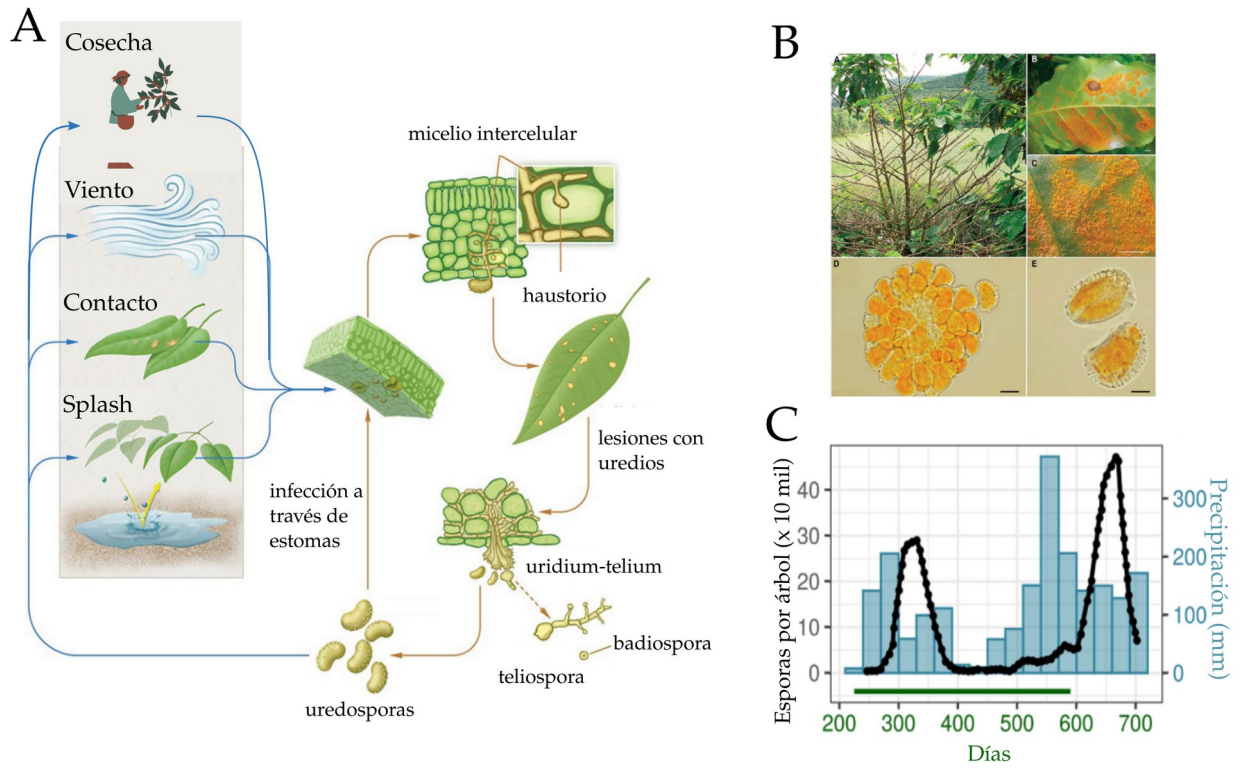

Figura 2. A. Ciclo de vida de la roya del café. Modificado de Vandermeer y Perfecto (2018) e imagen tomada de rumka_vodki. **B**. Efecto de la roya sobre las plantas de café y uredosporas en las hojas y vistas al microscopio. Tomado de Talhinhas et al. (2017). **C.** Patrón anual de la incidencia (esporas por árbol) de roya. Tomado de Mora Van Cauwelaert et al. (2023) basado en Boudrot et al. (2016).

2. El manejo de la roya del café

2.1. El enfoque clásico para el control de la roya

Los métodos para el control de la roya del café han ido cambiando a lo largo de los años, siguiendo el desarrollo científico general, el contexto socioeconómico y la región de estudio. McCook y Vandermeer (2015) proponen tres fases para la investigación y manejo de la roya: la fase colonial (1869-1945), la fase desarrollista (1945-1990) y la fase neoliberal (1990 en adelante).

Durante la fase colonial, la producción de café fue dirigida por los poderes europeos en sus colonias a través del mundo, despejando grandes áreas de bosques para suplir una cada vez mayor demanda desde los centros económicos (Clarence-Smith y Topik, 2003). Ante las pérdidas causadas por la nueva roya del café en el sureste asiático en 1869, los dueños de las plantaciones buscaron ayuda en sociedades privadas de científicos (Royal Botanic Garden en Kew; McCook y Vandermeer, 2015). Algunos de ellos, como Marshall Ward en los años 1870 realizaron las primeras descripciones detalladas del ciclo de vida del hongo al igual que sus procesos de infección y de dispersión (citado en Rayner, 1972). Sin embargo, muchos de estos estudios tenían un enfoque preventivo y no lograron dar cuenta de tratamientos ante la presencia de la enfermedad. La única medida implementada fue la búsqueda de variedades arábigas en el mundo, pero fracasó rotundamente por lo que en la mayoría de los casos se abandonó el cultivo (McCook y Vandermeer, 2015). Con el final de la segunda guerra mundial, el desarrollo de la industria química y el crecimiento económico generalizado, se inició la fase desarrollista. Durante este periodo, se firmó el Acuerdo Internacional del Café (ICA por sus siglas en inglés) y se crearon instituciones estatales como el INMECAFÉ en México (Instituto Mexicano del Café; Paré, 1990) que regulaban la producción e intercambio de café a lo largo del mundo al tiempo que promovían el estudio del cafeto. Estas instituciones lograron mantener precios relativamente altos y estables para los productores, lo que fue particularmente relevante en México en donde desde entonces cientos de miles de campesinos han vivido de la producción y venta de café (Flores Vichi, 2015). Desde dichos institutos se empezó a promover y a financiar los fungicidas sintéticos lo que dio pie a cientos de trabajos científicos que estudiaban la duración temporal de las fases del ciclo de vida de la roya y su relación con el

clima; esto con el fin de implementar una aplicación más efectiva de los fungicidas (e.g. Mulinge and Griffiths, 1974). Unos años más tarde, con el advenimiento de la genética mendeliana, se desarrollaron como método de control las cruzas de variedades robustas resistentes a la roya (*Coffee canephora*) con variedades arábicas (Avelino y Rivas, 2013). Este método se expandió rápidamente por su efectividad a corto plazo y se realizaron múltiples combinaciones de cruzas resistentes (*e.g*. Hibrido de Timor, Caturra, Catimor, Colombia; (Avelino y Rivas, 2013)) y mapas de resistencia a las nuevas variedades de roya (Eskes y Toma-Braghini, 1982; Silva et al., 2006). A inicios de los años ochenta, empezó una tercera fase, caracterizada por el fin de la guerra fría y el ascenso del neoliberalismo. En 1989 cerraron varios institutos estatales en apoyo a los cafetaleros y no se llegó a un nuevo acuerdo internacional de cuotas de producción y de precios (McCook y Vandermeer, 2015). En México hubo un adelgazamiento institucional del INMECAFÉ desde 1982 que resultó en su cierre definitivo unos años más tarde (Paré, 1990). Al no haber acuerdos internacionales, ciertos países incrementaron descontroladamente su producción y venta, generando oscilaciones en los precios internacionales nunca antes vistas (Avelino et al., 2015; McCook y Vandermeer, 2015). Las caídas periódicas en los precios del café, aunado a la reducción significativa de los apoyos estatales para fungicidas y créditos para la producción, llevaron al abandono o semiabandono (parcelas sin manejo y solo cosechadas) de cientos de hectáreas en Centroamérica. El abandono o la reducción abrupta en el uso de fungicidas en tierras manejadas por años con insumos externos y otras prácticas intensivas, junto a fenómenos meteorológicos y la evolución de nuevas variedades resistentes de roya, explicaron el brote regional y cuasi sincrónico del fitopatógeno durante "La Gran Roya" en Centroamérica (Avelino et al., 2015).

Hoy en día en México, este proceso histórico se refleja en una gran variedad de manejos de cafetales caracterizados como diferentes "síndromes de producción"(Andow y Hidaka, 1989). Este marco conceptual es útil para estudiar los efectos socio-ecológicos de diferentes síndromes de producción cafetera y entender cómo y por qué se mantienen en el tiempo (Ong y Liao, 2020; Vandermeer y Perfecto, 2012). Por un lado, existen cafetales industrializados que se caracterizan por ser monocultivos de gran extensión, sin árboles intercalados y con uso intensivo de fertilizantes y fungicidas. Los dueños de estas plantaciones cafetaleras suelen obtener su ganancia de la explotación de trabajadores asalariados, permanentes o temporales; y a través de la venta a mercados internacionales (López Echeverría, 2006). Esto se conoce como el

síndrome capitalista de producción (Ong y Liao, 2020). Por el otro, hay cafetales con manejos más ecológicos que se siembran en policultivo, con árboles de sombra, con un uso reducido de fertilizantes y bajo formas de tenencia comunitarias de la tierra (Lin, 2007; Moguel y Toledo, 1999; Soto-Pinto et al., 2000). Este segundo es el síndrome campesino de producción. Cabe mencionar que si bien estos dos extremos son los más comunes en México (Vandermeer y Perfecto, 2012), hay plantaciones que recuperan prácticas de uno u otro síndrome.

2.2. El manejo agroecológico: prevención, ecología y epidemiología

El enfoque agroecológico ante el estudio y manejo de un agroecosistema implica conocer sus determinantes históricas y sociales, al igual que su dimensión práctica y ecológica (Altieri et al., 1999). Para empezar, hacer un recuento histórico de los diferentes modos de control de la roya y su relación con factores socioeconómicos nos ayuda a entender por qué se implementan hoy en día ciertas prácticas, qué lógica científica o histórica tienen y por qué algunas funcionan mejor que otras, de acuerdo con la región. El recuento también vislumbra el papel que han jugado o pueden jugar los manejos ecológicos y preventivos para la roya del café y el tipo de preguntas que podemos hacer desde la ciencia para implementarlos de manera efectiva.

Muchas de las prácticas preventivas y ecológicas han sido desplazadas por técnicas que maximizan la producción y reducen las pérdidas a corto plazo, y que implican una constante entrada de capital y obtención de ganancia (McCook y Vandermeer, 2015). Sin embargo, desde los primeros años de registro de roya ha habido prácticas agrícolas y estudios con enfoques sistémicos. Empezando con el trabajo pionero de Marshall-Ward, quien propuso el uso de árboles para cortar el viento y la transmisión de esporas, la siembra de diversas variedades de café y de otros cultivos en las parcelas y enfatizó el papel de ciertos organismos para el control poblacional de la roya (Ayres, 2005; Rayner, 1972). Unos 50 años más tarde, toda una generación de científicos y científicas sentó las bases para entender la temporalidad del proceso de infección de la roya y su relación con los métodos de dispersión y los eventos meteorológicos, tomando como base la epidemia de roya en Etiopía y en Kenya (Becker y Kranz, 1977; Bock, 1962a; Cannell, 1974; Nutman y Roberts, 1970; Rayner, 1961). Por otro lado, desde los años noventa a la actualidad, los trabajos desde el CIRAD (Centro de Cooperación Internacional en Investigación Agronómica para el Desarrollo) en Francia y el CATIE (Centro Agronómico Tropical de Investigación y Enseñanza) en Costa Rica han explorado la relación del ciclo de vida del hongo

con las características microclimáticas de las parcelas y los tipos de manejo agrícola (Avelino et al., 1991, 2004, 2006). A través de análisis multivariados y experimentos empíricos han mostrado el impacto no lineal de ciertas prácticas, como la presencia de sombra o la poda, sobre la magnitud o la persistencia de la roya en las parcelas (Avelino y Rivas, 2013; Gagliardi et al., 2020; López-Bravo et al., 2012; Zewdie et al., 2020). Desde otro grupo de investigación proveniente de la escuela agroecológica (Altieri et al., 1999; Levins y Wilson, 1980), Perfecto y Vandermeer han estudiado y sistematizado por más de treinta años las interacciones de las comunidades bióticas presentes en sistemas cafetaleros con manejos ecológicos (Perfecto y Vandermeer, 2016; Vandermeer et al., 2019). Una de las bases conceptuales de este grupo es el estudio de agroecosistemas sin plagas o "sanos" y no solamente aquellos "enfermos". Entre otras cosas, han descrito algunos de los enemigos naturales directos de la roya y sus relaciones en redes bióticas más grandes (González González et al., 2021; Hajian-Forooshani et al., 2023; Jackson et al., 2012). Por otro parte, han estudiado las relaciones de no consumo en los cafetales, en donde la presencia de una especie puede afectar la relación biótica de otras dos sin afectar directamente sus densidades poblaciones (Levine et al., 2017). Se ha argumentado teórica y experimentalmente que estas interacciones en comunidades bióticas incrementan la estabilidad del sistema ante el crecimiento de la diversidad (Bairey et al., 2016; Xiao et al., 2020). Como parte del trabajo doctoral de Cecilia González González, validamos esta hipótesis reproduciendo la red de interacción del cafetal (Fig. 3) y modelando su estabilidad estructural ante diferentes tipos de perturbaciones en comparación a redes aleatorias con las mismas propiedades estructurales (ver **apéndice 2** y (González González et al., 2021)). Así, las propiedades comunitarias pueden impedir el crecimiento desmedido de algunos de los nodos (especies) de la red, evitando que se vuelvan plagas (González González et al., 2021).

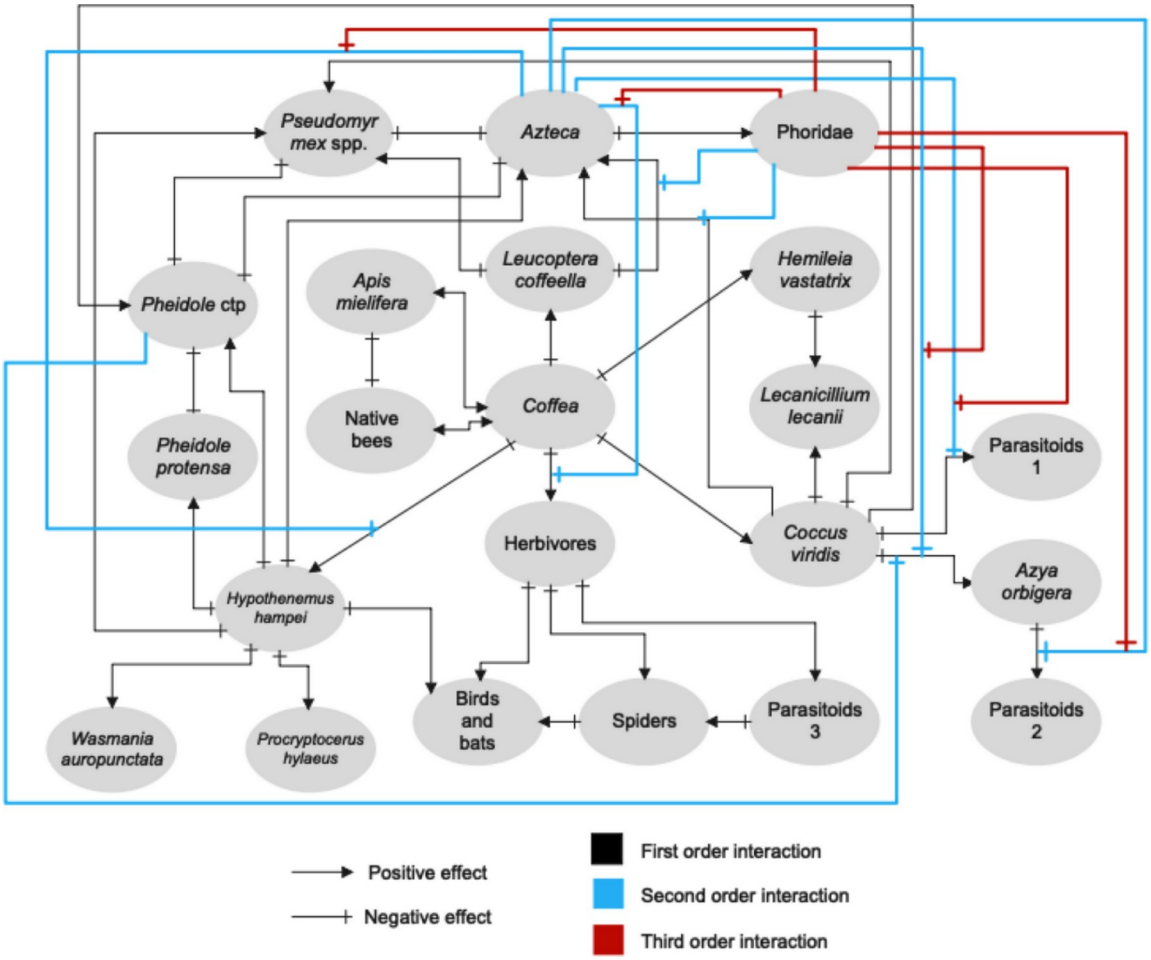

Figura 3. Red de interacciones bióticas asociadas al cafetal. En este modelo, sistematizado a partir de los estudios en el Soconusco, Chiapas, la roya del café (*H. vastatrix*) solo tiene un depredador directo: el hongo blanco (*Lecanicillium lecanii*). Pero este crece con la presencia de escamas de café (*Coccus viridis*) que por su parte tienen relaciones con muchas otras especies de la red. Así el control biológico generado por el hongo blanco está determinado por la estabilidad general de la red biótica. Imagen tomada de González González et al. (2021)

3. El estudio de la dispersión y el manejo de la parcela

3.1. La dimensión espacial y temporal en el estudio de la roya del café

Uno de los grandes retos en el estudio de los agroecosistemas y la generación de plagas es que son fenómenos que suceden a diversas escalas temporales y espaciales (Zadoks, 1999). En el estudio de la roya del café u otros sistemas pátogeno-hospedero esto se refleja en el hecho de que en una parcela, no todas las plantas son infectadas de manera simultánea a lo largo de la temporada (Li et al., 2022). El éxito de la infección y el impacto epidemiológico va a estar determinado por la interacción de componentes sésiles (las plantas) y componentes móviles (las esporas de los hongos) en los periodos de tiempo estudiados. Por ello, es importante estudiar los arreglos espaciales de los hospederos (Keeling, 1999; Vandermeer et al., 2018)) y sus contextos paisajísticos (Avelino et al., 2012; Beasley et al., 2022). Por otro lado, también es central estudiar el movimiento espacial del hongo; es decir, sus mecanismos y escalas de dispersión (Becker y Kranz, 1977). Ambos procesos dependen de los diversos manejos agrícolas en campo (Merle et al., 2020). Uno de los ejes centrales de esta tesis fue dar luz sobre algunas de estas interacciones. Para ello, revisamos primero los mecanismos de dispersión y lo reportado en la literatura sobre su papel en el crecimiento de la epidemia. Después revisamos su relación con diferentes tipos de manejo. Sobre estos exploramos algunas de las lagunas que se quieren responder en este trabajo.

3.2. **La dispersión de la roya, sus escalas y mecanismos**

Los modos de dispersión de la roya, sus escalas y su importancia relativa en la epidemia de roya fueron objeto de debate durante gran parte del siglo XX y XXI (ver **apéndice 1**). Toda una escuela iniciada por Marshall Ward se enfocó en entender el papel del viento para el movimiento de las esporas. En 1961, Rayner afirmó que las turbulencias de viento golpeteaban las hojas y liberaban las esporas de los uridios para su dispersión. No obstante, en los mismos años se realizó una serie de estudios experimentales donde se sugirió que la fuerza del viento no era relevante para despegar las esporas y que además, teóricamente, la velocidad terminal de

las mismas (diferencia entre la fuerza de gravedad y el empuje del aire) era demasiado alta para permitirles viajar largas distancias (Bock, 1962b; Nutman y Roberts, 1970; Waller, 1972). A su vez, estos autores demostraron que las gotas de agua liberaban una gran cantidad de esporas y que las podían mover entre hojas y plantas vecinas (Bock, 1962b; Guzman y Gomez, 1987). Esto coincide con los hallazgos recientes de Li et al. (2023) quienes también demuestran que el agua puede transportar esporas desde hojas caídas e infectadas para reiniciar un ciclo de infección. El impacto de este tipo de dispersión a escala de parcela todavía no se conoce enteramente, o dicho de otro modo, qué tanto se expande la epidemia a lo largo de la parcela basándose únicamente en la dispersión por *splash* a partir de un foco de infección. Ahora bien, años más tarde, en un estudio central para el tema general de la dispersión de esporas Becker & Kranz (1977) reportaron con equipos más sofisticados la presencia de esporas en el aire a diferentes alturas de la planta y hasta a miles de metros de altitud. Este trabajo experimental acabó con las dudas del papel del viento en la dispersión entre plantas y a escala regional. Aunado a esto, se volvió a calcular la velocidad terminal obteniendo un valor mucho más bajo, lo que sugería que teóricamente las esporas sí podían viajar largas distancias en suspensión en el aire (Bowden et al., 1971). Desde entonces, el papel del viento ha sido continuamente estudiado tanto por estudios teóricos (Dupont et al., 2022) como experimentales (Gagliardi et al., 2020). En años recientes, Vandermeer y colaboradores añadieron que el contacto mismo entre plantas cercanas también debía ser considerado como un mecanismo de dispersión (Vandermeer et al., 2018). Becker y Kranz también sugirieron que los insectos tenían un papel menor en la dispersión (ver también Crowe, 1963) y mostraron que la ropa de los trabajadores era un medio potencialmente eficaz para la transmisión de esporas (Becker y Kranz, 1977). El papel de la dispersión por humanos también fue observado por Waller quien notó que los focos de infección de roya estaban cerca de los caminos y los centros de habitación (Waller 1979 citado en Waller, 1981). Además, vale la pena mencionar que el crecimiento de la epidemia se correlaciona temporalmente con el momento de la cosecha (Avelino et al., 1991, 1993). Esto puede deberse a que tanto la cosecha como la infección están relacionadas con la maduración de los frutos, pero también puede ser que la cosecha misma esté incrementando la dispersión e incidencia del hongo. El movimiento de los trabajadores durante la cosecha y el alcance que puede tener en el crecimiento de la epidemia no ha sido estudiado en sistemas cafetaleros. Las pocas aproximaciones al estudio del movimiento de personas durante el proceso de cosecha se han

realizado en otros sistemas agrícolas (Brown et al., 2007; Reynolds et al., 2018). Además, contrariamente a otros métodos de dispersión, la cosecha humana está directamente condicionada por el manejo, por ejemplo en qué meses se lleva a cabo o cuántas horas se cosecha por día. A una escala regional, los dos mecanismos centrales para el movimiento de esporas son el viento (Bowden et al., 1971) pero también el movimiento de personas (Ramírez-Camejo et al., 2022). Para más detalles de cada uno de los mecanismos y escalas espaciales, el lector puede referirse al **apéndice 1.**

Otra serie de estudios se han enfocado en entender la dinámica temporal de los modos de dispersión de la roya y su relación con la estacionalidad (Bock, 1962c; Boudrot et al., 2016; Rosas et al., 2021). En la figura 4, realizamos una representación cualitativa de la relación entre las escalas espaciales y temporales de la roya en donde actúan cada uno de los modos de dispersión (Fig. 4). Agregamos también la relación con el ciclo de infección, el crecimiento de la roya, el ciclo agrícola, las prácticas de manejo y la estacionalidad, tomando como base la región de la zona cafetalera del Soconusco en Chiapas. Lo primero a observar es que el papel del agua para mover las esporas entre hojas infectadas o entre plantas es solo relevante durante la época de lluvias o con lluvias intermitentes (Bock, 1962b; Li et al., 2023). La dispersión por *splash* puede iniciar desde el inicio de la temporada lluviosa pero es hasta que las condiciones son óptimas para la infección, en particular cuando los frutos ya están maduros, que promueve el crecimiento acelerado de la epidemia (Avelino y Rivas, 2013). En este momento del año, arranca la cosecha y la dispersión por los trabajadores, hasta después del fin de la temporada de lluvias (Mora Van Cauwelaert et al., 2023). Avanzando en el año y en temporada de secas, el papel del viento parece ser más relevante, llevando las esporas a zonas distintas de la parcela o a diferentes regiones (Boudrot et al., 2016). Finalmente, durante todo el año, el contacto entre plantas y el movimiento por insectos puede ampliar la dispersión al interior de las parcelas (Becker and Kranz, 1977; Vandermeer et al., 2018) y el viento o el movimiento de seres humanos por diferentes regiones puede iniciar nuevos focos de infección en regiones alejadas (Bowden et al., 1971; Ramírez-Camejo et al., 2022).

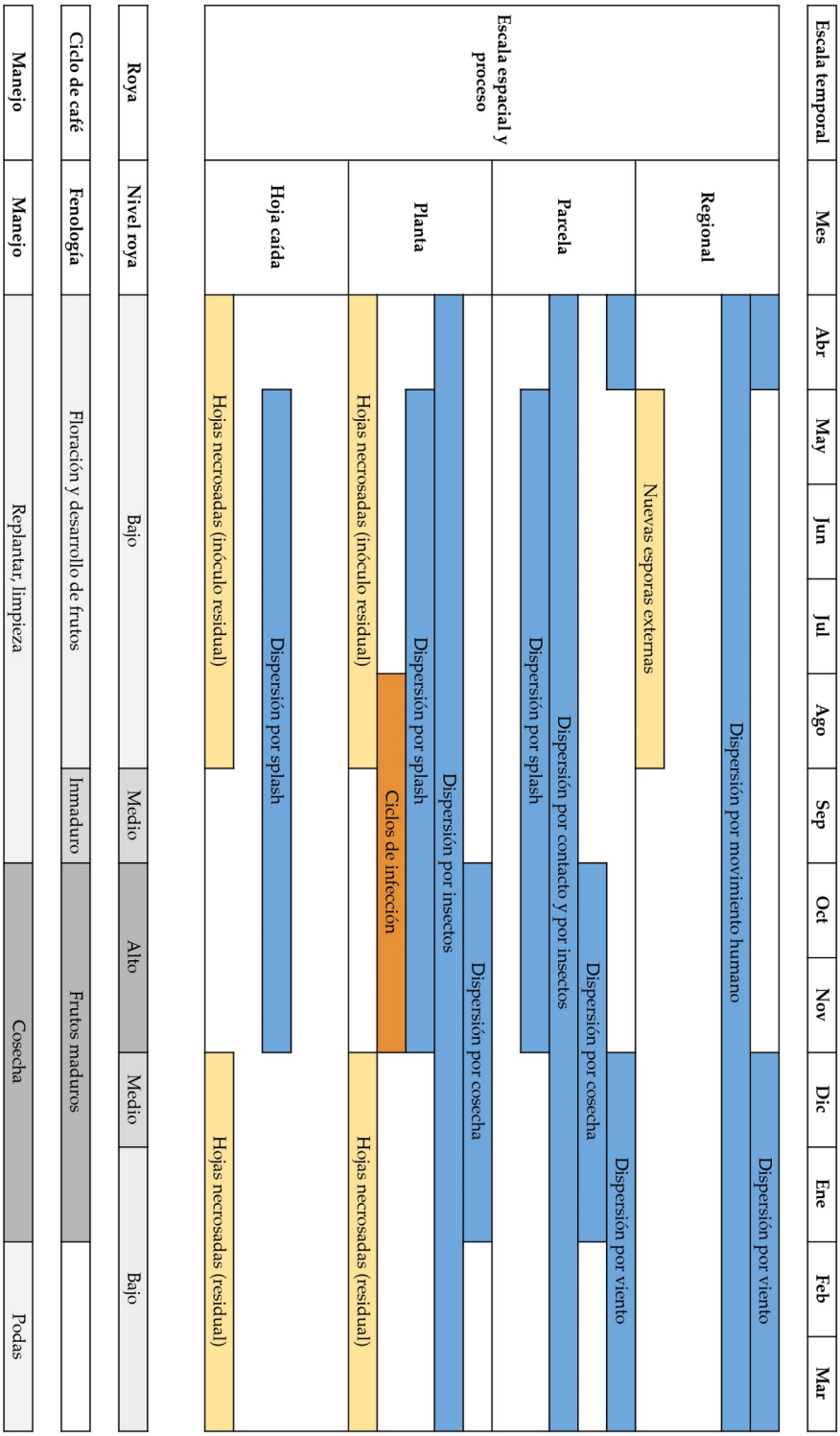

Figura 4. Escalas temporales y espaciales a las que actúan los diferentes modos de dispersión de la roya. El mapa es autoría plena del autor y se construye con base en lo revisado en el **apéndice 1**. Escala regional: entre regiones o entre parcelas, escala parcela: al interior de una parcela agrícola, escala planta: entre las hojas de la planta, escala hoja caída: entre hojas caídas y la planta. Los colores indican los diferentes procesos en el ciclo de vida de la roya según Avelino y Rivas (2013): la formación del inóculo residual (amarillo), la infección (naranja) y la dispersión (azul).

3.3. Relación de los modos de dispersión con el manejo agrícola

A nivel de parcela, la densidad de siembra, el arreglo espacial de las plantas, la presencia de árboles como barreras o la organización de la cosecha u otras actividades dependen del manejo y el objetivo de la producción, es decir, dependen del síndrome de producción (Vandermeer y Perfecto, 2012). Cada uno de estos factores interactúa con la dispersión y la incidencia de la epidemia de roya.

Para empezar, el arreglo espacial y la densidad de siembra cambia el tamaño de las redes de plantas que están contacto entre sí. Cuando las plantas se siembran en arreglos regulares y a altas densidades, la roya puede dispersarse velozmente llevando a crecimientos explosivos de la epidemia (Hajian-Forooshani y Vandermeer, 2021). En cambio, cuando las plantas están sembradas en cúmulos, la infección no avanza tan velozmente y disminuye de manera global. El arreglo espacial de las plantas depende de la edad de la plantación o de la dinámica de renovación de las plantas en la parcela (Hajian-Forooshani y Vandermeer, 2021). Por otro lado, la cantidad de sombra generada por los árboles intercalados en la parcela modifica la dispersión por viento y por lluvia y, por lo tanto, la incidencia general de la roya (Gagliardi et al., 2020; Vandermeer et al., 2015). Estos autores muestran además que las características funcionales de los árboles de sombra afectan de manera diferencial el movimiento de las esporas. En un trabajo en la misma línea, Dupont et al. (2022) cuantifican la dinámica de los vientos en los campos agrícolas y su relación con la dispersión de esporas. El manejo agrícola también se refleja en el tipo de variedades sembradas. La presencia de variedades resistentes y su disposición espacial puede generar barreras genéticas para el movimiento del hongo (Kushalappa y Eskes, 1989). A su vez, la organización de la forma y la fecha de inicio y término de la cosecha, producto también del síndrome de producción (Jiménez-Soto, 2021), puede impactar directamente la dispersión de la roya. La temporada de cosecha puede durar entre tres y cinco meses según la región, y cada planta puede ser cosechada hasta cinco veces dependiendo de los momentos de maduración del café (Jiménez-Soto, 2021; Masarirambi et al., 2009). Finalmente, el manejo y su efecto sobre la dispersión también se refleja en una escala regional, sobre todo con relación a la extensión del cultivo en el paisaje y al ecosistema en donde se siembra. Los cafetales pueden ir desde pequeñas parcelas de una hectárea rodeadas por fragmentos de bosque primario o secundario, hasta extensiones de 300 ha de café (Garedew et al., 2019; Moguel y Toledo, 1999).

En un trabajo del 2012, Avelino y colaboradores, encontraron que la variable que mejor explicaba la incidencia de roya en cafetales de Costa Rica era la cantidad de pastizal circundante a la plantación; probablemente por el incremento que causaba en la turbulencia de viento y dispersión de esporas al interior de las parcelas (Avelino et al., 2012). En esta misma escala regional Beasley y colaboradores realizaron un modelo espacialmente explícito en donde mostraron que a partir de cierto umbral de agregación de las fincas, aumenta significativamente la velocidad de transmisión de la roya a nivel de paisaje (Beasley et al., 2022).

4. Los modelos matemáticos en agroecología

Abarcar la complejidad espacio-temporal de los agroecosistemas no es tarea sencilla. En general, para estudiar la realidad siempre tenemos que hacer una abstracción de la misma. Esta implica reducir o agrupar variables con el afán de buscar generalidades sobre el fenómeno (Levins, 1966). La abstracción o modelación de la realidad puede verse como un experimento en laboratorio con variables controladas, una categorización de ecosistemas, un análisis multivariado o un conjunto de ecuaciones mecanísticas tipo depredador-presa. Ninguno de estos modelos son completos y veraces por sí solos, sino que se contradicen o complementan, y en esa interacción se generan conocimientos sobre los fenómenos estudiados (Levins y Wilson, 1980).

Para poder construir un entendimiento mecanístico de la relación entre algunos modos de dispersión de la roya y el manejo agrícola, utilizaremos modelos dinámicos computacionales. Estos permiten poner a prueba escenarios que difícilmente pueden estudiarse sistemáticamente en campo tales como diferentes arreglos de siembra, modos de dispersión o trayectorias de cosecha. En última instancia, generan hipótesis de relaciones y procesos que ayudan a diseñar nuevos experimentos. En el caso de las plagas y de la roya en particular, existe una gran literatura de modelos epidemiólogicos, multivariados y dinámicos. En ciertos casos, hay modelos complicados que arrojan tendencias sencillas sobre la relación de la epidemiología con el paisaje o la dispersión (Djuikem et al., 2021; Papaïx et al., 2014). En otros, se revelan comportamientos complicados a partir de ecuaciones simples (Vandermeer y Rohani, 2014). Con relación a la dispersión, existe una separación entre modelos continuos (Dupont et al., 2022; Vandermeer y Rohani, 2014) y modelos discretos (Park et al., 2001) o según el tipo de formalismo que usan para modelar la dispersión. Existen modelos de difusión simple (Park et al., 2001), otros con comportamientos más complejos y realistas (Dupont et al., 2022) o caminatas aleatorias con diferentes distribuciones como vuelos de Lévy (Dannemann et al., 2018). En este trabajo vamos a emplear dos modelos computacionales espacialmente explícitos con diferentes supuestos con respecto al mecanismo de infección, al arreglo espacial de las plantas y al modo de dispersión (ver cap 1 y 3). Además, usaremos modelos espacio-estado para el análisis de trayectorias obtenidas en campo (Patterson et al., 2008).

PLANTEAMIENTO DEL PROBLEMA

Las formas de control de la roya son muy variadas y reflejan el proceso y enfoques históricos y económicos del manejo de plagas en la agricultura. Algunas de ellas se basan en detener el proceso de infección del hongo ya sea a través de variedades resistentes, de fungicidas químicos, o modificando las condiciones microambientales para el proceso de infección. Otras prácticas incluyen a los enemigos naturales o a la comunidad ecológica en general. Otras más se basan en el estudio del proceso de dispersión. En esta lógica, disminuir la dispersión mantiene localizados los focos de infección e impide que se alcancen nuevos hospederos y se vuelva a reproducir el patógeno. La roya, al dispersarse por uredosporas, puede transmitirse por factores bióticos y abióticos en escalas espaciales y temporales muy variadas. El impacto de la dispersión sobre la incidencia general depende también del arreglo espacial de las plantas, modificada directamente por el tipo de manejo agrícola. Sin embargo, muchas de las relaciones entre la dispersión, sus escalas o tipos de manejo siguen siendo descriptivas. Además, la importancia relativa de cada modo de dispersión no es clara. En particular, hay pocos modelos mecanísticos espacialmente explícitos que relacionen los modos de dispersión con la incidencia general de roya en cafetales con diferentes manejos agrícolas. En este trabajo queremos avanzar en esta dirección. La primera relación que nos interesó estudiar fue el papel de la dispersión por *splash* en plantaciones con diferentes arreglos espaciales de siembra (primer capítulo y apéndice 3). Sabemos de los múltiples trabajos experimentales realizados que el *splash* puede mover las esporas de una planta a sus vecinas cercanas. Ahora bien, no es claro qué tanto se puede expandir la epidemia a lo largo de parcelas con diferentes arreglos de siembra únicamente con este mecanismo, tomando en cuenta la ventana temporal en la que el *splash* está presente. Por otro lado, nos pareció relevante que el papel del movimiento de las personas durante la cosecha en la dispersión del hongo no esté suficientemente explorado, ni tampoco su relación con el

síndrome de producción cafetalera. Lo primero que hicimos fue caracterizar estadísticamente este movimiento a partir de datos obtenidos en plantaciones de gran escala y estudiar qué factores ambientales y de manejo –relacionados con el síndrome general de producción-- podían modificar las trayectorias observadas (segundo capítulo y apéndice 4). En el tercer y último capítulo (y apéndice 5), exploramos con un modelo dinámico si uno de los factores propuestos en el capítulo anterior --la asincronía en la maduración de los frutos de café-- era suficiente para explicar las diferencias en las trayectorias de los cosechadores y, sobre todo, qué papel jugaban éstas en la dispersión e incidencia de la roya en parcelas con diferentes densidades de siembra.

OBJETIVOS

Objetivo General

Analizar el impacto de dos modos de dispersión de la roya del café (*splash* y movimiento humano) sobre su incidencia en parcelas con diferentes manejos agrícolas, a saber, distintas formas de cosecha, densidades y arreglos espaciales de siembra.

Objetivos particulares

1. Analizar con un modelo compartimentalizado y parametrizado el impacto de la dispersión por medio del *splash* sobre la temporalidad y la magnitud de la incidencia de roya en parcelas con diferentes arreglos espaciales de siembra.

2. Caracterizar el movimiento espacial de los cosechadores en plantaciones cafetaleras de gran escala, los factores de manejo agrícola que determinan dichos movimientos y su relación con el síndrome de producción.

3. Analizar con un modelo cualitativo el papel de la asincronía en la maduración de los frutos para generar diferentes trayectorias de movimiento durante la cosecha y evaluar el impacto de estas sobre la dispersión e incidencia de la roya en parcelas con diferentes densidades de siembra.

CAPÍTULO I. Dispersión por *splash* e incidencia de la roya en parcelas con diferentes arreglos de siembra.

Síntesis del capítulo

La incidencia de roya, medida como el porcentaje de hojas o de plantas infectadas por unidad de tiempo, crece aceleradamente a finales de la temporada de lluvias hasta llegar a un pico máximo conocido como incidencia máxima (Avelino et al., 1993). La incidencia máxima determina la cantidad de hojas que caerán prematuramente y el impacto que tendrá en la producción agrícola del siguiente año (Cerda et al., 2017; Mulinge y Griffiths, 1974; Rosas et al., 2021). La incidencia alcanzada en una parcela depende de la interacción entre los ciclos de infección y los procesos de dispersión entre hojas y entre plantas (Avelino y Rivas, 2013). En particular, durante la temporada de lluvias, cuando las condiciones son óptimas para la infección del hongo, uno de los modos de dispersión presentes es el *splash*. De acuerdo con algunos autores, el *splash* por sí mismo explica el crecimiento acelerado y la incidencia máxima (Bock, 1962b). Tanto la dispersión como la infección están mediados por factores climáticos y genéticos, lo que modifica la incidencia máxima de la epidemia (Avelino et al., 2004). No obstante, hay una gran variabilidad en la incidencia máxima y en el tiempo que dura la fase de crecimiento hasta entre parcelas vecinas con condiciones ambientales y bióticas similares (Li et al., 2022). En algunos sitios, la epidemia puede arrancar hasta dos o tres semanas después que en las regiones vecinas.

En este capítulo, partimos de la hipótesis de que la variabilidad en la incidencia máxima y en la temporalidad del retraso o de la fase de crecimiento epidémico entre parcelas similares puede deberse principalmente a la relación entre la dispersión por *splash* entre planta y planta y el arreglo espacial de la siembra a nivel de parcela. En la mayoría de los estudios experimentales esta relación está oculta ya que reportan la incidencia de la epidemia en las parcelas como un promedio de la incidencia individual (porcentaje de hojas infectadas). Proponemos entonces que la incidencia máxima de la epidemia en una parcela estará determinada por qué tanto logra

expandirse la roya a partir de ciertas plantas infectadas a toda la parcela, a través del *splash* durante el tiempo que dure la temporada de lluvias. La efectividad de la dispersión dependerá de la distancia entre las plantas de café y, por lo tanto, del arreglo espacial de la siembra.

Para poner a prueba nuestra hipótesis, hicimos primero una sistematización de series de tiempo de la epidemia de la roya y de la temporada de lluvias en diferentes sitios para estimar la variación en la incidencia máxima y en el número de días de cada fase del proceso epidémico. Además, construimos un modelo compartimentalizado a nivel de planta que reprodujera el ciclo de infección de la roya y su dinámica de dispersión por *splash* entre plantas. Los modelos compartimentalizados o SIR (Susceptible-Infectado-Recuperado) han sido ampliamente usados para capturar las características generales de los brotes epidémicos tanto en animales como en plantas (Cunniffe y Gilligan, 2010; Gilligan, 2002). Esencialmente, buscan determinar los mecanismos que subyacen la no linealidad de la incidencia epidémica, dividiendo la población estudiada en compartimentos (e.g. hojas susceptibles, infectadas, caídas) y determinando las diferentes reglas de transición entre cada uno. En nuestro modelo definimos los compartimentos como plantas con hojas susceptibles (S) y hojas infectadas (I) y agregamos un compartimiento de esporas libres (X) que pudiera dispersarse por difusión simple a las plantas vecinas (Gubbins et al., 2000). Los parámetros de transición entre compartimientos fueron parametrizados con los datos de la revisión bibliográfica, lo que nos permitió trabajar con escalas temporales realistas. A través del modelo exploramos la relación entre la dispersión por *splash* con la infección y con diferentes arreglos de siembra en una parcela (*i.e.* plantas agregadas, espaciadas, en hileras o aleatoriamente sembradas). A su vez, evaluamos la incidencia de roya en diferentes escenarios cambiando las condiciones iniciales de infección y la tasa de caída de las hojas infectadas a nivel de planta.

De manera general encontramos que las curvas epidémicas de roya tienen dos fases marcadas desde el inicio de la temporada de lluvias: una fase de retraso entre el inicio de las lluvias y el inicio del crecimiento de la incidencia y una fase de crecimiento en sí. Ambas fases son muy variables y la fase de crecimiento en sí se correlaciona temporalmente con la temporada de cosecha. Esto puede ser causado indirectamente por la relación entre la maduración de los frutos y el incremento de la susceptibilidad de las hojas ante la roya, ambas traslapadas con la temporada de cosecha. Pero, como exploramos en los capítulos siguientes, la propia cosecha podría reforzar la dispersión y, por lo tanto, la incidencia de la roya. Con el

modelo mecanístico obtuvimos fases de crecimiento con una duración equivalente a lo reportado en campo. En particular, observamos que la incidencia promedio fue reflejo de la dispersión espacial de la roya a través de la parcela. Cuando las plantas están sembradas de manera agregada, la dispersión de la roya por medio del *splash* conjunto a los ciclos de infección en cada nueva planta, alcanza a infectar toda la parcela antes del final de la temporada de lluvias, aun con tasas bajas de dispersión (esto es, con valores bajos de difusión). Esto resulta en una incidencia máxima del casi 80%. En este sentido, sembrar a altas densidades puede siempre llevar a epidemias grandes. Por otro lado, si no se rebasa un umbral de agregación de las plantas, la incidencia máxima de la parcela cae considerablemente, particularmente con tasas de difusión bajas. Esto se debe a que la roya no alcanza a dispersarse y a reproducirse en todas las plantas de la parcela antes de que se terminen las condiciones climáticas óptimas para la infección. En particular, cuando las plantas están más espaciadas entre sí, la incidencia promedio aumenta de forma escalonada con el tiempo, producto de la asincronicidad temporal en la infección individual de cada planta. A nivel de planta, observamos que una mayor tasa de caída de las hojas infectadas reduce considerablemente la incidencia máxima a nivel de parcela, lo que hace pensar que quitar y llevarse las hojas infectadas puede reducir la incidencia de la epidemia, aunque implique un esfuerzo importante en campo. Finalmente, una menor infección inicial en cada planta retrasó el inicio de la fase de crecimiento. En este sentido, el retraso observado en campo no se debe únicamente a condiciones fisiológicas de maduración del café, sino también a la cantidad de inóculo residual, lo que se debe tomar en cuenta para las prácticas de manejo.

Ecological Modelling 475 (2023) 110206

Contents lists available at ScienceDirect

Ecological Modelling

journal homepage: www.elsevier.com/locate/ecolmodel

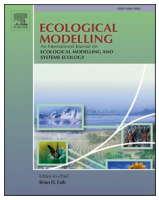

Dispersal and plant arrangement condition the timing and magnitude of coffee rust infection

Emilio Mora Van Cauwelaert [a,b,*], Cecilia González González [a,c], Denis Boyer [d], Zachary Hajian-Forooshani [e], John Vandermeer [e], Mariana Benítez [a,*]

[a] Laboratorio Nacional de Ciencias de la Sostenibilidad, Instituto de Ecología, Universidad Nacional Autónoma de México, Mexico City C.P. 04510, Mexico
[b] Posgrado en Ciencias Biomédicas, Universidad Nacional Autónoma de México, Mexico City C.P. 04510, Mexico
[c] Posgrado en Ciencias Biológicas, Universidad Nacional Autónoma de México, Mexico City C.P. 04510, Mexico
[d] Instituto de Física, Universidad Nacional Autónoma de México, Mexico City C.P. 04510, Mexico
[e] Department of Ecology and Evolutionary Biology, University of Michigan, Ann Arbor, MI, United States

ARTICLE INFO

Keywords:
Coffee-leaf-rust infection
Dispersal
Epidemiology
Dynamical modeling

ABSTRACT

One central issue in coffee-leaf rust (*Hemileia vastatrix*) epidemiology is to understand what determines the intensity and the timing of yearly infections in coffee plantations. However, most experimental and theoretical studies report infection as an average at the plot level, obscuring the role of potentially key factors like rust dispersal or the planting pattern. Here, we first review the rust epidemic patterns of different sites, which reveal large variability in the duration and magnitude of the different epidemiologic phases. We then present a spatially explicit and parametrised model, where the host population is subdivided into discrete patches linked through spore dispersal, modeled as simple diffusion. With this model, we study the role of the planting arrangement, the dispersal intensity and plant-level variables on the maximum average tree infection (MATI) and its timing. Our results suggest that the epidemic timeline can be divided into two phases: a time lag and a growth phase *per se.* The model shows that the combination of the dispersal magnitude and plant aggregation modifies the MATI and the time to MATI, mainly by preventing some plants from reaching their maximum peak during the epidemic. It also affects the epidemic curves, which can have a stepped, or a rather smooth pattern in plots with otherwise similar conditions. The initial rust infection modulates the time lag before the epidemic and the infected leaf-fall rate drastically changes the MATI. These findings highlight the importance of explicitly considering the spatial aspects of coffee agroecosystems when measuring and managing rust infection, and help us to further understand the spatio-temporal dynamics of ecological systems in general.

1. Introduction

The first recorded epidemic of the coffee rust disease, caused by the fungus *Hemileia vastatrix,* broke out in Ceylon (now Sri Lanka) in 1869 (Talhinhas et al., 2017). Since then, coffee rust has spread across the continents, reaching virtually all the coffee plantations areas on earth (Avelino et al., 2006; McCook and Vandermeer, 2015). This is particularly relevant for farmers who depend economically on these crops.

One central issue in coffee rust epidemiology is to understand what determines the intensity of a one-year infection (Avelino et al., 2006; Gagliardi et al., 2020; Kushalappa and Eskes, 1989; Motisi et al., 2022). Similarly, many epidemiologists have sought to estimate the time to maximum infection for the design of specific control practices (Ananth, 1969; Burdekin, 1964). Both questions have been studied within the "disease triangle" framework (Stevens, 1960). In this sense, scientists and farmers have studied the pathogen's properties such as its genetics (Carvalho et al., 2011), the host resistance and phenology (Avelino et al., 1993; Silva et al., 2006), and disease environmental drivers such as the temperature, humidity or precipitation (Avelino et al., 2015). Nevertheless, there is a large amount of variability in the intensity and timing of the different epidemiological phases of the coffee rust epidemic that remains unexplained, even between neighbouring coffee plots with the same environmental and biotic conditions (Li et al., 2022). For example, in some plantations, when the abiotic and biotic conditions

* Corresponding authors at: Laboratorio Nacional de Ciencias de la Sostenibilidad, Instituto de Ecología, Universidad Nacional Autónoma de México, Mexico City C.P. 04510, Mexico.
E-mail addresses: emiliomora92@ciencias.unam.mx (E. Mora Van Cauwelaert), mbenitez@iecologia.unam.mx (M. Benítez).

https://doi.org/10.1016/j.ecolmodel.2022.110206
Received 7 May 2022; Received in revised form 27 October 2022; Accepted 3 November 2022

for rust invasion are met, the infection may not start right away: there is a highly variable time lag (Boudrot et al., 2016; Mulinge and Griffiths, 1974).

To explain this variability, previous research has mainly focused on the infection phase *per se* (where susceptible leaves are infected by coffee rust spores and become infective; Talhinhas et al., 2017) and has overlooked another epidemiological phase: dispersal. Dispersal is the process by which spores are transported from one place to another, across different scales, ranging from the intraleaf, interleaf, or even the inter-plot scale (Becker and Kranz, 1977; Boudrot et al., 2016; Vandermeer et al., 2018). Overall, the intensity of an epidemic is highly related to the rates of infection and dispersal during each season (Avelino et al., 2015). Analysis of dispersal is thus called for, and, by its very nature, must incorporate a spatial approach (Avelino et al., 2012). There are effectively two distinct scales of dispersal: first, the large scale mediated by the wind and resulting from a "rain" of spores over large areas (between plots or between farms; Becker and Kranz, 1977; Bowden et al., 1971; Kushalappa and Eskes, 1989), and second, the local scale, corresponding to neighbouring plants in a plot and/or leaves on the same plant, caused mainly by insect vectors, splash, wind gusts, and human action during harvest (Becker and Kranz, 1977; Vandermeer et al., 2018). In this work, we will focus on the local plant-to-plant dispersal scale in a plot.

Intuitively higher local dispersal should lead to more severe epidemics in a plot. However, despite the importance of a nuanced understanding of rust epidemic dynamics within plots, most empirical studies on coffee rust epidemics report rust prevalence in terms of averages within a plot and not on individual trees (Bock, 1962a; Burdekin, 1964). This method reduces the sampling errors and smooths the epidemic curves but may obscure the relationship between plant and plot dynamics mediated by dispersal. Besides, coffee plantations can be arranged in rows or follow a more random arrangement depending on the age, type (rustic or conventional), or size of the plantation (Hajian-Forooshani and Vandermeer, 2021; Moguel and Toledo, 1999). Therefore coffee rust dispersal effect might be modulated by these planting patterns (Hajian-Forooshani and Vandermeer, 2021; Vandermeer et al., 2018). Finally, the relative importance of the dispersal between plants and the plant-level infection dynamics (such as the initial infection or the rust-infected leaf-fall rate) on the plot-level rust epidemics, has not been fully assessed or considered in current dynamic models (but see Park et al., 2001).

A dynamical modeling approach at both the plant and plot scales can help to disentangle such multi-scaled relations and processes, and shed light on the role of dispersal on the maximum infection prevalence (we will refer here to maximum infection) and the time to reach it in coffee plantations. We hypothesise that spatial dynamics and coffee rust dispersal might also play a role in the variability of the timing and magnitude of the different rust epidemiological phases in coffee plots with otherwise similar biotic and abiotic conditions. We thus seek to explore the determinants of (a) the plot-averaged maximum infection and (b) its timing, using a parametrised epidemiological SIX (Susceptible-Infected-eXternal inoculum) model in a spatially structured host population. With this model we analyze the role of the intensity of rust dispersal, planting arrangements, initial infection, and plant-level dynamics (such as the fall rate of an infected leaf) on the epidemiological outcomes.

2. Methods

We first reviewed quantitative and qualitative data on the maximum infection and the number of days to reach this maximum in different coffee systems. From these data, we estimated the duration of the different coffee rust epidemiological phases and their variability, and used them for future validation of the model. Secondly, we built a spatially explicit model to study the role of planting arrangement, dispersal intensity, plant-level dynamics, and initial conditions on the variability detected in the spatially-averaged maximum coffee rust infection and its timing. Details are presented below, but the overall work route was the following: We first constructed the model and parametrised it. Then, we implemented different computational scenarios at the plant and plot level, and studied their effect on the maximum infection, growth phase and time lags.

2.1. Reviewing the qualitative dynamics of coffee rust infection

To study the qualitative behavior of coffee rust infections, we reviewed literature reporting data on coffee rust at coffee sites with different climatic, orographic, and management conditions. We used data from studies that presented at least a 12 month time series, rainfall pattern, and, in some cases, the harvesting period. We explored publications reporting all these data from the 1960′s to the present. Since most of the reviewed works do not report Tables or do not follow a uniform procedure, we extracted both the rainfall and coffee rust infection data directly from the graphs, using WebPlotDigitizer (Drevon et al., 2017; Rohatgi, 2020). We transformed all dates to their corresponding julian day number and all the precipitation histograms to millimetres. Some graphs started on day 250 (September 7th) and others on day 1 (January 1st) (Fig. 2). We considered three time series from Chiapas, México (Avelino et al., 1991; Vandermeer et al., 2018); two from Central America (Quetzaltenango, Guatemala and Turrialaba, Costa Rica) (Avelino et al., 1993; Boudrot et al., 2016); one from South India (Mysore) (Ananth, 1969); and three from Kenya (East Riff, Ruiru and Kiambu) (Becker and Kranz, 1977; Bock, 1962a; Mulinge and Griffiths, 1974). In the case of Ruiru, Kenya, rainfall was not directly reported, so we used the rainfall pattern reported for Nairobi, which has similar climatic conditions (Ndolo et al., 2017).

In some cases, coffee rust infection was reported as the average percentage of rust-infected leaves per tree, in others, as spores counted per tree or spores in the immediate vicinity. Rainfall was reported on a daily or monthly basis, and we grouped the daily data in months. When the harvesting period was reported, we added it manually, adding a ten day-error to each end. For each site, we reviewed the duration of the different epidemiological phases, the maximum infection reached and their relationship with rainfall and harvesting period. We defined the beginning of the rainy season as the middle of the first month that averaged precipitations higher than 50 mm, and the beginning of the epidemic growth period *per se* as the moment when the increase in the reported percentage of infected leaves in the trees was higher than 0.1 per day. The time between these two points was defined as the time lag. Other characteristics of the plantations such as the climatic, orographic, and management conditions are included in the supplementary material S2. The general timings and magnitudes of infection on these sites were also compared to the predictions of our parametrised model.

2.2. SIX model construction

We modeled the dynamics of multiple individual plants, including both infection and internal leaf-to-leaf spore dispersal processes, coupled in a plot through a plant-to-plant dispersal mechanism. The overall modeling strategy is shown in Fig. 1 and can be summarised as follows. We first defined a 10×10 lattice (100 cells) with sink boundaries and 50 trees (N) in four different scenarios of planting arrangements: aggregated, random, rows, and spaced (Fig. 1B). These arrangements aim to represent the different patterns reported in coffee plots, where trees can be closely surrounded by other trees (aggregated), or have direct neighbours in one specific direction (rows), or have no direct neighbours (spaced) or have a random arrangement. Black squares represent the trees with susceptible or infected leaves as well as the immediate space around the tree where external uredospores may be present. White squares represent regions of space where only uredospores might be present ($S = I = 0$ in Eq. (2.2)) (Fig. 1B). We characterised the four different planting arrangements with a distance-between-plant index $\langle H \rangle$ defined as (Eq. (2.1)):

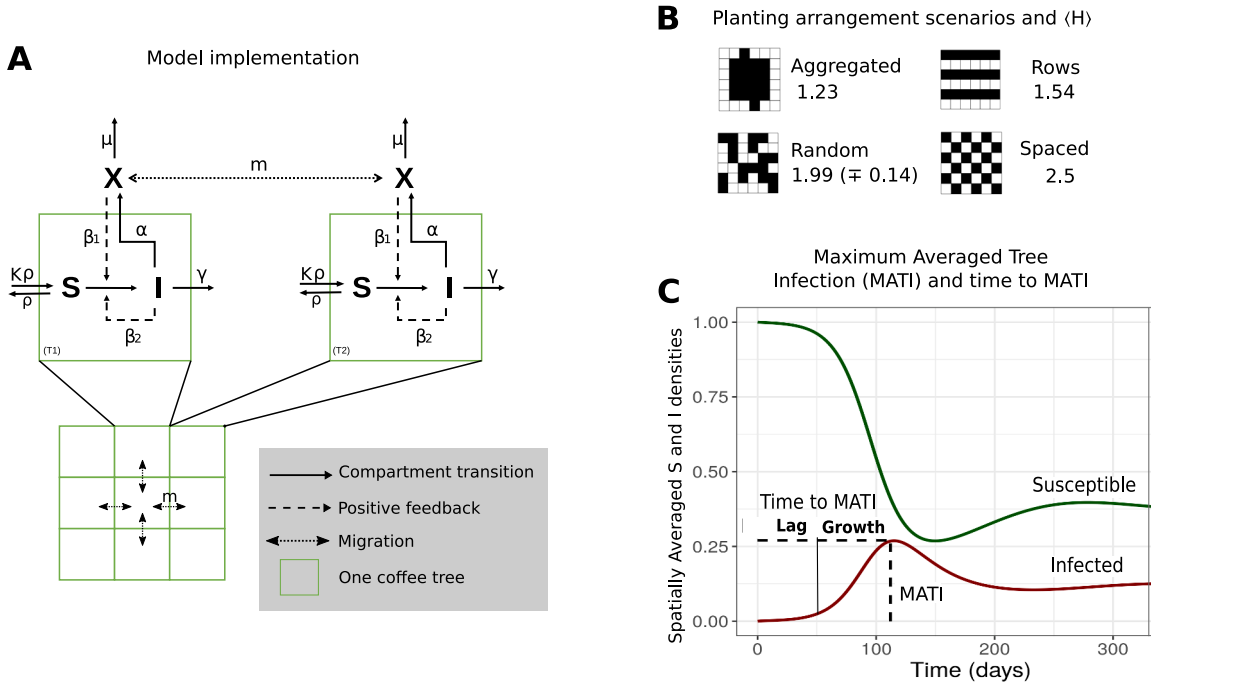

Fig. 1. Model Diagram and the different planting patterns considered. A. Model scheme; *S*: Susceptible leaves, *I*: Infected Leaves, *X*: External spores. B. Different planting arrangements and their distance-between-plants index $\langle H \rangle$. The black squares indicate the presence of a tree and the number is the $\langle H \rangle$ value for that pattern. All the arrangements contain 50 trees in a 10 × 10 lattice (here we depict a 6 × 6 lattice with the same planting density only for visualisation purposes). C. Basic dynamics for *S* and *I*, Maximum Average Tree Infection (MATI) and time to MATI (divided in two parts: the time lag (*Lag*) and the growth *per se* (*Growth*)). *X* follows dynamics similar to *I* (see Fig. S1.1). Here $\gamma = 0.056$, $\alpha = 0.65$, $\beta_1 = \beta_2 = 0.035$, $\rho = 0.011$ and $\mu = 0.2$ (estimated parameters shown in Table 1).

$$\langle H \rangle = \frac{N}{\sum_{i=1}^{N} H_i} \qquad H_i = \frac{\sum_{j=1}^{4} 1 \Big/ d_{ji}}{4} \tag{2.1}$$

where N is the number of plants per plot, and H_i is the average of the inverse distance (number of squares) between plant i and its four closest neighbours j (d_{ji}) along the horizontal and vertical axis. If there are no neighbours along a particular direction, we set $1/d_{ji} = 0$. In the case of the random arrangement, we ran 30 configurations and presented the average. Since we chose the same number of trees for all the scenarios ($N = 50$), $\langle H \rangle$ only depends on the spatial arrangement of plants (Fig. 1B).

Each tree follows the two main phases of the coffee rust life cycle: host-pathogen interaction (invasion) and pathogen dispersal, whose dynamics are schematized in Fig. 1A and are described by the following system of coupled differential equations (Eq. (2.2)):

$$\begin{aligned} \frac{dS_i}{dt} &= \rho(K - S_i) - \beta_1 X_i \frac{S_i}{K} - \beta_2 I_i \frac{S_i}{K} \\ \frac{dI_i}{dt} &= \beta_1 X_i \frac{S_i}{K} + \beta_2 I_i \frac{S_i}{K} - \gamma I_i \\ \frac{dX_i}{dt} &= \alpha I_i - \mu X_i + m\left(\sum_{j=1}^{V_i} X_{ji} - V_i X_i\right) \end{aligned} \tag{2.2}$$

where S_i and I_i are the amounts of susceptible and infected leaves in tree i. I_i represents the state where the infected leaf has already produced new infective spores. X_i represents the number of infective external uredospores (from now on "external spores"; supplementary material S3; Bock, 1962b) in square i, with or without a tree. X_i does not include spores in the leaves or between them, only the ones that are outside the tree. Host reproduction (*i.e.* leaf production and leaf-fall rate of susceptible leaves) is represented by the so-called monomolecular growth (Cunniffe and Gilligan, 2010), where the natural (or non-infected) leaf-fall rate is represented by ρ and leaf production rate is equivalent to $K\rho$ where K is the carrying capacity of susceptible leaves. We took $K = 1$ for simplicity but our results can be rescaled by using reported values for K (Burdekin, 1964). This assumes that the new leaf production rate equals the leaf-fall rate of susceptible leaves. The transition from S to I is subdivided into primary infection arising from the external spores (X) and secondary infection occurring by transmission from already infected leaves (I). In both cases, the growth in infection is proportional to the fraction of remaining susceptible leaves S/K, and to the rates (β_1, β_2), respectively. Infected leaves can fall and leave the I compartment at a rate γ that must be higher than the non-infected leaf-fall rate (ρ). Spores detach from infected leaves and become suspended in the air or fall on the ground, filling the X compartment at a rate α. External spores die at rate μ both in squares with and without trees (black and white cells in Fig. 1B). Finally, m is the diffusion rate, which represents the rate at which spores are dispersed to the neighbouring squares. Let us denote as V_i the number of immediate neighbours of square i (ranging from two to four depending on the location of the square in the lattice), and X_{ji} the amount of X in the j-th neighbour of i. Non-directed dispersal is modeled by a diffusion process that takes place from one plant to its four immediate neighbouring squares, mimicking short ranged rust dispersal mediated by splash and plant-to-plant contact in our two-directional planting arrangements. Note that equivalent scenarios could be modeled using an 8 neighbourhood vicinity, but in order to create the spaced arrangement we would have to push trees further away from each other. In empty squares, $S_i = I_i = 0$, so the spores have the following dynamic:

$$\frac{dX_i}{dt} = m\left(\sum_{j=1}^{V_i} X_{ji} - V_i X_i\right).$$

All the parameters are summarised in Table 1.

Our model is a spatially extended case of the SIRX (Susceptible-Infected-Removed-eXternal inoculum) models analyzed by Cunniffe and Gilligan (2010) and Gubbins et al. (2000), originally developed for insect-pathogen interactions but widely used for plant-pathogen associations (Swinton and Anderson, 1995). Here we did not include the Removed compartment (R) since its dynamic is determined by the other compartments and does not impact the whole infection process (this assumption is discussed in the Discussion section). In this sense, our model can be referred to as a SIX model. We assume that infection happens in non-resistant coffee trees with "well-mixed leaves", when the conditions for the development of coffee rust are optimal (sufficient susceptible leaves and humidity Nutman et al., 1963). Factors like plant or rust variability are not explicitly considered, nor the change in abiotic conditions. In this work we do not study the equilibrium points but rather some of the most relevant transient dynamics of coffee rust epidemics like the duration of the growth phase or the maximum infection, as well as the probability of rust invasion in each individual plant (but see Cunniffe and Gilligan, 2010 for the linear analysis of the model and the supplementary material S1 for the equilibrium points). The invasion criteria is summarised by the parameter R_0 which is defined as (Eq. (2.3)):

$$R_0 = \frac{\beta_2 + \frac{\beta_1 \alpha}{\mu}}{\gamma} \tag{2.3}$$

If R_0 is less than 1, the single plant system always reaches a-non infective equilibrium. If $R_0 \geq 1$, I and X "invade" and S decreases (see Fig. S1.1 and Cunniffe and Gilligan, 2010 for the main mathematical results on this model).

2.3. Plant level parameterization and simulation conditions

We selected the infected leaf-fall rate (γ) as the sole plant-level

Table 1
Estimated parameter ranges, definition, estimation methods and used values for SIX model simulations.

Parameter	Definition	Inverse of the time it takes:	Estimation Method	Explanation of the estimation	Units	Range	Used values for simulations
Estimated parameters							
ρ	Natural leaf fall rate	One newly mature susceptible leaf (S) to fall	In field measurement (a) Data-Based Estimation (b, c)	Time reported in the field as GDD (a). We also fitted data of leaf development in trees, where coffee rust infection was negligible, to a basic leaf growth equation (b, c).	1/t	[0.009–0.013]	[0.011]
β1 and β2	Primary and secondary infection rate	One susceptible leaf (S), in contact with one external package of infective spores (X) or with one infected leaf (I), to become infected	In field measurement (d, e)	Time well documented in several field studies (d, e).	$N_{inf}/(N_{sp}$ t) and 1/t	[0.03–0.04]	[0.035]
α	Recruitment rate	One package of spores (X) to leave the plant system from one infected leaf (I)	Data-Based Estimation (f, g, d, h, i)	Estimation based on reports on the number of spores produced per infected leaf and per unit of time, as well as on the relationship between the number of spores in a leaf and the number of spores surrounding the plant system (f, g, d, h, i)	$N_{sp}/(N_{inf}$ t)	[0.1–1.2]	[0.65]
μ	Spore death rate	A new spore to become non-viable.	Data-Based Estimation (j, k)	The spore viability through time has been studied (j, k). We used their data to fit our model.	1/t	[0.1–0.3]	[0.2]
γ	Infected leaves fall rate ($\gamma = \rho + \rho I$)	A newly infected leaf (I) to fall	Data-Based Estimation (c)	Time is shorter than the natural leaf fall time. As far as we know, the former time is not explicitly reported so we used (c) results on susceptible and infected fallen leaves to estimate the leaf fall differences.	1/t	ρ+ [0.004]	[0.015–0.14]
Non-estimated parameters							
K	Carrying capacity of susceptible leaves	NA	NA	NA	N_{leaf}	NA	1
m	Diffusion rate	One package of spores to be fully transported to a 4N-vicinity neighbour square.	NA	NA	1/t	NA	[0.001 – 0.1]

The letters indicate the direct reference used: a- Rakocevic and Takeshi (2018) b- Mulinge and Griffiths (1974), c- Firman and Wallis (1965), d- Bock (1962a), e- Leguizamón-Caycedo et al. (1998), f-Gagliardi et al. (2020), g- Boudrot et al. (2016),h- Rayner (1961), i- Silva-Acuña et al. (1999), j- Nutman et al. (1963), k- Deepak et al. (2012). GDD: Growing Degree Days. N_{sp}: number of infective packages of external spores, N_{leaf}: number of susceptible leaves, N_{inf}: number of infected leaves. NA: Not Applicable.

variable and fixed the other parameters of the SIX equation (primary and secondary infection, recruitment, leaf-growth, and spore-death rates). We chose the infected leaf-fall rate as it is a variable that can be directly modified by human management (e.g. removing and bagging away the infected leaves). The other parameters such as the infection rates are affected by multiple environmental, genetic and management processes and are more difficult to control. Besides, this decision reduces our computational explorations and simplifies the interpretation of the results. To choose the values of the plant-level parameters correctly and work with meaningful timescales, we estimated the range of each plant or spore parameter from reported data (Table 1) (Bock, 1962a; Boudrot et al., 2016; Deepak et al., 2012; Firman and Wallis, 1965; Gagliardi et al., 2020; Leguizamón-Caycedo et al., 1998; Mulinge and Griffiths, 1974; Nutman et al., 1963; Rakocevic and Takeshi Matsunaga, 2018; Rayner, 1961; Silva-Acuña et al., 1999). We then set each parameter to the mean value for our general simulations, but we included a sensitivity analysis of our results, using the lowest and highest values of the estimated ranges. The infected leaf-fall rate (γ) was varied above its estimated mean to account for leaf-removal practices that shorten the time for a rusted leaf to fall (e.g. selective pruning), but we restricted its maximum value to simulate scenarios where rust invades the system (this is, where $R_0 \geq 1$ considering the other estimated parameters; Eq. (2.3)) . The detailed methods for the estimation of each parameter are available in the supplementary material S3. To summarise, the model parameters can be estimated from the characteristic time-scale (in days) of a given known process. We first looked for studies that reported those times directly or indirectly. If these data were not available, we fitted specific time-series of leaf infection to linear or exponential models (Table 1).

2.4. Simulations and measured variables: MATI and time to MATI

With the chosen parameters, we explored the effect of the leaf-fall rate of infected leaves (γ), the initial proportion of infected leaves per tree (I_0), the planting patterns, and the different plant-to-plant diffusion rates (m) on the maximum averaged tree infection (henceforth; MATI) and the time to reach this maximum (in days) (Fig. 1C). The MATI is obtained by averaging tree infection over all trees in the plot for every time step, and then by identifying its overall maximum. This is a common indicator to measure rust infections in the field. The time to MATI was divided into a time lag and a growth period *per se*, following the same criteria used in real time series (see Section 2.1 and Fig. 1C). The results were then compared with the magnitudes measured in Section 2.1 and analyzed in each combination of scenarios.

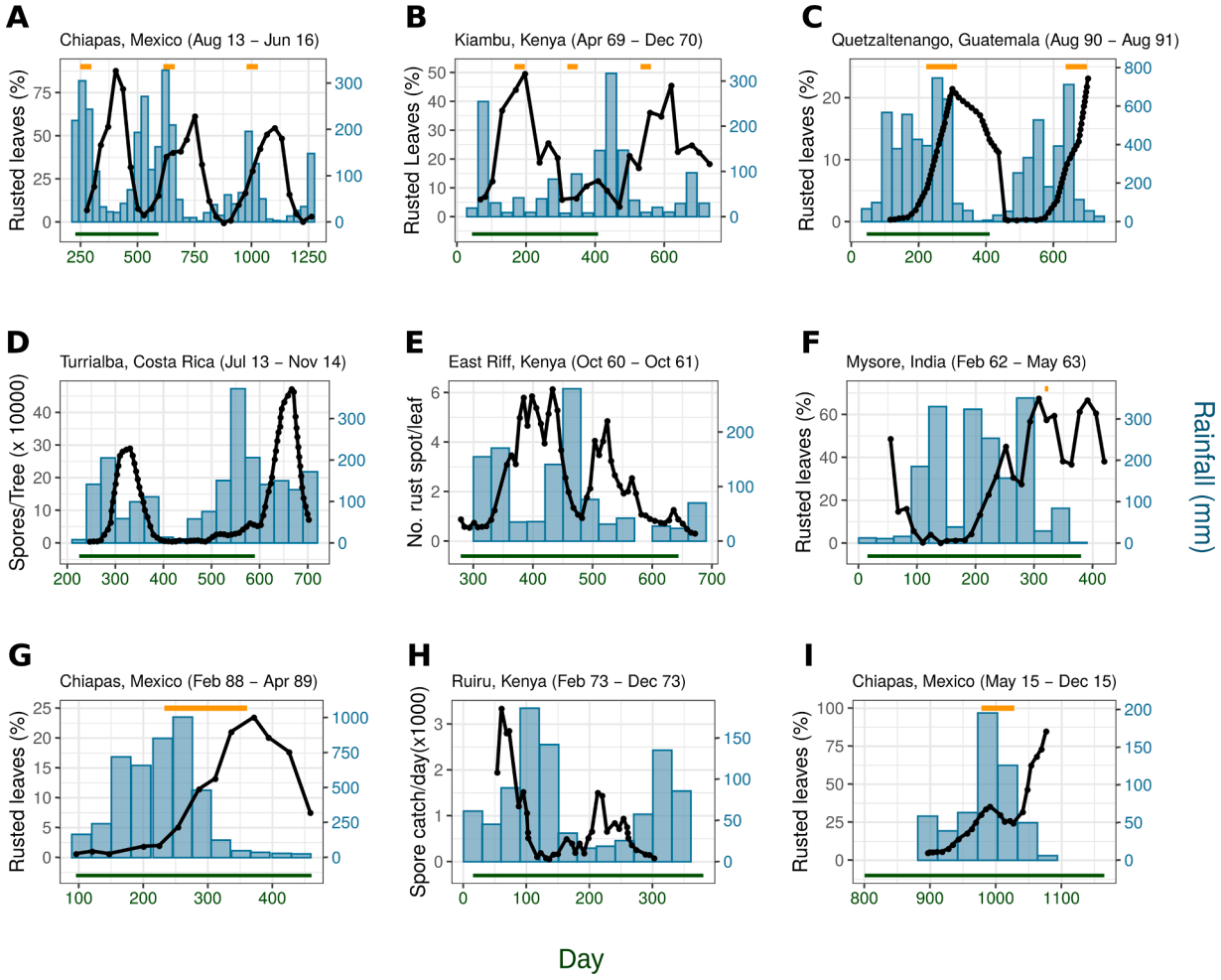

Fig. 2. Coffee rust infection dynamics in relation to annual rainfall and harvesting period. The black line represents the amount of rust infection, measured as the average percentage of rusted leaves per tree (A, B, C, F, G, I), or the average number of rust spots per leaf (E), or the number of spores per tree (D), or above the tree (H). The bars represent the monthly rainfall (mm). The orange horizontal segment in figures A, B, C, F, G and I shows the reported harvesting period and the green horizontal line in the bottom of each graph stands for the 365-day period. The plots are ordered from the longest to the shortest period recorded. The references for each plot are: A (Vandermeer et al., 2018), B (Mulinge and Griffiths, 1974), C (Avelino et al., 1993), D (Boudrot et al., 2016), E (Bock, 1962a), F (Ananth, 1969), G (Avelino et al., 1991), H (Becker and Kranz, 1977; Ndolo et al., 2017), I (Vandermeer et al., 2018). For more details, see supplementary material 2.

2.4.1. One-plant level simulations

We first ran simulations of the SIX model at the single-tree level ($N = 1$, $m = 0$ and $i = 1$), studying the effect of both the γ and I_0 on the MATI and the time to MATI. In this scenario, the MATI is the maximum local tree infection. We varied the leaf-fall rate of infected leaves (γ) from 0.015 to 0.14 and the initial proportion of infected leaves per tree (I_0) from 0.001 to 0.1 (72 scenarios in total). Each simulation started with I_0 infected leaves ($I = I_0$), $1 - I_0$ susceptible leaves ($S = 1 - I_0$), no external uredospores ($X = 0$) and ran for 30 000 integration steps using the Euler method ($\Delta t = 0.01$). This method is a standard and common integration procedure for solving discretized partial differential equations in lattices (Koch and Meinhardt, 1994; Elder et al., 1992) and is sufficiently robust and precise for all our modeled scenarios and quantities of interest (with a $\Delta t = 0.02$, there were no differences in the results within the range of precision used (Fig. S1.6)). These integration steps represented 300 days, after parameter calibration. The beginning of the simulation corresponds to the start of the optimal conditions for infection (when humidity is sufficient, and leaves are susceptible) and we chose 300 days to be the maximum time for the rust to reach the maximum peak of infection in one year (following the times reported in Fig. 2). After this, rust infection is assumed to decrease. This time limit sets a maximum simulation time.

2.4.2. Plot-level simulations

The next step was to run the full model in the 10×10 lattice to include the effects of spatial arrangement and diffusion rate on the MATI and time to MATI. We defined scenarios with the four different planting arrangements (aggregated, spaced, random and rows), one initially infected tree in the centre of the lattice ([x,y] = [5,6]), two values of initially infected leaves ($I_0 = 0.001$ and $I_0 = 0.1$), and five different levels of diffusion rate (m) across three orders of magnitude (ranging from 0.001 to 0.1; or expressed in log for a better visualisation, from -3 to -1). We also chose two of the values of γ used in the single plant dynamic (0.015, 0.056) to compare the plant and plot-level results. For the random planting, we took averages over 30 simulations for each combination of the parameters. For each scenario we obtained the MATI and the time to MATI as a function of the diffusion rate, initial infection and $\langle H \rangle$. We also included the time evolution of the average tree infection with two representative diffusion values ($\log(m) = -3$, $\log(m) = -2$). As we consider $t \leq 300$ days, the results of the scenarios can be divided into two cases: **a.** when an infection peak is attained before the 300 days and **b.** when the optimal conditions for rust cease before the peak is reached (creating a maximum at 300 days). Finally, in order to explore the relationship between individual and average dynamics, we registered the values of each tree's maximum infection and timing and grouped the number of trees that reached a high level of infection (more than 70% of infected leaves) during the same 15-day period. Focusing both on the level of infection of individual trees and their degree of temporal overlapping can shed light on the determinants of the average infection dynamics.

2.4.3. Computational implementation

The model and simulations were implemented in the *Python* 3.7.3 programming language, using the modules *NumPy, SciPy, Pandas, Seaborn* and ran on the LANCIS facilities, at the Ecology Institute of UNAM. The data analyzes and figures were done in *Rstudio* 1.2.1335 using *plyr, dplyr, tidyverse, ggplot2* and *patchwork* libraries and *Inkscape 1.0.* All code and data to reproduce results in the work can be accessed at https://github.com/tenayuco/dispersion_plant_arrangement_coffeerust_infection

3. Results

3.1. Trends in qualitative dynamics coffee rust infection: seasonality and variability in time lags, growth phase and maximum infection

Fig. 2 depicts different coffee rust infection dynamics observed in nine sites, the corresponding rainfall, and, when reported, the harvesting period. Each infection is measured either as the average percentage of rusted leaves per tree or as the average number of spores, during at least one year (green bar at the bottom of each plot). Plotting the time series together enables us to visualise similarities and differences. Firstly, rust infection follows a basic epidemiological cycle consisting of a time lag in relation to the beginning of the rainy season, followed by a growth and a decline phase.

Coffee rust infection also seems to have a rain-forced periodicity: the growth phase always starts after the onset of the rain season (this is clearer for Fig. 2A–C where more than one year is reported). This forced periodicity is related to the first phases of the coffee rust infection cycle, where rain is necessary for spores liberation and invasion. The infection reaches a maximum value and declines when the rain season is ongoing (D, H) or has ended (A, C, F, G). In Kenya, where there are two rainy seasons per year, we observe two peaks of infection (Fig. 2B,E,H). The second peaks are substantially lower than the first peaks in East Riff and Ruiru Sites but they are qualitatively relevant to the general dynamics (B, H), as they show that a new infection process began.

The time lag is 82 days on average (ranging from 24.5 (B) to 146 days (C); see Table S1.1). In sites with two rainy seasons, the lag shortens (Fig. 2B,E,H). In some cases, coffee rust infection is negligible during the lag (Fig. 2C,D,F,G). The growth phase takes 119 days on average, ranging from 68 (I) to 181 days (C) (Table S1.1). It is worth noting that the coffee rust infection cycle takes about 30 days, therefore rust probably undergoes multiple infection cycles during one epidemiological phase, as discussed in Kushalappa and Eskes (1989). The "time to maximum infection" comprises the time lag and the growth phase and ranges from 95 (I) to 325 days (C). The maximum average tree infection ranges in turn from 20 to 80% of infected leaves per tree. Therefore, the timing and intensity of an infection at a given site are largely variable. Interestingly, the harvesting period correlates with the build-up (growth phase) (Fig. 2A,C,G,I) (see the discussion section). All values for the MATI and time to MATI are summarised in Table S1.1.

3.2. Estimation of the parameters of the SIX model in a rust-infected scenario

We estimated the natural (non-infected) leaf-fall time, primary and secondary infection, and spore death rates directly from reported data (supplementary material S3; Table 1). The leaf-fall time of susceptible leaves ($1/\rho$) ranges between 74 and 108 days. β_1 and β_2 can both be interpreted as the inverse of the time taken for one susceptible leaf to become infected, either for being in contact with external spores or with an infected leaf. If we assume that one package of external spores infects one leaf at a time (this is $N_{sp}/N_{inf} = 1$) both times are equal and range from 25 to 30 days ($1/\beta_1$ and $1/\beta_2$). Finally, the uredospore viability goes from 3 to 10 days ($1/\mu$) (Table 1). The time taken for a newly infected leaf to fall ($\boldsymbol{1/\gamma}$) was estimated indirectly as how much shorter this time was in comparison to $1/\rho$. Infected leaves take on average from 35 to 53 days less than susceptible leaves to fall.

We express γ as $\rho + \rho_I$, where ρ_I is the increment in leaf-fall rate due to coffee rust infection. The recruitment rate (α) range is broad [0.1–1.2] since it was estimated indirectly from several studies (Table 1). We use $\rho = 0.011$, hence the mean value of γ is equal to 0.015 (Table 1). Given the values chosen for the other parameters here, the invasion criterion can be expressed as $R_0 = 0.15/\gamma \geq 1$ (see Eq. (2.3) and Fig. S1.1). In this sense, to simulate rust infected scenarios and to account for leaf-removal practices (see Section 2.3), γ was varied between 0.015 to 0.14 ($R_0 \in [1, 10]$).

3.3. In one-plant simulations, γ affects both the MATI and time to MATI, and I_0 affects the time to MATI through the time lag

Fig. 3A,B display the maximum averaged tree infection (MATI) and the days to MATI, for one-tree simulations ($N = 1$), varying the leaf-fall

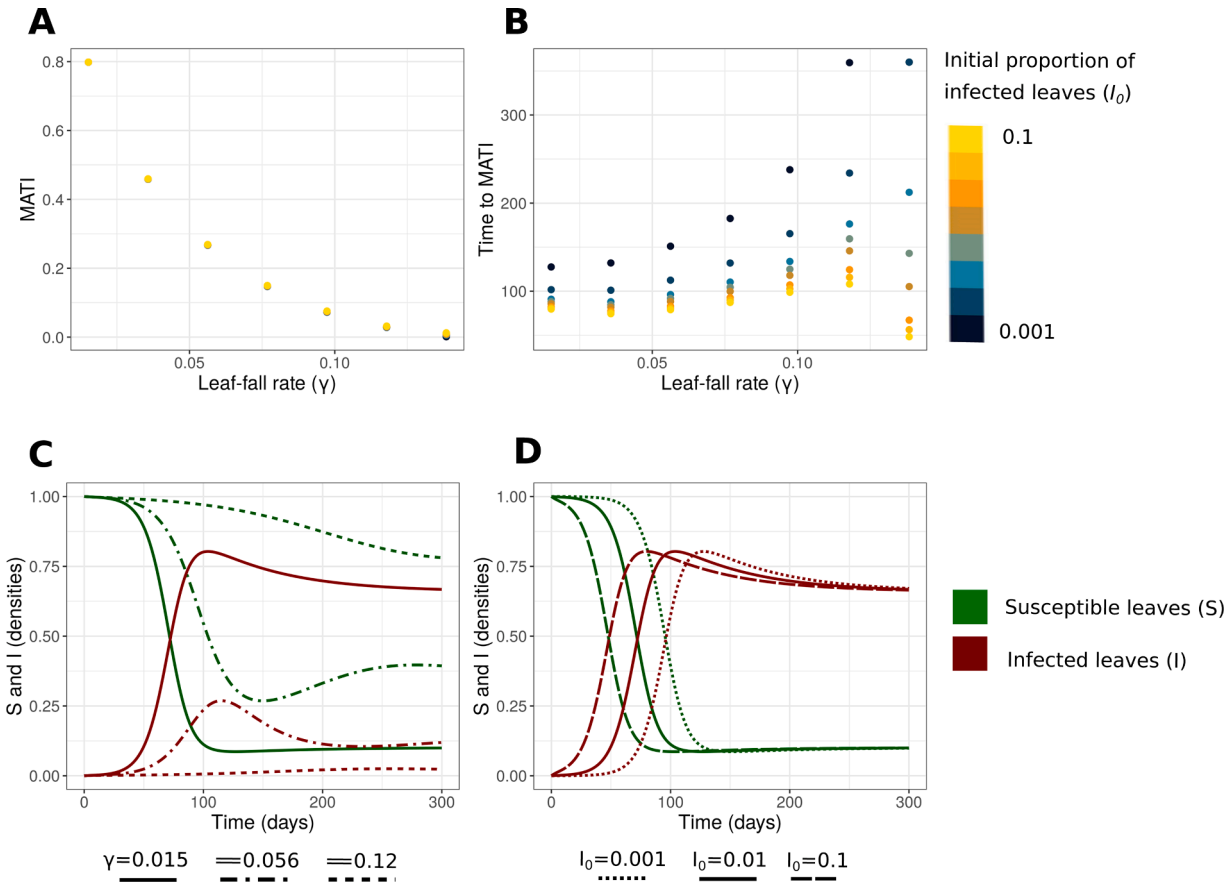

Fig. 3. MATI and time to MATI in isolated coffee plants ($N = 1$). A, B: MATI and days to MATI in function of the leaf-fall rate of infected leaves (γ) and initial proportion of infected Leaves (I_0). C: Example of infection dynamics for susceptible and infected leaves (see Fig. S1.2 for the evolution of the spores X) with different values of γ and a fixed $I_0 = 0.01$. D: Example of infection dynamics with different values of I_0 and a fixed $\gamma = 0.015$. The values of α, β_1, β_2, ρ and μ are shown in Table 1.

rate (γ) and initial proportion of infected leaves (I_0). MATI decreases with the infected leaf-fall rate (Fig. 3A,C). When γ is equal 0.015, the maximum infection is around 75%. When γ is higher than 0.1, MATI drops to zero. This effect is independent of the number of infected leaves in the systems' equilibria predicted by R_0 (Section 2.3; Fig. S1.3; see Fig. S1.1 for the influence of γ on equilibria and stability). I_0 does not affect the MATI whatsoever (Fig. 3D). Time to MATI is affected by both γ (Fig. 3B,C) and I_0 (Fig. 3B,D). In general, when γ increases, the time to reach MATI increases because the curve flattens (Fig. 3C), affecting the growth phase duration but not necessarily the time lag (see Fig. 2). On the other hand, when I_0 is low, the time to MATI increases without changing the MATI (Fig. 3B,D). In other terms, I_0 affects the time lag but not the growth phase *per se* (Fig. 3D). When MATI drops to 0 (with high values of γ) the time to MATI is not relevant since the maximum infection can be reached at the beginning of the simulation.

3.4. *In the spatially explicit model, diffusion rate and the planting arrangement jointly modify MATI and days to MATI in a threshold-dependent manner and modify the curves of infection, while I_0 modulates the time lag and γ decreases the MATI in all scenarios*

We plotted in Fig. 4 the MATI and time to MATI for each combination of planting arrangement, diffusion, and initial conditions (I_0), and in Fig. 5 the time evolution of the average tree infection with two representative diffusion values ($\log(m) = -3$, $\log(m) = -2$). We used two values of γ (0.015, 0.056) but as the results were qualitatively similar, we only present the plots here for $\gamma = 0.015$ (but see Fig. S1.7 for the case of $\gamma = 0.056$). As we explained in the methods sections, results are divided into two cases: **a.** when an infection peak is attained before the 300 days and **b.** when the optimal conditions for rust cease before the peak is reached (creating a maximum at 300 days).

The variations of the time to MATI and MATI for all the combinations of scenarios fall within the range reviewed in Section 3.1 (see Fig. 2 and Tables S1.1 and S1.2). In all the spatial arrangements, when diffusion rate increases, MATI increases, and days to MATI decrease (Fig. 4).

In the aggregated planting arrangement MATI is always reached before 300 days (ranging from 116 to 287 days) and has values above 70% of infected leaves, only slightly modified by the diffusion rate. In the rows, random and spaced arrangement the change of diffusion rate has a more pronounced effect on the MATI. When the diffusion rate is minimal ($\log(m) = -3$) the time to MATI is 300 days (case b; Figs. 4 and 5). In those scenarios, MATI reaches values that range between 35% and 55% of infected leaves, depending on how advanced the infection was at 300 days. If the diffusion rate is larger (more than -2.5 or -2 depending on the arrangement and the initial infection), the time to MATI becomes less than 300 days for these three arrangements (varying between 151 and 294 days). In these scenarios, an infection peak is reached before the end of optimal conditions (*i.e.* before the end of the simulation; case **a**).

In other terms, for lower values of diffusion rate ($\log(m) = -3$) the change of the diffusion rate affects the MATI according to a critical distance between plants ($\langle H \rangle$): when $\langle H \rangle$ is higher than 1.5, this change greatly modifies the MATI (Figs. 4 and S1.4), when $\langle H \rangle$ is lower than this threshold, the MATI is slightly affected. For higher values of the diffusion rate ($\log(m) > -3$), the differences in aggregation become less relevant. Interestingly, in all scenarios, the diffusion rate modifies the growth time *per se* (that varies between 151 and 205 for $\log(m) = -3$,

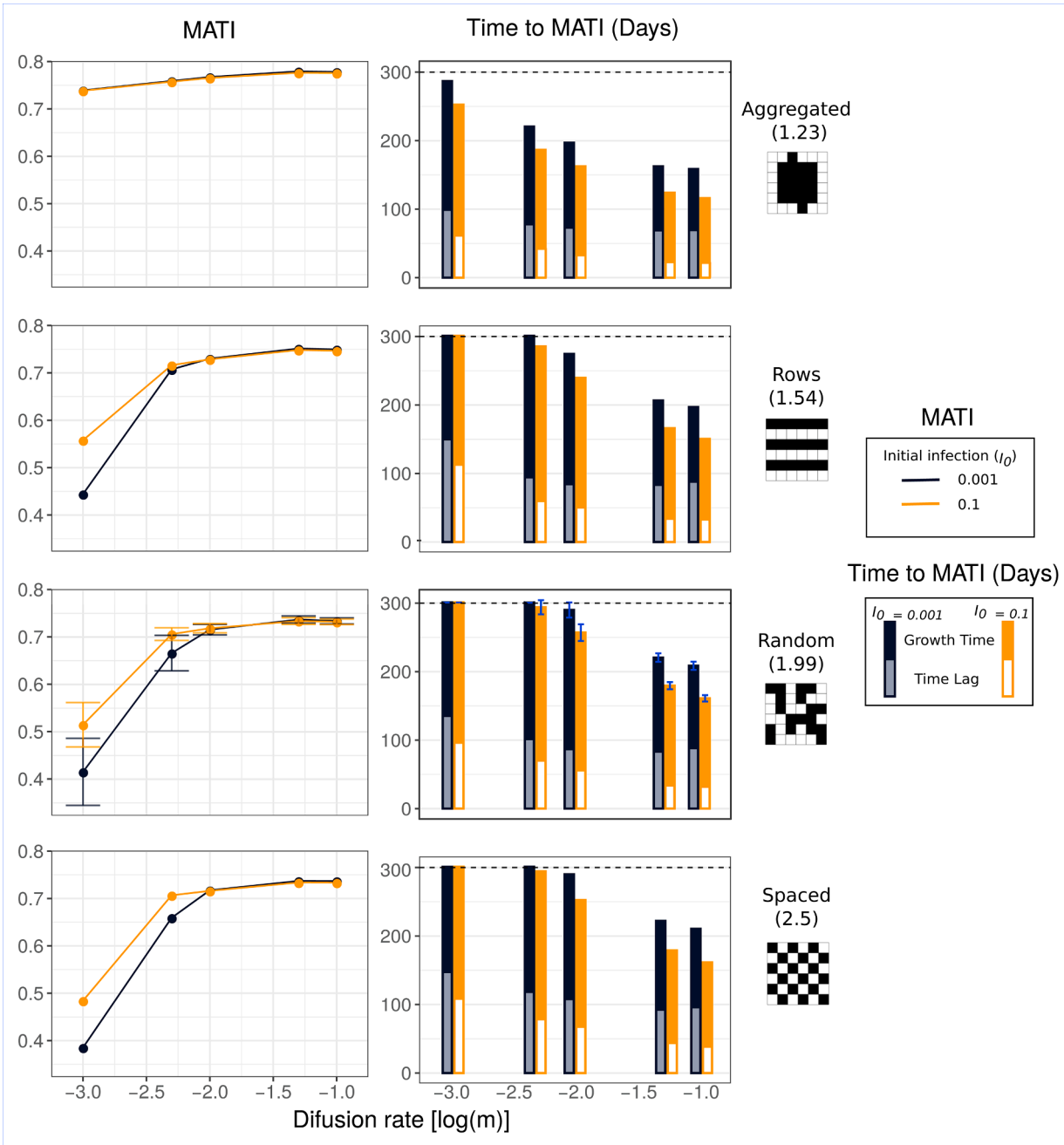

Fig. 4. MATI and time to MATI for all simulations. Simulations of four different planting arrangements (aggregated, random, rows and spaced, with their respective distance-between-plants index $\langle H \rangle$) with five levels of diffusion rate (log(m) between −3 and −1) and two levels of I_0 (0.001 and 0.1, dark and orange lines, respectively). The bars representing the time to MATI are divided into the time lag and the growth period *per se* (light blue vs black and light orange vs dark orange). The dotted line represents the 300 days limit of the simulations. For the random arrangement, each point/bar represents a 30-simulation average, and the error bars the standard deviation. The values of α, β_1, β_2, ρ and μ are shown in Table 1. We used $\gamma = 0.015$ (see Fig. S1.7 for $\gamma = 0.056$).

and 89 and 129 for log(m) = −1) (see Fig. 4 and Table S1.2). For low diffusion rates, this results in flatter curves leading to lower MATI (Fig. 5).

Moreover, differences in planting arrangements do modify the qualitative average tree infection dynamics, creating smoother or rougher curves (Fig. 5). In particular, the spaced arrangement combined with a low diffusion rate, generates multiple steps in the epidemiological dynamics (Fig. 5). This is similar to what we observe in Fig. 2B or H. Random and row planting arrangements did not present any relevant differences between them.

I_0 mainly affects the time lag (that varies between 70 and 150 days when $I_0 = 0.001$ and between 22 and 113 days when $I_0 = 0.1$) (see Fig. 4 and Table S1.2). The curves of Fig. 5 are thus shifted along the time axis as I_0 varies. It is noteworthy that the time lag can be higher than in the one-plant simulation scenarios (that go from 10 to 50 days as I_0 is varied). This increase in the time lag can lead to a lower MATI if the curve of infection does not reach a maximum peak and is still increasing at the end of the simulation (Figs. 4 and 5).

All of our results were qualitatively robust to the variation of the other plant-level parameters within their estimated range, except for the lowest value of α ($\alpha = 0.1$) that significantly decreases the MATI in all scenarios (Fig. S1.7). Finally, as in the plant-level simulation, the MATI decreases and the time to MATI increases when the infected leaf-fall rate (γ) increases (Fig. S1.7.B), especially for values greater than the

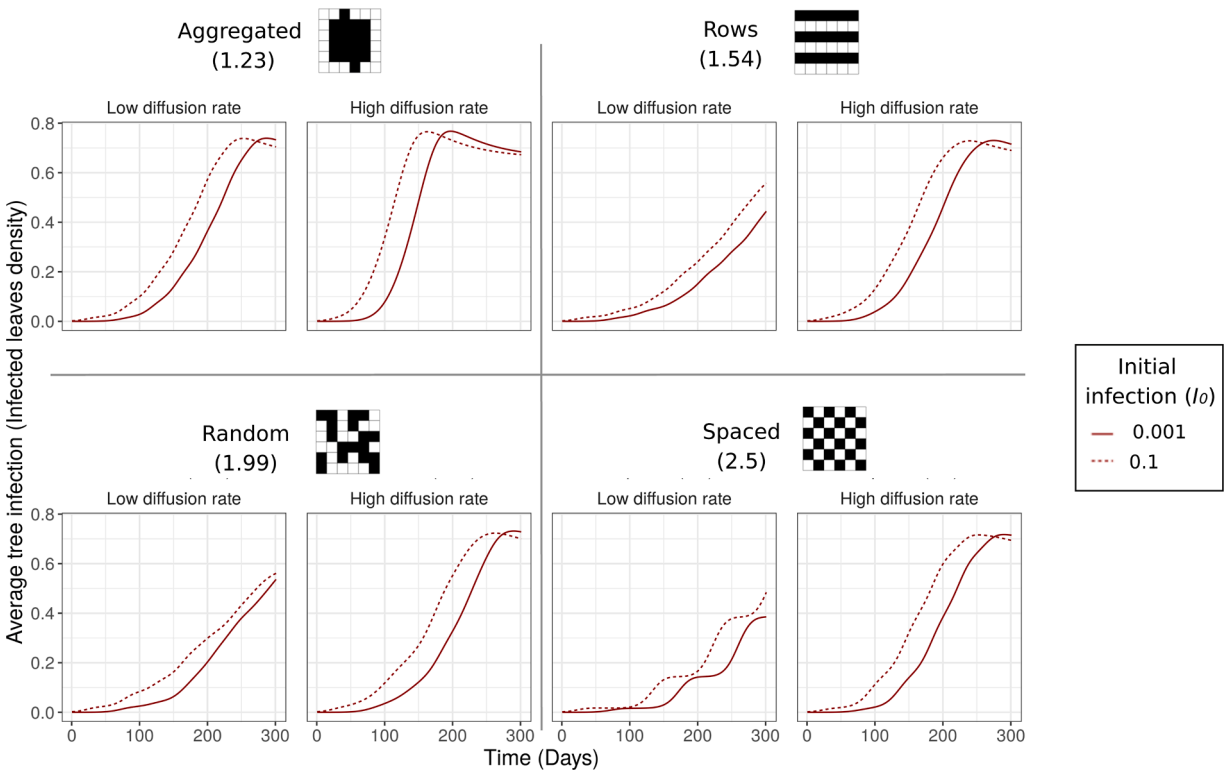

Fig. 5. Examples of average tree infection dynamics for plants in a plot. Simulations of four different planting arrangements (aggregated, random, rows and spaced) with two levels of diffusion (low: $\log(m) = -3$, high: $\log(m) = -2$) and two levels of I_0 (0.001 and 0.1). The lines represent averages over all the trees of the plot at a given time. The values of α, β_1, β_2, ρ and μ are shown in Table 1. We used $\gamma = 0.015$.

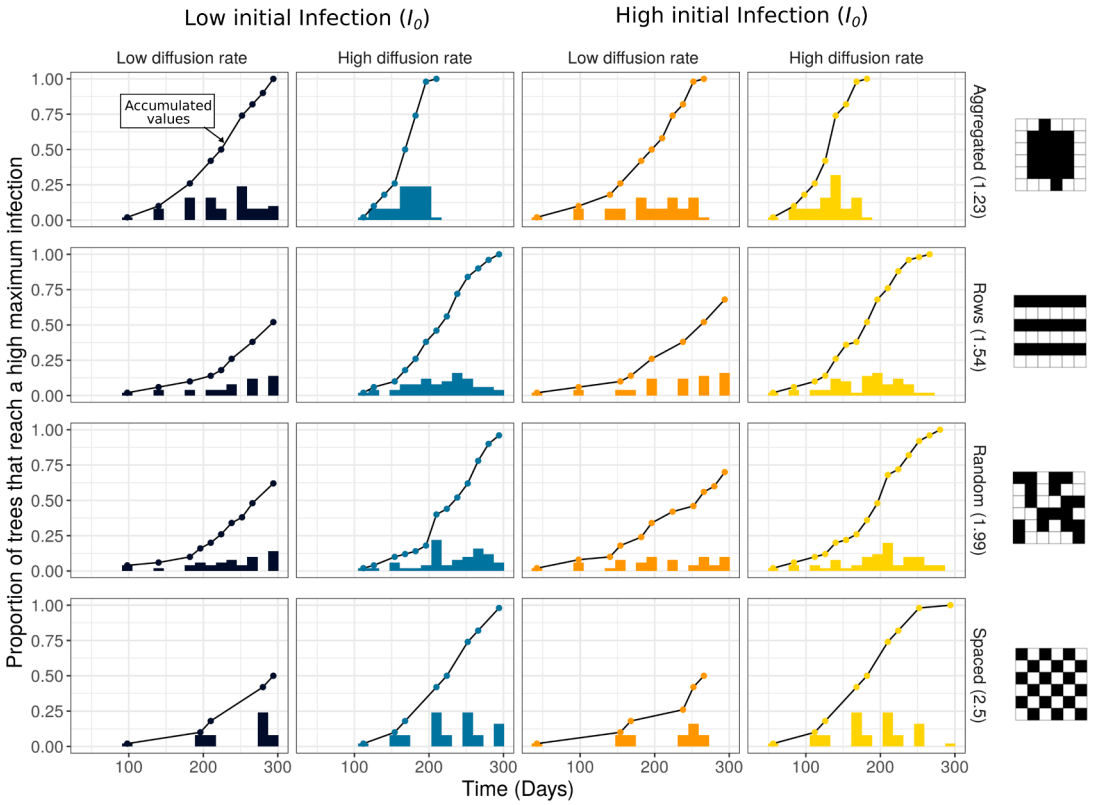

Fig. 6. Proportion of trees that reach a high maximum infection (>0.7 of infected leaves) during the same 15-day period. Histograms for the different planting arrangements (aggregated, random, rows and spaced) with two levels of diffusion (low: $\log(m) = -3$, high: $\log(m) = -2$) and two levels of I_0 (0.001, 0.1; dark/blue and orange/yellow colors, respectively). The black dotted line represents the corresponding accumulated proportion of trees in the plot that reach a high maximum infection. The values of α, β_1, β_2, ρ and μ are shown in Table 1. We used $\gamma = 0.015$.

estimated range ($\gamma = 0.056$).

3.5. The MATI and time to MATI are determined by the number of individual plants that reach a high level of infection before the end of the simulation, and their degree of temporal overlapping

The level of infection of individual trees and their degree of temporal overlapping determine the average infection dynamics. Both variables are affected by the diffusion rate and the planting arrangement. We represent in Fig. 6 the proportion of trees that reached a high level of infection (>70% of infected leaves) during the same 15-day period, and the accumulated proportion of corresponding highly infected trees (dotted line), which indicates how much the epidemic has expanded in space up to a given time (see supplementary material S4 for a full plot visualisation and refer to Fig. S1.5 for the values of each tree's maximum infection and timing).

Planting arrangement substantially influences the overlap between individual tree dynamics. This explains the different shapes of the average infection curves (Fig. 5) as well as the changes in MATI and time to MATI. When plants are spaced, in rows, or randomly distributed, the distribution of the number of highly infected trees over time is broader than in the aggregated pattern, especially when diffusion is high (Fig. 6; yellow and light blue bars). This means that in the first three scenarios the temporal overlap of highly infected trees decreases, which causes a lower MATI compared to the aggregated pattern (Figs. 4 and 6).

The diffusion rate, combined with the planting pattern, affects both the overlap and the individual times at which the maximum individual infection is reached. When diffusion is low (dark blue vs light blue, and orange vs yellow bars in Fig. 6) the distribution is spread out and slightly shifted to the right (see also the accumulated curve). At low diffusion, for the spaced, rows and random patterns, only 50 to 75% of the trees reach the 70% of infected leaves threshold before the end of the simulation. The other trees with low levels of infection will contribute little to the average tree infection value, lowering the MATI (Figs. 4, 5 and S1.5). In the aggregated pattern or when diffusion is high, all the trees reach 70% of infected leaves (the accumulated curves sum up to 1). Interestingly, high values of $\langle H \rangle$ (which characterises rows, random and spaced arrangements) combined with a low diffusion rate (dark and orange bars) generate isolated outbreaks of highly infected trees (Fig. 6). In particular, in the spaced pattern, individual trees reach high infections at well separated times, explaining the multi-stepped dynamics of the spatially averaged prevalence in Fig. 5. Fig. 6 also shows that a lower amount of initially infected leaves (I_0) delays the initial infection without significantly changing the dynamics.

4. Discussion

One of the central issues in coffee rust epidemiology is to understand the factors that explain the great variability in the magnitude of the infection peaks and their timing, both at the plant and plot levels (Avelino et al., 1991; Li et al., 2022; Rosas et al., 2021). To address this issue, many studies have focused on the microclimate (Avelino et al., 2006), plant resistance (Talhinhas et al., 2017), or the susceptibility of leaves during specific stages of the coffee crop cycle (Salgado et al., 2008). Nevertheless, none of these approaches has succeeded to fully explain the differences in timing and intensity of the epidemics occurring in plots from the same site with equivalent meteorological and plant genetic conditions. Here we hypothesised that spatial patterns created by rust dispersal in different planting arrangements might be affecting both variables.

We first documented known trends for the timing and magnitude of the epidemic peak, as well as their variability, by comparing epidemiological curves from different sites (Fig. 2). From this analysis we distinguish two phases in the epidemic timeline: a time lag and a growth phase *per se* (Fig. 2 and Table S1.1). We also noted that the harvesting period correlated with the build-up or growth phase (Fig. 2A,C,G,I). This is consistent with harvesting and rust infection being related to fruit development and fruit load (Avelino et al., 1993; Motisi et al., 2022; Salgado et al., 2008). Nevertheless, the movements of workers during harvesting might also promote rust dispersal and reinforce the infection (Motisi et al., 2022). Our parameterised SIX model recreates the coffee rust epidemic and helps us to explore some of the mechanisms that may determine properties of the maximum peak and its timing (Figs. 3–6). The values of the maximum average tree infection (MATI) and time to MATI were within the range reported in field studies. This qualitatively validates the estimates of the model parameters, and supports that different planting arrangements and different diffusion rates might provide possible explanations to the variation observed in real dynamics.

In particular, we showed that both the planting arrangement and the diffusion rate jointly modify the MATI and time to MATI by preventing some plants from reaching their maximum peak (Figs. 4–6), thus explaining part of the variability observed in plots with otherwise similar conditions. In particular the aggregated spatial arrangement highly increases the MATI compared to the other planting arrangements that did not present quantitative differences between them (see video in supplementary material S4). The effects of the planting arrangement are noticeable in the different curves of Fig. 5, which can be multi-stepped, or smooth (like some of the curves from real data presented in Fig. 2). The multi-stepped pattern is associated with a higher distance between plants, in particular in the spaced pattern, where plants have no direct neighbours. In this sense, the differences of the effect of planting patterns on the MATI and curves of infection were more related with a planting aggregation threshold (or a minimal distance between plants) than with the spatial arrangements *per se*. Moreover, a low I_0 increases the time it takes to reach the maximum peak of infection at the plant level and plot level, due to delays in the start of the growth phase (Figs. 4 and 5). The time lag differences reported in sites with similar phenological timing (Li et al., 2022) can thus be explained by differences in the initial infection and planting arrangements, and not only by the positive correlation between fruit charge and plant susceptibility to infection (Avelino et al., 1993; Salgado et al., 2008). Finally, we found that high infected leaf-fall rate (γ) strongly affects the whole-plot infection dynamics and we hypothesise that this quantity is a key aspect for coffee-rust monitoring or intervention at the plot scale (Park et al., 2001).

These results have a practical significance regarding coffee rust management. They highlight the importance of reducing rust dispersal rates, either by having other trees in the plot or by planting coffee plants at larger distances (independently of the spatial arrangement *per se*) in order to uncouple individual dynamics and reduce plot infection. In particular, one should avoid the aggregated arrangement, this is, $\langle H \rangle$ values larger than 1.5 (Fig. S1.4; Video S4). This result complements those of Hajian-Forooshani and Vandermeer (2021), who tested different critical dispersal distances between coffee plants and reported that the regularity of the planting arrangement pattern modulates the time to reach fully rust-infected coffee plots. This is relevant for farmers, who balance their planting density according to their production necessities and the risk of plot epidemic (Ehrenbergerová et al., 2018). In general, conventional coffee management produces very densely aggregated planting patterns that might be prone to coffee-leaf rust invasion, contrarily to more rustic or ecological coffee plantations that intercalate different kinds of trees between the coffee plants (Moguel and Toledo, 1999). Besides, Boudrot et al. (2016) and Gagliardi et al. (2020) reported that the functional traits of plants related to shade (foliage density, shade percentage) modify the relative importance of wind and rainfall in uredospore dispersal across the plot. Understanding the role of the initial infection and dispersal rate on the time lag is also relevant for rust-control procedures that rely heavily on the timing of the epidemic, such as pruning, management of shade (Boudrot et al., 2016; Liebig et al., 2019; Soto-Pinto et al., 2000), or fungicide application (Burdekin, 1964; Mulinge and Griffiths, 1974). Additionally, the leaf-fall

rate of infected leaves can also be modified with management practices but may have an ambiguous effect on the maximum infection: on the one hand, farmers could decrease the maximum infection by removing and bagging away the infected leaves continuously (thus decreasing the source of new reinfections from infected leaves either on the ground or in the plant system); but on the other hand, due to the farmers' movement between the trees, removing the leaves could trigger the dispersal of uredospores by contact and further propagate the epidemic.

The present model also allows us to make recommendations on the ways coffee rust prevalence can be measured and monitored. Here we worked with the average tree infection because it is one of the more common ways of measuring coffee rust prevalence in coffee plots (Fig. 2). Nevertheless, this variable is highly dependent on the progression of the infection in the chosen plants and their degree of temporal overlap due to spatial factors (Fig. 6). Additionally, the average over trees can be an inappropriate measure for the plot infection when individual infections follow a non-normal distribution that changes during the epidemic. Even if we supposed the infection to follow a normal distribution, the mean without the variance would not be sufficient. Other ways of measuring plot infection in the field could consist in drawing spatially explicit plot infection maps (Li et al., 2022; Rosas et al., 2021; Vandermeer et al., 2018).

In our model, we considered rust dispersal from one plant to its four closest neighbours through splash and leaf-to-leaf contact. This assumption was linked to the spatial arrangements that were only significantly different in the 4-neighbour vicinity. However, in future work it will be important to consider other mechanisms and models for spore dispersal that consider an 8-neighbour range or long-range dispersal. On the one hand, it is known that changing the neighbourhood of interaction can change the probability of plot invasion (Park et al., 2001). Also, having a different dispersal rate depending on whether the plants are in contact or not, can lead to critical transitions in infection dynamics (Hajian-Forooshani and Vandermeer, 2021; Vandermeer et al., 2018). On the other hand, if we were to consider other dispersal mechanisms such as wind gusts or human action during harvesting (Becker and Kranz, 1977), the planting arrangements might play a less important role in plot infection. This is because spores would reach farther trees and attenuate the relevance of the plot geometry. In those scenarios, the amount of shade-trees that can act as wind barriers would be crucial to reduce dispersal (Gagliardi et al., 2020) and uncouple the individual tree infection dynamics. Moreover, the model considers only one initially infected tree located in the centre of the plot. Other choices should not qualitatively change our results, but might have an effect on the general times of infection. The effect of multiple sources of infection should also be studied in future works. It is also important to keep in mind that our model assumes that infected fallen leaves are removed from the system (bagged away, for example) and cannot spread infection to neighbouring plants or reinfect. In many sites, these fallen leaves with spores likely contribute in a meaningful way to infecting plants (Zachary Hajian-Forooshani, personal obs). This could be added in the future by defining an additional R compartment in the SIX equation. Nevertheless, as coffee leaf rust is a biotroph, the survival of spores in the fallen leaves is expected to be limited.

Weather covariates like high rainfalls might also influence plant-level parameters such as the recruitment of spores from infected leaves (α) by washing off spores from the leaves. This is likely to strongly affect the general dynamics of infection (e.g. reducing the maximum infection; Figs. 2 and S1.7; Motisi et al., 2022) and should be considered in future works.

Finally, our model represents coffee rust infection but does not assess coffee production reduction. This relationship is not necessarily linear and must be considered for any practical recommendations (Cerda et al., 2017).

Control and management practices of coffee rust disease have commonly underestimated the role of dispersal and the relationship between plant and plot dynamics. Our work contributes to a better understanding of this relationship and can be used as a null-model to study the role of specific dispersal mechanisms, such as wind, splash or human mobility (see for example, Avelino et al., 2012; Becker and Kranz, 1977; Gagliardi et al., 2020; Hajian-Forooshani and Vandermeer, 2021). It mostly aimed at exploring the general and qualitative mechanisms behind the patterns observed in real systems (Fig. 2). Adding context-specific conditions would enable us to do some data-fitting and quantitative comparisons in a more detailed way than the general times of MATI and time to MATI presented here.

Recreating and understanding the main mechanisms of coffee rust dispersal is crucial to the development of a preventive approach to epidemics. It informs the management processes that seek to balance the different effects that some practices have on the infection and dispersal stages, in order to design resilient agroecological coffee systems to coffee rust or other epidemics.

CRediT authorship contribution statement

Emilio Mora Van Cauwelaert: Conceptualization, Data curation, Formal analysis, Investigation, Methodology, Software, Visualization, Writing – original draft. **Cecilia González González:** Methodology, Software, Visualization, Writing – review & editing. **Denis Boyer:** Conceptualization, Methodology, Formal analysis, Software, Writing – review & editing. **Zachary Hajian-Forooshani:** Methodology, Validation, Visualization. **John Vandermeer:** Formal analysis, Writing – review & editing. **Mariana Benítez:** Conceptualization, Methodology, Funding acquisition, Supervision, Visualization, Writing – review & editing.

Declaration of Competing Interest

The authors declare that they have no known competing financial interests or personal relationships that could have appeared to influence the work reported in this paper.

Data Availability

All code and data to reproduce results in the work can be accessed at https://github.com/tenayuco/dispersion_plant_arrangement_coffeerust_infection.

Acknowledgments

EMVC is a doctoral student from the Programa de Doctorado en Ciencias Biomédicas, Universidad Nacional Autónoma de México and has received CONACyT scholarship 686776. MB acknowledges financial support from UNAM-DGAPA-PAPIIT (IN207819). CGG acknowledged the graduate program Posgrado en Ciencias Biológicas, Universidad Nacional Autónoma de México and CONACyT scholarship 743257. EMVC thanks Fabian Aguirre for all the discussions and guidance in mathematical analysis and Elisa Lotero for her help and support. The authors thank Rodrigo García Herrera for technical support and two anonymous reviewers for very detailed comments that greatly improved the paper. We also thank members of *La Parcela* Laboratory for their valuable comments and suggestions. This article covers part of the requirements for EMVC to obtain his PhD Degree in the doctoral program.

Supplementary materials

Supplementary material associated with this article can be found, in the online version, at doi:10.1016/j.ecolmodel.2022.110206.

References

Ananth, K.C., 1969. Timing and frequency of spraying for control of coffee leaf rust in southern india. Exp. Agric. 5, 117–123. https://doi.org/10.1017/S0014479700004336.

Avelino, J., Cristancho, M., Georgiou, S., Imbach, P., Aguilar, L., Bornemann, G., Läderach, P., Anzueto, F., Hruska, A.J., Morales, C., 2015. The coffee rust crises in Colombia and Central America (2008–2013): impacts, plausible causes and proposed solutions. Food Secur. 7, 303–321. https://doi.org/10.1007/s12571-015-0446-9.

Avelino, J., Muller, R.A., Cilas, C., Velasco Pascual, H., 1991. Développement et comportement de la rouille orangée du caféier (*Hemileia vastatrix* Berk. et Br.) dans des plantations en cours de modernisation, plantées de variétés naines, dans le sud-est du Mexique. Café, Cacao, Thé 35, 21–37. https://agritrop.cirad.fr/416561/.

Avelino, J., Romero-Gurdián, A., Cruz-Cuellar, H.F., Declerck, F.A.J., 2012. Landscape context and scale differentially impact coffee leaf rust, coffee berry borer, and coffee root-knot nematodes. Ecol. Appl. 22, 584–596. https://doi.org/10.1890/11-0869.1.

Avelino, J., Toledo, J.C., Medina, B., 1993. Développement de la rouille orangée (*Hemileia vastatrix*) dans une plantation du sud-ouest du Guatemala et évaluation des dégâts qu'elle provoque. In: Proceedings of the ASIC 15th International Conferen Coffee Science, pp. 293–302. https://agritrop.cirad.fr/466977/.

Avelino, J., Zelaya, H., Merlo, A., Pineda, A., Ordoñez, M., Savary, S., 2006. The intensity of a coffee rust epidemic is dependent on production situations. Ecol. Model. 197, 431–447. https://doi.org/10.1016/j.ecolmodel.2006.03.013.

Becker, S., Kranz, J., 1977. Vergleichende Untersuchungen zur Verbreitung von *Hemileia vastatrix* in Kenia/comparative studies on dispersal of Hemileia vastratrix in Kenya. Z. Planzenschultz J. Plant Dis. Prot. 84, 526–539. https://www.jstor.org/stable/43213550.

Bock, K.R., 1962a. Seasonal periodicity of coffee leaf rust and factors affecting the severity of outbreaks in Kenya Colony. Trans. Br. Mycol. Soc. 45, 289–300. https://doi.org/10.1016/s0007-1536(62)80068-0.

Bock, K.R., 1962b. Dispersal of uredospores of *Hemileia vastatrix* under field conditions. Trans. Br. Mycol. Soc. 45, 63–74. https://doi.org/10.1016/s0007-1536(62)80035-7.

Boudrot, A., Pico, J., Merle, I., Granados, E., Vílchez, S., Tixier, P., De Melo Virginio Filho, E., Casanoves, F., Tapia, A., Allinne, C., Rice, R.A., Avelino, J., 2016. Shade effects on the dispersal of airborne *Hemileia vastatrix* uredospores. Phytopathology 106, 527–580. https://doi.org/10.1094/PHYTO-02-15-0058-R.

Bowden, J., Gregory, P.H., Johnson, C.G., 1971. Possible wind transport of coffee leaf rust across the Atlantic Ocean. Nature 229 (5285), 500–501. https://doi.org/10.1038/229500b0.

Burdekin, D.A., 1964. The effect of various fungicides on leaf rust, leaf retention and yield of coffee. East Afr. Agric. For. J. 30, 101–104. https://doi.org/10.1080/00128325.1964.11661972.

Carvalho, C.R., Fernandes, R.C., Carvalho, G.M.A., Barreto, R.W., Evans, H.C., 2011. Cryptosexuality and the genetic diversity paradox in coffee rust, *Hemileia vastatrix*. PLoS One 6, 1–7. https://doi.org/10.1371/journal.pone.0026387.

Cerda, R., Avelino, J., Gary, C., Tixier, P., Lechevallier, E., Allinne, C., 2017. Primary and secondary yield losses caused by pests and diseases: assessment and modeling in coffee. PLoS One 12, 1–17. https://doi.org/10.1371/journal.pone.0169133.

Cunniffe, N.J., Gilligan, C.A., 2010. Invasion, persistence and control in epidemic models for plant pathogens: the effect of host demography. J. R. Soc. Interface 7, 439–451. https://doi.org/10.1098/rsif.2009.0226.

Deepak, K., Hanumantha, B.T., Sreenath, H.L., 2012. Viability of coffee leaf rust (*Hemileia vastatrix*) urediniospores stored at different temperatures. J. Biotechnol. Biomater. 02, 2–4. https://doi.org/10.4172/2155-952x.1000143.

Drevon, D., Fursa, S.R., Malcolm, A.L., 2017. Intercoder reliability and validity of web plot digitizer in extracting graphed data. Behav. Modif. 41, 323–339. https://doi.org/10.1177/0145445516673998.

Ehrenbergerová, L., Kučera, A., Cienciala, E., Trochta, J., Volařík, D., 2018. Identifying key factors affecting coffee leaf rust incidence in agroforestry plantations in Peru. Agrofor. Syst. 92, 1551–1565. https://doi.org/10.1007/s10457-017-0101-x.

Elder, K.R., Viñals, J., Grant, M., 1992. Dynamic scaling and quasiordered states in the two-dimensional Swift-Hohenberg equation. Phys. Rev. A 46, 7618. https://doi.org/10.1103/PhysRevA.46.7618.

Firman, I.D., Wallis, J.A.N., 1965. Low-volume spraying to control coffee leaf rust in Kenya. Ann. Appl. Biol. 55, 123–137. https://doi.org/10.1111/j.1744-7348.1965.tb07875.x.

Gagliardi, S., Avelino, J., Beilhe, L.B., Isaac, M.E., 2020. Contribution of shade trees to wind dynamics and pathogen dispersal on the edge of coffee agroforestry systems: a functional traits approach. Crop Prot. 130, 105071 https://doi.org/10.1016/j.cropro.2019.105071.

Gubbins, S., Gilligan, C.A., Kleczkowski, A., 2000. Population dynamics of plant-parasite interactions: thresholds for invasion. Theor. Popul. Biol. 57, 219–233. https://doi.org/10.1006/tpbi.1999.1441.

Hajian-Forooshani, Z., Vandermeer, J., 2021. Emergent spatial structure and pathogen epidemics: the influence of management and stochasticity in agroecosystems. Ecol. Complex. 45, 100872 https://doi.org/10.1016/j.ecocom.2020.100872.

Koch, A.J., Meinhardt, H., 1994. Biological pattern formation: from basic mechanisms to complex structures. Rev. Mod. Phys. 66 (4), 1481. https://doi.org/10.1103/RevModPhys.66.1481.

Kushalappa, A.C., Eskes, A.B., 1989. Advances in coffee rust research. Annu. Rev. Phytopathol. 27, 503–531. https://doi.org/10.1146/annurev.py.27.090189.002443.

Leguizamón-Caycedo, J.E., Orozco-Gallego, L., Gómez-Gómez, L., 1998. Períodos de incubación (pi) y de latencia (pl) de la roya del cafeto en la zona cafetera central de colombia. Cenicafé 49, 325–339. https://www.cenicafe.org/es/publications/arc049(04)325-339.pdf.

Li, K., Hajian-Forooshani, Z., Su, C., Perfecto, I., Vandermeer, J., 2022. Reduced rainfall and resistant varieties mediate a critical transition in the coffee rust disease. Sci. Rep. 12, 1–9. https://doi.org/10.1038/s41598-022-05362-0.

Liebig, T., Ribeyre, F., Läderach, P., Poehling, H.M., van Asten, P., Avelino, J., 2019. Interactive effects of altitude, microclimate and shading system on coffee leaf rust. J. Plant Interact. 14, 407–415. https://doi.org/10.1080/17429145.2019.1643934.

McCook, S., Vandermeer, J., 2015. The big rust and the red queen: long-term perspectives on coffee rust research. Phytopathology 105, 1164–1173. https://doi.org/10.1094/PHYTO-04-15-0085-RVW.

Moguel, P., Toledo, V.M., 1999. Biodiversity conservation in traditional coffee systems of Mexico. Conserv. Biol. 13, 11–21. https://doi.org/10.1046/j.1523-1739.1999.97153.x.

Motisi, N., Bommel, P., Leclerc, G., Robin, M.H., Aubertot, J.N., Arias Butron, A., Merle, I., Treminio, E., Avelino, J., 2022. Improved forecasting of coffee leaf rust by qualitative modeling: design and expert validation of the ExpeRoya model. Agr.Syst 197, 26. https://doi.org/10.1016/j.agsy.2021.103352.

Mulinge, S.K., Griffiths, E., 1974. Effects of fungicides on leaf rust, berry disease, foliation and yield of coffee. Trans. Br. Mycol. Soc. 62, 495–507. https://doi.org/10.1016/s0007-1536(74)80061-6.

Ndolo, I.J., John Muthama, N., Oludhe, C., Kinyuru Nganga, J.S., Odingo, R., 2017. Diagnosis of urbanization and seasonal rainfall over the City of Nairobi. J. Meteorol. Relat. Sci. 10, 25–34. https://doi.org/10.20987/jmrs.3.01.2017.

Nutman, F.J., Roberts, F.M., Clarke, R.T., 1963. Studies on the biology of *Hemileia vastatrix* Berk. & Br. Trans. Br. Mycol. Soc. 46, 27–44. https://doi.org/10.1016/s0007-1536(63)80005-4.

Park, A.W., Gubbins, S., Gilligan, C.A., 2001. Invasion and persistence of plant parasites in a spatially structured host population. Oikos 94, 162–174. https://doi.org/10.1034/j.1600-0706.2001.10489.x.

Rakocevic, M., Takeshi Matsunaga, F., 2018. Variations in leaf growth parameters within the tree structure of adult Coffea arabica in relation to seasonal growth, water availability and air carbon dioxide concentration. Ann. Bot. 122, 117–131. https://doi.org/10.1093/aob/mcy042.

Rayner, R.W., 1961. Spore liberation and dispersal of coffee rust *Hemileia vastatrix* B. et Br. Nature 191, 725. https://doi.org/10.1038/191725a0.

Rohatgi, A., 2020. WebPlotDigitizer (Version 4.4) [Computer software]. https://automeris.io/WebPlotDigitizer.

Rosas, J., de Assis Silva, S., de Almeida, S., Medauar, C., Moraes, W., de Souza Lima, J., 2021. Spatial and temporal behavior of coffee rust in C . canephora and its effects on crop yield. Eur. J. Plant Pathol. https://doi.org/10.1007/s10658-021-02352-2.

Salgado, P.R., Favarin, J.L., Leandro, R.A., De Lima Filho, O.F., 2008. Total phenol concentrations in coffee tree leaves during fruit development. Sci. Agric. 65, 354–359. https://doi.org/10.1590/S0103-90162008000400005.

Silva-Acuña, R., Maffia, L.A., Zambolim, L., Berger, R.D., 1999. Incidence-severity relationships in the pathosystem Coffea arabica-*Hemileia vastatrix*. Plant Dis. 83, 186–188. https://doi.org/10.1094/PDIS.1999.83.2.186.

Silva, M.D.C., Várzea, V., Guerra-Guimarães, L., Azinheira, H.G., Fernandez, D., Petitot, A.S., Bertrand, B., Lashermes, P., Nicole, M., 2006. Coffee resistance to the main diseases: leaf rust and coffee berry disease. Braz. J. Plant Physiol. 18, 119–147. https://doi.org/10.1016/j.ijepes.2005.11.005.

Soto-Pinto, L., Perfecto, I., Castillo-Hernandez, J., Caballero-Nieto, J., 2000. Shade effect on coffee production at the northern Tzeltal Zone of the state of Chiapas, Mexico. Agric. Ecosyst. Environ. 80, 61–69. https://doi.org/10.1016/S0167-8809(00)00134-1.

Stevens, R.B., Horsfall, J.G., Dimond, A.E., 1960 (Eds). Plant Pathology, An Advanced Treatise, 3. Academic Press, NY, pp. 357–429.

Swinton, J., Anderson, R.M., 1995. Model frameworks for plant-pathogen interaction. In: Grenfell, B.T., Dobson, A.P. (Eds.), Ecology of Infectious Diseases in Natural Populations. Publications of the Newton Institute, Cambridge, pp. 280–294. https://doi.org/10.1017/CBO9780511629396.011.

Talhinhas, P., Batista, D., Diniz, I., Vieira, A., Silva, D.N., Loureiro, A., Tavares, S., Pereira, A.P., Azinheira, H.G., Guerra-Guimarães, L., Várzea, V., Silva, M.C., 2017. The coffee leaf rust pathogen *Hemileia vastatrix*: one and a half centuries around the tropics. Mol. Plant Pathol. 18, 1039–1051. https://doi.org/10.1111/mpp.12512.

Vandermeer, J., Hajian-Forooshani, Z., Perfecto, I., 2018. The dynamics of the coffee rust disease: an epidemiological approach using network theory. Eur. J. Plant Pathol. 150, 1001–1010. https://doi.org/10.1007/s10658-017-1339-x.

CAPÍTULO II. Trayectorias de cosecha en plantaciones de gran escala: determinantes ecológicas y de manejo

Síntesis del capítulo

En el capítulo anterior exploramos la relación entre la dispersión por *splash* de la roya y el arreglo espacial de las plantas de café. En particular, resaltamos el efecto de las densidades altas de siembra sobre el impacto de la epidemia cuando se considera únicamente la dispersión por *splash*. Varias observaciones han sugerido que el movimiento de las personas puede también tener relevancia para la dispersión en la parcela (Waller, 1981). Especialmente durante la cosecha, en donde decenas de personas recorren de 4 a 5 veces cada una de las plantas con café (Masarirambi et al., 2009)y en donde hay una tasa alta de transferencia de esporas a través de la ropa (Becker y Kranz, 1977), el impacto sobre el desarrollo de la epidemia puede ser muy alto. Aunado a lo anterior, la forma de cosecha también es afectada por el manejo agrícola y depende del tipo de tenencia y organización para el trabajo de la tierra, así como del tamaño de la plantación. Es decir, depende del síndrome de producción (Vandermeer y Perfecto, 2012).

Por ejemplo, en algunas zonas cafetaleras, como en el Soconusco en Chiapas, las plantaciones son del orden de cientos de hectáreas y son propiedad privada adquirida durante el Porfiriato (López Echeverría, 2006). Estas fincas tienen manejos agrícolas muy variados, desde cafetales de sol hasta cafetales orgánicos de sombra, y la cosecha es realizada por trabajadores eventuales "temporaleros" o trabajadores fijos pagados a destajo, conocidos como tapiscadores. Los tapiscadores trabajan de tres a cuatro meses a lo largo de la maduración del grano y reciben un pago diario por kilo o por volumen de cosecha (Jiménez-Soto, 2021). Trabajan de 8 a 10 horas al día para maximizar la cosecha en diferentes regiones de la plantación conocidas como *pantes* (del nahuatl *pantli*). Este manejo impacta sobre la salud de los tapiscadores y de sus familias (Jiménez-Soto, 2021). Aquí argumentamos que, además, esta forma de cosecha puede tener un impacto ecológico, en particular a través de la dispersión de roya.

El movimiento de los trabajadores durante la cosecha no ha sido descrito de manera sistemática ni su relación con el síndrome de producción que caracteriza a estas fincas cafetaleras de gran escala; aún menos el impacto que pueda tener para la dispersión de la roya u otros patógenos de las plantas. En este capítulo realizamos una primera descripción y análisis del movimiento de los tapiscadores a partir un seguimiento en campo que realizamos en dos fincas cafetaleras del Soconusco, entre octubre y noviembre del 2021. La primera finca, que de ahora en adelante se denominará "orgánica", se caracteriza por ser un cafetal de sombra con casi 100 especies de árboles y con una alta biodiversidad asociada. La segunda, la finca "convencional", es un sistema de café de sol con algunos árboles dispersos y con un uso frecuente de fungicidas y fertilizantes. Primero registramos y analizamos por medio de modelos de espacio-estado (Patterson et al., 2008) las trayectorias de 6 trabajadores en un día de cosecha en cada una de las dos fincas. Los modelos espacio-estado son usados en el contexto de la ecología del movimiento para caracterizar las trayectorias de animales individuales quienes tienen diferentes comportamientos o estados (e.g. forrajeo, exploración) durante su movimiento (Michelot y Blackwell, 2019; J. M. Morales et al., 2004). Estos estados se reflejan en características del propio movimiento como la longitud de los pasos (*i..e.* distancia tomada entre dos puntos marcados) o el ángulo relativo entre paso y paso (Michelot y Blackwell, 2019). Medimos a su vez la cantidad de árboles cosechados y el área visitada por cosechador. Realizamos también entrevistas semi-estructuradas y exploramos los factores que afectan de forma cualitativa el movimiento de los tapiscadores a lo largo de día y su relación con el síndrome de producción de estas fincas.

El análisis de espacio-estado diferenció dos tipos de estados en cada una de las fincas: cuando los árboles tienen frutos, los tapiscadores se quedan en una vecindad cercana del *pante* y generan distribuciones con pasos usualmente cortos (*estado colecta*); cuando se acaban los frutos, deben moverse a otra región del *pante* o incluso de la plantación, generando distribuciones con pasos de hasta 100 m hasta el siguiente árbol (*estado búsqueda*). En la finca orgánica, el estado *búsqueda* generó una distribución de longitud de pasos con una cola más larga que en la finca convencional. Esto se traduce en relocalizaciones de los trabajadores a diferentes partes de la finca, resultando en una área visitada significativamente mayor durante la cosecha. De acuerdo con las entrevistas esto puede ser explicado por la asincronicidad en la maduración del café, el tamaño del pante o el número de trabajadores por zona de cosecha. A su vez, las trayectorias en

la finca orgánica eran menos regulares que en la finca convencional, probablemente por el arreglo espacial de las plantas, afectado por la forma de manejo de la sombra en el cafetal y la edad de la plantación. Las trayectorias con más árboles visitados por día, y con una mayor cantidad de pasos largos pueden incrementar de manera potencial la dispersión de roya a diferentes zonas de la plantación. En este sentido, la interacción entre el paisaje y el movimiento de los vectores de patógenos puede mediar el surgimiento de plagas (como sugieren (White et al., 2018)) Existen diferentes medidas que se pueden tomar para reducir este impacto, como evitar trabajar a finales de la temporada en donde hay una mayor asincronicidad en la maduración de las plantas y una menor carga frutal –y, por lo tanto, un mayor desplazamiento diario de los tapiscadores.

Harvesting trajectories in large-scale coffee plantations: ecological and management drivers and implications

Emilio Mora Van Cauwelaert[a, b, *], Denis Boyer[c], Estelí Jiménez-Soto[d], Cecilia González González[a] and Mariana Benítez[a, *]

a. Laboratorio Nacional de Ciencias de la Sostenibilidad, Instituto de Ecología, Universidad Nacional Autónoma de México, Mexico City, C.P. 04510, México

b. Posgrado en Ciencias Biomédicas, Universidad Nacional Autónoma de México, Mexico City, C.P. 04510, México

c. Instituto de Física, Universidad Nacional Autónoma de México, Mexico City, C.P. 04510, México

d. School of Geosciences, College of Arts and Sciences, University of South Florida USF, USA

*mbenitez@iecologia.unam.mx, *emiliomora92@ciencias.unam.mx

0. Abstract

Coffee is produced under different management practices, land tenure systems and scales, categorized as Syndromes of Production. In particular, the so-called "Capitalist Syndrome" is based upon large-scale and high-density planting farms with a high input of human labor and exploitation. This syndrome results in practices, like high planting density, that may promote the development and dispersal of important pests like coffee leaf rust (CLR). It can also reflect on the spatial movement of the harvesters who could bear and disperse CLR across the plantations. However, the spatial movement of the harvesters has not yet been described, nor its relationship with the scale, management, or ownership of the plantation, and even less its ecological implications for CLR or other potential pest dispersal. Here we present a description and qualitative analysis of the spatial movement of farmworkers during harvesting in two large-scale landlord-owned capitalist plantations: an organic and a conventional plantation. We recorded and analyzed with state-space models the spatial movements of the workers during harvesting in both plantations. We then constructed a driver tree for harvest dynamics, which incorporated qualitative variables related to climate, as well as coffee plant and management aspects reported by the harvesters. Our model differentiated two kinds of movements: when trees have berries, harvesters remain in the same rows or nearby (Collect state; 94 to 98% of the steps); when not, harvesters make longer steps within the harvesting zone or move to another area of the plantation (Search state; 2 to 6% of the steps). The organic plantation had a longer tail step-length distribution than the conventional plantation for the search state, resulting in a significantly higher visited area per worker ($p<0.005$). This might be related to a) a lower fruit charge or ripening synchronization when we took the data or b) smaller harvesting locations or the number of harvesters per location. Harvesting movements that explore a wider area, either by visiting more trees or by changing locations on the same day, could create more foci of CLR infection across the plantation. To reduce the possible impact of human dispersal of pathogens, we suggest shorter trajectories by working fewer hours a day, avoiding harvesting at the end of the coffee maturation season when few trees have berries and harvesters have to travel longer distances, or even skipping infected plants. This calls for an organic coffee management that could prevent diseases, increase diversity, and guarantee just and safe conditions for workers.

KEYWORDS

Syndromes of production; state-space models; harvesting movement; coffee leaf rust dispersal

1. Introduction

In recent decades, the increased industrialization of agroecosystems has gathered significant attention due to its profound negative social and ecological consequences (Raven and Wagner, 2021). This trend is characterized by prioritizing short-term gains in productivity through practices such as intensified use of synthetic fertilizers and pesticides, high-density monoculture planting, a reduced presence of native trees, and the precarity of human labor (Ong and Liao, 2020; Raven and Wagner, 2021). Agricultural industrialization and environmental change have led to increases in pest populations (Andow, 1983), biodiversity decline (Raven and Wagner, 2021), and are also associated with a higher likelihood of zoonotic disease outbreaks (Jones et al., 2013; Perfecto et al., 2023). Adding to these challenges are the heightened demands on human labor and precarious social conditions experienced in large-scale industrial agricultural systems (Mapes, 2010), a social phenomenon that imparts more complexity to agroecosystem management and processes.

Coffee agroecosystems exhibit a large variety of management practices that reinforce each other and that can be defined as "syndromes of production", a conceptual framework useful to evaluate social and ecological dynamics across distinct agricultural paradigms (Andow and Hidaka, 1989; Moguel y Toledo, 1999; Ong and Liao, 2020; Vandermeer and Perfecto, 2012). Coffee production syndromes can be mainly distinguished by shade management (shade or sun coffee plantations; Vandermeer and Perfecto, 2012) or by the type of land tenure and scale of production (large-scale capitalist or small-scale peasant-owned coffee plantations; Ong and Liao, 2020). In this sense, coffee agroecosystems are model systems to understand how different syndromes of production affect ecological processes such as the planned and associated biodiversities (Mas and Dietsch, 2004) but also social aspects like the worker's conditions (Jiménez-Soto, 2021).

In the large-scale capitalist syndrome, decisions and practices follow a maximization of profit rule (Ong and Liao, 2020); it is typically based upon large-scale and high-density planting farms with a high input of human labor and exploitation, although it may have specific ecological practices according to organic or conventional coffee markets (Perfecto et al., 2019). This syndrome of coffee production results in practices that may promote the development and spread of important pests

(Avelino et al., 2006; Hajian-Forooshani et al., 2016). For instance, the coffee leaf rust (CLR) can travel across the coffee plantations through direct leaf contact, water splash, or local turbulent wind conditions (Becker and Kranz, 1977; Vandermeer et al., 2018), but its effectiveness of dispersal and impact can be modulated by management practices like the planting density (Mora Van Cauwelaert et al., 2023), the presence of wind-barrier trees in the plantation (Gagliardi et al., 2020), or the biotic communities of natural enemies (Jackson et al., 2012), all determined to some degree by the syndrome of production (Vandermeer and Perfecto, 2012; McCook and Vandermeer). In this regard, increased agricultural simplification and industrialization of coffee agroecosystems have led to massive outbreaks of CLR around the globe (Avelino et al., 2015; McCook and Vandermeer, 2015). Some studies have proposed that harvesters can also bear CLR spores during harvesting (Becker and Kranz, 1977; Waller, 1981). The range of movement and duration of the daily harvest are also determined by the type, ownership, size and by the agricultural characteristics of the coffee plantations. This relates to the general framework of movement ecology where one can wonder why an individual moves, how and where, as well as the role of external factors (Nathan et al., 2008). In most landlord-owned large-scale coffee plantations, harvesters are paid by piecework and work several hours to maximize the daily harvest (Jiménez-Soto, 2021; López Echeverría, 2006). These practices affect the social and health conditions of the workers, which are often precarious. We argue that the movement of the harvesters under labor-intensive plantation conditions could also have an ecological impact, like modulating the human dispersal of some pathogens like coffee leaf rust (CLR). In fact, other studies have stressed the relation between the landscape structure, individual movement behavior, and pathogen transmission for predicting and understanding disease dynamics (Manlove et al., 2022; White et al., 2018).

However, the spatial movement of the harvesters in plantations within this syndrome of production has not been described yet, nor its relationship with the scale, management, or ownership of the plantation, and even less its ecological implications for CLR or other potential pest dispersal. Here we present a description and qualitative analysis of the spatial movement of farmworkers during harvesting in two large-scale landlord-owned plantations (~300 ha) with two different types of management: an organic shaded production coffee plantation and a sun-grown production with few

scattered trees. Specifically, we asked 1) how to statistically characterize the spatial trajectories of workers during harvesting, 2) how different features of the plantations, determined within a specific syndrome of production, affect these trajectories, and 3) what are the socio-ecological consequences of the harvesting movement in these large scale plantations.

We first recorded and analyzed with state-space models the spatial movements of the workers during harvesting, as well as their differences between both plantations. We then constructed a driver tree for harvest dynamics, which incorporated qualitative variables related to climate, as well as coffee biology and management aspects reported by the harvesters during interviews and noted through our own observations. We also highlighted the relationship between these variables and the syndrome of production. Finally, we put in conversation the patterns and dynamics of the spatial movement of harvesters with the social conditions associated with the large-scale capitalist syndrome and the possible implications in pathogen dynamics such as CLR spread.

2. Methods

2.1. Site of study

We selected two coffee large-scale plantations located in the Soconusco region of Chiapas, Mexico. This region has a tropical wet and dry climate (Koppen classification, Aw), with a rainy season from May to October, an annual mean temperature of 27 °C, and a precipitation of 2800 mm (Villarreal-Treviño et al., 2015). The first one (organic plantation, henceforth) is an organic shaded coffee plant plantation with a high plant diversity of up to 200 species. The second one (the conventional plantation) has a lower shade cover dominated by few *Inga sp*, uses pesticides, and has a high rate of coffee tree renovation to increase the productivity of regions affected by coffee leaf rust (CLR). Both plantations are approximately 300 ha, are landlord-owned and produce different coffee varieties for exportation. Harvesting is carried out by permanent or temporary workers from Central America, primarily Guatemala and El Salvador, from October to February, depending on the previous rainy season. Workers are paid by piecework, either by weight or volume, and live in precarious conditions (Jiménez-Soto, 2021). During harvest, the foreman assigns the harvesters and their families specific areas called "*pante*" (a Nahuatl word referring to agricultural locations of variable size) to

work during one or multiple days. Harvesters remain in these locations during the day or travel to another region when all the trees in the *pante* are already harvested.

2.2. Data Collection

We carried out field research for three weeks between October and November of 2021. We accompanied 12 families of harvesters during their harvesting day, six on each plantation, after their explicit consent to our research. The trajectories were labeled from C1 to C6 and from O1 to O6 for the conventional and organic plantations, respectively. We worked with them for six hours (including resting and eating pauses), completing three tasks: i) We recorded the movement of one harvester from each family by marking the location of every newly harvested tree, ii) we carried out semi-structured walking interviews (Evans and Jones, 2011) with each family and participant observation during harvesting to assess the factors that determined the different trajectories and to gather information about the whole syndrome of production, and iii) we participated in harvest, as one team member acquired the necessary harvesting skills along with experienced harvesters and donated their daily harvest to contribute to the family process.

2.2.1. Trajectories data

We added a waypoint for each consecutive visited tree using the satellite remote sensing Global Positioning System (GPS) Garmin 65. This system is ideal to analyze fine-scale movement patterns as its relative distance error between two consecutive recorded points is small (<0.5 m) (Breed and Severns, 2015). The recorded tracks were homogenized and curated by removing the pauses and normalizing the UTM coordinates. We defined the step length as the distance between two harvested trees; this distance provides a good proxy of the general movement of harvesters and is also relevant to understand how patterns of movement could explain the dispersal of CLR or other potential pests from one tree to another. Every pair of trees closer than one meter was considered as the same point (Vandermeer et al., 2018).

2.2.1 Walking interviews

We designed a questionnaire to gather information on the organization of harvest and applied it as a walking interview with the harvesters (Evans and Jones, 2011). We included questions about the period of the harvesting season, the number of times each plot was harvested, and the differences in the harvesting dynamics along the season between both plantations (organic and conventional). In particular, we asked who decided the size of the groups, the starting point, and the daily length of harvest. We also asked the harvesters directly about the factors that affected the motion of harvesting within each plant and between the plants. We added questions about the CLR control in both plantations and, last but not least, about the origins and social conditions of the harvesters. Before this process, we explained the purpose of the study and gave an informative letter to each of the participants to obtain their informed consent to participate in the study. The data was complemented with personal observations on the characteristics and times of harvesting per plant, the size of the families, and the differences in topography and ecological management between both plantations

2.3. Movement analysis and qualitative drivers of motion

We analyzed the harvester movement data using state-space models (Patterson et al., 2008) and organized the factors that influence the motion in a qualitative driver tree. All data analyses and figures were done in *Rstudio* 2023.03.1+446 using *plyr, dplyr, tidyverse, ggplot2, patchwork* libraries, and *Inkscape 1.0 and yEd 3.23.2.* All code and data required to reproduce results in the work can be accessed at https://github.com/tenayuco/harvestDistribution and it is further explained in supplementary material.

2.3.1. Movement analysis, state-space models and differences between the plantations

We analyzed the harvesters' movement using multi-state distribution models. State-space models are typically used in the context of movement ecology analysis to characterize the trajectories of individual animals that are assumed to have different behaviors or states (eg. foraging, exploring, migrating) during the recorded movement (Michelot and Blackwell, 2019; Morales et al., 2004;

Patterson et al., 2008). These behaviors are derived by characteristics like the relative angle between two steps, or the step length. We used this approach to statistically quantify differences in the daily movement of the harvesters (for the complete details, refer to Supplementary Material).

We first fitted the step length frequency distributions of the six recorded trajectories of each plantation to models of one and two-states distributions (i.e. models assuming that the observed movements are generated by one or by two behavioral states during harvest). In the two-state case, we termed the behaviors as "Collect" and "Search". In all cases, we used two different fitting distributions, namely, the Gamma (G(x)) and Weibull (W(x)) functions (see Equations (1-3); Fig.S1.3; Table S1.2). For $\boldsymbol{x}$ and $\boldsymbol{\alpha > 0}$, these normalized probability density functions (PDFs) are given by the following formula:

$$W(x) = \frac{\alpha}{\lambda}\left(\frac{x}{\lambda}\right)^{\alpha-1} e^{-(x/\lambda)^{\alpha}} \tag{1}$$

$$G(x) = \frac{\frac{1}{\lambda}\left(\frac{x}{\lambda}\right)^{\alpha-1} e^{-(x/\lambda)}}{\Gamma(\alpha)} \tag{2}$$

$$\Gamma(\alpha) = \int_0^{\infty} y^{\alpha-1} e^{-y} dy \tag{3}$$

where $\boldsymbol{x}$ is the step length (in m), $\boldsymbol{\alpha}$ is a shape parameter (no units), $\boldsymbol{\lambda}$ a scale parameter (in m) and $\boldsymbol{\Gamma(\alpha)}$ the gamma function (Pishro-Nik, 2014). In the two-state case, the Search state should typically be characterized by a significantly larger $\boldsymbol{\lambda}$ than the Collect state. In each fitting process, we used the forward algorithm implemented in the *movehmm* library (Michelot et al., 2016) with 1000 combinations of prior parameters from uniform distributions that included the mean and the maximum step lengths of the data (Table 1). For the analysis, the steps were time-irregular and we assumed no differences between the harvesters. We compared the Gamma and Weibull models, as well as the

one-state and two-state models, using the Akaike (AIC) criteria (Michelot et al., 2016). As the two-states distribution of the Gamma family (equation 2-3) generated a lower AIC for both plantations, we chose it to assign to each step of the trajectories one of the two states (Search and Collect), using Hidden Markov Models (HMM) and the Viterbi algorithm (Zucchini et al., 2016). Hidden Markov models (HMMs) assume that the distribution that generates an observation Zt (a step-length) depends on the state St of an underlying and unobserved Markov process. In brief, this procedure jointly fits the two-state distribution of step-lengths and establishes a sequence of states using a maximum likelihood procedure (Patterson et al. 2008; Zucchini et al., 2016). It first assigns to each step the most likely state and then corrects the state using a global decoding procedure with the whole sequence (Zucchini et al., 2016). Finally, we explored the differences in the obtained distributions for each state (Search and Collect) between both plantations and their implications in the number of trees and surface area visited. We divided the total area into squares with different sizes (from 1 to 40 m wide) to account for the effect of the grain size and assumed that a square was visited if at least one visited tree fell within it. We tested the significance of the difference between the means for each measurement using the Wilcoxon test (w) or the Student test (st) depending on the normality of the residuals.

2.3.2. Qualitative drivers of the spatial trajectories

To understand the qualitative drivers of harvesters' trajectories we organized the variables obtained during the walking interviews to analyze their relation with the longitude, the direction of the trajectories, or the presence of short and long tailed step-length distributions. We separated the variables into two categories: environmental or coffee biology-related (e.g. rainfall or coffee ripening synchronization) and those that could be directly affected by management decisions or, in general, by the syndrome of production (e.g. coffee variety, size of the *pantes*). Finally, we connected these variables when they influenced each other and categorized the connection into direct and indirect drivers. Direct drivers included those whose modification affected the trajectory. Indirect factors affected direct factors (but not the trajectory itself).

3. Results

3.1 The movement of the harvesters can be described by two-state distribution models with qualitative differences between the plantations

Harvesters visited 94.5 trees on average (± 25.6) during the three to four hours recorded daily, excluding pauses. The average time between each visited tree was 2.3 min (± 1.8 mins). The spatial trajectories of the 12 harvesters were largely determined by the initial pattern of coffee trees (Fig.1). Within these patterns some harvesters followed more or less specific coffee tree rows (C_1 to C_3, C_5, O_6) or jumped from one row to another or other regions, depicting more randomized trajectories (C_4, C_6, O_2 to O_5) (Fig. 1). The aggregated distribution of the step lengths of harvesters in each plantation (n=6) is represented in Fig. 2. In both plantations the distribution is skewed to the right. In the conventional plantation the mean step length is 4.2 m and the median is 3.2 m whereas in the organic plantation these values are 6 m and 4.5 m, respectively. In some cases, harvesters could travel up to 50 m from one tree to another (conventional plantation), or even more than 100 m (organic plantation) (see inset boxplots in Fig.2).

Models with two distinct state distributions provided a better fit to the aggregated step length distribution as they exhibited lower general AICs, for both Gamma and Weibull distributions, than models with only one state (Table 1 and Fig. S1.5). In particular, the Gamma family with two states had the lowest AIC in both plantations (Table 1). Each step along the trajectories was assigned a state in Fig. 1 according to the distributions of Fig.2. In our work, the states are interpreted as a proxy for the situation during harvest. We named the first state “Collect”, where the worker remains in the same vicinity of the *pante* harvesting nearby plants (Fig.1). The PDF of this state is qualitatively similar in both plantations (Table 1, Fig. 2) and encompasses steps from 1 to 8.6 m in the conventional plantation (94% of the steps) and from 1 to 18 m in the organic plantation (98% of the steps) (Fig.2). In the second state, the “Search” state, harvesters traveled to another zone of the *pante* or to another *pante* when the current one had been completely harvested (Fig. 1). This second Search state is described by two qualitatively different PDFs depending on the plantation (Table 1, Fig.2). In the conventional plantation, it includes steps from 7.4 to 44 m and represents movements within the *pante*

(6% of steps, blue line in Fig. 1 and Fig.2). In the organic plantation, this state includes steps from 21 to 117 m long and represents mainly movements between *pantes* or relocalizations (2% of steps, blue line in Fig. 1 and Fig.2). Also note that in the organic plantation, the shape parameter α is close to 1 in the Search state (exponential distribution) while it is above 3 in the Collect state (distribution with a maximum at a finite step length). In the conventional plantation, the difference between the two states is less pronounced.

Table 1- Best models for each plantation and distribution family, for one and two-state models (State 1=Collect, State 2=Search). We added the prior parameters for parameter P1 (mean and shape for gamma and weibull, respectively) and P2 (standard deviation and scale for gamma and weibull, respectively) (Michelot et al., 2016). We show the minimal negative likelihood (minNegL), AIC values and the final parameters obtained and transformed to shape and scale following the following relations: $\alpha = \mu^2/\sigma^2$, $\lambda = \sigma^2/\mu$, where α:shape, λ:scale, μ:mean, σ:standard deviation. The parameters in bold are the ones we used for the analysis (equations (2)-(3)).

Farm	**Number of states**	**Family**	**Priors P1**	**Priors P2**	**minNegL**	**AIC**	**State 1**		**State 2**	
							Shape (α)	**Scale (λ)**	**Shape (α)**	**Scale (λ)**
Conventional	Two states	gamma	U(0.1, 10)	U(0.1, 20)	**1060**	**2134**	**4,95**	**0,70**	**2,45**	**4,10**
		weibull	U(0, 2.7)	U(0.1, 15)	1079	2172	1,46	10,12	2,42	3,87
	One state	gamma	U(0.1, 10)	U(0.1, 20)	1120	2244	2,85	1,22	NA	NA
		weibull	U(0, 2.7)	U(0.1, 15)	1170	2344	1,47	4,66	NA	NA
Organic	Two states	gamma	U(0.1, 10)	U(0.1, 20)	**1553**	**3119**	**3,20**	**1,56**	**1,14**	**29,00**
		weibull	U(0, 2.7)	U(0.1, 15)	1571	3156	1,96	5,47	0,97	21,25
	One state	gamma	U(0.1, 10)	U(0.1, 20)	1674	3351	1,92	3,68	NA	NA
		weibull	U(0, 2.7)	U(0.1, 15)	1722	3448	1,16	6,35	NA	NA

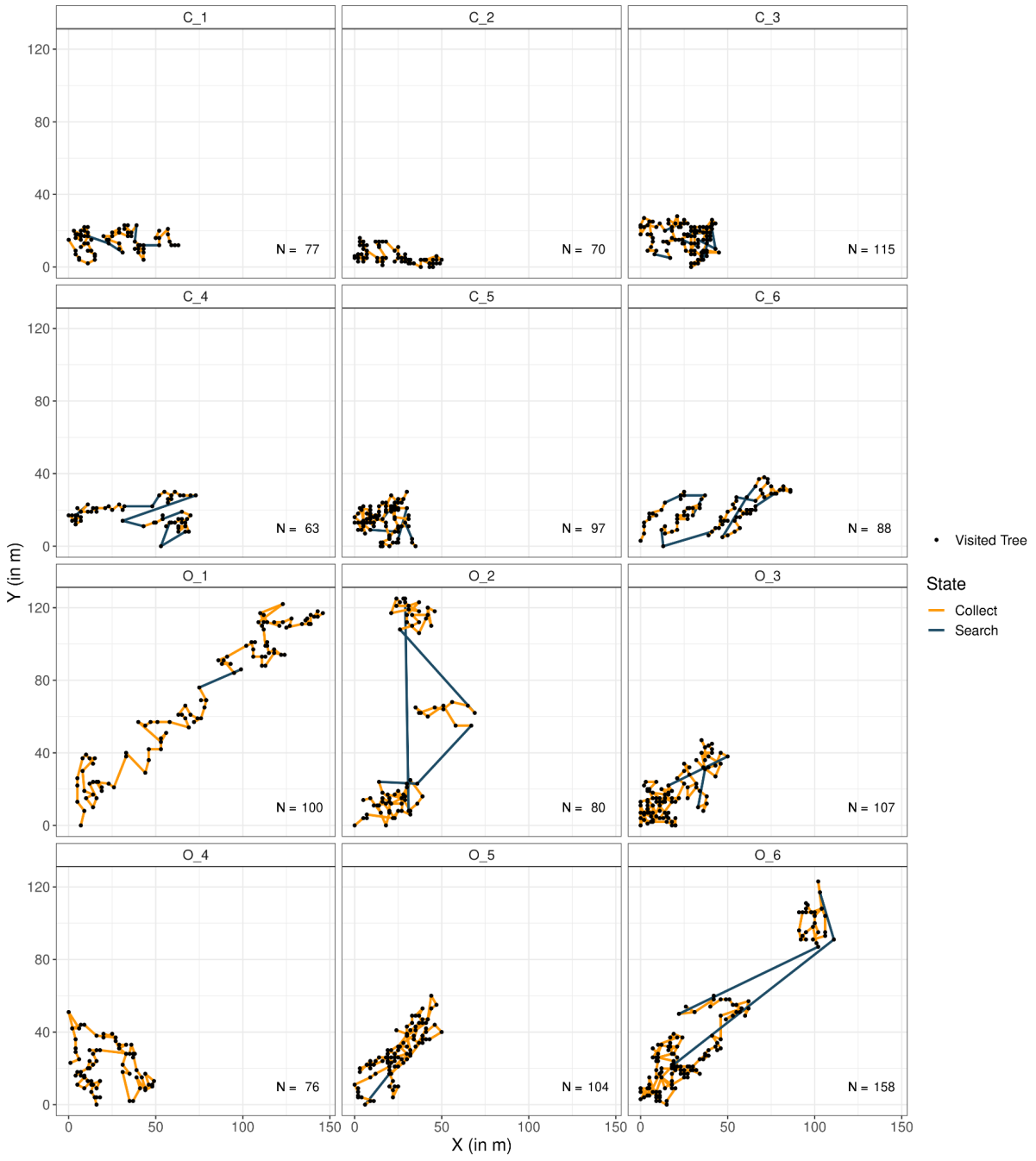

Figure 1. Harvesting trajectories from the conventional (C) and from the organic (O) plantations. We normalized the UTM coordinates from 0 to 150 m to represent the trajectories. The colors represent the most likely state to which each step belongs for each of the farms (orange: Collect, blue: Search; see the text for a full explanation). Each black point represents one harvested tree.

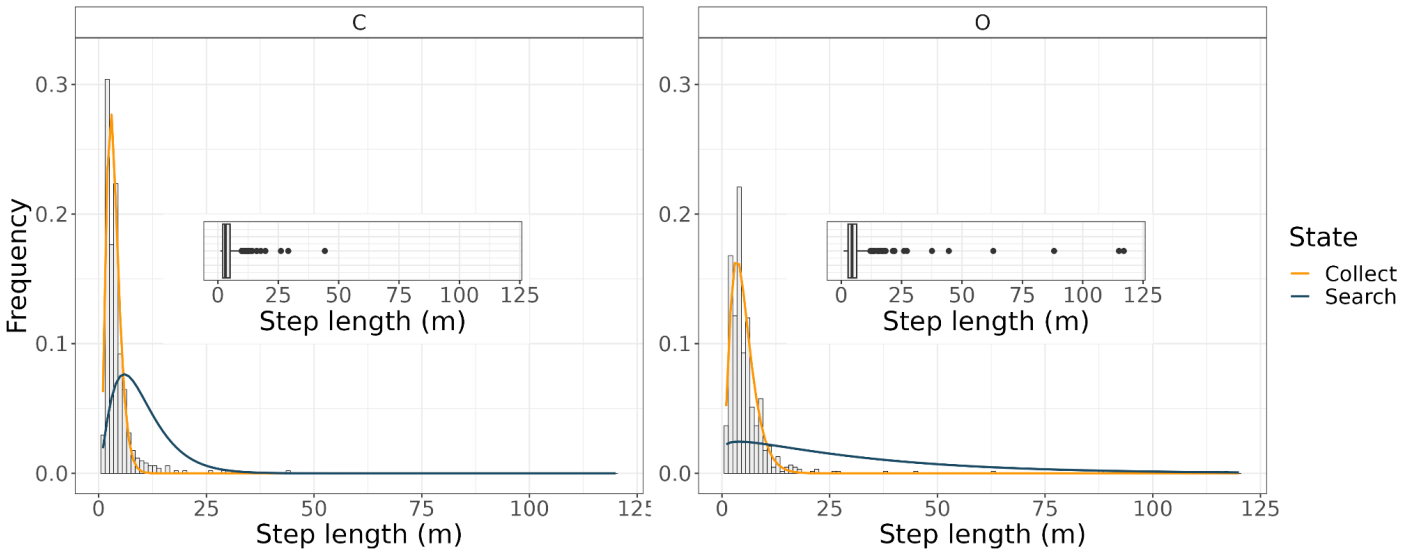

Figure 2. Histograms and box plots (insets) of the step lengths for the trajectories in each plantation and the probability density function of the gamma distributions for each of the two states. In the conventional plantation (C), the parameters of the gamma distribution (α, λ) are (4.95, 0.7) in the Collect state (orange line) and (2.45, 4.10) in the Search state (blue line). In the organic plantation (O) these parameters become (3.2, 1.56) for the Collect state t; and (1.14, 29) for the Search state . See Table 1 and equations (2)-(3).

3.2. Harvested trees and visited area per day are higher in the organic plantation

The average distance between trees within each *pante* is only slightly larger in the organic plantation (C: 3.8 ± 2.11 m; O: 4.8 ± 2.6 m; not significant). In this sense, the marked differences in the PDFs distributions of Search and Collect states between both plantations might be more related to the asynchronicity in fruit maturation between the trees and, to a lesser extent, to the initial planting pattern. The average number of trees visited per trajectory and per unit of time were higher in the organic than in the conventional plantation but the differences were not significant (Table 2). The higher number of harvested trees did not seem to correspond to differences in harvest weight per worker, which implies that, in the organic plantation, each tree had less mature berries when the data

was taken. This can be related either to fruit load or to ripening synchronicity differences between the two plantations.

The average traveled area per worker (approximated as the number of visited squares of given side length) was significantly higher in the organic plantation, for square units of 3, 5, 10 and 20 m side (Fig. 3). When the unit area is too small (1 m^2) or when the unit is too large (1600 m^2 or 40 m side) no significant differences are observed. The higher visited surface area might be the consequence of a higher presence of long steps (or relocalizations) during the harvesting day (Fig. 1 and Fig. 2). In some specific trajectories harvesters traveled up to 100 meters to reach the following tree. Finally it is worth mentioning that there was a significantly higher mean altitude difference within each *pante* in the organic plantation than in the conventional plantation, resulting in less uniform planting patterns in the organic plantation (Table 2).

Table 2- Differences in harvesting between both plantations. We show the mean for the six trajectories in each plantation and the standard deviation (±) for all the variables. We test the significance of the difference between the means using Wilcoxon test (w) or Student test (st) depending on the normality of the residuals. Only the altitude difference was significantly different between the two plantations ($p<0.005$).

Variable	**Plantation**		**Test difference between means**
	Conventional	**Organic**	
Hours recorded	3.5 (± 0.7)	3.9 (± 0.6)	NA
Trees harvested	85 (± 19) (s)	104 (± 29)	st
Trees harvested/hour	25 (± 7)	29 (± 5)	w
Altitude difference (m)	17 (± 9)	29 (± 12)	w ($p<0.005$)

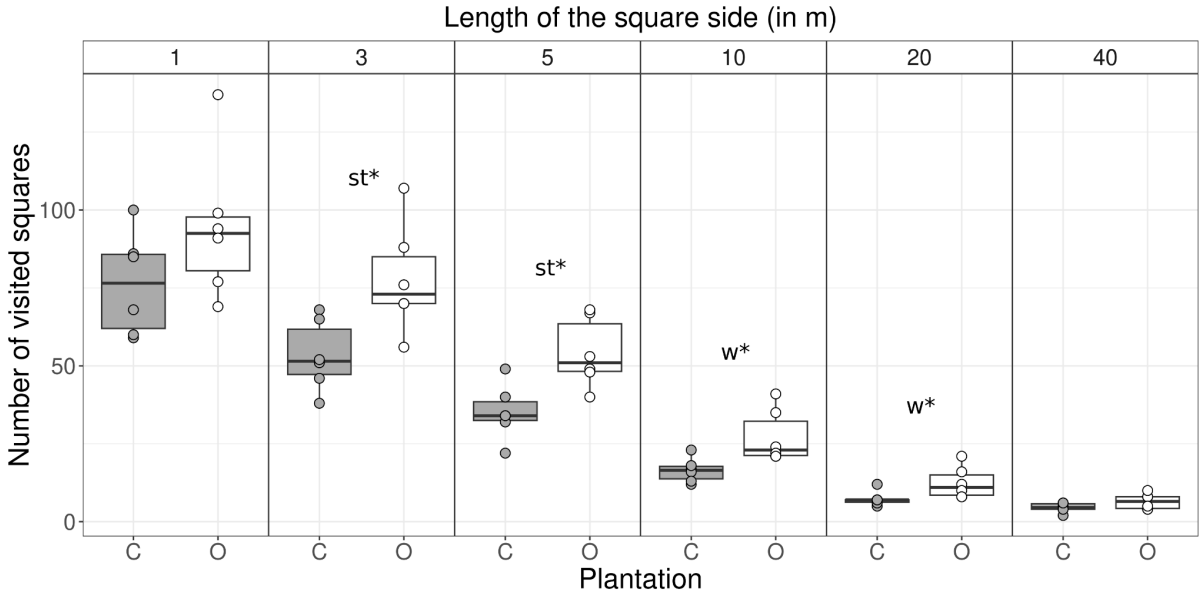

Figure 3. Surface area visited per harvester, obtained from visited squares of different sizes. Each dot represents the number of visited squares per harvester in each of the plantations (C-gray: conventional, O-white: organic). For the square unit areas where the differences between the two plantations were significant we added a * ($p<0.05$) and the used test of comparison between the two means (st: Student, w: Wilcoxon, n= 6).

3.3. Differences in trajectories of the harvesters are mediated by climate, the coffee biology and plantation variables, and most of them are modulated by management decisions.

The spatial movement of the harvesters, in particular the presence of longer steps (mainly in the state Search), as well as the daily length of the trajectory, can be directly and indirectly mediated by climate, topography, coffee biology characteristics, and coffee management variables (Fig. 4). The relationship between these variables give us some insights on the determinants of the syndrome of production and the reasons that might explain the differences and commonalities in the trajectory between both plantations.

According to the interviews and our additional observations (solid and dotted lines in Fig. 4, respectively), the harvester's trajectory might be directly affected by the number of mature berries in each of the trees (fruit load, D2) and the interplant maturation synchronicity (ripening synchronicity, D1). When trees have more berries, harvesters visit fewer trees and *pantes* per day, and their final

trajectory is shorter (Table 2, 3). Besides, to maximize their daily harvest, harvesters keep the same row when all the trees have berries, or jump from one row to another or even to another *pante*, when some trees are still immature. This results in more randomized patterns or larger step lengths along the day (state Search) (Fig.1). Ripening and fruit load depend on the coffee variety and age (N3, N5) and the date of harvest (N2, N4). Around the middle of the season, each coffee variety has a peak of berry maturation and synchronization between the trees. When we collected our data, trees were more homogeneously loaded in the conventional plantation than in the organic plantation, explaining in part the higher number of harvested trees in this plantation and the presence of larger step-lengths in the state Search (Fig. 1). This pattern could have been reversed in another period. It is worth mentioning that coffee ripening synchronicity is mostly mediated by the rainfall regularly during the flowering season (N1).

On the other hand, the spatial movement of harvesters is built upon the initial planting pattern (in rows, in groups, etc) and the *pante* size and shape (D5, D7). Both processes depend on the type of plantation (sun or shade-grown coffee) (N8, N11), the coffee variety (N7), and the topography of the field (N10, N11). Plant renovation dynamics also affect the planting pattern (N8). In the organic plantation individual plant renovations are more common, as well as the presence of other trees apart from coffee. This also defines more irregular patterns than in the conventional plantation without shade trees, where whole locations are removed and renovated every few years to increase short-term productivity. This reflects on the different degrees of randomization of the trajectories of the harvesters during harvest (Fig.1).

The number of harvesters (D3) per *pante* and the *pante* size (D7) could also determine the general pattern as it affects how fast families can harvest one location during the day and travel to another pante (long-steps in Fig. 1). The number of harvesters changes across the harvesting season following the coffee maturation process (N6). Finally, the number of working hours (D6) or the difficulty of harvesting a specific coffee variety (D4) also affect the trajectory length.

Most of these variables can be directly or indirectly affected by management decisions and ultimately depend on the specific syndrome of production of both plantations (green boxes in Fig. 4). For example, owners specify the starting and ending date of the harvesting season. Owners also

decide, mainly with profit-maximizing criteria, on the coffee varieties, the shade management, or the dynamics of plant renovation. As we saw, these factors will indirectly affect the final trajectory of the harvesters. Management can also determine the motion of harvesters by changing the working hours or the number of people by *pante*, or the distance between *pantes*. In this sense, the recorded trajectories of both plantations, their lengths, and patterns are the product of a specific syndrome of production with two different shade and management practices.

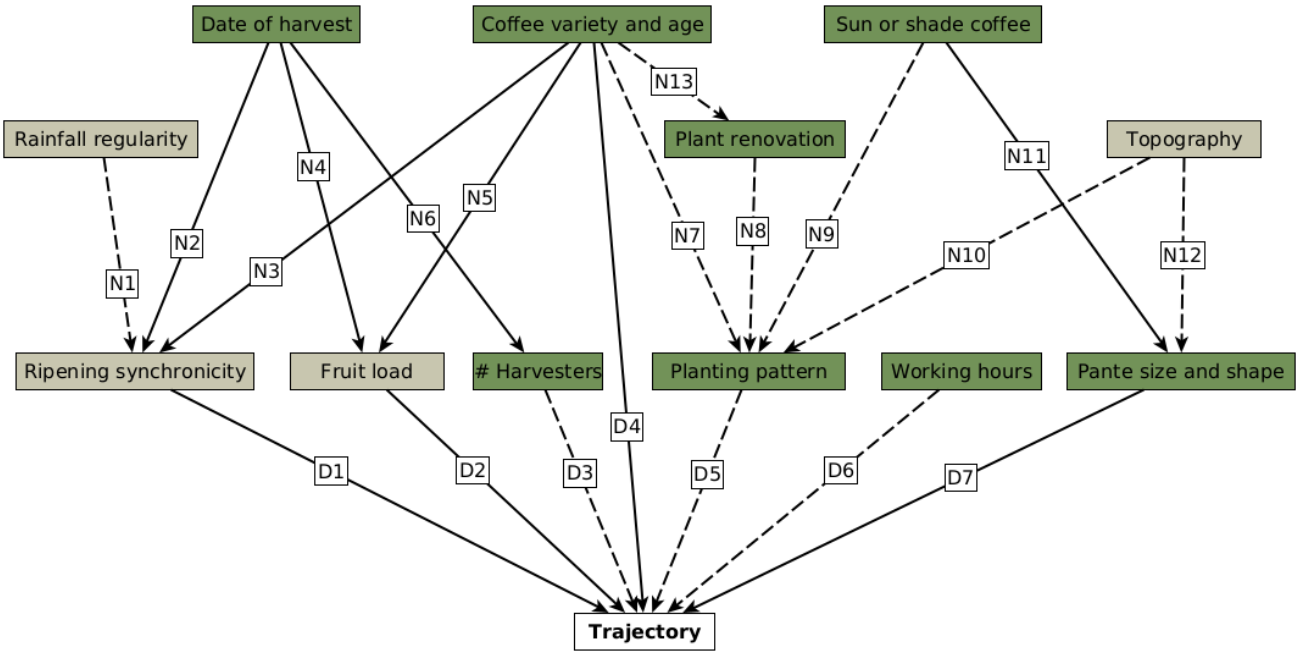

Figure 4. Qualitative drivers of the spatial trajectories of the harvesters during harvesting. The nodes represent the variables that interplay with the trajectory and the edges the causal relationships between them. The color of the boxes indicates if the variable is environmental or coffee biology related (gray), and if it can be directly modified by the management of the plantation (green). Note that the modification of these variables affects all the variables downstream. The letter in the label of the edges indicates whether the effect on the trajectory is direct (D) or indirect (N). The explanation of each label is summarized in Table 3.

Table 3- Direct (D) and indirect (N) drivers of the trajectories of the harvesters. The relation between the nodes is shown in Fig. 4.

Variable	Affected by	Description	Edge	Source
Direct effects				
Trajectory	Ripening interplant synchronicity	If the majority of plants have red berries, the harvester stays in the same row. When some of them have immature berries, he jumps from one row to another to maximize harvest	D1	Harvester
	Fruit load	With a higher fruit load per tree, harvesters visit less trees and *pantes* per day	D2	Harvester
	Number of harvesters	With multiple harvesters on the field, *pantes* are finished more rapidly. Individual dynamics are randomized and move away from the planting pattern.	D3	Pers. Obs
	Coffee variety and age	Some varieties are harder to harvest making harvesters visit less trees and *pantes* per day	D4	Harvester
	Planting pattern	The trajectory is built upon the initial planting pattern	D5	Pers. Obs.
	Working hours	More working hours implies more visited trees and *pantes* per day	D6	Pers. Obs.
	Pante's size and shape	The shape of the *pante* defines how often a harvester "turns" or keeps straight. Smaller *pantes* are harvested more rapidly	D7	Harvester
Indirect effects				
Ripening interplant synchronicity	Rainfall regularity	Ripening uniformity is determined by the temporal and spatial regularity of rainfall during flowering	N1	Pers. Obs.
	Date of the harvest	Ripening is variable across the harvesting season	N2	Harvester
	Coffee variety and age	Some varieties present a more uniform ripening than others	N3	Harvester
Fruit load	Date of harvest	Fruit load is variable across the harvesting season	N4	Harvester
	Coffee variety and age	Some varieties present more berries than other	N5	Harvester
Number of harvesters	Date of harvest	At the beginning or end of the harvesting season, there are less harvesters in the field	N6	Harvester
Planting pattern	Coffee variety and age	Some varieties are sow closer to each other modifying the general pattern	N7	Pers. Obs.
	Plant renovation	The plant renovation dynamics randomizes (when individual trees are removed) or uniforms (when complete locations are removed) the general pattern along the years.	N8	Pers. Obs.
	Sun or Shade coffee	Polycultures have a higher distance between trees than monocultures and tend to be more heterogeneous	N9	Pers. Obs.

	Topography of the field	Higher variability in the topography within a plot creates non-uniform planting patterns	N10	Pers. Obs.
***Pante* size and shape**	Sun or Shade coffee	The presence of trees in polycultures defines less uniform *pantes*	N11	Harvester
	Topography of the field	Topography conditions the boundaries of the *pante*	N12	Pers. Obs.
Plant renovation	Coffee variety and age	The rate of plant renovation depends on the age of the plantation and the productive years of each variety	N13	Pers. Obs.

4. Discussion and conclusions

Coffee is produced under a large variety of management practices, land tenure systems, and scales. In Mexico, one finds community-owned rustic coffee plantations as well as large-scale landlord-owned sun, and sometimes shaded, coffee plantations (Moguel and Toledo, 1999). Here we draw upon the conceptual framework of the "syndromes of production" to evaluate some of the social and ecological dynamics within a given agricultural paradigm (Andow and Hidaka, 1989; Ong and Liao, 2020; Vandermeer and Perfecto, 2012). In particular, we maintain that the two studied plantations (organic and conventional) in the Sonocusco region are part of a general capitalist syndrome of production characterized by large-scale plantations where landlords extract surplus value from the work of permanent and temporary workers and sell their product to conventional or organic markets (López Echeverría, 2006; Ong and Liao, 2020). The distinction in their markets reflects differences in their specific management and ecological practices. The organic plantation has an integrated management system that results in higher associated biodiversity, pest control, and lower plant renovation, but also in better worker's health conditions by removing pesticides (Soto-Pinto et al., 2000; Jiménez-Soto, 2021). Besides, it values quality over quantity in coffee production, which reduces the plant renovation rate and prioritizes planting high-quality arabica plants.

Our study aimed to understand how distinct agricultural managements in large-scale plantations drive differences in patterns of human movement that can potentially impact CLR spread in the environment, as well as working conditions. We found that two-state space models can describe harvester's trajectories well. This is in line with our observations in the field where we differentiate

two kinds of movements: when trees have berries, harvesters remain in the same rows or nearby (Collect state: short to medium steps); when no berries are in sight or when they have finished a *pante*, harvesters move to another zone of the *pante* or to another *pante* chosen by the foreman (Search state: medium to long steps). These behaviors are similar to general foraging patterns in other agroecosystems (Reynolds et al., 2018) or to the trajectories generated by deterministic models where a walker visits the closest unvisited site among a collection of point-like sites irregularly distributed in a landscape (Santos et al., 2007). The organic shaded plantation had longer steps both in the Collect state (within the *pante*) and specially in the Search state (relocalizations between *pantes*) in the same amount of time and, according to our qualitative analysis this could be related to *a)* a lower fruit charge or ripening synchronization when we took the data or *b)* smaller *pantes* or the number of harvesters per *pante.* This resulted in a higher number of visited areas of different sizes (Fig. 3). The heterogeneity in trajectories in this plantation seems to be related to the presence of other trees, plant renovation dynamics, or even to the topographic context,as also discussed by Hajian-Forooshani and Vandermeer, (2021) and Soto-Pinto et al., (2000).

In this sense, the spatial movements of the harvesters are the result of their interactions with biological and climatic factors and also depend on plantation characteristics and management decisions. This goes along the line of the unifying paradigm of movement ecology first introduced in the context of animals (Nathan et al 2008). For example, the ripening synchronization can be affected by the regularity of the rainfall during flowering and the temperature (Kath et al., 2021), or by the distribution of shade (Henrique Marquezine Leite et al., 2022). Nevertheless, the owners decide when to end the harvesting season. As was reported by other studies, it is common for the owners to encourage harvesters to stay until the end of the season by increasing the value of the harvest load, or to directly force them to remain in the fields by delaying their payment (Jiménez-Soto, 2021). This promotes harvesting when plants have highly asynchronous ripening and low fruit load, setting the scenario for longer daily trajectories with a higher proportion of medium to long steps across the region.

There are several potential socio-ecological implications of the different harvesters' trajectories on coffee rust dispersal. Here we did not report any data related to CLR or other potential

pests but we can hypothesize that visiting more trees per day, without the possibility of changing clothing could increase the dispersal and impact of CLR (as observed by Becker and Kranz (1977)). Besides, CLR or other pathogens are also dispersed from plant to plant through water splash or leaf-to-leaf contact, creating localized foci of infection (Vandermeer et al., 2018). Changing *pante* several times (Fig. 1, organic plantation) could connect these foci of infection or bear the pathogens to different parts of the landscape and start new infections. The square units depicted in Fig. 3 could be thought of as a proxy of these foci. In this sense, the spatial heterogeneity in coffee maturation creates fragmented host-landscapes that interact with the movement of harvesters and could increase the CLR or other pathogens' outbreaks (as suggested by White et al., 2018). Nonetheless, these hypotheses need to be tested, theoretically or empirically. These implications would not mean promoting managements that could homogenize the coffee ripening or fruit charge (e.g., homogenous sun coffee varieties, controlled irrigations) to reduce the spatial movement of harvesters during the harvesting. Coffee production and the incidence of specific pathogens as CLR are multifactorial processes (Avelino et al., 2006) and decisions that could reduce human dispersal can promote another dimension of the epidemic. For example, removing the shade trees to avoid irregular ripening (Henrique Marquezine Leite et al., 2022) also increases the CLR wind-mediated dispersal (Gagliardi et al., 2020). They also do not mean placing responsibility on the harvesters as they are temporary or permanent workers paid daily by piecework, working precariously for several hours to maximize the daily harvest in landlord-owned plantations guided by the generation of profit.

Our findings call for organic coffee management that could prevent diseases, increase diversity, and guarantee just and safe conditions for workers. In particular, to reduce the possible impact of human dispersal of pathogens during harvesting, we suggest the need for shorter trajectories by working fewer hours a day, avoiding harvesting at the beginning or end of the coffee maturation season when few trees have berries and harvesters have to travel longer distances, or even skipping infected plants. These measures can reduce short-term productivity but sustain long-term productivity. In this sense, to be implemented, coffee farmers should overcome the business-as-usual politics of large-scale capitalist coffee agroecosystems.

5. Acknowledgements

EMVC is a doctoral student from the Programa de Doctorado en Ciencias Biomédicas, Universidad Nacional Autónoma de México, and has received CONACyT scholarship 686776. MB acknowledges financial support from UNAM-DGAPA-PAPIIT (IN207819). EMVC, CGG and MB thanks Gustavo Bautista, Gabriel Domínguez and Elisa Lotero for the discussions and precious help during the fieldwork. EMVC especially thanks Elisa Lotero for her patience and support and the people from La Parcela for their ideas and friendship. Finally the authors dedicate this work to all the harvester families in both plantations and in other regions, that feed the world under social conditions that must be overturned .

6. References

Andow, D., 1983. The extent of monoculture and its effects on insect pest populations with particular reference to wheat and cotton. Agriculture, Ecosystems and Environment 9, 25–35. https://doi.org/10.1016/0167-8809(83)90003-8

Andow, D.A., Hidaka, K., 1989. Experimental natural history of sustainable agriculture: syndromes of production. Agriculture, Ecosystems & Environment 27, 447–462. https://doi.org/10.1016/0167-8809(89)90105-9

Avelino, J., Cristancho, M., Georgiou, S., Imbach, P., Aguilar, L., Bornemann, G., Läderach, P., Anzueto, F., Hruska, A.J., Morales, C., 2015. The coffee rust crises in Colombia and Central America (2008–2013): impacts, plausible causes and proposed solutions. Food Security 7, 303–321. https://doi.org/10.1007/s12571-015-0446-9

Avelino, J., Zelaya, H., Merlo, A., Pineda, A., Ordoñez, M., Savary, S., 2006. The intensity of a coffee rust epidemic is dependent on production situations. Ecological Modelling 197, 431–447. https://doi.org/10.1016/j.ecolmodel.2006.03.013

Becker, S., Kranz, J., 1977. Comparative Studies on Dispersal of Hemileia vastratrix in Kenya.

Zeitschrift für Pflanzenkrankheiten und Pflanzenschutz / Journal of Plant Diseases and Protection 84, 526–539. https://www.jstor.org/stable/ 43213550

Breed, G. A., & Severns, P. M. (2015). Low relative error in consumer-grade GPS units make them ideal for measuring small-scale animal movement patterns. *PeerJ*, *3*, e1205. https://doi.org/10.7717/peerj.1205

Evans, J., Jones, P., 2011. The walking interview: Methodology, mobility and place. Applied Geography 31, 849–858. https://doi.org/10.1016/j.apgeog.2010.09.005

Gagliardi, S., Avelino, J., Beilhe, L.B., Isaac, M.E., 2020. Contribution of shade trees to wind dynamics and pathogen dispersal on the edge of coffee agroforestry systems: A functional traits approach. Crop Protection 130, 105071. https://doi.org/10.1016/j.cropro.2019.105071

Hajian-Forooshani, Z., Rivera Salinas, I.S., Jiménez-Soto, E., Perfecto, I., Vandermeer, J., 2016. Impact of Regionally Distinct Agroecosystem Communities on the Potential for Autonomous Control of the Coffee Leaf Rust. Environ Entomol 45, 1521–1526. https://doi.org/10.1093/ee/nvw125

Hajian-Forooshani, Z., Vandermeer, J., 2021. Emergent spatial structure and pathogen epidemics: the influence of management and stochasticity in agroecosystems. Ecological Complexity 45, 100872. https://doi.org/10.1016/j.ecocom.2020.100872

Henrique Marquezine Leite, P., Evangelista De Oliveira, R., Durrer Bigaton, A., Vilela, G., Fontanetti, A., 2022. Shade influence of the temporary canopy of an agroforestry system on coffee fruit ripening. CS 16, 1–11. https://doi.org/10.25186/.v16i.1974

Jackson, D., Skillman, J., Vandermeer, J., 2012. Indirect biological control of the coffee leaf rust, Hemileia vastatrix, by the entomogenous fungus Lecanicillium lecanii in a complex coffee agroecosystem. Biological Control 61, 89–97. https://doi.org/10.1016/j.biocontrol.2012.01.004

Jiménez-Soto, E., 2021. The political ecology of shaded coffee plantations: conservation narratives and the everyday-lived-experience of farmworkers. Journal of Peasant Studies 48, 1284–1303. https://doi.org/10.1080/03066150.2020.1713109

Jones, B.A., Grace, D., Kock, R., Alonso, S., Rushton, J., Said, M.Y., McKeever, D., Mutua, F.,

Young, J., McDermott, J., Pfeiffer, D.U., 2013. Zoonosis emergence linked to agricultural intensification and environmental change. Proc. Natl. Acad. Sci. U.S.A. 110, 8399–8404. https://doi.org/10.1073/pnas.1208059110

Kath, J., Mittahalli Byrareddy, V., Mushtaq, S., Craparo, A., Porcel, M., 2021. Temperature and rainfall impacts on robusta coffee bean characteristics. Climate Risk Management 32, 100281. https://doi.org/10.1016/j.crm.2021.100281

López Echeverría, M.E., 2006. Identidad, autonomía y cultura: El espíritu del capitalismo en las Fincas Cafetaleras Alemanas en el Soconusco (1850-2006).

Manlove, K., Wilber, M., White, L., Bastille‐Rousseau, G., Yang, A., Gilbertson, M. L., ... & Pepin, K. M. (2022). Defining an epidemiological landscape that connects movement ecology to pathogen transmission and pace‐of‐life. *Ecology Letters*, *25*(8), 1760-1782. https://doi.org/10.1111/ele.14032

Mapes, K., 2010. Sweet tyranny: Migrant labor, industrial agriculture, and imperial politics. University of Illinois Press.

Mas, A.H., Dietsch, T.V., 2004. Linking Shade Coffee Certification to Biodiversity Conservation: Butterflies and Birds in Chiapas, Mexico. Ecological Applications 14, 642–654. https://doi.org/10.1890/02-5225

McCook, S., Vandermeer, J., 2015. The Big Rust and the Red Queen: Long-term perspectives on coffee rust research. Phytopathology 105, 1164–1173. https://doi.org/10.1094/PHYTO-04-15-0085-RVW

Michelot, T., Blackwell, P.G., 2019. State‐switching continuous‐time correlated random walks. Methods Ecol Evol 10, 637–649. https://doi.org/10.1111/2041-210X.13154

Michelot, T., Langrock, R., Patterson, T.A., 2016. moveHMM: an R package for the statistical modelling of animal movement data using hidden Markov models. Methods Ecol Evol 7, 1308–1315. https://doi.org/10.1111/2041-210X.12578

Moguel, P., Toledo, V.M., 1999. Biodiversity conservation in traditional coffee systems of Mexico. Conservation Biology 13, 11–21. https://doi.org/10.1046/j.1523-1739.1999.97153.x

Mora Van Cauwelaert, E., González González, C., Boyer, D., Hajian-Forooshani, Z., Vandermeer, J.,

Benítez, M., 2023. Dispersal and plant arrangement condition the timing and magnitude of coffee rust infection. Ecological Modelling 475, 110206. https://doi.org/10.1016/j.ecolmodel.2022.110206

Morales, J.M., Haydon, D.T., Frair, J., Holsinger, K.E., Fryxell, J.M., 2004. Extracting More Out of Relocation Data: Building Movement Models as Mixtures of Random Walks. Ecology 85, 2436–2445. https://doi.org/10.1890/03-0269

Nathan, R., Getz, W. M., Revilla, E., Holyoak, M., Kadmon, R., Saltz, D., & Smouse, P. E. (2008). A movement ecology paradigm for unifying organismal movement research. *Proceedings of the National Academy of Sciences*, *105*(49), 19052-19059. https://doi.org/10.1073/pnas.0800375105

Ong, T.W.Y., Liao, W., 2020. Agroecological Transitions: A Mathematical Perspective on a Transdisciplinary Problem. Front. Sustain. Food Syst. 4, 91. https://doi.org/10.3389/fsufs.2020.00091

Patterson, T. A., Thomas, L., Wilcox, C., Ovaskainen, O., & Matthiopoulos, J. (2008). State–space models of individual animal movement. *Trends in ecology & evolution*, *23*(2), 87-94. https://doi.org/10.1016/j.tree.2007.10.009

Perfecto, I., Chaves, L.F., Fitch, G.M., Hajian-Forooshani, Z., Iuliano, B., Li, K., Medina, N., Morris, J., Otero-Jiménez, N., Rivera-Salinas, I.S., Chenyang, S., Vandermeer, J., White, A., and Williams-Guillén, K. 2023. Looking beyond land-use and land-cover change: Zoonoses emerge in the agricultural matrix. One Earth, 6(9), 1131-1142. https://doi.org/10.1016/j.oneear.2023.08.010

Perfecto, I., Jiménez-Soto, M. E., & Vandermeer, J. 2019. Coffee landscapes shaping the Anthropocene: forced simplification on a complex agroecological landscape. *Current Anthropology*, *60*(S20), S236-S250. https://doi.org/10.1086/703413

Pishro-Nik, H. (2014). *Introduction to probability, statistics, and random processes* (p. 732). Blue Bell, PA, USA: Kappa Research, LLC

Raven, P. H., & Wagner, D. L. (2021). Agricultural intensification and climate change are rapidly decreasing insect biodiversity. *Proceedings of the National Academy of Sciences*, *118*(2),

e2002548117.https://doi.org/10.1073/pnas.2002548117

Reynolds, A., Ceccon, E., Baldauf, C., Medeiros, T.K., Miramontes, O., 2018. Lévy foraging patterns of rural humans. PLoS ONE 13, 1–16. https://doi.org/10.1371/journal.pone.0199099

Santos, M.C., Boyer, D., Miramontes, O., Viswanathan, G.M., Raposo, E.P., Mateos, J.L., Da Luz, M.G.E., 2007. Origin of power-law distributions in deterministic walks: The influence of landscape geometry. Phys. Rev. E 75, 061114. https://doi.org/10.1103/PhysRevE.75.061114

Soto-Pinto, L., Perfecto, I., Castillo-Hernandez, J., Caballero-Nieto, J., 2000. Shade effect on coffee production at the northern Tzeltal Zone of the state of Chiapas, Mexico. Agriculture, Ecosystems and Environment 80, 61–69. https://doi.org/10.1016/S0167-8809(00)00134-1

Vandermeer, J., Hajian-Forooshani, Z., Perfecto, I., 2018. The dynamics of the coffee rust disease: an epidemiological approach using network theory. European Journal of Plant Pathology 150, 1001–1010. https://doi.org/10.1007/s10658-017-1339-x

Vandermeer, J., Perfecto, I., 2012. Syndromes of production in agriculture: Prospects for social-ecological regime change. Ecology and Society 17. https://doi.org/10.5751/ES-04813-170439

Villarreal-Treviño, C., Penilla-Navarro, R.P., Vázquez-Martínez, M.G., Moo-Llanes, D.A., Ríos-Delgado, J.C., Fernández-Salas, I., Rodríguez, A.D., 2015. Larval habitat characterization of Anopheles darlingi from its northernmost geographical distribution in Chiapas, Mexico. Malar J 14, 517. https://doi.org/10.1186/s12936-015-1037-0

Waller, J.M., 1981. The recent spread of some tropical plant diseases. Tropical Pest Management 27, 360–362. https://doi.org/10.1080/09670878109413805

White, L. A., Forester, J. D., & Craft, M. E. (2018). Disease outbreak thresholds emerge from interactions between movement behavior, landscape structure, and epidemiology. *Proceedings of the National Academy of Sciences*, *115*(28), 7374-7379. https://doi.org/10.1073/pnas.1801383115

Zucchini, W., MacDonald, I.L., Langrock, R., 2016. Hidden markov models for time series: an introduction using R, Second edition. ed, Monographs on statistics and applied probability. CRC Press, Taylor & Francis Group, Boca Raton.

CAPÍTULO III. Dispersión por cosecha e incidencia de la roya en parcelas con diferentes densidades de siembra

Síntesis del capítulo

En el capítulo anterior realizamos un análisis de las trayectorias asociadas al movimiento de los trabajadores durante la cosecha en dos plantaciones de gran escala y de las razones que explican las diferencias entre uno y otro tipo de movimiento. En particular, en algunas de las trayectorias de los cosechadores, observamos la presencia de saltos largos entre diferentes regiones de la plantación (conocidos como *pantes*); posiblemente promovidos por la asincronía en la maduración de los frutos o por el número de trabajadores por *pante*. Algunos estudios han enfatizado la relación entre la estructura del paisaje, el movimiento de las personas y la transmisión de los patógenos (Manlove et al., 2022; White et al., 2018). En el caso de la roya del café, ciertos autores han sugerido el papel que pueden tener los cosechadores sobre la dispersión y el impacto regional de la epidemia (Avelino y Rivas, 2013; Waller, 1981). Sin embargo, solo unos pocos se han detenido a medir la transferencia real de esporas entre las hojas de café y la ropa y todavía no hay estudios experimentales sobre el impacto real de este movimiento en campo con relación a los otros modos de dispersión (Becker y Kranz, 1977). Además, como se sugirió anteriormente, estudiar el impacto de este mecanismo de dispersión es relevante dado que puede ser modificado por decisiones de manejo (o por el síndrome de producción), ya sea de manera directa decidiendo cómo cosechar, o de manera indirecta a través de la configuración espacial o la densidad de siembra.

El objetivo de este capítulo fue construir un modelo computacional que pudiera arrojar luz, en primer lugar, sobre las condiciones necesarias para generar trayectorias de cosecha similares a las observadas en campo, con o sin presencia de saltos largos. Pusimos específicamente a prueba el papel de la asincronía en la maduración de los frutos entre árboles y el papel del número de cosechadores por parcela. En segundo lugar, evaluamos el efecto de

estos movimientos sobre la dispersión y sobre la incidencia general de la roya en parcelas con diferentes densidades de siembra. Para ello simulamos parcelas con dos tipos de asincronía en la maduración de los frutos: donde todas las plantas tenían carga de frutos (sincrónico) y en donde solo la mitad estaban cargadas (asincrónico). Sobre estas parcelas definimos una regla de cosecha en donde cada individuo cosechara la planta más cercana con frutos y evaluamos el tipo de trayectorias generadas. Después, para medir el efecto del movimiento sobre la incidencia de roya, generamos parcelas con diferentes densidades de siembra y un porcentaje inicial de plantas infectadas, y definimos dos formas de dispersión: uno basal de dispersión por contacto entre planta y planta (Vandermeer et al., 2018) y uno de dispersión mediada por el movimiento de los cosechadores.

Encontramos que la maduración asíncrona de las plantas fue suficiente para explicar la presencia de saltos largos, en particular hacia el final de la cosecha en donde hay una escasez generalizada de árboles con frutos. La dispersión por el movimiento durante la cosecha aumentó la incidencia de roya en todos los escenarios, en comparación a las parcelas en donde solo la dispersión por contacto estaba presente. El efecto fue mayor (hasta 15% de incremento) con trayectorias con saltos largos y en plantaciones con densidades intermedias de siembra (2000 plantas/ha). A densidades bajas las nuevas infecciones generadas durante la cosecha se quedan localizadas en conjuntos aislados de plantas. A mayor densidad, casi todas las plantas se infectan por la dispersión por contacto entre plantas, por lo que en la cosecha se infectan pocos nuevos conjuntos de plantas. Este resultado, aunado al del capítulo anterior, hace pensar en decisiones de manejo que puedan aprovechar las ventajas que confiere la maduración asíncrona de café, al tiempo que reduzcan los impactos negativos que generan en la dispersión y en el desarrollo de fitopatógenos.

Interplay between harvesting, planting density and ripening time affects coffee leaf rust dispersal and infection

Emilio Mora Van Cauwelaert[a, b, *], Kevin Li[c], Zachary Hajian-Forooshani[d], John Vandermeer[e] and Mariana Benítez[a, *]

a. Laboratorio Nacional de Ciencias de la Sostenibilidad, Instituto de Ecología, Universidad Nacional Autónoma de México, Mexico City, C.P. 04510, México

b. Posgrado en Ciencias Biomédicas, Universidad Nacional Autónoma de México, Mexico City, C.P. 04510, México

c. School of Environment and Sustainability, University of Michigan, Ann Arbor, MI 48108, USA

d. German Centre for Integrative Biodiversity Research (iDiv), Martin Luther University Halle, Leipzig, Germany

e. Department of Ecology and Evolutionary Biology, University of Michigan, Ann Arbor, Michigan, USA

*mbenitez@iecologia.unam.mx, *emiliomora92@ciencias.unam.mx

ABSTRACT

Coffee leaf rust (*CLR; Hemileia vastatrix*) is one of the principal coffee diseases and has caused devastating loss of production around the globe. This fungus disperses between plants or regions through direct contact, water splash, or local turbulent wind conditions. Some studies have proposed that coffee harvesters can also bear CLR during harvesting. Their different trajectories depend on management and coffee plant characteristics, like the planting density or the ripening synchronicity, but also on the social organization of the plantation. However, it is not clear how relevant these movements are for CLR dispersal and plot-level infection in plots with other modes of CLR dispersal and different planting densities. Here we present a qualitative computational model to explore the role of coffee ripening synchronicity and the number of workers per plot in reproducing the different movement trajectories observed in the field. We then evaluate how these trajectories modify rust dispersal and change CLR infection in plots with increasing planting densities. We found that interplant asynchronous ripening and tree scarcity generate trajectories with long steps. In our model, the number of workers does not modify the trajectories. The harvest dispersal significantly increases coffee plot infection (up to 15%) compared to scenarios where only local mechanisms for CLR dispersal (contact-mediated or splash) are present. This effect is maximal for trajectories with long steps and in plantations with medium planting densities. At larger planting densities, plants are all already infected due to the local CLR dispersal. Our results aim to spur discussion on practices that could reduce the impact of harvesting and specific trajectories, in scenarios where one can benefit from asynchronous maturation of berries and shaded plantations. Some examples of practices include reducing the long-distance movements during the same day, for instance, by avoiding harvesting at the end of the harvest season when trees ripening asynchronicity and CLR levels are higher.

KEYWORDS

Coffee leaf rust dispersal; harvesting movement; coffee ripening; dynamical modelling; planting density

1. INTRODUCTION

The life cycle of pathogens in plants can be divided broadly into two stages: the infection stage where the organism invades the host and reproduces, and the dispersal stage where new replicates of the pathogen move from one host to the other (Avelino et al., 2004; Pangga et al., 2011). The rate and extent at which both stages are completed largely determine the magnitude of the epidemic and the crop loss (Avelino et al., 2004). Contrary to epidemics in non-sessile organisms, the host's density and spatial arrangement play a central role in plants, as they can modify the range and dynamics of the pathogen's dispersal (Keeling, 1999; Vandermeer et al., 2018; Papaïx et al.; 2015). In agriculture, this spatial structure depends on management factors (Beasley et al., 2022), plant-to-plant interactions (Li et al., 2020), and also on the topography of the field, among others (Soto-Pinto et al., 2000). Additionally, the interaction of the arrangement of the hosts and the disease depends on the characteristic transmission's distance of dispersal (Park et al., 2001; Hajian-Forooshani and Vandermeer, 2021). Studying these spatial relationships is crucial for an ecological approach to pest management that does not rely on synthetic pesticides, or solely on resistant plant varieties that focus on the infection stage (Avelino et al; 2004).

Coffee leaf rust (CLR), caused by *Hemileia vastatrix* Berk. & Br is one of the principal coffee diseases and has caused devastating loss of production in different coffee sites around the globe (McCook and Vandermeer, 2015; Talhinhas et al., 2017). Its mechanisms for dispersal have been amply studied (Becker and Kranz, 1977; Kushalappa and Eskes, 1989; Li et al., 2023; Vandermeer et al., 2018) and thus provide a great model to explore the disease's spatially explicit dynamics and its relations with the host's spatial arrangement and density (Beasley et al., 2022; Gagliardi et al., 2020; Hajian-Forooshani and Vandermeer, 2021; Mora Van Cauwelaert et al., 2023). CLR forms urediniospores that can travel to neighboring coffee

plants through direct contact, water splash, or local turbulent wind conditions (Kushalappa and Eskes, 1989). The urediniospores may also ascend to the atmosphere and travel to other plantations (Becker and Kranz, 1977; Vandermeer and Rohani, 2014). For each of these ways of dispersal, there are agroecological management proposals to reduce the spread, like reducing the density or clustering of the plantations (Beasley et al., 2022; Ehrenbergerová et al., 2018), avoiding regular patterns that can make the epidemic thrive through contact or splash-mediated dispersal (Hajian-Forooshani and Vandermeer, 2021; Mora Van Cauwelaert et al., 2023; Li et al., 2023), but also planting different trees within the plots and in the borders to reduce local and regional wind dispersal (Avelino et al., 2022; Boudrot et al., 2016; Gagliardi et al., 2020)

It has been observed that workers can also disperse CLR within the plot and between regions (Becker and Kranz, 1977; Ramírez-Camejo et al., 2022; Schieber and Zentmyer, 1984). At the plot scale, this relates to the fact that some foci of infection occur close to harvesting paths and human settlements (Waller, 1982, 1972) and that the build-up of the epidemic correlates with the harvesting season (Avelino et al., 1993, 1991; Mora Van Cauwelaert et al., 2023). However, it is unclear how relevant the dispersal by harvesters is for the whole epidemic in contrast to other modes of dispersal, and what agroecological measures could be implemented to reduce its impact.

Besides, the dynamics of harvesting in coffee plantations depend on the scale, land tenure regimes, goal of production, and specific ecological practices; or on what has been called "the syndrome of production" (Andow and Hidaka, 1989; Perfecto et al., 2019). In large-scale and landlord-owned plantations, the trajectory of paid workers during harvest depends on the interaction of management decisions with biological factors (Masarirambi et al., 2009; Mora Van Cauwelaert et al., in press). In particular, we show in previous studies that the daily movement of harvesters in large-scale plantations has two states: short steps between coffee plants or long steps across the plot or between the plots (Mora Van

Cauwelaert et al., in press). The difference in the proportion of each state during the daily harvest presumably relies on the maturation synchronization of the berries or the number of workers in the plot (Mora Van Cauwelaert et al., in press). These different trajectories could play an important role in CLR dispersal and its impact on plantations with distinct managements or planting density characteristics.

Here we present a mathematical model to study the workers' spatial movement during coffee harvesting and its contribution to CLR dispersal and infection at a plot level. We first explore if the different spatial trajectories drawn by the workers in large-scale plantations (with or without long steps; Mora Van Cauwelaert et al., in press) can be reproduced in simulated coffee plots with different berries maturation synchronicity and number of workers in the plot. We then evaluate how these trajectories modify rust dispersal and change the final average CLR infection in plots with increasing planting densities. Finally, we discuss the implications of our results in a broader context of different syndromes of coffee production.

2. METHODS

The objective of implementing a model was twofold: i) characterize some of the sufficient factors (ripening asynchronicity and number of workers) to reproduce the reported trajectories of the workers during the harvest and ii) explore the effect of these trajectories for dispersal and average rust infection in coffee plots with different planting densities. We first describe the procedure illustrated in Figure 1 and the different simulated scenarios. Then, we explain the analyses for each of the objectives.

2.1 Model Description

Coffee infection and dispersal process. We simulated coffee plants in a plot as N randomly placed points in a 100 x 100 m square with non-periodic boundaries. As we fixed the area, N represents the average planting density per ha of coffee plantations. Each plant had one of two states of infection: ***susceptible*** or ***infected*** (with rust spores present) (Fig. 1A). An infected plant can disperse and infect neighboring plants by two mechanisms. Through ***contact-mediated dispersal***, infected plants infect all 1.5 m apart or less susceptible neighbors. This mimics the local dispersion of rust either by contact between two nearby plants or by splash (as proposed by Vandermeer et al., 2018). The process creates networks of infected nearby plants where each pair of plants are 1.5 m apart or less (gray and black circles in Fig. 1A). The ***worker-mediated dispersal*** occurs when a worker harvests an infected plant and reaches a susceptible plant in the following step (yellow circle in Fig.1A). When an infected plant infects susceptible neighbors at time step t, these become infected at *t+1*. Each unit represents roughly 30 days, this is, the time needed for rust to complete a cycle of infection (Leguizamon et al., 1998).

Coffee ripening and harvesting motion. Additionally, each plant can have berries (***present***) or no (***absent***) (Fig.1B). We defined two coffee interplant ripening scenarios. In the Synchronous scenario (S), all the plants have ripe berries at the date of harvest. In the Asynchronous scenario (A), only 50% randomly selected plants have ripe berries at harvest (Fig. 1B). The presence of berries defines the harvesting motion: at the date of harvest each worker starts harvesting in a plant with berries, collects it (changing the status of berries of that plant to ***absent***), and moves to the closest plant with berries (Fig.1A). This cycle repeats until half of the plants in the plots are visited (Fig.1A). Depending on the number of plants harvested and number of workers, the process represents one or multiple working days (one worker collects around 30 plants per hour; Mora Van Cauwelaert et al., *in press*).

Whole model dynamic. We start the simulations with a small percentage of infected plants (T0 in Fig.1A) and run five cycles of contact-mediated dispersal and infection (these five cycles mimic the five months from the beginning of CLR buildup to the peak of harvesting; Mora Van Cauwelaert et al., 2023). At the time of harvest (TH = 5 time steps) almost all the plants in the same contact-mediated networks with one or more initially infected plants are infected (gray circles in Fig. 1A). These infected networks define the extent to which the pathogen spreads with contact mediated dispersal but without any harvesting. In the non-control scenarios, the harvesting takes place at TH. During the harvest, new infections emerge (yellow circles in Fig. 1A). After this harvesting event, we generate seven new cycles of contact-mediated dispersal and infection in which the newly infected plants spread the rust across their contact-mediated networks (black circles in Fig.1B). The whole simulation represents the maximum rust spread during one year, without acknowledging for leaf loss or other mechanisms or climate factors that in practice reduce the general infection (Kushalappa and Eskes, 1989). This is useful to compare the expansion of rust in our

different scenarios. In the control scenarios, no harvesting process takes place and the simulations run an equivalent time than the non-control scenarios.

2.2. Scenarios and measurements

We first characterized the trajectories and the distribution of steps simulated under two scenarios of coffee ripening (A and S), five planting densities (500, 1000, 2000, 3000, and 5000 plants per ha), and two quantities of simulated workers (1 and 5) (totalling 20 scenarios). We then took the last 160 steps of trajectories drawn in planting density of 3000 plants/ha to compare them with data that presented a similar average of harvested trees in plantations with different levels of ripening synchronicity (Mora Van Cauwelaert et al., in press). In particular, we took two examples from a large-scale organic plantation with an asynchronous ripening at the date of harvest ("organic plantation", henceforth) and two from a slightly shaded, large-scale non-organic plantation with synchronous ripening at the date of harvest (conventional plantation). Both plantations had a planting density between 3000 to 4000 plants/ha.

Secondly, we used our model to explore the effect of these simulated trajectories (20 scenarios) on the plot average rust infection, compared to control non-harvesting scenarios (5 additional scenarios, one for each planting density). We replicated each scenario 30 times to account for the random initial arrangement of plants. Each simulation started with 20% of infected plants (We show results for other initial infections in the supplementary material). To further explore the mechanisms behind our results, we registered the newly infected plants during harvest (yellow circle in Fig.1A) and the newly infected network after harvest and their size (black circles in Fig. 1A).

The model and simulations were implemented in the *Python* 3.10.6 programming language, using the modules *NumPy, SciPy, Pandas, and Seaborn*, and ran on the LANCIS facilities, at the Ecology Institute of UNAM. The data analyses and figures were done in

192 *Rstudio* 2023.03.1+446 using *plyr, dplyr, tidyverse, ggplot2, patchwork* libraries, and *Inkscape 1.0.*

193 All code and data required to reproduce results in the work can be accessed at

194 https://github.com/tenayuco/toyModel_harvest.

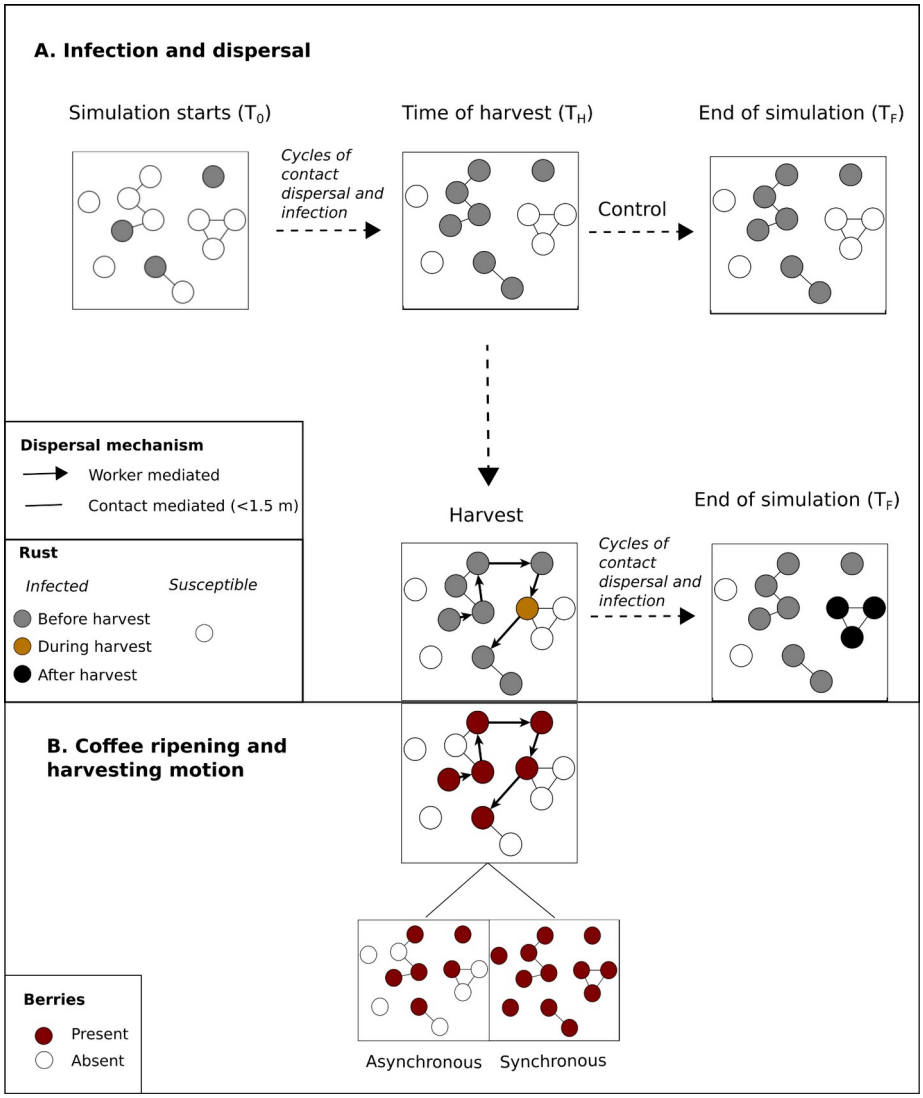

195

196 **Fig. 1. Model structure and dynamics.** ***(A) Infection and dispersal***. Plants can have two states of
197 infection: infected or susceptible (white circles). Infected plants can be infected before the harvest
198 (gray circles), during the harvest (yellow circles) or after the harvest (black circles). Black edges
199 represent pairs of plants that are 1.5 m apart or less and can be infected through contact-mediated
200 dispersal. Black arrows represent the movement of the harvester. We depict the start of the simulation
201 (T_0), the five cycles of contact dispersal and infection until the time of harvest (T_H) and the two
202 possible scenarios afterwards: the control scenario where no harvesting takes place, and the harvest
203 scenario where harvesters can create new infections (yellow circle) that might disperse to the
204 neighbors after new seven cycles of contact-mediated dispersal and infection. ***(B). Coffee ripening and***
205 ***harvest motion***. Plants can have two states of berries: with berries (red circles) or without (white
206 circles). We illustrate the two coffee ripening scenarios explained in the text. In the synchronous
207 scenario all the plants have berries at the time of harvest and in the asynchronous scenario, half have
208 berries and the other half do not.. The presence of berries determines the trajectory of the worker
209 (black arrows) during harvest.

3. RESULTS

3.1. Coffee ripening synchronization produces two qualitatively different harvesting trajectories that are equivalent to the trajectories of the workers in large-scale plantations

The deterministic movement of the simulated workers across randomly distributed plants generates random trajectories. (Fig.2 and Fig.S1.1). For both synchronization scenarios, the distribution of step length is positively skewed and can be approximated with continuous lognormal and exponential distributions (Fig.S1.3). Within each planting density, the mode is equivalent (Table S1.1). Under the asynchronous ripening scenario, the trajectory exhibits medium to large steps (30 to 100 m) and produces a heavy-tailed distribution (Fig.2). In the synchronous scenario, the steps are smaller than 30 m, creating a short-tailed distribution (Fig.2). In the asynchronous scenario the workers also explore a larger area of the plot.

Interestingly, the presence of large steps (>30 m) is not directly related to the initial low density of plants with berries in the asynchronous scenario. In fact they are not present in any of the equivalent and sometimes lower planting densities in the synchronous scenarios (Fig. S1.1 and Fig. S1.2). Large steps are concentrated near the end of the harvesting process (Fig. S1.2) for all planting densities, suggesting they are related to an increasing scarcity of trees with berries during the harvesting in the asynchronous scenario. Finally, we note that the number of simulated workers does not generate significantly different trajectories (Fig.S1.1). Hence we model only one worker in the plot in the following analysis.

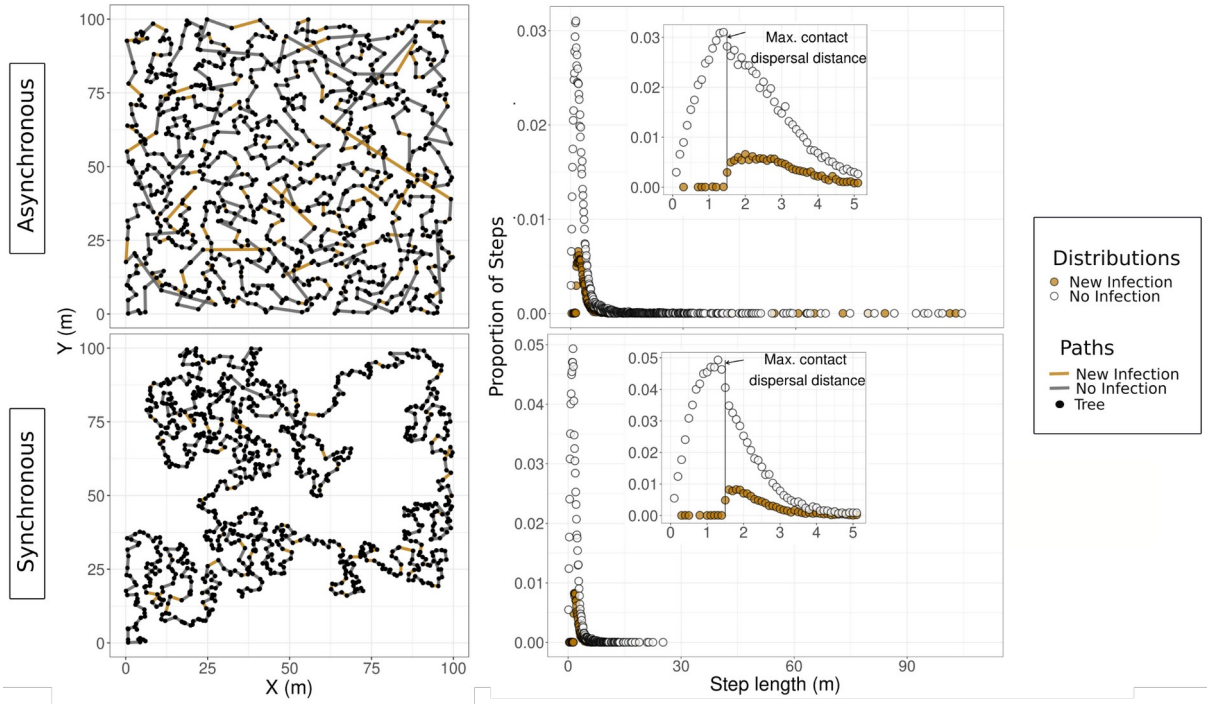

Figure 2. Simulated trajectories (left column) under two scenarios of coffee ripening and their respective step distribution (right column). The trajectories show one of the repetitions but the distributions are calculated over 30 repetitions. The color depicts if the harvesting step generated a new infection (this is, if the worker travels from one infected plant to one susceptible one) (yellow lines and dots) or no (gray lines and white dots). The line in the inset represents the maximum contact-mediated dispersal distance between plants. In the distribution we can distinguish two qualitative distributions of steps: with and without large steps. The modes of the skewed distributions are 1.7 and 1.3 for the asynchronous and synchronous scenarios, respectively. For the presented data, N= 2000, w= 1. The trajectories for other planting densities and number of workers are presented in Fig. S1.1.

The generated trajectories for the last 160 trees at a planting density of 3000 plants/ha are qualitatively similar to in-field trajectories drawn by workers in two large-scale coffee plantations with equivalent planting density (3000 to 4000 plants/ha) but that differed in their ecological management and their ripening synchronicity at the date of harvest (Fig. 3). This implies that the coffee ripening differences and the scarcity of trees with berries at the end of harvesting in our model might be sufficient to reproduce the short and large steps observed in the field. This behavior corresponds to observed jumps by the workers between coffee plots when a zone is depleted during the same day (to maximize daily harvest). Contrarily, synchronous ripening or a short harvesting process (before reaching the scarcity of trees; Fig. S1.2) would enable workers to stay in the same area during the day (Fig.3).

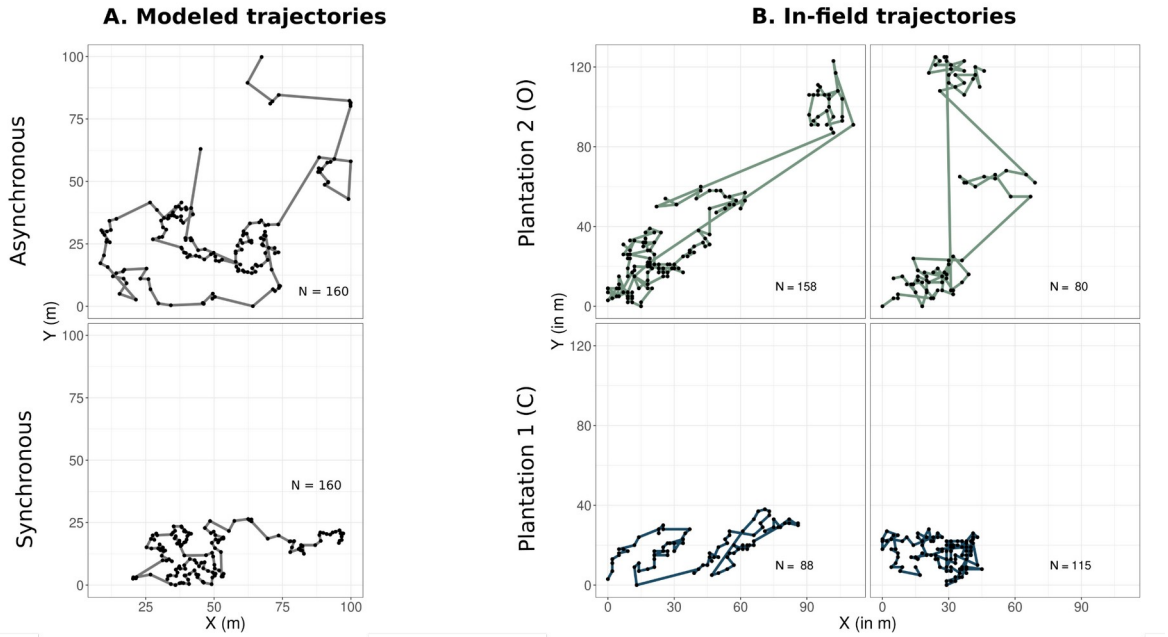

Fig. 3. Comparison of the model with in-field trajectories. A. Two examples of the modeled trajectories for the last 160 plants, drawn under the asynchronous and the synchronous scenarios, with N= 3000 plants/ha and w=1. **B.** Examples of in-field registered trajectories from Mora Van Cauwelaert et al. (in press). Organic plantation (green line) is a large-scale shaded and organic plantation with an asynchronous ripening at the date of harvest. Conventional plantation (blue line) is a slightly shaded, non-organic large-scale plantation with synchronous ripening at the date of harvest). For both plantations 160 plants were visited on average (see Mora Van Cauwelaert et al., in press for more details). Both plantations are around 300 ha, with a planting density between 3000 to 4000 plants per ha.

3.2. Dispersal during harvesting increases final rust infection specially for trajectories with large steps.

In this section we analyze the effect of the different generated simulated trajectories (with large steps from the asynchronous ripening scenario, and without large steps from the synchronous scenario) on the average rust in the plot. Higher planting density increases the plot-average infection in scenarios where only contact-mediated dispersal is present (control; gray line in Fig. 4A). Nonetheless, for each planting density, adding the harvesting event increases the final infection compared to the control (orange and blue lines in Fig. 4A).

The difference between the average rust with harvesting and without harvesting follows a non-linear curve for both kinds of trajectories with increasing planting density (orange and blue boxes in Fig. 4B). The maximum effect of harvesting with large steps lies at 2000 plants/ha (~15% average rust increase), and between 1000 and 2000 plants/ha for trajectories without these steps (~ 8% increase) (Fig. 4. B). At 5000 plants/ha, the impact of harvesting drops for both scenarios as almost all the plants are already infected by contact (Fig4. A and B). Harvesting with large steps increases rust infection more than without these steps, especially at medium densities (2000 plants/ha; more than 6% of rust infection difference (Fig. 4B). Only at very low densities (500 plants/ha) the difference between both scenarios is not distinct from zero.

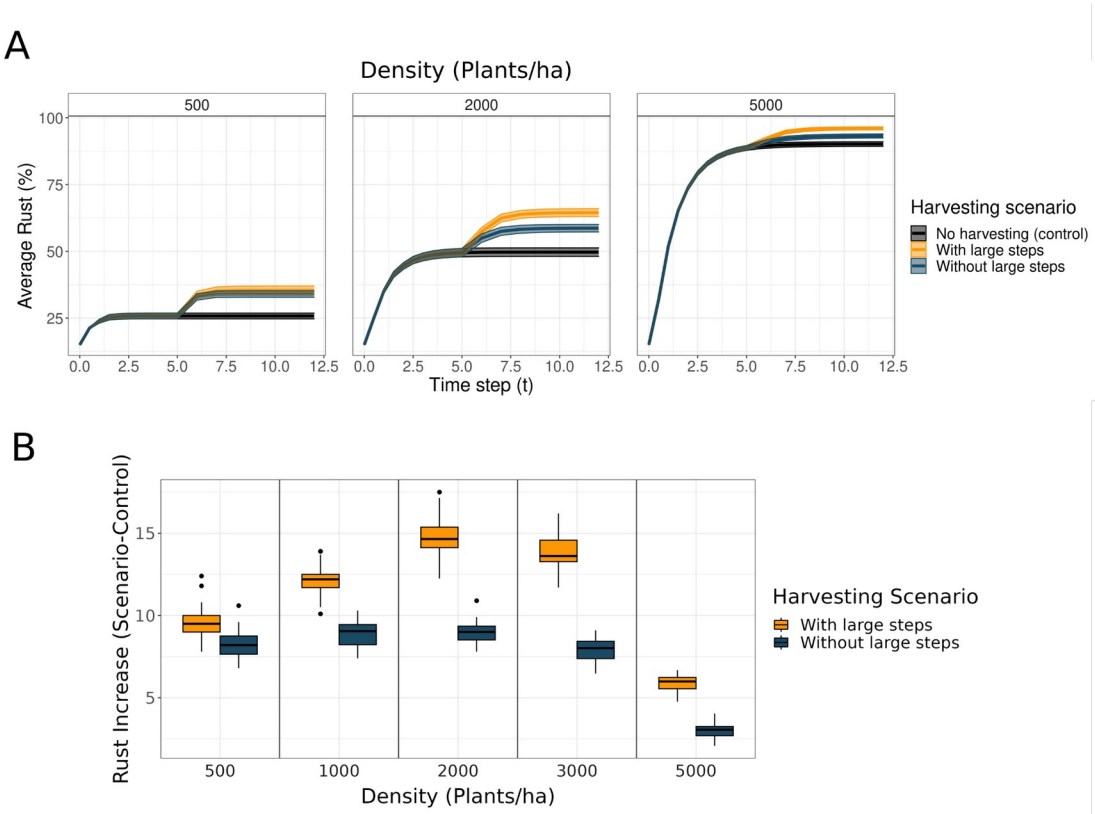

Figure 4. Effect of different harvesting trajectories on the average plot rust infection. ***A.*** Full time series of the average rust for three planting densities, for the control and the two harvesting trajectories generated under the coffee ripening scenarios (**A**; gray: control, orange: trajectories with large steps, blue: trajectories without large steps). The time series for 1000 and 3000 plants/ha were equivalent. **B.** Rust's increase due to the harvesting for each of the trajectories (harvesting scenario - control) for the five different planting densities (orange box: with large steps, blue: without large steps). In all simulations, we started with 20% of infected plants at T_0. We fixed 1 worker per plot.

3.3. The interaction between the number of new infected networks of plants and their size underlies the effect of harvesting on plot average infection

In Fig.2, we differentiate the steps that carried infection (yellow dots) from those that didn't (white dots). We observe that before 1.5 meters, the frequency of worker-mediated dispersal events (steps during harvest that promotes new infections) is almost zero. This distance corresponds to the contact-mediated infection reach: almost all the plants within this reach should be already infected at T_H (Fig.1). When we explore the proportion of worker-mediated dispersal events larger than 1.5 m, we observe that the values drop as we increase the density and that there is no difference between coffee ripening scenarios (Fig.S1.4). In this sense, the maximum rust's increase at medium densities (Fig. 4B) is not directly related to the proportion of new infections created during harvest.

In Fig.5 we show the proportion of infected networks of plants after the harvest event and the new cycles of contact-mediated infections (AH) (black circles in Fig.1 and the subplot in Fig.5) and their mean size. We include the product of both magnitudes as a proxy for the number of infected plants after the harvest event and the new rounds of infection (plants that would not be infected otherwise). For both trajectories with and without large steps, the proportion of new infected networks of plants decreases as planting density increases (black lines with circles dots in Fig. 5). This makes sense since the connectivity between plants increases with density, making almost all the plants already infected before harvest (gray dots in the subplot in Fig.5). On the contrary, the average size of new infected networks after harvest increases with planting density (black lines with triangle dots in Fig. 5). The estimated number of newly infected plants after the harvest (as an interaction of the number of networks and their mean size) follows a non-linear behavior in both scenarios that peaks between 2000 and 3000 plants (red dashed line with square points, Fig.5). This

curve is equivalent to the observed increase of infection in Fig. 4 and might be the mechanism underlying its nonlinear behavior.

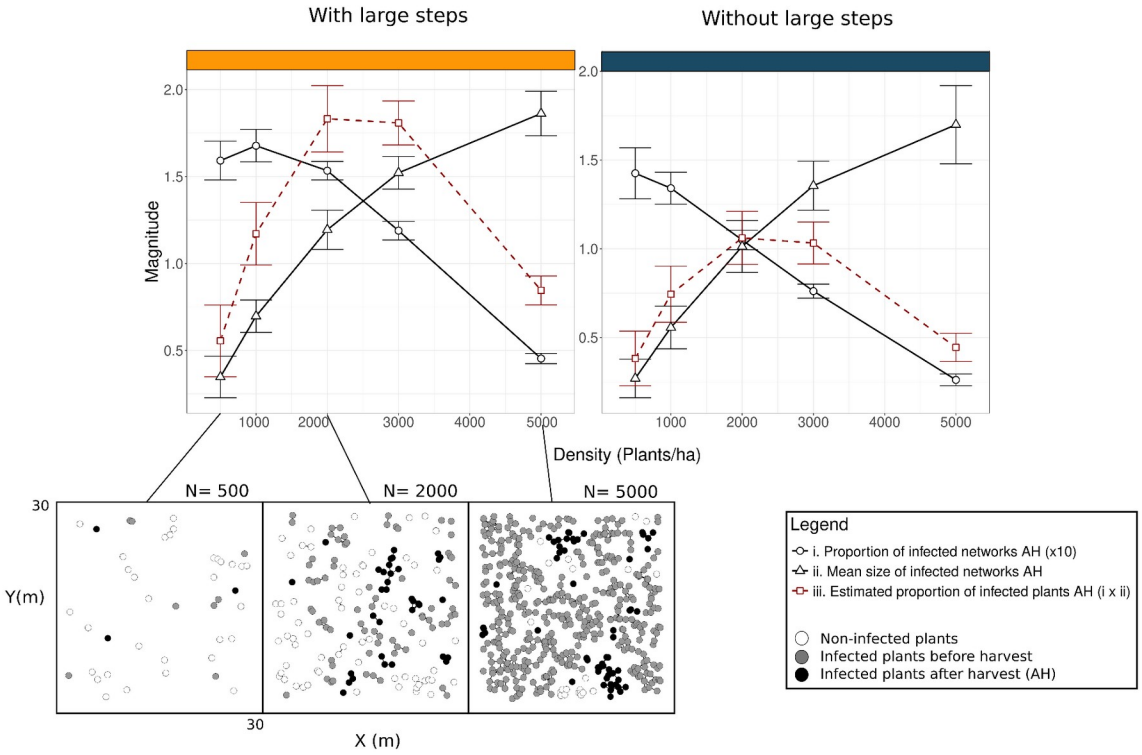

Fig. 5. Relationship between the trajectories of harvesting and the infected networks during the infection dynamic. We have one plot for the scenario with large steps (orange) and one for the scenarios without large steps (blue). In each plot, we present the proportion of new infected networks of plants after harvest/total plant visited; black lines with circles dots), the mean size of these network (black lines with triangle dots) and the multiplication of these factors as a proxy of the proportion of new infected plants (red dashed line with square points). In the below figure, we show three examples (at 500, 2000 and 5000 plants/ha) of the spatial disposition of susceptible plants (white circle), plants infected before the harvest (gray circle) and plants infected after harvest and the new cycles of contact-mediated infection (black circles). For visualization purposes we multiplied the proportion of infected networks by 10.

4. DISCUSSION AND CONCLUSIONS

Understanding the relationship between the spatial arrangement of the hosts and the different modes of dispersal of CLR is central to developing preventive strategies to reduce the impact of the pathogen on crop production (Hajian-Forooshani and Vandermeer, 2021). Here we present a model to study the determinants of the movement of the workers in the field during harvesting and its relevance in CLR dispersal and infection at the plot level. Our results suggest that we can reproduce random walks or large relocalizations by regulating the coffee ripening synchronicity and the scarcity of trees with berries at the end of harvest. Relocalizations in deterministic walks on a random set of points have been documented for other systems (Brown et al., 2007) and simulated in rectangle domains (Boyer, 2008; Santos et al., 2007) or varying the size of the targets (Boyer et al., 2006). These studies present specific widths or target size uniformity ranges where the modeled workers fail to find closer unvisited points and "jump" to another zone of the area (Boyer, 2008; Boyer et al., 2006). Concerning the CLR impact, we found that increasing the planting density where only contact-mediated dispersal was present increases the final CLR at the plot level. This is in line with other studies (Hajian-Forooshani and Vandermeer, 2021; Zambolim, 2016; Mora Van Cauwelaert, et al. 2023) and emphasizes planting at lower densities to avoid big bursts of the pathogen (Ehrenbergerová et al., 2018). The harvest event magnifies the final CLR infection for all scenarios and densities. Its effect is more important for medium densities (2000 to 3000 plants/ha), which is a common density of coffee plots owned by small-scale farmers (Soto-Pinto et al., 2000). If densities are too high, harvesting becomes irrelevant as the plot is already infected. Other modes of dispersal, such as wind-mediated relocalizations from neighbor plantations, were not included (as in (Hajian-Forooshani and Vandermeer, 2021; Vandermeer and Rohani, 2014). This assumption stands for the rainy seasons where

local contact is more relevant to build the initial epidemic (Boudrot et al., 2016). The different types of trajectories generated under the two coffee ripening scenarios changed the plot average CLR and varied nonlinearly with increasing planting density. Movements with medium and large steps promote new foci of infection (Zadoks and Van Den Bosch, 1994) that eventually become newly infected networks with optimum size and number at planting densities between 2000 to 3000 plants/ha. It is important to note that we modeled a random arrangement of the plants in the lattice. This assumption is likely valid for old plantations and shaded coffee managements (Moguel and Toledo, 1999) but should be revisited for aggregated or uniform patterns.

While we observe an increase in CLR in the asynchronous scenario, our results do not imply that asynchronous ripening conducts *per se* to higher rust. On the one hand, the medium to large steps are not generated due to the asynchronous ripening alone, but mainly due to the scarcity of closer trees at the end of harvest in that scenario. This would also be the case for large-scale landlord owned plantations where the workers are paid by the daily harvest (Jiménez-Soto, 2021); even if the following plant is hundreds of meters distant, it becomes necessary for them to reach it within the same day (Mora Van Cauwelaert et al., in press). In these plantations it is also common to force the workers to harvest at the end of the season when only few scattered trees still have berries (Mora Van Cauwelaert et al., in press). On the other hand, the simulated trajectories in the two coffee ripening scenarios suppose otherwise similar conditions on the plot. But in the field, asynchronous ripening is associated with characteristics that change these conditions and that can reduce the general rust impact. For example, the susceptibility of coffee plants to rust increases with fruit charge (Salgado et al., 2008). Hence, the asynchrony in the maturation of berries due to erratic rainfalls, or simply due to different coffee varieties (DaMatta et al., 2007), generates a mixed spatial pattern of resistant and susceptible plants that could reduce rust dispersal. On the other hand, shade trees in the plot form different patches of maturation (and the

potential for large steps during harvest) but also create barriers to wind-mediated rust dispersal (Gagliardi et al., 2020).

Our study aims to spur discussion on practices that can reduce the impact of harvesting and specific trajectories, in scenarios where one can benefit from asynchronous maturation of berries and shaded plantations (Ehrenbergerová et al., 2018; Liebig et al., 2019; Soto-Pinto et al., 2000). This is crucial as almost all the plantations have or will have this kind of ripening (DaMatta et al., 2007; Masarirambi et al., 2009), especially in the predicted climate scenarios of increasingly erratic rainfalls (Avelino et al., 2015; Huang et al., 2012; Rana et al., 2014). Along with planting different genetic varieties (Silva et al., 2006) or having other species of trees inside the plot and between them (Avelino et al., 2022), our results show the importance of reducing long-distance movements during the same day by avoiding harvesting at the end of the harvest season when trees ripening asynchronicity and CLR levels are higher (Avelino et al., 1991; Mora Van Cauwelaert in press); or simply skipping rust-infected trees and working fewer hours a day, even if this represents a short term decrease in harvested berries. These practices presuppose the right to decide how and when to harvest the coffee plantations.

We hope this mechanistic model will contribute to educating our intuition on the relationships between host spatial disposition and dispersal. With this approach, we try to build working hypotheses for an agroecological approach to pest management that does not rely solely on the control of the infection stage of the pathogen, but also on preventive measures that focus on the dispersal of the fungus.

5. ACKNOWLEDGMENTS

EMVC is a doctoral student from the Programa de Doctorado en Ciencias Biomédicas, Universidad Nacional Autónoma de México, and has received CONACyT scholarship 686776 and support from the Programa de Apoyo a los Estudios del Posgrado (PAEP) for his research stay at the University of Michigan (USA). MB acknowledges financial support from UNAM-DGAPA-PAPIIT (IN207819). JV acknowledges financial support from the US National Science Foundation, grant number DEB-1853261. EMVC thanks the people from La Parcela and Perfectomeer lab for their great ideas and friendship, and specially the GEO organization for their continuing strike for a living wage. EMVC and MBK are also thankful to Gustavo Bautista, Gabriel Domínguez, Elisa Lotero and Cecilia González for the discussions and help during the fieldwork. The authors thank Denis Boyer and Alfonso Valiente for the valuable feedback on the results and Rodrigo García Herrera for his technical support.

6.REFERENCES

Andow, D.A., Hidaka, K., 1989. Experimental natural history of sustainable agriculture: syndromes of production. Agriculture, Ecosystems & Environment 27, 447–462. https://doi.org/10.1016/0167-8809(89)90105-9

Avelino, J., Cristancho, M., Georgiou, S., Imbach, P., Aguilar, L., Bornemann, G., Läderach, P., Anzueto, F., Hruska, A.J., Morales, C., 2015. The coffee rust crises in Colombia and Central America (2008–2013): impacts, plausible causes and proposed solutions. Food Security 7, 303–321. https://doi.org/10.1007/s12571-015-0446-9

Avelino, J., Gagliardi, S., Perfecto, I., Isaac, M., Liebig, T., Vandermeer, J., Merle, I., Hajian-Forooshani, Z., Tabeuguia Motisi, N., 2022. Tree effects on coffee leaf rust at field and landscape scales. Plant Disease 107. https://doi.org/10.1094/pdis-08-21-1804-fe

Avelino, J., Muller, R.A., Cilas, C., Velasco Pascual, H., 1991. Développement et comportement de la rouille orangée du caféier (Hemileia vastatrix Berk. et Br.) dans des plantations en cours de modernisation, plantées de variétés naines, dans le sud-est du Mexique. Café, Cacao, Thé 35, 21–37. https://agritrop.cirad.fr/416561/

Avelino, J., Toledo, J.C., Medina, B., 1993. Développement de la rouille orangée (Hemileia vastatrix) dans une plantation du sud-ouest du Guatemala et évaluation des dégâts qu'elle provoque. ASIC 15th International Conference on Coffee Science 293–302. https://agritrop.cirad.fr/466977/

Avelino, J., Willocquet, L., Savary, S., 2004. Effects of crop management patterns on coffee rust epidemics. Plant Pathology 53, 541–547. https://doi.org/10.1111/j.1365-3059.2004.01067.x

Beasley, E.M., Aristizábal, N., Bueno, E.M., White, E.R., 2022. Spatially explicit models predict coffee rust spread in fragmented landscapes. Landscape Ecology 37, 2165–2178. https://doi.org/10.1007/s10980-022-01473-1

474 Becker, S., Kranz, J., 1977. Comparative Studies on Dispersal of Hemileia vastratrix in Kenya.
475 Zeitschrift fur Planzenschultz- Journal of Plant Diseases and Protection 84, 526–539.
476 https://www.jstor.org/stable/ 43213550
477 Boudrot, A., Pico, J., Merle, I., Granados, E., Vílchez, S., Tixier, P., De Melo Virginio Filho, E.,
478 Casanoves, F., Tapia, A., Allinne, C., Rice, R.A., Avelino, J., 2016. Shade effects on the
479 dispersal of airborne Hemileia vastatrix uredospores. Phytopathology 106, 527–580.
480 https://doi.org/10.1094/PHYTO-02-15-0058-R
481 Boyer, D., 2008. Intricate dynamics of a deterministic walk confined in a strip. Europhys.
482 Lett. 83, 20001. https://doi.org/10.1209/0295-5075/83/20001
483 Boyer, D., Ramos-Fernández, G., Miramontes, O., Mateos, J.L., Cocho, G., Larralde, H.,
484 Ramos, H., Rojas, F., 2006. Scale-free foraging by primates emerges from their
485 interaction with a complex environment. Proceedings of the Royal Society B:
486 Biological Sciences 273, 1743–1750. https://doi.org/10.1098/rspb.2005.3462
487 Brown, C.T., Liebovitch, L.S., Glendon, R., 2007. Lévy Flights in Dobe Ju/'hoansi Foraging
488 Patterns. Hum Ecol 35, 129–138. https://doi.org/10.1007/s10745-006-9083-4
489 DaMatta, F.M., Ronchi, C.P., Maestri, M., Barros, R.S., 2007. Ecophysiology of coffee growth
490 and production. Braz. J. Plant Physiol. 19, 485–510. https://doi.org/10.1590/S1677-
491 04202007000400014
492 Ehrenbergerová, L., Kučera, A., Cienciala, E., Trochta, J., Volařík, D., 2018. Identifying key
493 factors affecting coffee leaf rust incidence in agroforestry plantations in Peru.
494 Agroforestry Systems 92, 1551–1565. https://doi.org/10.1007/s10457-017-0101-x
495 Gagliardi, S., Avelino, J., Beilhe, L.B., Isaac, M.E., 2020. Contribution of shade trees to wind
496 dynamics and pathogen dispersal on the edge of coffee agroforestry systems: A
497 functional traits approach. Crop Protection 130, 105071.
498 https://doi.org/10.1016/j.cropro.2019.105071

499 Hajian-Forooshani, Z., Vandermeer, J., 2021. Emergent spatial structure and pathogen
500 epidemics: the influence of management and stochasticity in agroecosystems.
501 Ecological Complexity 45, 100872. https://doi.org/10.1016/j.ecocom.2020.100872
502 Huang, W.-C., Chiang, Y., Wu, R.-Y., Lee, J.-L., Lin, S.-H., 2012. The Impact of Climate
503 Change on Rainfall Frequency in Taiwan. Terr. Atmos. Ocean. Sci. 23, 553–564.
504 https://doi.org/10.3319/TAO.2012.05.03.04(WMH)
505 Jiménez-Soto, E., 2021. The political ecology of shaded coffee plantations: conservation
506 narratives and the everyday-lived-experience of farmworkers. Journal of Peasant
507 Studies 48, 1284–1303. https://doi.org/10.1080/03066150.2020.1713109
508 Keeling, M.J., 1999. The effects of local spatial structure on epidemiological invasions.
509 Proceedings of the Royal Society B: Biological Sciences 266, 859–867.
510 https://doi.org/10.1098/rspb.1999.0716
511 Kushalappa, A.C., Eskes, A.B., 1989. Advances in Coffee Rust Research. Annual Review of
512 Phytopathology 27, 503–531. https://doi.org/10.1146/annurev.py.27.090189.002443
513 Leguizamón-Caycedo, J.E., Orozco-Gallego, L., Gómez-Gómez, L., 1998. Períodos de
514 incubación (pi) y de latencia (pl) de la roya del cafeto en la zona cafetera central de
515 Colombia. Cenicafé 49, 325–339.
516 Li, C., Hoffland, E., Kuyper, T.W., Yu, Y., Zhang, C., Li, H., Zhang, F., Van Der Werf, W.,
517 2020. Syndromes of production in intercropping impact yield gains. Nat. Plants 6,
518 653–660. https://doi.org/10.1038/s41477-020-0680-9
519 Li, K., Hajian-Forooshani, Z., Vandermeer, J., Perfecto, I., 2023. Coffee leaf rust (Hemileia
520 vastatrix) is spread by rain splash from infected leaf litter in a semi-controlled
521 experiment. J Plant Pathol. https://doi.org/10.1007/s42161-023-01404-2
522 Liebig, T., Ribeyre, F., Läderach, P., Poehling, H.M., van Asten, P., Avelino, J., 2019.
523 Interactive effects of altitude, microclimate and shading system on coffee leaf rust.

524 Journal of Plant Interactions 14, 407–415.
525 https://doi.org/10.1080/17429145.2019.1643934
526 Masarirambi, M.T., Chingwara, V., Shongwe, V.D., 2009. The effect of irrigation on
527 synchronization of coffee (Coffea arabica L.) flowering and berry ripening at
528 Chipinge, Zimbabwe. Physics and Chemistry of the Earth, Parts A/B/C 34, 786–789.
529 https://doi.org/10.1016/j.pce.2009.06.013
530 McCook, S., Vandermeer, J., 2015. The Big Rust and the Red Queen: Long-term perspectives
531 on coffee rust research. Phytopathology 105, 1164–1173.
532 https://doi.org/10.1094/PHYTO-04-15-0085-RVW
533 Moguel, P., Toledo, V.M., 1999. Biodiversity conservation in traditional coffee systems of
534 Mexico. Conservation Biology 13, 11–21. https://doi.org/10.1046/j.1523-
535 1739.1999.97153.x
536 Mora Van Cauwelaert, E., Boyer, D., Jímenez- Soto, E., Benitez, M., Harvesting trajectories in
537 large-scale coffee plantations: ecological and management drivers and implications.
538 Biorxiv
539 Mora Van Cauwelaert, E., González González, C., Boyer, D., Hajian-Forooshani, Z.,
540 Vandermeer, J., Benítez, M., 2023. Dispersal and plant arrangement condition the
541 timing and magnitude of coffee rust infection. Ecological Modelling 475, 110206.
542 https://doi.org/10.1016/j.ecolmodel.2022.110206
543 Pangga, I.B., Hanan, J., Chakraborty, S., 2011. Pathogen dynamics in a crop canopy and their
544 evolution under changing climate: Pathogen dynamics and evolution. Plant
545 Pathology 60, 70–81. https://doi.org/10.1111/j.1365-3059.2010.02408.x
546 Papaïx, J., Burdon, J.J., Zhan, J., Thrall, P.H., 2015. Crop pathogen emergence and evolution
547 in agro-ecological landscapes. Evolutionary Applications 8, 385–402.
548 https://doi.org/10.1111/eva.12251

549 Park, A.W., Gubbins, S., Gilligan, C.A., 2001. Invasion and persistence of plant parasites in a
550 spatially structured host population. Oikos 94, 162–174.
551 https://doi.org/10.1034/j.1600-0706.2001.10489.x
552 Perfecto, I., Jiménez-Soto, M. E., & Vandermeer, J. 2019. Coffee landscapes shaping
553 the Anthropocene: forced simplification on a complex agroecological landscape.
554 *Current Anthropology*, *60*(S20), S236-S250. https://doi.org/10.1086/703413
555 Perfecto, I., Vandermeer, J., 2016. Coffee Agroecology: A New Approach to Understanding
556 Agricultural Biodiversity, Ecosystem Services and Sustainable Development,
557 American Entomologist. https://doi.org/10.1093/ae/tmw084
558 Ramírez-Camejo, L.A., Keith, L.M., Matsumoto, T., Sugiyama, L., Fukada, M., Brann, M.,
559 Moffitt, A., Liu, J., Aime, M.C., 2022. Coffee Leaf Rust (Hemileia vastatrix) from the
560 Recent Invasion into Hawaii Shares a Genotypic Relationship with Latin American
561 Populations. JoF 8, 189. https://doi.org/10.3390/jof8020189
562 Rana, A., Foster, K., Bosshard, T., Olsson, J., Bengtsson, L., 2014. Impact of climate change on
563 rainfall over Mumbai using Distribution-based Scaling of Global Climate Model
564 projections. Journal of Hydrology: Regional Studies 1, 107–128.
565 https://doi.org/10.1016/j.ejrh.2014.06.005
566 Salgado, P.R., Favarin, J.L., Leandro, R.A., De Lima Filho, O.F., 2008. Total phenol
567 concentrations in coffee tree leaves during fruit development. Scientia Agricola 65,
568 354–359. https://doi.org/10.1590/S0103-90162008000400005
569 Santos, M.C., Boyer, D., Miramontes, O., Viswanathan, G.M., Raposo, E.P., Mateos, J.L., Da
570 Luz, M.G.E., 2007. Origin of power-law distributions in deterministic walks: The
571 influence of landscape geometry. Phys. Rev. E 75, 061114.
572 https://doi.org/10.1103/PhysRevE.75.061114
573 Schieber, E., Zentmyer, G.A., 1984. Coffee Rust in Western Hemisphere. Plant Disease 68,
574 89–93.

575 Silva, M.D.C., Várzea, V., Guerra-Guimarães, L., Azinheira, H.G., Fernandez, D., Petitot,
576 A.S., Bertrand, B., Lashermes, P., Nicole, M., 2006. Coffee resistance to the main
577 diseases: Leaf rust and coffee berry disease. Brazilian Journal of Plant Physiology 18,
578 119–147. https://doi.org/10.1016/j.ijepes.2005.11.005
579 Soto-Pinto, L., Perfecto, I., Castillo-Hernandez, J., Caballero-Nieto, J., 2000. Shade effect on
580 coffee production at the northern Tzeltal Zone of the state of Chiapas, Mexico.
581 Agriculture, Ecosystems and Environment 80, 61–69.
582 https://doi.org/10.1016/S0167-8809(00)00134-1
583 Talhinhas, P., Batista, D., Diniz, I., Vieira, A., Silva, D.N., Loureiro, A., Tavares, S., Pereira,
584 A.P., Azinheira, H.G., Guerra-Guimarães, L., Várzea, V., Silva, M. do C., 2017. The
585 coffee leaf rust pathogen Hemileia vastatrix: one and a half centuries around the
586 tropics. Molecular Plant Pathology 18, 1039–1051.
587 https://doi.org/10.1111/mpp.12512
588 Vandermeer, J., Hajian-Forooshani, Z., Perfecto, I., 2018. The dynamics of the coffee rust
589 disease: an epidemiological approach using network theory. European Journal of
590 Plant Pathology 150, 1001–1010. https://doi.org/10.1007/s10658-017-1339-x
591 Vandermeer, J., Rohani, P., 2014. The interaction of regional and local in the dynamics of the
592 coffee rust disease. http://arxiv.org/abs/1407.8247
593 Waller, J.M., 1982. Coffee rust-epidemiology and control. Crop Protection 1, 385–404.
594 https://doi.org/10.1016/0261-2194(82)90022-9
595 Waller, J.M., 1972. Coffee rust in latin america. PANS Pest Articles and News Summaries 18,
596 402–408. https://doi.org/10.1080/09670877209412699
597 Zadoks, J.C., Van Den Bosch, F., 1994. On the Spread of Plant Disease: A Theory on Foci.
598 Annu. Rev. Phytopathol. 32, 503–521.
599 https://doi.org/10.1146/annurev.py.32.090194.002443
600 Zambolim, L., 2016. Current status and management of coffee leaf rust in Brazil. Tropical
601 Plant Pathology 41, 1–8. https://doi.org/10.1007/s40858-016-0065-9

CONCLUSIONES




Conclusiones por capítulo

Capítulo I.

1- El crecimiento de la incidencia de la roya en las parcelas tiene una fase de retraso desde el inicio de la temporada de lluvias hasta la fase de crecimiento en sí de la epidemia. Ambas fases son muy variables temporalmente y juntas pueden tomar entre 95 y 325 días. La fase de crecimiento se traslapa con el periodo de cosecha.

2. Al sobrepasar un umbral de agregación de siembra, la dispersión por splash (entre planta y planta) conjuntamente a los ciclos de infección, son suficientes para infectar parcelas completas de 50 plantas a partir de un solo foco de infección, durante la temporada de lluvias. Esto lleva a incidencias a nivel de parcela del 80%.

3. Debajo del umbral de agregación, el alcance de la infección hacia todas las plantas de la parcela disminuye, generando curvas escalonadas de incidencia y llegando a niveles de 40% de incidencia cuando acaba la temporada de lluvias.

4. Una menor infección inicial de las plantas aumenta la duración del retraso inicial, y una mayor tasa de caída de las hojas disminuye la infección en cada planta. Ambas se reflejan en una menor incidencia máxima en la parcela.

Capítulo II

1. La trayectoria durante la cosecha se puede describir mediante un modelo de distribución de dos estados que corresponden a dos comportamientos cualitativamente distintos: el asociado a la cosecha de plantas vecinas en el *pante* (estado *colecta*) y el asociado al movimiento de los tapiscadores a otra zona del *pante* o de la plantación (estado *búsqueda*).

2. En la parcela que identificamos como orgánica, el estado *búsqueda* genera una distribución con pasos de hasta 100 m entre diferentes zonas de la plantación, lo que se deriva en una mayor área visitada por día. Esto puede deberse a una mayor asincronicidad en la maduración de los frutos

o a una menor carga frutal cuando se tomaron los datos, o incluso a un mayor número de tapiscadores por área de cosecha.

3. Las trayectorias con más árboles visitados por día, y con una mayor cantidad de pasos largos pueden incrementar de manera potencial la dispersión de roya u otros patógenos a diferentes zonas de la plantación.

4. El tipo de cosecha se deriva del síndrome de producción de plantaciones cafetaleras que siguen un criterio de maximización de ganancia a corto plazo. Implementar manejos que reduzcan la posible dispersión de la roya, al tiempo que garanticen condiciones dignas de trabajo, podría llevar a una reducción de la cosecha a corto plazo, lo que implicaría modificar el propio síndrome y objetivo de la producción.

Capítulo III

1. La maduración asíncrona de las plantas promueve la presencia de saltos largos en la trayectoria de cosecha, en particular hacia el final del evento de cosecha en donde hay una escasez generalizada de árboles sin frutos.

2. La dispersión por el movimiento de los cosechadores aumenta significativamente la incidencia de roya en comparación a parcelas en donde solo la dispersión por contacto entre plantas está presente. El efecto del movimiento sobre el incremento de roya es mayor con trayectorias con una mayor presencia de saltos largos (15% de incremento en la incidencia) .

3. El efecto de la cosecha es mayor a densidades intermedias de siembra. A densidades bajas las nuevas infecciones generadas durante la cosecha se quedan localizadas en conjuntos aislados de plantas. A mayor densidad, casi todas las plantas se infectan por la dispersión por contacto entre plantas, por lo que en la cosecha se infectan pocos nuevos conjuntos de plantas.

4. La asincronía en la maduración del café está asociada con prácticas que reducen el impacto de la roya (variabilidad genética, presencia de sombra) y mantienen la biodiversidad. Por ello, es importante encontrar formas de reducir los saltos largos que puedan dispersar los patógenos en estos escenarios, tales como evitar la cosecha cuando hay una escasez generalizada de árboles con frutos.

Conclusiones generales

A lo largo de esta tesis buscamos explorar el papel de los modos de dispersión de la roya del café sobre su incidencia en cafetales con diferentes manejos agrícolas. Pusimos a prueba por medio de modelos computacionales y modelos estadísticos el efecto de dos mecanismos de dispersión: la dispersión entre planta y planta por medio del *splash* y una dispersión de corto y largo alcance por medio de las personas durante la cosecha. Evaluamos su efecto sobre la incidencia de roya en parcelas con diferentes manejos agrícolas, simulados mediante cambios en la densidad o en el arreglo de siembra de las plantas de café, pero también simulados a través de diferentes trayectorias de cosecha. Aunado a esto revisamos la relación entre estas diferentes formas de manejo y el síndrome general de producción de café .

Analizar la relación de procesos epidémicos con el manejo agrícola es relevante. Regresa el énfasis sobre el desarrollo de prácticas preventivas ante el surgimiento de estas plagas de importancia económica y social. Cuando los organismos no son pensados como plagas en sí, sino como indicadores de perturbación de un agroecosistema, podemos entender que en varios sitios del mundo la roya esté presente en el cafetal, sin por ello implicar una afectación para las y los productores (H. Morales y Perfecto, 2000; Perfecto y Vandermeer, 2016). En este sentido, el manejo agroecológico de la roya debe buscar promover mecanismos autónomos, es decir, nada o poco dependientes de insumos externos, que mantengan cada organismo de la comunidad en niveles poblacionales aceptables y promuevan la biodiversidad. Además, debe buscar mantener una producción agrícola sostenible en el tiempo y garantizar condiciones de trabajo y salud dignas para las productoras.

Cada mecanismo de dispersión puede tener uno o varios manejos preventivos asociados, buscando evitar que la roya llegue a las parcelas o, si ya está en ellas, que no se expanda descontroladamente. En el caso de la dispersión por viento se ha propuesta la siembra de

árboles corta viento con diferentes características funcionales para reducir su impacto (Gagliardi et al., 2020; Rayner, 1972). En el caso de la dispersión entre planta y planta (por *splash* o por contacto entre ramas), se ha sugerido evitar arreglos de siembra regulares o densos que pueden llevar a transiciones críticas en el crecimiento de la epidemia (Hajian-Forooshani and Vandermeer, 2021). Tener otros cultivos en la parcela también aumenta la distancia entre plantas de café, lo que reduce su dispersión entre planta y planta e impacto.

Esto va acorde a nuestros resultados. Tanto en el primer modelo matemático compartimentalizado con dispersión por *splash* (capítulo I) como en los escenarios control del modelo cualitativo de cosecha–en dónde sólo la dispersión por contacto entre planta y planta estaba presente-- (capítulo III), sobrepasar un umbral de agregación de las plantas lleva a un crecimiento no lineal en la incidencia de la roya a nivel de parcela. Esto no implica únicamente reducir la densidad de siembra: se pueden pensar arreglos espaciales de plantas por grupos alejados entre sí, lo que evita la dispersión de la roya a toda la parcela (Hajian-Forooshani y Vandermeer, 2021).

La dispersión por *splash* es mayor durante la temporada de lluvias e interactúa con la constante producción de esporas generadas en los nuevos ciclos de infección (Avelino y Rivas, 2013). En este sentido, tiene un papel mayor en el crecimiento de la epidemia, pero también está limitada por la propia duración de la temporada de lluvias (Bock, 1962c). En nuestro modelo, observamos que si la roya no alcanza a dispersarse a toda la parcela antes del final de la temporada de lluvias, la incidencia alcanzada ese en ciclo se reduce considerablemente. Por ello, algunas medidas para reducir la incidencia de la roya pueden incluir retrasar el inicio de la epidemia reduciendo el inóculo inicial en las plantas, inhibir la reproducción de hongo quitando las hojas infectadas, o retrasar la dispersión de planta a planta alejando las plantas de café entre sí. En cambio, la dispersión por contacto entre plantas no está directamente limitada por la temporada de lluvias y puede actuar durante todo el año. La única limitación es que las esporas ya no se reproducen cuando la humedad relativa es muy baja (Nutman et al., 1963) por lo que la magnitud de esporas transportadas por este mecanismo debería ser menor. El papel del contacto entre plantas puede sobre todo aumentar la cantidad de inóculo residual para la siguiente temporada de infección.

Por otro lado, en este trabajo exploramos el papel de dispersión por el movimiento de los humanos durante la cosecha. Nuestros resultados muestran que el manejo de gran escala dentro

de un síndrome de producción capitalista promueve trayectorias de cosecha diarias muy largas, y cuando se combina con periodos de asincronía en la maduración del cafeto, particularmente a inicios o finales de la temporada, se generan saltos que conectan zonas lejanas de las plantaciones. Esto tiene un potencial muy alto para el movimiento de esporas, sobre todo a finales de la temporada de cosecha en donde, además, hay una mayor incidencia de roya (Avelino et al., 1993). Así, además de lo mencionado anteriormente, para evitar una dispersión importante de fitopatógenos, un manejo agroecológico debería promover jornadas de cosecha menos largas –haciéndolo a su vez menos extenuante para los trabajadores-- y que no se concentren a finales de la temporada en donde la carga frutal es baja y la asincronía en la maduración entre árboles es muy alta. Estas medidas implican una reducción a corto plazo de la producción diaria o de la temporada, en pos de una producción sostenible a largo plazo, por lo que presupone la capacidad social de decidir cómo y para qué se produce café, en qué escalas y con qué prácticas.

Esperamos que nuestra aproximación, en gran parte teórica y con modelos mecanísticos, puede contribuir a educar la intuición sobre el efecto de los modos de dispersión de la roya sobre a incidencia de roya y su relación con las diferentes formas de producir y manejar los agroecosistemas de café. Nuestro objetivo es que sea un paso más para el diseño de manejos agrícolas que sean sostenibles, productivos y socialmente justos.

REFERENCIAS

Altieri, M. A., Hecht, S., Liebman, M., Madgoff, F., Norgaard, R., y Sikor, T. O. (1999). *Agroecología: Bases científicas para una agricultura sustentable*. Nordan Comunidad.

Andow, D. A. (1983). The extent of monoculture and its effects on insect pest populations with particular reference to wheat and cotton. *Agriculture, Ecosystems and Environment*, *9*(1), 25–35. https://doi.org/10.1016/0167-8809(83)90003-8

Andow, D. A., y Hidaka, K. (1989). Experimental natural history of sustainable agriculture: Syndromes of production. *Agriculture, Ecosystems & Environment*, *27*(1–4), 447–462. https://doi.org/10.1016/0167-8809(89)90105-9

Avelino, J., Cristancho, M., Georgiou, S., Imbach, P., Aguilar, L., Bornemann, G., Läderach, P., Anzueto, F., Hruska, A. J., y Morales, C. (2015). The coffee rust crises in Colombia and Central America (2008–2013): Impacts, plausible causes and proposed solutions. *Food Security*, *7*(2), 303–321. https://doi.org/10.1007/s12571-015-0446-9

Avelino, J., Muller, R. A., Cilas, C., y Velasco Pascual, H. (1991). Développement et comportement de la rouille orangée du caféier (Hemileia vastatrix Berk. Et Br.) dans des plantations en cours de modernisation, plantées de variétés naines, dans le sud-est du Mexique. *Café, Cacao, Thé*, *35*(1), 21–37. https://agritrop.cirad.fr/416561/

Avelino, J., y Rivas, G. (2013). La roya anaranjada del cafeto. *HAL Id : hal-01071036*.

Avelino, J., Romero-Gurdián, A., Cruz-Cuellar, H. F., y Declerck, F. A. J. (2012). Landscape context and scale differentially impact coffee leaf rust, coffee berry borer, and coffee root-knot nematodes. *Ecological Applications*, *22*(2), 584–596. https://doi.org/10.1890/11-0869.1

Avelino, J., Toledo, J. C., y Medina, B. (1993). Développement de la rouille orangée (Hemileia vastatrix) dans une plantation du sud-ouest du Guatemala et évaluation des dégâts qu'elle provoque. *ASIC 15th International Conference on Coffee Science*, 293–302. https://agritrop.cirad.fr/466977/

Avelino, J., Willocquet, L., y Savary, S. (2004). Effects of crop management patterns on coffee rust epidemics. *Plant Pathology*, *53*(5), 541–547. https://doi.org/10.1111/j.1365-3059.2004.01067.x

Avelino, J., Zelaya, H., Merlo, A., Pineda, A., Ordoñez, M., y Savary, S. (2006). The intensity of a coffee rust epidemic is dependent on production situations. *Ecological Modelling*, *197*(3–4), 431–447. https://doi.org/10.1016/j.ecolmodel.2006.03.013

Ayres, P. G. (2005). *Harry Marshall Ward and the fungal thread of death*. APS Press.

Bairey, E., Kelsic, E. D., y Kishony, R. (2016). High-order species interactions shape ecosystem diversity. *Nature Communications*, *7*(1), 12285. https://doi.org/10.1038/ncomms12285

Beasley, E. M., Aristizábal, N., Bueno, E. M., y White, E. R. (2022). Spatially explicit models predict coffee rust spread in fragmented landscapes. *Landscape Ecology*, *37*(8), 2165–2178. https://doi.org/10.1007/s10980-022-01473-1

Becker, S., y Kranz, J. (1977). Comparative Studies on Dispersal of Hemileia vastratrix in Kenya. *Zeitschrift für Pflanzenkrankheiten und Pflanzenschutz / Journal of Plant Diseases and Protection*, *84*(9), 526–539. https://www.jstor.org/stable/ 43213550

Bock, K. R. (1962a). Control of coffee leaf rust in Kenya Colony. *Transactions of the British Mycological Society*, *45*(3), 301–313. https://doi.org/10.1016/s0007-1536(62)80069-2

Bock, K. R. (1962b). Dispersal of uredospores of Hemileia vastatrix under field conditions. *Transactions of the British Mycological Society*, *45*(1), 63–74. https://doi.org/10.1016/s0007-1536(62)80035-7

Bock, K. R. (1962c). Seasonal periodicity of coffee leaf rust and factors affecting the severity of outbreaks in Kenya Colony. *Transactions of the British Mycological Society*, *45*(3), 289–300. https://doi.org/10.1016/s0007-1536(62)80068-0

Boudrot, A., Pico, J., Merle, I., Granados, E., Vílchez, S., Tixier, P., De Melo Virginio Filho, E., Casanoves, F., Tapia, A., Allinne, C., Rice, R. A., y Avelino, J. (2016). Shade effects on the dispersal of airborne Hemileia vastatrix uredospores. *Phytopathology*, *106*(6), 527–580. https://doi.org/10.1094/PHYTO-02-15-0058-R

Bowden, J., Gregory, P. H., y Johnson, C. G. (1971). Possible Wind Transport of Coffee Leaf Rust across the Atlantic Ocean. *Nature*, *229*(5285), 500–501. https://doi.org/10.1038/229500b0

Brown, C. T., Liebovitch, L. S., y Glendon, R. (2007). Lévy Flights in Dobe Ju/'hoansi Foraging Patterns. *Human Ecology*, *35*(1), 129–138. https://doi.org/10.1007/s10745-006-9083-4

Cannell, M. G. R. (1974). Factors affecting Arabica coffee bean size in Kenya. *Journal of Horticultural Science*, *49*(1), 65–76. https://doi.org/10.1080/00221589.1974.11514552

Carvalho, C. R., Fernandes, R. C., Carvalho, G. M. A., Barreto, R. W., y Evans, H. C. (2011). Cryptosexuality and the Genetic Diversity Paradox in Coffee Rust, Hemileia vastatrix. *PLoS ONE*, *6*(11), 1–7. https://doi.org/10.1371/journal.pone.0026387

Cerda, R., Avelino, J., Gary, C., Tixier, P., Lechevallier, E., y Allinne, C. (2017). Primary and secondary yield losses caused by pests and diseases: Assessment and modeling in coffee. *PLoS ONE*, *12*(1), 1–17. https://doi.org/10.1371/journal.pone.0169133

Clarence-Smith, W. G., y Topik, S. (Eds.). (2003). *The global coffee economy in Africa, Asia and Latin America, 1500-1989*. Cambridge University Press.

Crowe, T. J. (1963). Possible insect vectors of the uredospores of Hemileia vastatrix in Kenya. *Transactions of the British Mycological Society*, *46*(1), 24–26.

Cunniffe, N. J., y Gilligan, C. A. (2010). Invasion, persistence and control in epidemic models for plant pathogens: The effect of host demography. *Journal of the Royal Society Interface*, *7*(44), 439–451. https://doi.org/10.1098/rsif.2009.0226

Dannemann, T., Boyer, D., y Miramontes, O. (2018). Lévy flight movements prevent extinctions and maximize population abundances in fragile Lotka-Volterra systems. *Proceedings of the National Academy of Sciences of the United States of America*, *115*(15), 3794–3799. https://doi.org/10.1073/pnas.1719889115

Dennill, G. B., y Moran, V. C. (1989). On insect-plant associations in agriculture and the selection of agents for weed biocontrol. *Annals of Applied Biology*, *114*(1), 157–166. https://doi.org/10.1111/j.1744-7348.1989.tb06796.x

Djuikem, C., Grognard, F., Wafo, R. T., Touzeau, S., y Bowong, S. (2021). Modelling coffee leaf rust dynamics to control its spread. *Mathematical Modelling of Natural Phenomena*, *16*, 26. https://doi.org/10.1051/mmnp/2021018

Dupont, S., Irvine, M. R., Motisi, N., Allinne, C., Avelino, J., y Bagny Beilhe, L. (2022). Wind-flow dynamics and spore-like particle dispersal over agroforestry systems: Impact of the tree density distribution. *Agricultural and Forest Meteorology*, *327*, 109214. https://doi.org/10.1016/j.agrformet.2022.109214

Eskes, A. B., y Toma-Braghini, M. (1982). The effect of leaf age on incomplete resistance of coffee to Hemileia vastatrix. *Netherlands Journal of Plant Pathology*, *88*(6), 219–230. https://doi.org/10.1007/BF02000128

Flores Vichi, F. (2015). La producción de café en México: Ventana de oportunidad para el sector agrícola de Chiapas. *Revista Espacio I+D Innovación más Desarrollo*, *4*(7), 174–194. https://doi.org/10.31644/IMASD.7.2015.a07

Gagliardi, S., Avelino, J., Beilhe, L. B., y Isaac, M. E. (2020). Contribution of shade trees to wind dynamics and pathogen dispersal on the edge of coffee agroforestry systems: A

functional traits approach. *Crop Protection*, *130*(December 2019), 105071. https://doi.org/10.1016/j.cropro.2019.105071

Garedew, W., Lemessa, F., y Pinard, F. (2019). Landscape context and plot features influence the epidemics of coffee leaf rust (Hemileia vastatrix) in southwest Ethiopia. *Archives of Phytopathology and Plant Protection*, *52*(1–2), 71–89. https://doi.org/10.1080/03235408.2019.1580177

Gilligan, C. A. (2002). An epidemiological framework for disease management. En *Advances in Botanical Research* (Vol. 38). https://doi.org/10.1016/s0065-2296(02)38027-3

González González, C., Mora Van Cauwelaert, E., Boyer, D., Perfecto, I., Vandermeer, J., y Benítez, M. (2021). High-order interactions maintain or enhance structural robustness of a coffee agroecosystem network. *Ecological Complexity*, *47*, 100951. https://doi.org/10.1016/j.ecocom.2021.100951

Gubbins, S., Gilligan, C. A., y Kleczkowski, A. (2000). Population dynamics of plant-parasite interactions: Thresholds for invasion. *Theoretical Population Biology*, *57*(3), 219–233. https://doi.org/10.1006/tpbi.1999.1441

Guzman, O., y Gomez, L. (1987). Permanence of free water on coffee leaves. *Experimental Agriculture*, *23*(1987), 213–220.

Hajian-Forooshani, Z., Perfecto, I., y Vandermeer, J. (2023). Novel community assembly and the control of a fungal pathogen in coffee agroecosystems. *Biological Control*, *177*, 105099. https://doi.org/10.1016/j.biocontrol.2022.105099

Hajian-Forooshani, Z., y Vandermeer, J. (2021). Emergent spatial structure and pathogen epidemics: The influence of management and stochasticity in agroecosystems. *Ecological Complexity*, *45*, 100872. https://doi.org/10.1016/j.ecocom.2020.100872

Hawaï-Deparment of Agriculture. (2020). *Coffee Leaf Rust Confirmed on Hawaï Island*. https://hdoa.hawaii.gov/blog/main/nr20-17-clrconfirmedonhawaiiisland/

Hilje, L., Araya, M. C., y Valverde, B. E. (2003). Pest management in Mesoamerican agroecosystems. En J. Vandermeer (Ed.), *Tropical Agroecosystems*. CRC Press.

Jackson, D., Skillman, J., y Vandermeer, J. (2012). Indirect biological control of the coffee leaf rust, Hemileia vastatrix, by the entomogenous fungus Lecanicillium lecanii in a complex coffee agroecosystem. *Biological Control*, *61*(1), 89–97. https://doi.org/10.1016/j.biocontrol.2012.01.004

Jiménez-Soto, E. (2021). The political ecology of shaded coffee plantations: Conservation narratives and the everyday-lived-experience of farmworkers. *Journal of Peasant Studies*, *48*(6), 1284–1303. https://doi.org/10.1080/03066150.2020.1713109

Keeling, M. J. (1999). The effects of local spatial structure on epidemiological invasions. *Proceedings of the Royal Society B: Biological Sciences*, *266*(1421), 859–867. https://doi.org/10.1098/rspb.1999.0716

Kim, K., y McPheron, B. A. (Eds.). (1993). *Evolution of insect pests: Patterns of variation*. Wiley.

Kushalappa, A. C., y Eskes, A. B. (1989). Advances in Coffee Rust Research. *Annual Review of Phytopathology*, *27*(1), 503–531. https://doi.org/10.1146/annurev.py.27.090189.002443

Levine, J. M., Bascompte, J., Adler, P. B., y Allesina, S. (2017). Beyond pairwise mechanisms of species coexistence in complex communities. *Nature*, *546*(7656), 56–64. https://doi.org/10.1038/nature22898

Levins, R. (1966). The Strategy of Model Building in Population Biology. *American Scientist*, *54*(4), 421–421. https://www.jstor.org/stable/27836590

Levins, R., y Wilson, M. (1980). Ecological Theory and Pest Management. *Annual Review of Entomology*, *25*(1), 287–308. https://doi.org/10.1146/annurev.en.25.010180.001443

Li, K., Hajian-Forooshani, Z., Su, C., Perfecto, I., y Vandermeer, J. (2022). Reduced rainfall and resistant varieties mediate a critical transition in the coffee rust disease. *Scientific Reports*, *12*(1), 1–9. https://doi.org/10.1038/s41598-022-05362-0

Li, K., Hajian-Forooshani, Z., Vandermeer, J., y Perfecto, I. (2023). Coffee leaf rust (Hemileia vastatrix) is spread by rain splash from infected leaf litter in a semi-controlled experiment. *Journal of Plant Pathology*. https://doi.org/10.1007/s42161-023-01404-2

Lin, B. B. (2007). Agroforestry management as an adaptive strategy against potential microclimate extremes in coffee agriculture. *Agricultural and Forest Meteorology*, *144*(1–2), 85–94. https://doi.org/10.1016/j.agrformet.2006.12.009

López Echeverría, M. E. (2006). *Identidad, autonomía y cultura: El espiritú del capitalismo en las Fincas Cafetaleras Alemanas en el Soconusco (1850-2006)*. http://tesiuami.izt.uam.mx/uam/aspuam/presentatesis.php?recno=13595&docs=UAMI13595.pdf

López-Bravo, D. F., Virginio-Filho, E. de M., y Avelino, J. (2012). Shade is conducive to coffee rust as compared to full sun exposure under standardized fruit load conditions. *Crop Protection*, *38*, 21–29. https://doi.org/10.1016/j.cropro.2012.03.011

Manlove, K., Wilber, M., White, L., Bastille-Rousseau, G., Yang, A., Gilbertson, M. L. J., Craft, M. E., Cross, P. C., Wittemyer, G., y Pepin, K. M. (2022). Defining an epidemiological landscape that connects movement ecology to pathogen transmission and pace-of-life. *Ecology Letters*, *25*(8), 1760–1782. https://doi.org/10.1111/ele.14032

Masarirambi, M. T., Chingwara, V., y Shongwe, V. D. (2009). The effect of irrigation on synchronization of coffee (Coffea arabica L.) flowering and berry ripening at Chipinge, Zimbabwe. *Physics and Chemistry of the Earth, Parts A/B/C*, *34*(13–16), 786–789. https://doi.org/10.1016/j.pce.2009.06.013

McCook, S., y Vandermeer, J. (2015). The Big Rust and the Red Queen: Long-term perspectives on coffee rust research. *Phytopathology*, *105*(9), 1164–1173. https://doi.org/10.1094/PHYTO-04-15-0085-RVW

Merle, I., Pico, J., Granados, E., Boudrot, A., Tixier, P., de Melo Virginio Filho, E., Cilas, C., y Avelino, J. (2020). Unraveling the complexity of coffee leaf rust behavior and development in different coffea arabica agroecosystems. *Phytopathology*, *110*(2), 418–427. https://doi.org/10.1094/PHYTO-03-19-0094-R

Michelot, T., y Blackwell, P. G. (2019). State-switching continuous-time correlated random walks. *Methods in Ecology and Evolution*, *10*(5), 637–649. https://doi.org/10.1111/2041-210X.13154

Moguel, P., y Toledo, V. M. (1999). Biodiversity conservation in traditional coffee systems of Mexico. *Conservation Biology*, *13*(1), 11–21. https://doi.org/10.1046/j.1523-1739.1999.97153.x

Mora Van Cauwelaert, E., González González, C., Boyer, D., Hajian-Forooshani, Z., Vandermeer, J., y Benítez, M. (2023). Dispersal and plant arrangement condition the timing and magnitude of coffee rust infection. *Ecological Modelling*, *475*, 110206. https://doi.org/10.1016/j.ecolmodel.2022.110206

Morales, H., y Perfecto, I. (2000). Traditional knowledge and pest management in the Guatemalan highlands. *Agriculture and Human Values*, *17*(1), 49–63. https://doi.org/10.1023/A:1007680726231

Morales, J. M., Haydon, D. T., Frair, J., Holsinger, K. E., y Fryxell, J. M. (2004). Extracting More Out of Relocation Data: Building Movement Models as Mixtures of Random Walks. *Ecology*, *85*(9), 2436–2445. https://doi.org/10.1890/03-0269

Mulinge, S. K., y Griffiths, E. (1974). Effects of fungicides on leaf rust, berry disease, foliation and yield of coffee. *Transactions of the British Mycological Society*, *62*(3), 495–507. https://doi.org/10.1016/s0007-1536(74)80061-6

Nutman, F. J., y Roberts, F. M. (1970). Coffee leaf rust. *PANS Pest Articles and News Summaries*, *16*(4), 606–624. https://doi.org/10.1080/09670877009413428

Nutman, F. J., Roberts, F. M., y Clarke, R. T. (1963). Studies on the biology of Hemileia vastatrix Berk. & Br. *Transactions of the British Mycological Society*, *46*(1), 27–44. https://doi.org/10.1016/s0007-1536(63)80005-4

Ong, T. W. Y., y Liao, W. (2020). Agroecological Transitions: A Mathematical Perspective on a Transdisciplinary Problem. *Frontiers in Sustainable Food Systems*, *4*, 91. https://doi.org/10.3389/fsufs.2020.00091

Papaïx, J., Adamczyk-Chauvat, K., Bouvier, A., Kiêu, K., Touzeau, S., Lannou, C., y Monod, H. (2014). Pathogen population dynamics in agricultural landscapes: The Ddal modelling framework. *Infection, Genetics and Evolution*, *27*, 509–520. https://doi.org/10.1016/j.meegid.2014.01.022

Paré, L. (1990). ¿Adelgazamiento del INMECAFE o de los pequeños productores de café? *Sociológica - Universidad Autonoma Metropolitana*, *5*(13).

Park, A. W., Gubbins, S., y Gilligan, C. A. (2001). Invasion and persistence of plant parasites in a spatially structured host population. *Oikos*, *94*(1), 162–174. https://doi.org/10.1034/j.1600-0706.2001.10489.x

Patterson, T., Thomas, L., Wilcox, C., Ovaskainen, O., y Matthiopoulos, J. (2008). State–space models of individual animal movement. *Trends in Ecology & Evolution*, *23*(2), 87–94. https://doi.org/10.1016/j.tree.2007.10.009

Perfecto, I., y Vandermeer, J. (2016). Coffee Agroecology: A New Approach to Understanding Agricultural Biodiversity, Ecosystem Services and Sustainable Development. En *American Entomologist* (Vol. 62). https://doi.org/10.1093/ae/tmw084

Quezada, J. R., y DeBach, P. (1973). Bioecological and population studies of the cottony-cushion scale, *Icerya purchasi* Mask., and its natural enemies, *Rodolia cardinalis* Mul. And *Cryptochaetum iceryae* Will., in southern California. *Hilgardia*, *41*(20), 631–688. https://doi.org/10.3733/hilg.v41n20p631

Ramírez-Camejo, L. A., Keith, L. M., Matsumoto, T., Sugiyama, L., Fukada, M., Brann, M., Moffitt, A., Liu, J., y Aime, M. C. (2022). Coffee Leaf Rust (Hemileia vastatrix) from the Recent Invasion into Hawaii Shares a Genotypic Relationship with Latin American Populations. *Journal of Fungi*, *8*(2), 189. https://doi.org/10.3390/jof8020189

Rayner, R. W. (1961). Germination and penetration studies on coffee rust (Hemileia vastatrix B. & Br.). *Annals of Applied Biology*, *49*(3), 497–505. https://doi.org/10.1111/j.1744-7348.1961.tb03641.x

Rayner, R. W. (1972). *Micología, historia y biología de la roya del cafeto*. Instituto Interamericano de Ciencias Agricolas de la OEA. Centro Tropical de Enseñanza e Investigación.

Reynolds, A., Ceccon, E., Baldauf, C., Medeiros, T. K., y Miramontes, O. (2018). Lévy foraging patterns of rural humans. *PLoS ONE*, *13*(6), 1–16. https://doi.org/10.1371/journal.pone.0199099

Rosas, J., de Assis Silva, S., de Almeida, S., Medauar, C., Moraes, W., y de Souza Lima, J. (2021). Spatial and temporal behavior of coffee rust in C. canephora and its effects on crop yield. *European Journal of Plant Pathology*. https://doi.org/10.1007/s10658-021-02352-2 Spatial

Schieber, E. (1972). Economic Impact of Coffee Rust in Latin America. *Annual Review of Phytopathology*, *10*(1), 491–510. https://doi.org/10.1146/annurev.py.10.090172.002423

Silva, M. D. C., Várzea, V., Guerra-Guimarães, L., Azinheira, H. G., Fernandez, D., Petitot, A. S., Bertrand, B., Lashermes, P., y Nicole, M. (2006). Coffee resistance to the main diseases: Leaf rust and coffee berry disease. *Brazilian Journal of Plant Physiology*, *18*(1), 119–147. https://doi.org/10.1016/j.ijepes.2005.11.005

Soto-Pinto, L., Perfecto, I., Castillo-Hernandez, J., y Caballero-Nieto, J. (2000). Shade effect on coffee production at the northern Tzeltal Zone of the state of Chiapas, Mexico. *Agriculture, Ecosystems and Environment*, *80*(1–2), 61–69. https://doi.org/10.1016/S0167-8809(00)00134-1

Sylvain, P. G. (1958). Ethiopian coffee—Its significance to world coffee problems. *Economic Botany*, *12*(2), 111–139. https://doi.org/10.1007/BF02862767

Talhinhas, P., Batista, D., Diniz, I., Vieira, A., Silva, D. N., Loureiro, A., Tavares, S., Pereira, A. P., Azinheira, H. G., Guerra-Guimarães, L., Várzea, V., y Silva, M. do C. (2017). The coffee leaf rust pathogen Hemileia vastatrix: One and a half centuries around the tropics. *Molecular Plant Pathology*, *18*(8), 1039–1051. https://doi.org/10.1111/mpp.12512

Urbina, H., y Aime, M. C. (2023). The first USA continental record of coffee leaf rust (*Hemileia vastatrix*) on coffee (*Coffea arabica*) in southwest Florida, USA. *Plant Disease*, PDIS-09-23-1869-PDN. https://doi.org/10.1094/PDIS-09-23-1869-PDN

Van Den Bosch, R. (1979). The Pesticide Problem. *Environment: Science and Policy for Sustainable Development*, *21*(4), 12–42. https://doi.org/10.1080/00139157.1979.9929720

Van Driesche, R. G., y Bellows, T. S. (1996). Pest Origins, Pesticides, and the History of Biological Control. En R. G. Van Driesche y T. S. Bellows, *Biological Control* (pp. 3–20). Springer US. https://doi.org/10.1007/978-1-4613-1157-7_1

Vandermeer, J., Armbrecht, I., De La Mora, A., Ennis, K. K., Fitch, G., Gonthier, D. J., Hajian-Forooshani, Z., Hsieh, H. Y., Iverson, A., Jackson, D., Jha, S., Jiménez-Soto, E., Lopez-Bautista, G., Larsen, A., Li, K., Liere, H., MacDonald, A., Marin, L., Mathis, K. A., … Perfecto, I. (2019). The Community Ecology of Herbivore Regulation in an Agroecosystem: Lessons from Complex Systems. *BioScience*, *69*(12), 974–996. https://doi.org/10.1093/biosci/biz127

Vandermeer, J., Hajian-Forooshani, Z., y Perfecto, I. (2018). The dynamics of the coffee rust disease: An epidemiological approach using network theory. *European Journal of Plant Pathology*, *150*(4), 1001–1010. https://doi.org/10.1007/s10658-017-1339-x

Vandermeer, J., y Perfecto, I. (2012). Syndromes of production in agriculture: Prospects for social-ecological regime change. *Ecology and Society*, *17*(4). https://doi.org/10.5751/ES-04813-170439

Vandermeer, J., y Perfecto, I. (2018). *Ecological Complexity and Agroecology*. Routledge.

Vandermeer, J., y Rohani, P. (2014). *The interaction of regional and local in the dynamics of the coffee rust disease*. http://arxiv.org/abs/1407.8247

Vandermeer, J., Rohani, P., y Perfecto, I. (2015). *Local dynamics of the coffee rust disease and the potential effect of shade*. 1–6. https://doi.org/10.48550/arXiv.1510.05849

Waller, J. M. (1972). Coffee rust in latin america. *PANS Pest Articles and News Summaries*, *18*(4), 402–408. https://doi.org/10.1080/09670877209412699

Waller, J. M. (1981). The recent spread of some tropical plant diseases. *Tropical Pest Management*, *27*(3), 360–362. https://doi.org/10.1080/09670878109413805

White, L. A., Forester, J. D., y Craft, M. E. (2018). Disease outbreak thresholds emerge from interactions between movement behavior, landscape structure, and epidemiology. *Proceedings of the National Academy of Sciences*, *115*(28), 7374–7379. https://doi.org/10.1073/pnas.1801383115

Xiao, J., Li, Y., Chu, C., Wang, Y., Meiners, S. J., y Stouffer, D. B. (2020). Higher-order interactions mitigate direct negative effects on population dynamics of herbaceous plants during succession. *Environmental Research Letters*, *15*(7), 074023. https://doi.org/10.1088/1748-9326/ab8a88

Zadoks, J. C. (1999). Reflections on Space, Time and Diversity. *Annual Review of Phytopathology*, *37*, 1–17. https://doi.org/10.1146/annurev.phyto.37.1.1

Zewdie, B., Tack, A. J. M., Adugna, G., Nemomissa, S., y Hylander, K. (2020). Patterns and drivers of fungal disease communities on Arabica coffee along a management gradient. *Basic and Applied Ecology*, *47*, 95–106. https://doi.org/10.1016/j.baae.2020.05.002

APÉNDICES

Apéndice 1 - Factores climáticos, biológicos y de manejo que afectan el ciclo de vida de la roya (*Hemileia vastatrix*)

Tabla 1A- Factores que afectan el proceso de infección

Tabla 1B. Factores que afectan el proceso de dispersión

Tabla 1C. Factores que afectan la formación del inóculo inicial

Tabla 1A - Factores que afectan el proceso de Infección

Proceso	Unidad	Definición	Factores que influyen	Mecanismo	Referencias incluidas en (Avelino y Rivas, 2013)	Referencias adicionales
Germinación	**Hongo**	Proceso por el cual sale la hifa de la espora con recursos propios	Temperatura	La germinación óptima es bimodal 21 y 25ºC. El frio (5°C) previo promueve la germinación. De Jong: óptima entre 22 y 28°C.	Nutman et al., 1963	de Jong et al., 1987
			Obscuridad	En la obscuridad, la germinación es mayor	Nutman et al., 1963	
			Radiación	La radiación inhibe la esporulación	Avelino et al., 2004	
			Agua libre y sequìa	Al menos 6 horas continuas de lluvia. La humedad es esencial para germinación. La sequía interrumpe la germinación y reduce la viabilidad	Nutman et al., 1963; Avelino et al., 2004	
			Edad hoja	La "germinación" es mayor en hojas jovenes (sobre todo cuando hay una concentración baja de esporas)	Nutman et al., 1963	
Penetración	**Hongo**	Formación del apresorio para la penetración	Temperatura	13-16º, se tienen que alternar las temperaturas	de Jong et al., 1987	
			Agua libre	24-48 horas de agua es la condición óptima para que se logre la penetración	Kushalappa et al., 1983	
	Hoja	Invasión de estomas	Variación interhoja	Hay una variabilidad muy alta entre hojas de la misma edad, mismo árbol.	Nutman et al., 1963	
			Variación interplanta	Las plantas pueden tener diferente susceptibilidad genética	Cadena-Gómez y Buritica-Céspedes, 1980	
			Edad hoja	Hojas viejas (> 6 meses) y hojas muy jóvenes son poco receptivas. Hay un óptimo que son las hojas terciopelo. Esto tiene que ver con que los estómas estén bien formados. Esporas en suspensión	Eskes y Toma-Braghini, 1982	
				Las hojas más jóvenes generaron más apresorios que las hojas viejas. Desde esporas secas	Coutinho et al., 1994	
			Temperatura	40°C durante 4 exposiciones de 4-6 horas o más mata al patógeno y detiene el progreso de la enfermdad	Ribeiro et al., 1978	
Incubación	**Hoja - Hongo**	Invasión cámaras, ramas lateraes, hifas y haustorio y otras relaciones tróficas planta-hongo	Humedad del suelo y carga fructífera	Si hay alta humedad, hay poco estrés hídrico lo que facilita la penetración por estomas. Si hay mucha carga frutífera los cmpuestos fenolicos se van a los frutos y desprotegen las hojas	Chalfoun y de Carvalho, 1987	
			Temperatura	25ºC se acorta la latencia a 17.6 días, a 21ºC - 21.6 dìas, arriba de 40ºC muere la roya		Leguizamón-Caycedo, 1998
			Variedad planta	Se expresan las resistencias del cafeto a la roya	Silva et al., 2006	
Esporulación	**Hoja - Hongo**	Se invade camara, se forma protosoro, germina y sale por estoma: se forma esporóforo	Tamaño Ostiolo	300 mil a 2 millones de esporas. Color naranja. Una lesión puede producir hasta 400 mil esporas en 3 meses	Rayner, 1972	
			Otros organismos	Lecanicillium lecanii afecta indirectamente la presenciade esporas	Vandermeer et al., 2009; Jackson et al., 2012	
			Enemigos naturales	Los caracoles se comen las esporas		Hajian-Forooshani et al., 2023
				Las larvas de Mycodiplosis y Lestodiplosis consumen las esporas		Hajian-Forooshani et al., 2016
Tiempo totales	**Hoja**	Tiempo total entre dispersión/penetración y esporulación, entre más ciclos, más infección	Todos los anteriores	Asia: 12-16 días (Sri Lanka con lluvias) 15-16(Mysore) Kenya: 23 +- 1.9 (calor) 30.4 +- 4.0 (frío) Periodos de 5 semanas Colombia: 31.55 días (sombra) 34.59 días (sol))	Rayner, 1961; Mayne, 1960; Marshal Ward citado en Shrieber, 1972	Leguizamón-Caycedo et al., 1998; Bock, 1962b

Tabla 1B - Factores que afectan el proceso de Dispersión (actualizada)

Proceso	Unidad	Definición	Factores que influyen	Mecanismo	Referencias incluidas en (Avelino y Rivas, 2013)	Referencias adicionales
Liberación	**Hoja**	Separar las esporas de los clusters	Agua (PP o rocío)	La liberación de esporas sólo es posible con agua. El splash libera una gran cantidad de esporas	Nutman et al., 1960	
				El agua debe pasar de la parte de arriba a la de abajo para llegar a las esporas. Nutman y Roberts estimaron que se necesita 0.8 mm, Kushalappa estimó 1mm y Guzmán y Gómez 5mm	Guzman y Gomez, 1987; Kushalappa, 1983	Nutman y Roberts, 1970
			Viento o vibraciones	El viento y el golpeteo de las gotas de lluvia puede liberar las esporas en seco	Rayner, 1961	
				El viento necesita 19km/h para poder liberar las esporas, por lo que no es relevante.	Nutman et al., 1960	
	Hoja	Movimiento de esporas de una zona a otra de la hoja	Insectos	Las larvas de Mycodiplosis y Lestodiplosis puede mover las esporas a lo largo de la hoja		Crowe, 1963
			Agua	El agua mueve las esporas a lo largo de la hoja y también permite salirse de la hoja (las lesiones primarias dan origen a las secundarias por el movimiento de la gota a lo largo de la hoja)	Bock, 1962a	
		Movimiento de la parte adaxial a abaxial		El agua permite que las esporas depositadas en la parte alta de la hoja pasen a la parte baja de la hoja. Demasiado lluvia lava a las esporas de las hojas	Nutman, 1963; Bock, 1962a; Rayner, 1961a; Rayner, 1961b	
	IntraPlanta	Movimiento de esporas de una hoja a otra (intra planta o entre una planta y otra conectadas por el splash o por el contacto.	Agua	Las gotas de agua permiten que la espora pueda saltar de una hoja a otra. El pico de la enfermedad es causado por la lluvia y no por el viento. El splash puede mover una y otra vez las esporas, el viento suele hacerlo solo una vez	Nutman et al., 1960; Meredith, 1973; Nutman, 1963	
				Las gotas de agua permiten que la espora pueda saltar de una hoja a otra. <0.2 in no se dispersan (se secan las hojas). 0.2-0.25 in: solo dispersa si mucho inoculo. > 0.3 in es ideal.	Bock, 1962a	
				Hay una relación directa entre la cantidad de esporas en las hojas y la temporada de lluvia. Las distribuye por toda la planta	Bock, 1962b	Nutman y Roberts, 1970
				La lluvia tira las esporas a las partes más bajas de la planta en donde comienza infección. También por el inóculo inicial	Bock, 1962b	
				La lluvia y el splash dispersan entre plantas. Pero por unidad de gota no se ven tantas esporas. Ellos no ven la relación con la cantidad de roya en las hojas, sino en el agua	Becker and Kranz, 1977	
			Contacto	El contacto entre hojas (por el movimiento de las ramas con el viento) genera modulos de plantas. Los patrones de infección de las plantas están correlacionados estadisticamente con estos módulos		Vandermeer et al., 2018
			Cantidad de hojas	Aumenta el contacto entre hjas y plantas y se correlaciona con el incremento de la epidemia		Nutman y Roberts, 1970
	Interplantas	Movimiento de esporas de una planta a otra cuando no están en contacto por el splash o físicamente	Insectos	Hay diferentes órdenes que dispersan (ver lista). Pero no es tan relevante en órdenes de magnitud. Los insectos con esporas no tienen una vagilidad grande	Becker and Kranz, 1977	
				Lestodiplosis sp and Mycodiplosis, son parasitadas por avispas Leptasis kivuensis y Synopeas sp. Se cargan de esporas y las pueden transportar. Pueden empezar una lesión y volar varios metros.		Crowe, 1963
			Otras plantas o semillas	Otros tejidos vegetales y semillas pueden dispersar la espora pero no es tan relevante en órdenes de magnitud	Becker and Kranz, 1977; Waller, 1972	
			Viento x (secas)	El viento dispersa esporas en temporada de seca. Los picos de esporas en las hojas se correlacionan con los picos de esporas en aire.		Boudrot et al., 2016
			Viento x sol	El viento es el máximo dispersor en secas con café de sol. En el café de sombra no parece tener tanto efecto.		Boudrot et al., 2016
			Viento x hora del día	La dispersión por viento ocurre a inicios de la tarde cuando la humedad relativa es más baja y el viento más fuerte	Becker, 1977	
				Según la hora del día, las capturas de esporas sigue un pico (máximo a medio día-11 am). (37% de las horas con capturas)- El pico corresponde al pico de las ráfagas de viento. En la noche la dispersión es mínima		Boudrot et al., 2016
			Viento	Las uredosporas son encontradas continuamente en el aire. Tienen una bimodalidad sincronizada con la temporada de lluvias	Becker y Kranz, 1977	

Dispersión per se			Viento x árboles	Los árboles en la parcela disminuyen la velocidad del viento y por lo tanto la dispersión. Conforme son más densos, baja más el viento y se acumulan más esporas en las cercanía (no se sabe si afecta la dispersión lejana). Afecta el tipo de árbol y también su disposición en el espacio.		Gagliardi et al., 2020
			Agua x Sombra	La lluvia tienen más relevancia en la dispersión (y en la liberación) en el café de sombra, porque la gota alcanza un mayor tamaño y cae con más inercia		Boudrot et al., 2016
			Personas	En la cosecha hay muchas esporas pegadas a la ropa. Muestran experimentalmente como una gran cantidad puede a su vez regresar a la hoja del cafè	Becker and Kranz, 1977	
				Los foci máximos de infección estaban cerca de los caminos y los centros de habitación		Waller, 1979
	Interparcela	Movimiento de esporas de una parcela a otra, o de una región a la otra	Personas	El movimiento de las esporas a través de América se tuvo que haber hecho por personas (especulativo)	Waller, 1972	
				Los foci máximos de infección estaban cerca de los caminos y los centros de habitación		Waller, 1979
				En la cosecha hay muchas esporas pegadas a la ropa. Muestran experimentalmente como una gran cantidad puede a su vez regresar a la hoja del cafè	Becker y Kranz, 1977	
				La llegada de roya a Hawaï viajó ser por material contaminado o por la ropa de las personas y no por viento		Ramirez-Carmejo et al., 2022
				La dispersión de roya a través del desierto, montañas u oceanos se tuvo que hacer a través de las personas		Berihum and Alemu, 2022
			Geometría de fuente de infección	Muestra en un estudio teórico que si la fuente de infección se desarrollo en un punto o una franja, el gradiente de esporas en el aire cambia mucho.		Gregory, 1968
			Posición relativa a la dirección de los vientos	La cantidad e infección en downwind suele ser mayor que en upwind (en general, no solo para esporas), salvo si hay muchas fluctuaciones en la dirección del viento.		Gregory, 1968
			Viento	Las uredosporas se encontraron continuamente en las capas más altas (hasta 1000 m). Teoricamente pueden cubir hasta 200 km. Es un calculo que no toma en cuenta las corrientes de aire, solo la taza de hundimiento y el tamaño.	Becker y Kranz, 1977	
				La velocidad terminal es de 0.6 cm.s-1 en esporas simples y hasta 1.2cm.s-1 en clumps de esporas por lo que sí puede cubrir grandes distancias. Proponen que en 5-7 días pudo viajar de Angola a Brazil (siguiendo las corrientes de aire principales). En Angola se reporta en 1966, en Brazil (Bahia) en 1970	Bowden et al., 1971	
				Los patrones de diseminación de la roya (norte--> sur) siguieron la dirección de los vientos. Hasta se predijio acertadamente la infección en Sao paulo y el Paraná con base en la dirección del viento.	Schieber, 1972	
				El progreso de la roya a nivel continental en América Central y sur sigue el patrón de dispersión de enfermedades de larga distancia: la velocidad de la epidemia aumenta con la distancia desde la fuente		Mundt et al., 2009 citado en (Avelino et al., 2015)
				Se encontraron esporas a 1000 m de altura y a 150 km de un sitio de infección. Además hay correlación entre la distancia al sitio de infección y el número de esporas		Instituto Brasileiro de Café citado en (Schieber, 1972)
				Las esporas se caen rápidamente (se concentran más abajo). (velocidad terminal de 10 a 20 cm.s-1 muy alta) Son muy pocas en la época de secas. No generan el built up de la epidemia.	Bock, 1962a	
				El viento no es relevante por la velocidad de caída. La detección de esporas a 1000 m no es conclusiva porque no es fácil identificar que las uredosporas son de roya de café	Waller, 1972	
				La viabilidad baja por la T y sequía (poca agua o mucho sol). La espora no puede ser viable mucho tiempo en el aire.	Bock, 1962a; Nutman et al., 1963	

Anexo 1. Factores climáticos, biológicos y sociales que afectan el ciclo de vida de la roya (*Hemilieia vastatrix*)

Tabla 1A - Factores que afectan el proceso de Infección

Proceso	Unidad	Definición	Factores que influyen	Mecanismo	Referencias incluidas en (Avelino y Rivas, 2013)	Referencias adicionales
Germinación	**Hongo**	Proceso por el cual sale la hifa de la espora con recursos propios	Temperatura	La germinación óptima es bimodal 21 y 25ºC. El frio (5°C) previo promueve la germinación. De Jong: óptima entre 22 y 28°C.	Nutman et al., 1963	de Jong et al., 1987
			Obscuridad	En la obscuridad, la germinación es mayor	Nutman et al., 1963	
			Radiación	La radiación inhibe la esporulación	Avelino et al., 2004	
			Agua libre y sequìa	Al menos 6 horas continuas de lluvia. La humedad es esencial para germinación. La sequía interrumpe la germinación y reduce la viabilidad	Nutman et al., 1963; Avelino et al., 2004	
			Edad hoja	La "germinación" es mayor en hojas jovenes (sobre todo cuando hay una concentración baja de esporas)	Nutman et al., 1963	
Penetración	**Hongo**	Formación del apresorio para la penetración	Temperatura	13-16º, se tienen que alternar las temperaturas	de Jong et al., 1987	
			Agua libre	24-48 horas de agua es la condición óptima para que se logre la penetración	Kushalappa et al., 1983	
	Hoja	Invasión de estomas	Variación interhoja	Hay una variabilidad muy alta entre hojas de la misma edad, mismo árbol.	Nutman et al., 1963	
			Variación interplanta	Las plantas pueden tener diferente susceptibilidad genética	Cadena-Gómez y Buritica-Céspedes, 1980	
			Edad hoja	Hojas viejas (> 6 meses) y hojas muy jóvenes son poco receptivas. Hay un óptimo que son las hojas terciopelo. Esto tiene que ver con que los estómas estén bien formados. Esporas en suspensión	Eskes y Toma-Braghini, 1982	
				Las hojas más jóvenes generaron más apresorios que las hojas viejas. Desde esporas secas	Coutinho et al., 1994	
			Temperatura	40°C durante 4 exposiciones de 4-6 horas o más mata al patógeno y detiene el progreso de la enfermdad	Ribeiro et al., 1978	
Incubación	**Hoja - Hongo**	Invasión cámaras, ramas lateraes, hifas y haustorio y otras relaciones tróficas planta-hongo	Humedad del suelo y carga fructífera	Si hay alta humedad, hay poco estrés hídrico lo que facilita la penetración por estomas. Si hay mucha carga frutifera los cmpuestos fenolicos se van a los frutos y desprotegen las hojas	Chalfoun y de Carvalho, 1987	
			Temperatura	25ºC se acorta la latencia a 17.6 días, a 21ºC - 21.6 dìas, arriba de 40ºC muere la roya		Leguizamón-Caycedo, 1998
			Variedad planta	Se expresan las resistencias del cafeto a la roya	Silva et al., 2006	
Esporulación	**Hoja - Hongo**	Se invade camara, se forma protosoro, germina y sale por estoma: se forma esporóforo	Tamaño Ostiolo	300 mil a 2 millones de esporas. Color naranja. Una lesión puede producir hasta 400 mil esporas en 3 meses	Rayner, 1972	
			Otros organismos	Lecanicillium lecanii afecta indirectamente la presenciade esporas	Vandermeer et al., 2009; Jackson et al., 2012	
			Enemigos naturales	Los caracoles se comen las esporas		Hajian-Forooshani et al., 2023
				Las larvas de Mycodiplosis y Lestodiplosis consumen las esporas		Hajian-Forooshani et al., 2016
Tiempo totales	**Hoja**	Tiempo total entre dispersión/penetración y esporulación, entre más ciclos, más infección	Todos los anteriores	Asia: 12-16 días (Sri Lanka con lluvias) 15-16(Mysore) Kenya: 23 +- 1.9 (calor) 30.4 +- 4.0 (frío) Periodos de 5 semanas Colombia: 31.55 días (sombra) 34.59 días (sol))	Rayner, 1961; Mayne, 1960; Marshal Ward citado en Shrieber, 1972	Leguizamón-Caycedo et al., 1998; Bock, 1962b

Apéndice 2 - High-order interactions mantain or enhance structural robustness of a coffee agroecosystem network

Cecilia González González, Emilio Mora Van Cauwelaert, Denis Boyer, Ivette Perfecto ,

John Vandermeer Mariana Benítez

Ecological Complexity 47 (2021)

Ecological Complexity 47 (2021) 100951

Contents lists available at ScienceDirect

Ecological Complexity

journal homepage: www.elsevier.com/locate/ecocom

High-order interactions maintain or enhance structural robustness of a coffee agroecosystem network

Cecilia González González [a,b,*], Emilio Mora Van Cauwelaert [a,c], Denis Boyer [d], Ivette Perfecto [e], John Vandermeer [f], Mariana Benítez [a,*]

[a] Laboratorio Nacional de Ciencias de la Sostenibilidad, Instituto de Ecología, Universidad Nacional Autónoma de México, Mexico City, C.P. 04510, México
[b] Posgrado en Ciencias Biológicas, Universidad Nacional Autónoma de México, Mexico City, C.P. 04510, México
[c] Posgrado en Ciencias Biomédicas, Universidad Nacional Autónoma de México, Mexico City, C.P. 04510, México
[d] Instituto de Física, Universidad Nacional Autónoma de México, Mexico City, C.P. 04510, México
[e] School for Environment and Sustainability, University of Michigan, Ann Arbor, Michigan, U.S.A
[f] Department of Ecology and Evolutionary Biology, University of Michigan, Ann Arbor, Michigan, U.S.A

ARTICLE INFO

Keywords:
Ecological networks
Robustness
High order interactions
Species coexistence
Coffee agroecosystems

ABSTRACT

The capacity of highly diverse systems to prevail has proven difficult to explain. In addition to methodological issues, the inherent complexity of ecosystems and issues like multicausality, non-linearity and context-specificity make it hard to establish general and unidirectional explanations. Nevertheless, in recent years, high order interactions have been increasingly discussed as a mechanism that benefits the functioning of highly diverse ecosystems and may add to the mechanisms that explain their persistence. Until now, this idea has been explored by means of hypothetical simulated networks. Here, we test this idea using an updated and empirically documented network for a coffee agroecosystem. We identify potentially key nodes and measure network robustness in the face of node removal with and without incorporation of high order interactions. We find that the system's robustness is either increased or unaffected by the addition of high order interactions, in contrast with randomized counterparts with similar structural characteristics. We also propose a method for representing networks with high order interactions as ordinary graphs and a method for measuring their robustness.

1. Introduction

The link between an ecosystem's diversity, structure and functioning has long been debated in ecology. Both empirical and theoretical studies have tried to decipher the nature of their relationship and the factors that take part in shaping it. On the one hand, the existence of different definitions for these features has contributed to the difficulty of the task, while on the other hand, an intrinsic complexity stems from the very numerous elements, processes and scales that interact to give rise to these qualities (Ives and Carpenter 2007). Early ideas on the topic focused on the notion of stability, and maintained that diversity made ecosystems stable through species limiting each other's growth by predation or competition (Odum 1953; MacArthur 1955; Elton 1958). These notions were dramatically challenged by the work of Robert May (1972; 1973), who used linear stability analyses to show that communities modelled as random networks lose local stability as the number of species, the number of interactions, or their strength rise. These results caused commotion in the scientific community, as they seemed to contradict the very real biodiversity found around the world. Since then, two main extensions have helped reconcile theory with observation; mainly: the use of realistic community structures (Lawlor 1978; Lawlor 1980) and the complementation of linear stability analyses with other methods to assess ecosystem function from both a structural and a dynamical point of view like robustness, feasibility or structural stability (Landi et al., 2018). It is now generally recognized that diversity tends to positively correlate with some measures of ecosystem functioning, like stability, robustness or productivity. Nevertheless, this does not mean that diversity is the direct driver of these traits, rather, it should be regarded as an 'umbrella' indicator of many ecological mechanisms that are inherent to ecosystems and that are the actual determinants of the diversity-function relationships (McCann 2000). Such mechanisms and how they may favor the assembly and reproduction of highly diverse communities are now the focus of many studies (Chesson 2000; Levine et al., 2017).

* Corresponding authors.
E-mail addresses: ceci_g_g@ciencias.unam.mx (C. González González), mbenitez@iecologia.unam.mx (M. Benítez).

https://doi.org/10.1016/j.ecocom.2021.100951
Received 8 February 2021; Received in revised form 19 July 2021; Accepted 26 July 2021

Different mechanisms have since been proposed to enable the coexistence of species in highly diverse systems (Chesson 2000; Wright 2002; Adler et al., 2013; Levine et al., 2017). Recently, high order interactions (HOI) have been proposed as a key mechanism for the persistence of diverse communities (Bairey et al., 2016; Grilli et al., 2017). HOIs have been defined in subtly different ways and they have sometimes been equated with the concept of indirect effects (Worthen and Moore 1991; Billick and Case 1994; Sanchez 2019). Nevertheless, we align with those authors who have pointed out the strong differences between these two and define them as follows (Billick and Case 1994). Indirect effects are changes in interactions that are solely mediated by population densities (Levine 1976), and therefore pass from one species to another via the density changes in one or more intermediary species. These can also be called "interaction chains" (Wootton 1993). On the other hand, HOIs are functional modifications in the interaction of two species caused by a third one, and need not pass through any change in population densities (Wootton 1993). Indirect effects are a logical consequence of pairwise interactions whenever there are more than two species involved, while HOIs occur through additional mechanisms that cannot be extrapolated from isolated pairwise interactions. The importance of HOIs has been widely recognized, as they are quite common and can have substantial implications: ecosystem engineering, predatory adaptive behavior, changes in foraging, facilitation, mutualisms and many so-called trait-mediated effects commonly involve HOIs (Beckerman et al., 1997; Werner and Peacor 2003; Holt and Barfield 2012; Kéfi et al., 2012; Bairey et al., 2016). Bairey et al. (2016) computationally explored the role of HOIs on the linear stability and feasibility of systems described as virtual random networks and found that HOIs could indeed attenuate or even revert a negative relationship between the number of species and stability.

While the findings of Bairey et al. (2016) and other recent theoretical work have greatly contributed to our understanding of the relationship between HOIs and species coexistence (Grilli et al., 2017; Singh and Baruah, 2020; Li et al., 2020), they rely on hypothetical networks whose interactions are set randomly and do not represent known ecological interactions, or on the assessment of some focal species (Mayfield and Stouffer, 2017). It thus remains unclear how HOIs may affect the function of empirically-documented networks which, arguably, capture some aspects of their structure and dynamics in a more faithful manner. There are now some well-studied ecological and few agroecological networks that could help fill this important gap (Scheffer 1997; Yoon et al., 2004; Fortuna et al., 2014; Perfecto and Vandermeer, 2015; López Martínez 2017). Agroecosystems cover around 40% of the Earth's surface (Foley et al., 2005), represent a substantial part of the world's biodiversity, and have just recently begun to be analyzed from a network perspective (Bohan et al., 2013; López Martínez 2017). The insights gained from such a system-level approach hold the potential to guide our actions around major issues like autonomous pest control, disease outbreaks and biodiversity conservation in agricultural landscapes (Vandermeer et al., 2010, 2018; Ramos et al., 2018).

With this in mind, in the present study we updated and analyzed an empirically-based network for a coffee agroecosystem in southern Mexico. This biodiverse agroecosystem has been studied for about three decades and many of its species and interactions have been thoroughly described (Perfecto and Vandermeer 2015). Importantly, different HOIs have been found to play a key role in the dynamics of the main coffee pests and their natural enemies (Vandermeer et al., 2010; Perfecto et al., 2021), motivating discussions on different formalisms to integrate HOIs to ecological network analyses, which remain an underdeveloped area (Golubski et al., 2016; Battiston et al., 2020). Thus, we analyzed the coffee agroecosystem network from a structural perspective in order to investigate the effects of HOIs on the overall robustness of this system, defined as its capacity to remain connected in the face of node removal representing species loss. To this aim, we propose a method for representing networks with high order interactions as ordinary graphs and a method for measuring their robustness which is a modification of Piraveenan et al. (2013). Our work aims to contribute to the understanding of the mechanisms underlying species coexistence in highly diverse systems, as well as to provide novel insights that can inform management practices based on the biological understanding of agroecosystems.

2. Methods

2.1. Study site

The study site is "Finca Irlanda", a 320 ha coffee plantation situated on the highlands of El Soconusco, Chiapas (158,110 N, 928,200 W; 900 masl). Precipitation in the region averages 4500 mm per year and the vegetation type is seasonal tropical forest. Nevertheless, primary vegetation has been almost completely replaced by coffee plantations with different management intensities, aside from some tiny fragments of original forest kept in some farms. In Finca Irlanda, there is a portion of such original vegetation set aside for conservation, while the management of the surrounding productive area involves keeping the shade provided by native trees, which, among other practices, make it a highly biodiverse agroecosystem (Perfecto and Vandermeer, 2015).

It is convenient to detail some parts of the complex ecological web found in the study site. There are four main antagonists of coffee plants: the coffee leaf rust, *Hemileia vastatrix*, the coffee berry borer, *Hypothenemus hampei* (see Fig. 3d further), the coffee leaf miner, *Leucoptera coffeella*, and the coffee green scale, *Coccus viridis* (Fig. 3c). The last one keeps a spatially clustered mutualistic relationship with ants of the *Azteca* genus (Fig. 3e), which feed on the honeydew produced by the scales while protecting them from being eaten by a lady beetle, *Azya orbigera*. Thanks to this protection, the scale populations reach high levels within the clusters, which in turn increases their probability of being infected by the white halo fungus, *Lecanicillium lecanii*, a fungus that is also capable of infesting the coffee rust. By patrolling coffee plants where green scales feed, *Azteca* keeps other herbivores, like the berry borer beetle or the leaf miner from establishing big populations on these plants. However, all the effects that the *Azteca* ants have on the system are temporally inhibited by flies in the genus *Pseudacteon* (Family: Phoridae), who are parasitoids of the *Azteca* ants, and that cause them to retreat to their nests, hide or dramatically reduce their movement whenever they sense a fly nearby. This inhibition of *Azteca* leaves the scales and the coffee plants unprotected for a period of time, a lapse that has been proven to be ecologically relevant and that for example, is enough for allowing *Azya orbigera* to prey on the scales or oviposit underneath them, ensuring nourishment for their future larvae (Liere and Larsen 2010; Vandermeer et al., 2010).

The system here described exhibits different kinds of direct interactions like herbivory and parasitism, but also numerous HOIs (Table S1). For example, *Azteca* ants exert a second order interaction when they inhibit the predation interaction among *C. viridis* and *A. orbygera* by harrasing the latter, mostly without harming it (Vandermeer and Perfecto 2006; Liere and Larsen 2010; Vandermeer et al., 2010). An example of a third order interaction is the effect of the phorid flies, which by paralyzing or chasing away *Azteca* ants, inhibit the second order interaction they exerted and thus enable the predation of *C. viridis* by *A. orbygera* (Hsieh et al., 2012).

2.2. Network inference

We used a network approach to analyze the community under study. Species were represented as nodes whose connections were defined by the ecological interactions among them. In order to define the network's structure, we reviewed published information on this particular agroecosystem and integrated it in a common database.

The reviewing process began with a book that collects over 20 years of research in the area (Perfecto and Vandermeer 2015). All referenced papers that explained, observationally or experimentally, at least one

ecological interaction among a pair of species, were examined too. The type of interactions and the direction of their effects were extracted, including qualitative information about their strength, whenever available. If any of the papers in this first group made reference to other investigations in the area, those were also revised. All the information was integrated in a database organized as follows: *transmitter node (*e.g. *H. hampei), recipient node (*e.g. *Coffea), kind of interaction* (e.g. +/-), *description* (e.g. females of *H. hampei* bore into the coffee berries to oviposit and their larvae feed from it) and *reference* (listing of the articles that support the interaction). For HOIs, instead of a *recipient node*, a column was added with the *recipient interaction* (e.g. the presence of *Azteca* prevents *H. hampei* from boring into the coffee, inhibiting herbivory). Interactions that were uncertain, but suspected, were annotated but not considered for the construction of the network. Finally, the network was compared with smaller versions published previously and revised by experts.

We assumed that organisms in the empirically-grounded network co-occur, an assumption we regarded necessary in order to set up a model system in which we can interpret and keep track of the effects of HOI addition, without temporal changes as a confounding variable. This assumption is plausible because most of the field work underlying the network inference has been done in the same coffee plantation, a perennial system ("Finca Irlanda", in Southern Mexico), during summer, from May to August. Although seasonality in the study site is relatively mild, some fluctuations have been observed between the rainy (May to November) and dry seasons (December to April). However, interaction data underlying this network has been obtained during the rainy season, where organisms in the network exhibit altogether the largest population sizes.

2.3. Structure definition and general metrics

The structure of the network was visualized with the software *Gephi 0.9.2*. Because network-related methods only contemplate ensembles of nodes connected directly through edges (that is, first order interactions), it is not possible to define a network with edges connecting to other edges, which is the case of HOIs. For this reason, two versions of the network were created: the first one only captured the nodes and their first order interactions; the second one included HOI modified interactions as artificial pseudo-nodes, an artifact that allowed us to use the full force of network theory to analyze the system. Topological analyses were conducted on both versions of the network in order to quantify the effect of HOIs.

The transformation process of HOIs into pseudo-nodes is depicted in Fig. 1. Basically, an edge that was affected by a third node was labeled with a new pseudo-node (e. g. a pseudo-node named "predation"), so the third node now had a simple edge connecting it to the new pseudo-node. The same logic works for second, third or any higher order interactions. A similar procedure was suggested by Newman (2018), where interactions involving more than two nodes are introduced by adding new nodes belonging to a different category as part of a bipartite graph. This new node is connected by a single edge to each original node. However, this procedure is limited as bipartite graphs do not account for edges between nodes belonging to the same category.

Once both versions on the network were obtained, standard network metrics were quantified in order to characterize them and as a way of exploring how much pseudo-node addition changed the general structure of the network. In particular, we analyzed node relevance according to their centrality in both webs. For this, we used two commonly used metrics that can also be interpreted in ecological terms: i) *Degree*, which points to nodes directly linked to many nodes in the network and is the simplest and most widely used measure of node connectivity (Sharma and Surolia, 2013), and ii) *Betweenness centrality*, which helps identify nodes acting as "bridges" between nodes or groups of nodes in a network; it is used to find nodes that indirectly link many nodes of the network, and the removal of which may affect the communication between many pairs of nodes or groups of densely connected nodes (communities or modules) through the shortest paths between them. Thus, nodes with high betweenness centrality may largely influence the flow of matter and energy in ecological systems (Lu and Zhang, 2013; Raghavan Unnithan et al., 2014). Even though the structure-function relationship in ecological networks constitutes an old and still open field of research, some studies have at least partially validated the use of these metrics with functional data, expert knowledge or dynamical simulations (e.g. Endredi et al., 2018; Cagua et al., 2019; Yang et al., 2021; Arroyo-Lambaer et al., 2021; Gouveia et al., 2021; Zamkovaya

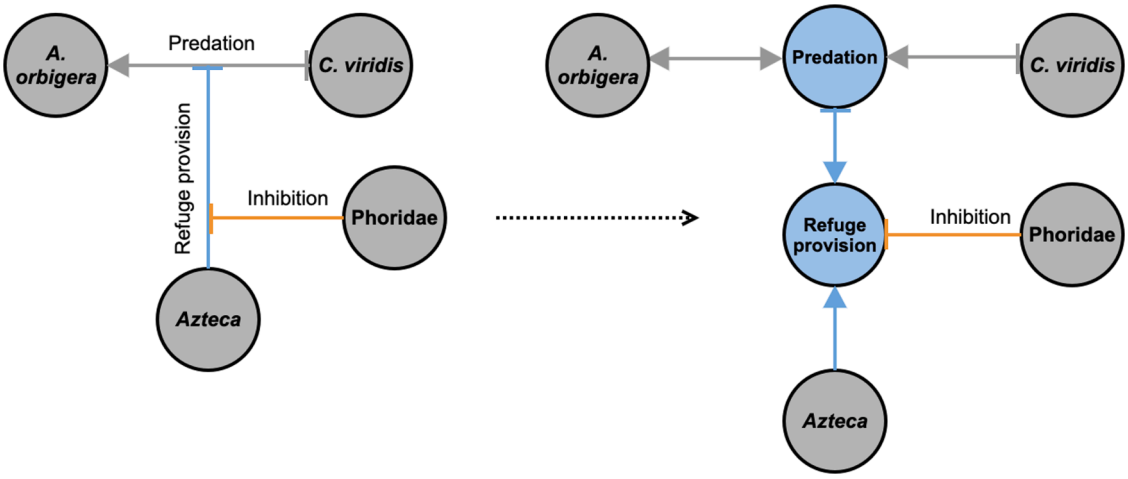

Fig. 1. Transformation process of second and third order interactions into pseudo-nodes. The grey nodes represent biological taxa and the blue nodes are pseudo-nodes representing ecological interactions which are modified by a HOI. First order edges are dark grey, second order edges are blue and third order edges are orange. Arrows represent positive effects, and crossed endpoints stand for negative effects. For example, the predatory interaction between *A. orbigera* and *C. viridis* is turned into a pseudo-node named *predation* in order to be modified by the refuge provision performed by *Azteca,* a second order interaction. The pseudo-node has two incoming positive arrows from the nodes that perform it because it needs both nodes to exist (*predation* could not occur without both prey and predator present). Likewise, refuge provision is inhibited by the presence of phorids, so it is turned into a second pseudo-node in order to be modified by the third order interaction performed by *Phoridae*. In the same way, this *refuge-provision* pseudo-node has incoming positive arrows both from *Azteca* and *predation*, because it would lose its meaning if any of them ceased to be present. (For interpretation of the references to colour in this figure legend, the reader is referred to the web version of this article.)

et al., 2021). All calculations were made with the software *Gephi 0.9.2*.

2.4. The effect of high order interactions on network robustness

We conducted a robustness analysis for both versions of the network (with and without HOIs). Robustness was measured by calculating the area under the curve that depicts the size of the biggest connected component as nodes are removed one by one from the network (Kasthurirathna et al., 2013; Piraveenan et al., 2013; Navarro Díaz 2015). This measure is compared with the area under the curve traced by a complete graph, that is, a graph where every possible pair of nodes is connected by an edge. Thus, following Eq. (1), the relationship between these two areas gives us a measure of robustness (for a full derivation of the equation see Piraveenan et al. (2013)).

$$R_1 = \frac{A_g}{A_c}(\%) = \frac{200\sum_{k=0}^{N} S_k - 100S_0}{N^2} \quad (1)$$

Where A_g is the area under the curve of the evaluated graph and A_c that of the fully connected graph. S_k is the size of the largest component after k nodes have been removed, S_0 denotes the initial largest component size, and N is the network size. According to the above equation, for a fully connected network of any size, the robustness coefficient (R) is always of 100% (taken from Kasthurirathna et al., 2013).

For the network that includes HOIs, only real nodes could be selected for removal, in order to avoid the biologically meaningless action of removing pseudo-nodes. Following this logic, whenever a node got selected for removal, any pseudo-node connected to it was also eliminated, since pseudo-nodes lose their meaning once the species causing the higher order effect is eliminated. Because this modification often resulted in the elimination of several nodes at the time, we modified Eq. (1) in order to control for it. In the Piraveenan et al. (2013) derivation, the area under the curve of the fully connected graph assumes one node removal per step in the x axis. If we assume n node removal per step (in order to control for pseudo-node removal in the evaluated graph), this area is $Ac = N2/2n$ and the robustness equation becomes:

$$R_n = \frac{A_g}{A_c}(\%) = \frac{200n\sum_{k=0}^{N'} S_k - 100nS_0}{N^2} \quad (2)$$

Where n is the average number of nodes removed at each step (1.54 in this network) and N' is the number of real nodes in the network (N minus the number of pseudo-nodes) . Eq. (1) is equivalent to Eq. (2) when $n = 1$ and there are no pseudo-nodes.

Hence, we used Eq. (1) for the network without HOIs and Eq. (2) for the network with HOIs. For each of these networks, two node removal methods were tested. With the first one, nodes were randomly selected and removed one by one until removing them all. This was done 200 independent times and a robustness average was obtained. The second method consisted of removing nodes by degree, from highest to lowest.

In order to discard the possibility that the differences between the networks with and without HOIs could be an artifact of the simple increase in node and edge number after HOI adition, we compared our results with three null models that had the same general metrics as these two webs but lacked the particular structural properties of the empirical pseudo-nodes. Following this setup, if HOIs actually confer a difference in robustness, that is, if their effect is not just due to the increase in node and edge number, we expected an increase in robustness as a result of HOI addition in the empirical web, but not in their null models. In order to test this, the robustness of each network with each removal method was also compared with the average robustness of 200 randomized but comparable networks, i.e. with the same number of nodes, average degree or interaction density. Three types of random networks were used: totally random networks (Erdős and Rényi 1960), small-world networks (Watts and Strogatz 1998) and scale-free networks (Barabási and Albert 1999). The first model generates random networks from a set of nodes in which the edges are independently created between any pair of nodes with a probability p. Because the structure of ecological networks is far from being random, we also used small-world and scale-free networks, which have been proved to share structural characteristics with many real world networks (Montoya and Solé 2002; Barabási and Bonabeau 2003). Small-world networks follow an algorithm that starts with a regular lattice where each node is connected to its k closest neighbors, and where each edge is then re-connected to a randomly chosen node with a certain probability, avoiding duplicates and self-loops. This construction produces networks with a high clustering coefficient and short paths, two particularities that have been found in many ecological webs (Montoya and Solé 2002). The last method builds networks with a preferential attachment mechanism, where nodes are added sequentially such that each new node is connected to a number m of existing nodes, where the probability to choose a node for connection is proportional to the number of links that this node already has. This creates networks with power-law degree distributions, another characteristic that has been widely found in ecological webs (Barabási and Bonabeau 2003). For the Erdös Rényi method we used the values $N = 34$ and $p = 0.095$, and $N = 22$ and $p = 0.145$ for networks representing cases with and without HOIs, respectively (where N is the number of nodes of the empirical web and p is taken from their density). For the Watts-Strogatz method, we chose $N = 34$, $k = 3$ and $p = 0.5$, and $N = 22$, $k = 3$ and $p = 0.5$ for networks representing cases with and without HOIs, respectively (where k is the average degree of the empirical web and p was arbitrarily chosen). For the Barabasi-Albert method we chose $N = 34$ and $m = 1$, and $N = 22$ and $m = 2$ for networks representing cases with and without HOIs, respectively (where m is chosen so that the resulting average degree matches the empirical average degree).

Because nodes in the empirical network with HOIs were removed along with their associated pseudo-nodes as discussed above, the randomized versions of this network needed to emulate this process too. This was done in the following way: First, we quantified the probability to remove a number n of pseudo-nodes with each real node removal in 100 simulations of the empirical network with HOIs. Then, in the randomized networks (composed of 34 nodes), a subset of 22 randomly chosen nodes was defined to stand for the real nodes, while the remaining 12 nodes stood for the pseudo-nodes. This random choice of pseudo-nodes in each simulation controls for any bias that could emerge from choosing pseudo-nodes with different centrality properties (i.e. the contrasting effects of choosing hubs and non-hubs to stand for pseudo-nodes). At each removal step, a node was removed (randomly or by degree as explained above) from the real nodes pool alongside with n nodes from the pseudo-node pool, with n drawn from the probability distribution derived from the mentioned simulations. Again, we used Eq. (1) for calculating robustness of the randomized versions of the network without HOIs and Eq. (2) for the randomized versions of the network with HOIs. With these numerical experiments we were able to compare, on the one hand, the robustness of the two versions of our network, that is, with and without HOIs, and on the other hand, each empirical robustness with their randomized analogues. One-way ANOVA tests were performed to test the significance of the differences in robustness among the networks with and without HOIs, as well as between their corresponding null models, with one ANOVA run for each of the four network structures (one empirical and three randomized null models) in each of the two node removal methods (i.e. eight total pairwise comparisons).

Using the same experimental design, we quantified secondary extinctions in order to complement the measure of robustness with a more direct and easily interpreted measure. For this, we counted the number of nodes that became isolated along with each node removal. Because isolated nodes by definition have no interactions with any other nodes in the system, we considered them to become extinct. Thus, taking the primary extinctions (sequential node removal) and the secondary extinctions (isolated nodes) into account, we quantified the proportion of remaining nodes in the community at each removal step. This approach

has been used by previous authors to assess and compare robustness across ecological systems (Cai and Liu 2016). Simulations were done with the library NetworkX 2.5 (Hagberg et al., 2008) in *Python 3.7.1*. and ANOVA tests were performed in *RStudio 1.2.1335* (RStudio Team 2020). Scripts are publicly available at: https://github.com/laparcela/CoffeeNetworkStructure

3. Results

3.1. Network inference

From literature revision, 48 interactions between 22 nodes were established out of 44 scientific papers and books, all conducted in our study site (Fig. 2). This information is organized in the supplementary material table S1.

3.2. Structure definition and general metrics

Two versions of the web were obtained with *Gephi,* the first one containing only first order interactions and the second one after adding pseudo-nodes for HOIs (Fig. 3).

Without HOIs, the network is composed of 22 nodes and 68 interactions, while incorporating HOIs makes it a network of 34 nodes and 104 interactions. Both networks have an approximate average degree of 3. Centrality analysis showed that *C. viridis, Coffea, H. hampei, Azteca, Pheidole* ctp. and *Pseudomyrmex* spp are the nodes with the highest rankings in both networks and for different centrality metrics (Fig. 4). Thus, even though HOI addition results in a larger web, relevant properties like connectivity and single-node centralities remain largely unaltered. Additional metrics for both versions of the network are available in Table S2.

3.3. The effect of high order interactions on network robustness

Fig. 5 presents the results of the robustness analyses for the empirical coffee networks with and without HOIs, as well as the results for the three different types of randomized networks with comparable structures. In the case of the empirical networks, the addition of HOIs did not significantly change the network robustness under random node removal, but robustness increased significantly under directed node removal. In contrast, for the three types of randomized networks that we used as null models, those with the same node number, edge degree and density as the empirical network with HOIs significantly lost robustness under the two node removal protocols, except for the completely random networks (Erdos-Renyi) under random removal, which showed no significant changes. Additionally, in the node removal by degree, taking HOIs into account made the empirical network more robust than all its randomized counterparts. Statistically significant differences are

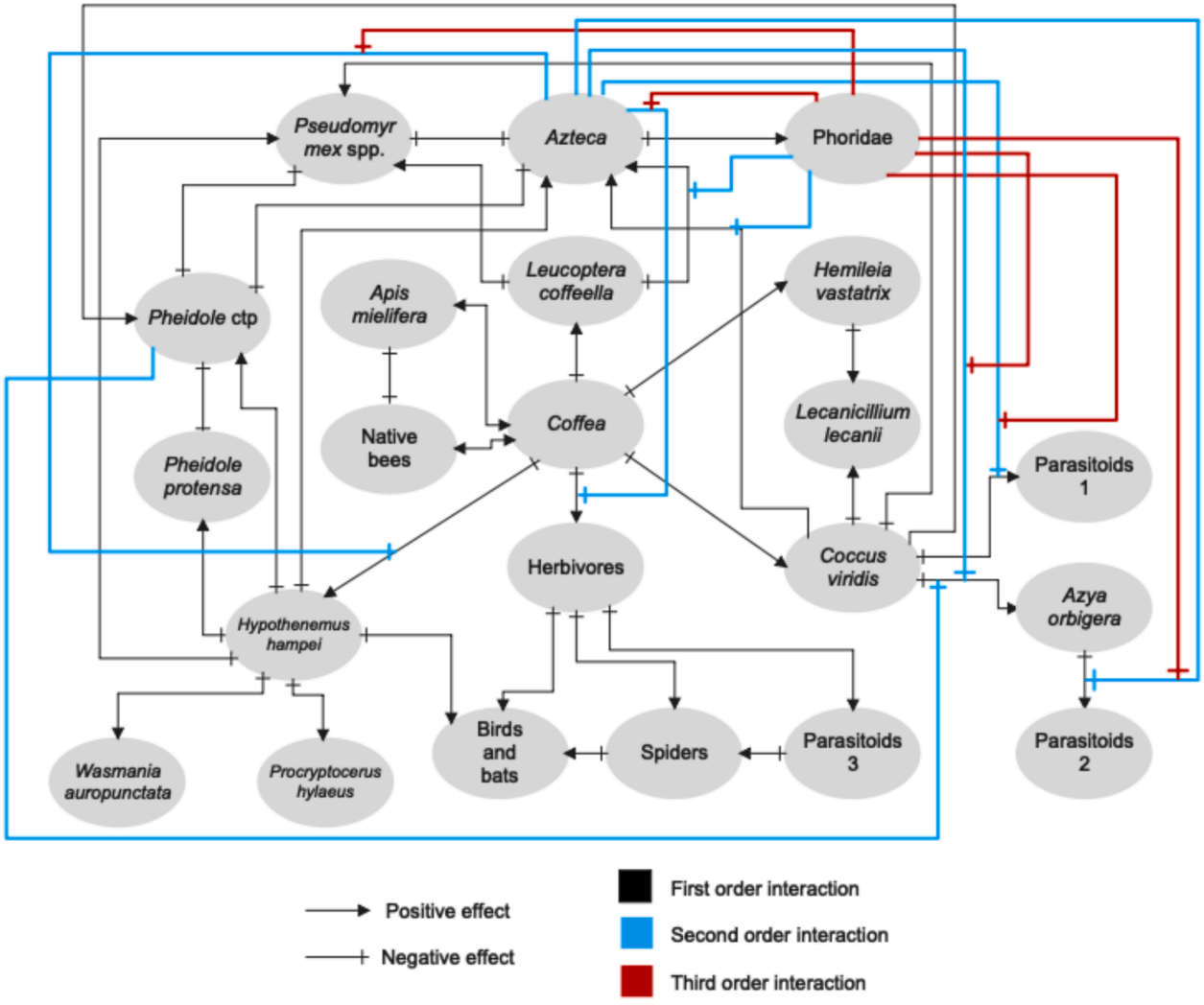

Fig. 2. Complete network before transformation from HOIs to pseudo-nodes. Black lines are first order interactions, blue lines are second order interactions and red lines are third order interactions. (For interpretation of the references to colour in this figure legend, the reader is referred to the web version of this article.)

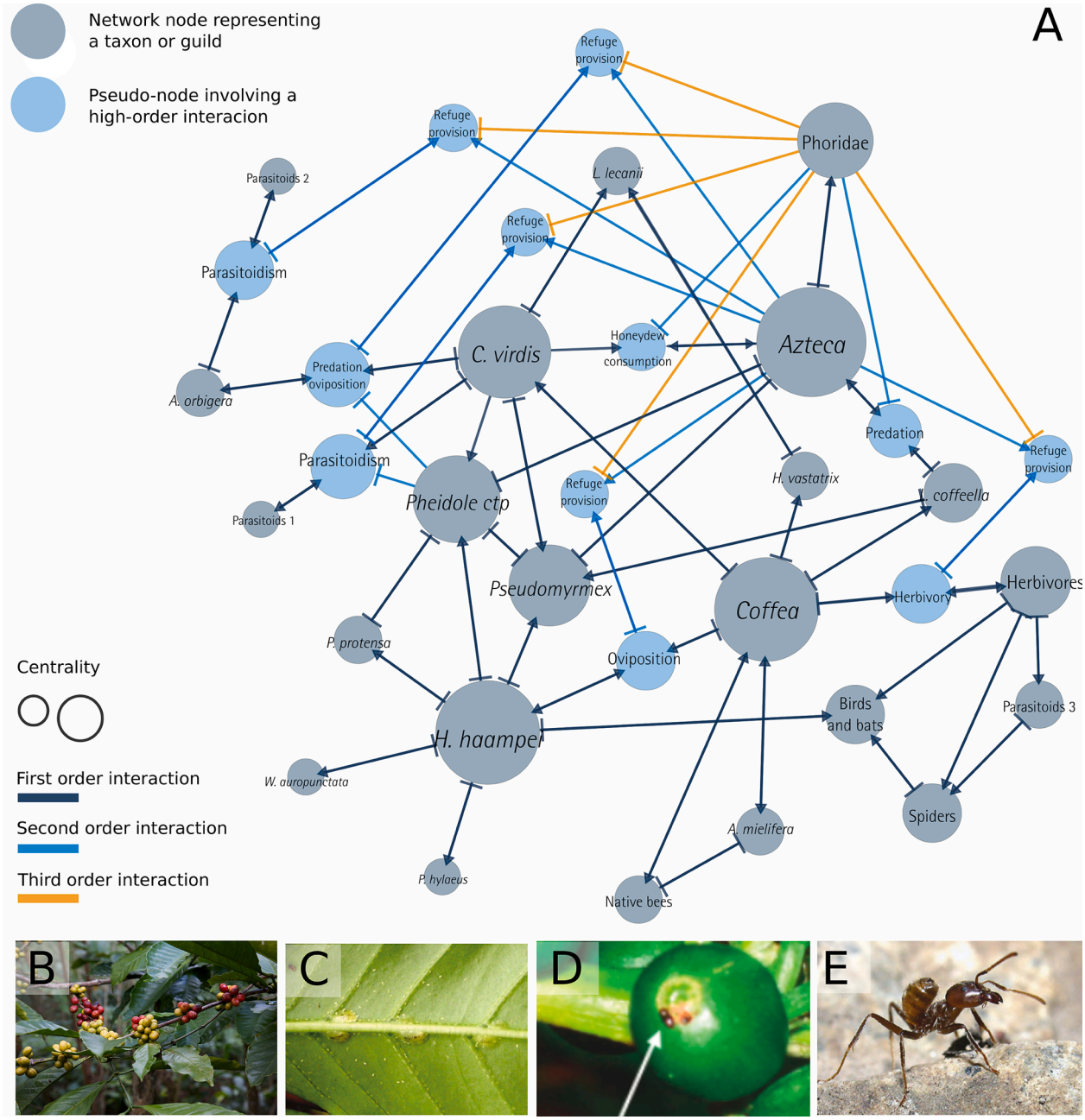

Fig. 3. A: Community network with first, second and third order interactions. Grey nodes represent biological taxa and blue nodes are pseudo-nodes representing ecological interactions which are subject to being modified by a HOI. Node size is determined by its degree. First order edges are grey, second order edges are blue and third order edges are orange. B: Coffee plants (*Coffea*). C: Coffee green scale (*Coccus viridis*), a potential pest in the system. D: Coffee berry borer (*Hypothenemus hampei*), one of the main coffee pests, about to penetrate a coffee grain. E: *Azteca* ant, an important regulator of this interaction network. Photographs: Wikimedia Commons by *Jmhullnot* at https://commons.wikimedia.org/wiki/File:CoffeeBerry.jpg (B), John Vandermeer (C, D), Alex Wild (E). (For interpretation of the references to colour in this figure legend, the reader is referred to the web version of this article.)

supported by p values <0.05 and large effect sizes as measured by *eta* squared, *epsilon* squared and *omega* squared indexes (Lakens 2013). The details of these statistical analyses can be found in the table S3 of the Supplementary material. Because all randomized analogues of the network with HOIs have the tendency to lose robustness, while the robustness of the actual empirical networks is either unchanged or increased by HOIs, we can say that the effects observed in the empirical networks are indeed a result of the particular structural properties conferred by HOI addition and not of simply increasing the number of interactions. Indeed, it seems that high order interactions favor robust network structures that may enable the coexistence of diverse systems.

In parallel, our quantification of secondary extinctions showed the same tendency (Fig. 6). The proportion of remaining nodes after sequential node removal and secondary extinctions shows that HOI addition results in a less abrupt diversity decline in the empirical networks, while the null models showed no differences (overlapped red and blue lines) or even a more abrupt diversity decline (more pronounced decline showed by the red lines). We believe this strengthens the results obtained by the robustness measure, and allows us to say with a clearer picture that HOIs increase the robustness of the system.

4. Discussion

We have integrated a vast set of empirical evidence into a coffee-

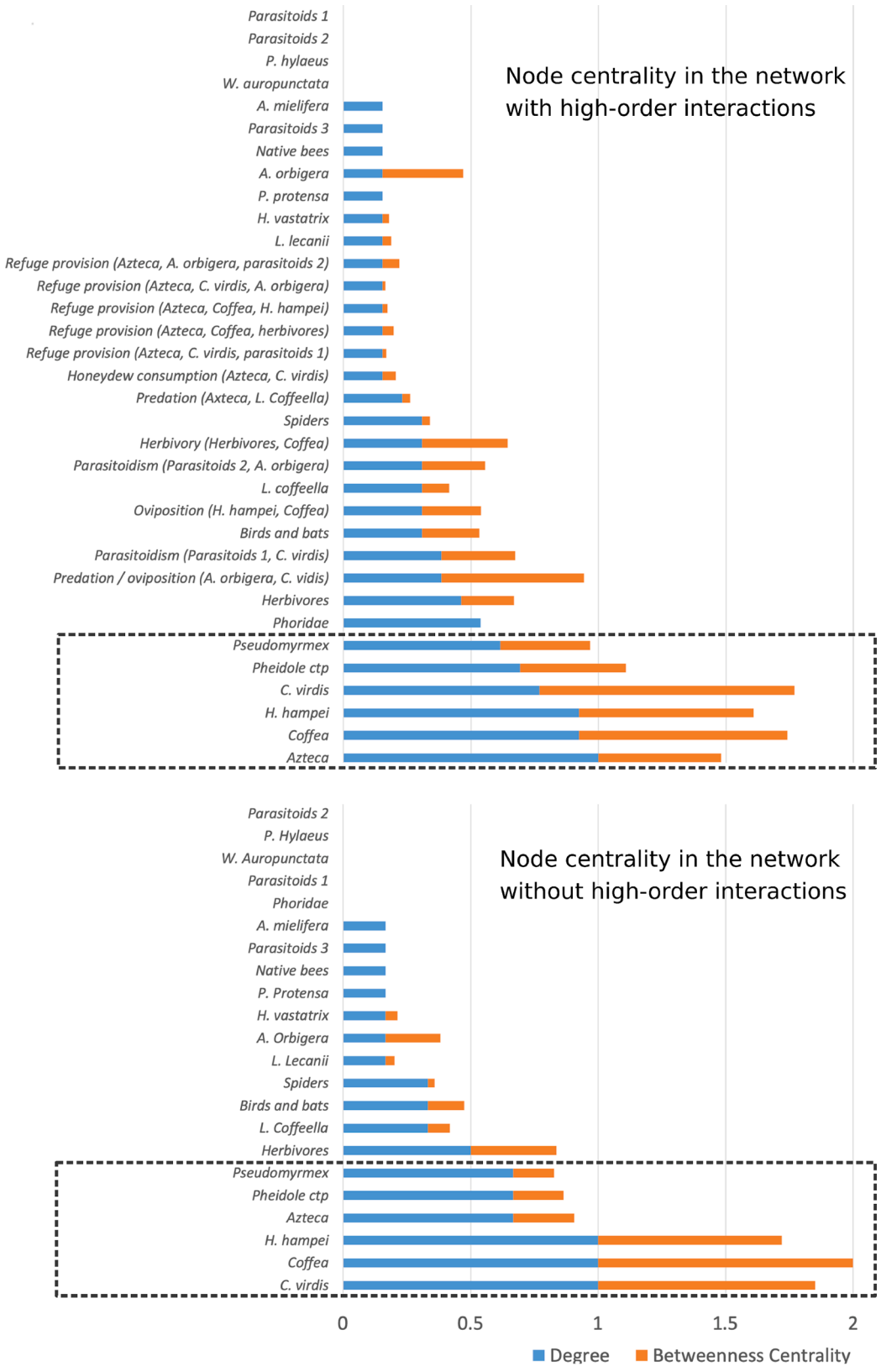

Fig. 4. Node centrality analysis for the network without HOIs (above) and with HOIs (below). *C. viridis, Coffea, H. hampei, Azteca, Pheidole* ctp and *Pseudomyrmex* spp are the highest ranking nodes in both networks.

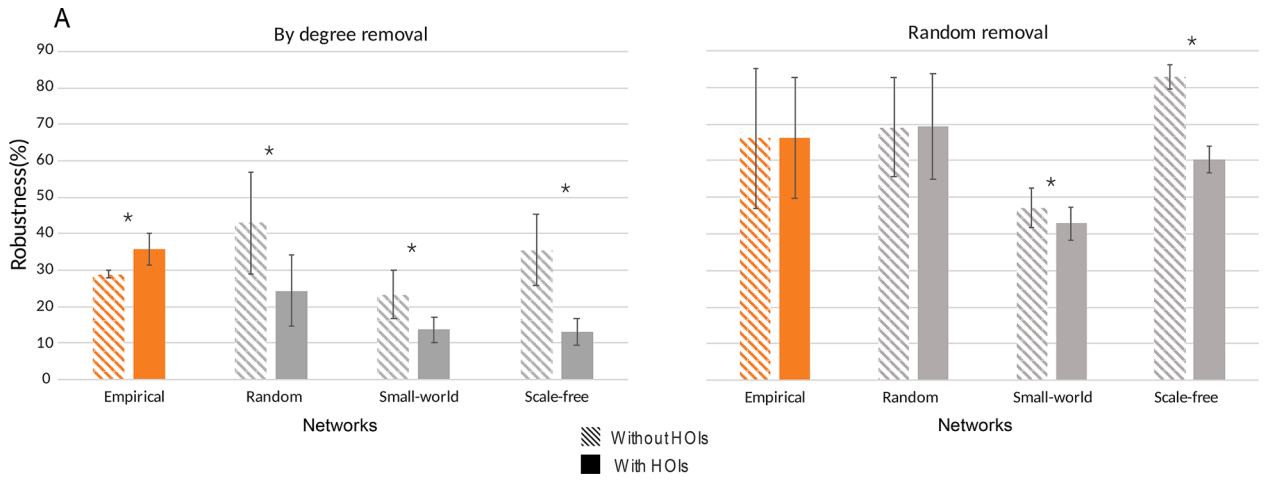

Fig. 5. Robustness of the coffee-associated network, with and without HOIs, as well as random, small-world and scale free networks with same *n,* mean degree and density. A: When removing nodes by degree, the empirical network (orange bars) is significantly more robust when HOIs are added, while the three types of randomized networks (grey bars) lose robustness when their structures are comparable to that with HOI addition. B: Under random node removal, the empirical web (orange bars) and the totally random networks (grey, left) are not significantly changed by the addition of HOIs; while small-world (grey, middle) and scale-free networks (grey, right) loose robustness under HOI addition.

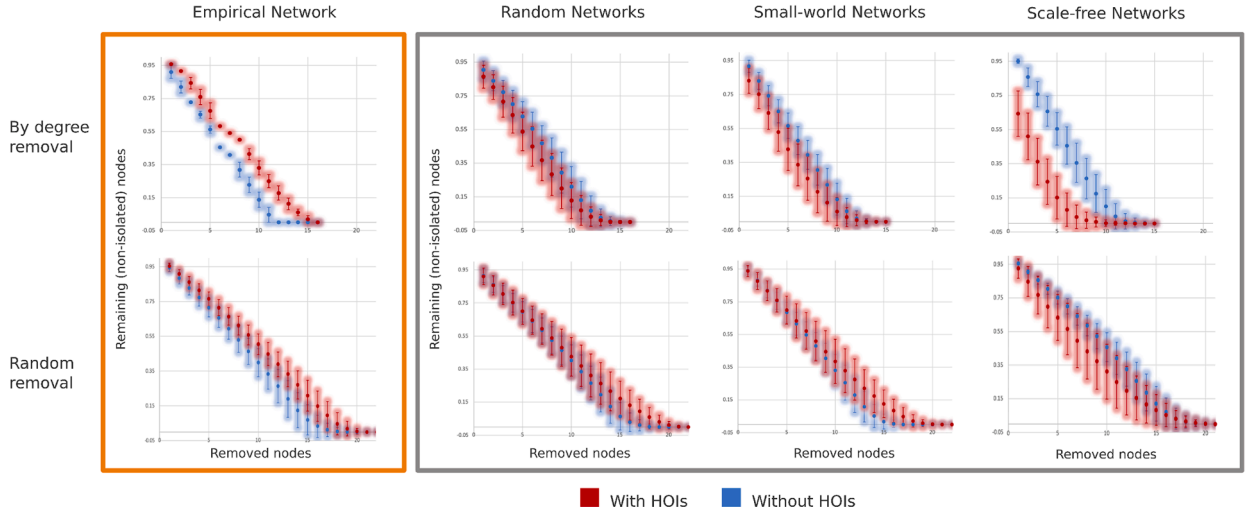

Fig. 6. Proportion of remaining nodes after sequential node removal and secondary extinctions. Left (marked in orange): empirical networks. Right (marked in gray): randomized networks. Above: Random node removal. Below: By degree node removal. In red we show the data of the networks with HOIs or similar general structure and in blue we show the data of the networks without HOIs or similar general structure. Each dot is the average of 200 networks and vertical shadows are standard deviations. HOI addition in the empirical networks (left) result in a slower diversity decline, while randomized null models (right) show the opposite or no tendency. (For interpretation of the references to colour in this figure legend, the reader is referred to the web version of this article.)

associated network that includes both simple and high order ecological interactions (Fig. 3). This network has enabled us to test the role of HOIs on the network's robustness for a system of great ecological and agricultural importance. We find that the robustness of the coffee-associated network structure, measured through an operational index and through a secondary extinction analysis, is unchanged or increased by HOI addition, and that random reconfigurations indicate that this effect is not simply due to edge addition (Fig. 5 and 6). This goes in agreement with previous studies considering hypothetical networks and different measures of system function like stability or feasibility, where the addition of simple interactions has been found to have negative repercussions on system function while HOI addition has a neutral or a positive effect (May 1972; Bairey et al., 2016; Grilli et al., 2017; Singh and Baruah, 2020; Li et al., 2020). Our results therefore support the idea that HOIs contribute to the maintenance of highly diverse ecological communities.

In our study, the robustness of the network was first evaluated with the change in size of the biggest connected component as the nodes were gradually removed, at random or by targeting nodes of higher degree first. This way of conceptualizing robustness assumes that the connection between network components is related to the function and integrity of the system, implying that a fully connected network can maintain its elements and overall functions better than a disaggregated or partially disconnected network (Albert et al., 2000; Dekker and Colbert 2004; Piraveenan et al., 2013; Sheykhali et al., 2020). Indeed, previous work on the coffee agroecosystem for which the network under study has been uncovered suggests that some agroecosystemic functions, such as pest control, rely on the dynamics of the whole system and on the documented interactions taking place (Vandermeer et al., 2010). In the particular case of agroecosystems, the integrity of the network, in other words the maintenance of its diversity, is also likely to be associated with yield and yield stability in the face of diverse perturbations

(Gaudin et al., 2015; Manns and Martin 2018). Additionally, we strengthened our analysis with a direct quantification of secondary extinctions along the primary node removal sequence. In this case, the assumption is simply that species loss results in co-extinctions whenever it leaves other species isolated. This second approach confirmed our results, supporting the idea that HOIs increase the robustness of the system and that the robustness index that we used is a good measure of the overall state of the system.

The node removal methods that we used have been explored in many ecological network studies, and our results confirm the general tendency of ecological networks to be less robust to directed loss of the most connected species than to random species loss (Dunne et al., 2002; Kaiser-Bunbury et al., 2010; Roopnarine 2010; Cai and Liu 2016). Thus, it is remarkable that under directed node removal, HOI addition bears the larger positive influence on robustness. While the extinction of the most connected species in most communities might be unlikely, given that they are often the most abundant ones (Dáttilo et al., 2014;Vázquez et al., 2005; Vázquez et al., 2007), we should bear in mind that we are dealing with an agroecosystem, which by definition if human-managed and which can be subjected to directed emotions (for example, in the case of pests). These intentional removals may very well be directed to largely abundant species, making the study of directed node removal all the more relevant.

While the coffee-associated system was studied here as an undirected network, the type and sign of its HOIs could inform the mechanism through which HOIs affect the overall robustness. For example, in this ecological system all documented HOIs are negative, meaning that they work as inhibitors of the ecological interaction they modify, thereby diminishing their intensity (although they sometimes form double negatives, as third order interactions inhibit previous inhibitions, amounting to a general positive effect). This may have several implications for the system's dynamics. For example, refuge provisioning, where one species protects another from one or several predators, may not only help explain prey survival (which is important for maintaining the predator), but also how predators avoid competitive exclusion (Vandermeer and Perfecto 2019). It is possible that these mechanisms, coupled with spatial and temporal heterogeneity, may create the necessary conditions for coexistence. However, it is important to bear in mind that individual HOIs may have effects in different directions. Especially in the case of agroecosystems, where effects are measured also in terms of human-based values like productivity, the effect of individual HOIs should not be universally assumed as positive. For instance, it has been shown that the ant *Wasmannia auropunctata* can indirectly protect the coffee leaf miner against potential predators, potentially limiting the effectiveness of biological control elements (Perfecto et al., 2021). Nevertheless, we could not compare the effects of positive and negative HOIs in this study as we worked with undirected networks, such a question remains an interesting pathway for future research.

The structural analyses of the coffee-associated network also allowed us to identify nodes with high centrality according to different metrics (Fig. 4). We identified five nodes that systematically exhibited a high centrality, independently of the centrality measure and the presence or absence of pseudo-nodes: *C. viridis, Coffea, H. hampei, Azteca, Pheidole* ctp. and *Pseudomyrmex* spp. This is in agreement with the crucial role of the coffee plant in this agroecosystem, as well as the effect of its potential pests and pest enemies in its growth and development (Vandermeer et al., 2010). However, at this point we cannot rule out the possibility that the high centrality of these nodes is due to a bias in sampling and research efforts. We therefore cautiously interpret the results on node degree and betweenness centrality; rather than highlighting specific nodes as potential keystone species or indicators, we used these metrics mainly to characterize the overall structure of the network and found that the high centrality of these nodes was generally unaltered by pseudo-node addition, which suggests that this method for representing HOIs is able to conserve key aspects of the network.

A key assumption in our analysis is that robustness depends upon network structure, a simplification that does not take temporal dynamics into account. The relationship between structure and function in networks is certainly unclear and remains an active and open field of research, with key questions largely unexplored. However, there is an important body of literature on this matter, from which some structural metrics and robustness analyses like the ones we used have emerged as potential indicators of network functioning and dynamics. For instance, computational and empirically-based studies on social-ecological systems have employed purely structural measures in order to identify nodes that can lead to large cascading effects, as well as potential indicators of overall system integrity (see for recent examples: Kaiser-Bunbury et al., 2010; Lü et al., 2016; Cai and Liu, 2016; Griffith et al., 2019; Horcea-Milcu et al., 2020; Puche et al., 2020; Cagua et al., 2019; Arroyo-Lambaer et al., 2021; Gouveia et al., 2021; Yang et al., 2021; Zamkovaya et al., 2021, among many others). Hence, even though the study of network structure alone cannot account for temporal phenomena, it has proven to be useful and valuable in its simplicity. On the other hand, dynamical approaches contribute with an important and complementary perspective, and there are novel methods being actively developed that promise to enrich our understanding of robustness in ecological systems (Neubert and Caswell 1997; Arnoldi et al., 2016; Saavedra et al., 2017; Saavedra et al., 2020). We are currently pursuing dynamical analyses that might help uncover the role of HOIs and highly central nodes on the dynamics of populations in the coffee-associated network. With these, we expect to be able to discuss the scope of the structural approach considered here in its relationship to spatial-temporal dynamics. Studies have historically found different relationships between the amount and type of interactions in a network and several measures of its stability and robustness (see Landi et al., 2018 for a thorough revision on this matter). Hence, complementing the present study with a dynamical analysis will allow us to get a more realistic vision of the system and what the consideration of HOIs may or may not entail.

To conclude, our results support the hypothesis that HOIs can contribute to the maintenance and robustness of highly diverse ecological systems, and agroecological systems in particular. In agreement with previous empirical and theoretical studies, our work points to the importance of agroecological management and practices that are based on a deep ecological understanding of productive systems, as well as to the importance of a high diversity of taxons and interactions for the robustness and functioning of agroecosystems.

Funding

CG acknowledged the graduate program Posgrado en Ciencias Biológicas, Universidad Nacional Autónoma de México and CONACyT scholarship. MB acknowledged financial support from UNAM-DGAPA-PAPIIT (IN207819). EM acknowledged the graduate program Posgrado en Ciencias Biomédicas, Universidad Nacional Autónoma de México and CONACyT scholarship. IP and JV acknowledged financial support from the grant number NSF DEB-185,326.

Author statement

All authors declare that they have seen and approved the final version of the manuscript being submitted. They warrant that the article is the authors' original work, that it hasn't been previously published and that it is not under consideration for publication elsewhere.

Declaration of Competing Interest

The authors declare that they have no known competing financial interests or personal relationships that could have appeared to influence the work reported in this paper.

Acknowledgements

The authors thank Blanca Estela Hernández Hernández and Yolanda Robledo Arratia for formatting and figure edition. We also thank members of *La Parcela* Laboratory and the two reviewers for their valuable comments and suggestions. This article covers part of the requirements to obtain the PhD Degree in the Posgrado en Ciencias Biológicas de la Universidad Nacional Autónoma de México.

Supplementary materials

Supplementary material associated with this article can be found, in the online version, at doi:10.1016/j.ecocom.2021.100951.

References

Adler, P.B., Fajardo, A., Kleinhesselink, A.R., Kraft, N.J., 2013. Trait-based tests of coexistence mechanisms. Ecol. Lett. 16 (10), 1294–1306. https://doi.org/10.1111/ele.12157.

Albert, R., Jeong, H., Barabási, A.L., 2000. Error and attack tolerance of complex networks. Nature 406 (6794), 378–382. https://doi.org/10.1038/35019019.

Arnoldi, J.F., Loreau, M., Haegeman, B., 2016. Resilience, reactivity and variability: a mathematical comparison of ecological stability measures. J. Theor. Biol. 389, 47–59. https://doi.org/10.1016/j.jtbi.2015.10.012.

Arroyo-Lambaer, D., Uscanga Castillo, A., Piña Tejeda, V.M., Vázquez-Barrios, V., Reverchon, F., Rosell, J.A., Escalante, A.E., Peña-Ramírez, V., Benítez, M., Wegier, A., 2021. Cognitive maps across multiple social sectors: shared and unique perceptions on the quality of agricultural soils in Mexico. Front. Sustain. Food Syst. 4, 292. https://doi.org/10.3389/fsufs.2020.522661.

Bairey, E., Kelsic, E.D., Kishony, R., 2016. High-order species interactions shape ecosystem diversity. Nat. Commun. 7 (1), 1–7. https://doi.org/10.1038/ncomms12285.

Barabási, A.L., Albert, R., 1999. Emergence of scaling in random networks. Science 286 (5439), 509–512. https://doi.org/10.1126/science.286.5439.509.

Barabási, A.L., Bonabeau, E., 2003. Scale-free networks. Sci. Am. 288 (5), 60–69. https://doi.org/10.1038/scientificamerican0503-60.

Battiston, F., Cencetti, G., Iacopini, I., Latora, V., Lucas, M., Patania, A., Young, J.G., Petri, G., 2020. Networks beyond pairwise interactions: structure and dynamics. Phys. Rep. 874, 1–92. https://doi.org/10.1016/j.physrep.2020.05.004.

Beckerman, A.P., Uriarte, M., Schmitz, O.J., 1997. Experimental evidence for a behavior-mediated trophic cascade in a terrestrial food chain. Proc. Natl Acad. Sci. 94, 10735–10738. https://doi.org/10.1073/pnas.94.20.10735.

Billick, I., Case, T.J., 1994. Higher order interactions in ecological communities: what are they and how can they be detected? Ecology 75 (6), 1529–1543. https://doi.org/10.2307/1939614.

Bohan, D.A., Raybould, A., Mulder, C., Woodward, G., Tamaddoni-Nezhad, A., Bluthgen, N., Pocock, M.J.O., Muggleton, S., Evans, D.M., Astegiano, J., Massol, F., Loeuille, N., Petit, S., Macfadyen, S., 2013. Networking agroecology: integrating the diversity of agroecosystem interactions. In: Woodward, D., Bohan, D.A. (Eds.), Advances in Ecological Research, 49. Academic Press, Amsterdam, pp. 1–67.

Cagua, E.F., Wootton, K.L., Stouffer, D.B., 2019. Keystoneness, centrality, and the structural controllability of ecological networks. J. Ecol. 107 (4), 1779–1790. https://doi.org/10.1111/1365-2745.13147.

Cai, Q., Liu, J., 2016. The robustness of ecosystems to the species loss of community. Sci. Rep. 6 (1), 1–8. https://doi.org/10.1038/srep35904.

Chesson, P., 2000. Mechanisms of maintenance of species diversity. Annu. Rev. Ecol. Syst. 31 (1), 343–366. https://doi.org/10.1146/annurev.ecolsys.31.1.343.

Dáttilo, W., Marquitti, F.M., Guimarães Jr., P.R., Izzo, T.J., 2014. The structure of ant–plant ecological networks: is abundance enough? Ecology 95 (2), 475–485. https://doi.org/10.1890/12-1647.1.

Dekker, A.H., Colbert, B.D., 2004. Network robustness and graph topology. In: Estevill-Castro, V. (Ed.), Proceedings of the 27th Australasian conference on Computer science, 26. Australian Computer Society, Darlinghurst, NSW, pp. 359–368.

Dunne, J.A., Williams, R.J., Martinez, N.D., 2002. Network structure and biodiversity loss in food webs: robustness increases with connectance. Ecol. Lett. 5 (4), 558–567. https://doi.org/10.1046/j.1461-0248.2002.00354.x.

Elton, C.S., 1958. Ecology of Invasions by Animals and Plants. Chapman & Hall, London.

Endrédi, A., Senánszky, V., Libralato, S., Jordán, F., 2018. Food web dynamics in trophic hierarchies. Ecol. Modell. 368, 94–103. https://doi.org/10.1016/j.ecolmodel.2017.11.015.

Erdős, P., Rényi, A., 1960. On the evolution of random graphs. Publications of the Mathematical Institute of the Hungarian. Academy of Sciences 5 (1), 17–60.

Foley, J.A., DeFries, R., Asner, G.P., Barford, C., Bonan, G., Carpenter, S.R., Stuart Chapin, F., Coe, M.T., Daily, G.C., Gibbs, H.K., Helkowski, J.H., Holloway, T., Howard, E.A., Kucharik, C.J., Monfreda, C., Patz, J.A., Colin Prentice, I., Ramankutty, N., Snyder, P.K., 2005. Global consequences of land use. Science 309 (5734), 570–574. https://doi.org/10.1126/science.1111772.

Fortuna, M.A., Ortega, R., Bascompte, J., 2014. The web of life. arXiv at https://arxiv.org/abs/1403.2575.

Gaudin, A.C., Tolhurst, T.N., Ker, A.P., Janovicek, K., Tortora, C., Martin, R.C., Deen, W., 2015. Increasing crop diversity mitigates weather variations and improves yield stability. PLoS ONE 10 (2), e0113261. https://doi.org/10.1371/journal.pone.0113261.

Golubski, A.J., Westlund, E.E., Vandermeer, J., Pascual, M., 2016. Ecological networks over the edge: hypergraph trait-mediated indirect interaction (TMII) structure. Trends Ecol. Evol. 31 (5), 344–354. https://doi.org/10.1016/j.tree.2016.02.006.

Gouveia, C., Móréh, Á., Jordán, F., 2021. Combining centrality indices: maximizing the predictability of keystone species in food webs. Ecol. Indic. 126, 107617 https://doi.org/10.1016/j.ecolind.2021.107617.

Grilli, J., Barabás, G., Michalska-Smith, M.J., Allesina, S., 2017. Higher-order interactions stabilize dynamics in competitive network models. Nature 548 (7666), 210–213. https://doi.org/10.1038/nature23273.

Griffith, G.P., Strutton, P.G., Semmens, J.M., Fulton, E.A., 2019. Identifying important species that amplify or mitigate the interactive effects of human impacts on marine food webs. Conservation Biology 33 (2), 403–412. https://doi.org/10.1111/cobi.13202.

Hagberg, A., Swart, P., S Chult, D., 2008. Exploring network structure, dynamics, and function using NetworkX. In: Varoquaux, G., Vaught, T., Millman, J. (Eds.), Proceedings of the 7th Python in Science Conference. SciPy Conferences. Pasadena, pp. 11–16.

Holt, R.D., Barfield, M., 2012. Trait-mediated effects, density dependence and the dynamic stability of ecological systems. In: Ohgushi, T., Schmitz, O., Holt, R.D. (Eds.), Trait-Mediated Indirect Interactions: Ecological and Evolutionary Perspectives. Cambridge University Press, New York, pp. 89–106.

Horcea-Milcu, I., Martín-López, B., Lam, D., Lang, D., 2020. Research pathways to foster transformation: linking sustainability science and social-ecological systems research. Ecol.Soc 25 (1), 13. https://doi.org/10.5751/ES-11332-250113.

Hsieh, H.Y., Liere, H., Soto, E.J., Perfecto, I., 2012. Cascading trait-mediated interactions induced by ant pheromones. Ecol.Evol 2 (9), 2181–2191. https://doi.org/10.1002/ece3.322.

Ives, A.R., Carpenter, S.R., 2007. Stability and diversity of ecosystems. Science 317 (5834), 58–62. https://doi.org/10.1126/science.1133258.

Kaiser-Bunbury, C.N., Muff, S., Memmott, J., Müller, C.B., Caflisch, A., 2010. The robustness of pollination networks to the loss of species and interactions: a quantitative approach incorporating pollinator behaviour. Ecol. Lett. 13 (4), 442–452. https://doi.org/10.1111/j.1461-0248.2009.01437.x.

Kasthurirathna, D., Piraveenan, M., Thedchanamoorthy, G., 2013. On the influence of topological characteristics on robustness of complex networks. J. Artif. Intell.Soft Comput. Res. 3 (2), 89–100. https://doi.org/10.2478/jaiscr-2014-0007.

Kéfi, S., Berlow, E.L., Wieters, E.A., Navarrete, S.A., Petchey, O.L., Wood, S.A., Boit, A., Joppa, L.N., Lafferty, K.D., Williams, R.J., Martinez, N.D., Menge, B.A., Blanchette, C.A., Iles, A.C., Brose, U., 2012. More than a meal… integrating non-feeding interactions into food webs. Ecol. Lett. 15 (4), 291–300. https://doi.org/10.1111/j.1461-0248.2011.01732.x.

Lakens, D., 2013. Calculating and reporting effect sizes to facilitate cumulative science: a practical primer for t-tests and ANOVAs. Front. Psychol. 4 (863) https://doi.org/10.3389/fpsyg.2013.00863.

Landi, P., Minoarivelo, H.O., Brännström, Å., Hui, C., Dieckmann, U., 2018. Complexity and stability of ecological networks: a review of the theory. Popul. Ecol. 60 (4), 319–345. https://doi.org/10.1007/s10144-018-0628-3.

Lawlor, L.R., 1978. A comment on randomly constructed model ecosystems. Am. Nat. 112 (984), 445–447. https://doi.org/10.1086/283286.

Lawlor, L.R., 1980. Structure and stability in natural and randomly constructed competitive communities. Am. Nat. 116 (3), 394–408. https://doi.org/10.1086/283634.

Levine, S.H., 1976. Competitive interactions in ecosystems. Am. Nat. 110 (976), 903–910. https://doi.org/10.1086/283116.

Levine, J.M., Bascompte, J., Adler, P.B., Allesina, S., 2017. Beyond pairwise mechanisms of species coexistence in complex communities. Nature 546 (7656), 56–64. https://doi.org/10.1038/nature22898.

Li, Y., Bearup, D., Liao, J., 2020. Habitat loss alters effects of intransitive higher-order competition on biodiversity: a new metapopulation framework. Proc. R. Soc. Lond. B Biol. Sci. 287 (1940), 20201571 https://doi.org/10.1098/rspb.2020.1571.

Liere, H., Larsen, A., 2010. Cascading trait-mediation: disruption of a trait-mediated mutualism by parasite-induced behavioral modification. Oikos 119 (9), 1394–1400. https://doi.org/10.1111/j.1600-0706.2010.17985.x.

López Martínez, R., 2017. Modelos dinámicos de redes ecológicas para un sistema productivo complejo: la milpa mexicana. Master degree thesis. Universidad Nacional Autónoma de México, México, p. 95.

Lü, L., Chen, D., Ren, X.-L., Zhang, Q.-M., Zhang, Y.-C., Zhou, T., 2016. Vital nodes identification in complex networks. Phys. Rep. 650, 1–63. https://doi.org/10.1016/j.physrep.2016.06.007.

Lu, L., Zhang, M., 2013. Edge Betweenness Centrality. In: Dubitzky, W., Wolkenhauer, O., Cho, K.H., Yokota, H. (Eds.), Encyclopedia of Systems Biology. Springer, New York, p. 36. https://doi.org/10.1007/978-1-4419-9863-7_874.

MacArthur, R.H., 1955. Fluctuations of animal populations and a measure of community stability. Ecology 36 (3), 533–536. https://doi.org/10.2307/1929601.

Manns, H.R., Martin, R.C., 2018. Cropping system yield stability in response to plant diversity and soil organic carbon in temperate ecosystems. Agroecol. Sustain. Food Syst. 42 (7), 724–750. https://doi.org/10.1080/21683565.2017.1423529.

May, R.M., 1972. Will a large complex system be stable? Nature 238 (5364), 413–414. https://doi.org/10.1038/238413a0.

May, R.M., 1973. Stability and Complexity in Model Ecosystems. Princeton Univ. Press, Oxford. https://doi.org/10.2307/j.ctvs32rq4.

Mayfield, M.M., Stouffer, D.B., 2017. Higher-order interactions capture unexplained complexity in diverse communities. Nat. Ecol. Evol. 1 (3), 1–7. https://doi.org/10.1038/s41559-016-0062.

McCann, K.S., 2000. The diversity–stability debate. Nature 405 (6783), 228–233. https://doi.org/10.1038/35012234.
Montoya, J.M., Solé, R.V., 2002. Small world patterns in food webs. J. Theor. Biol. 214 (3), 405–412. https://doi.org/10.1006/jtbi.2001.2460.
Navarro Díaz, M., 2015. Revisión y análisis comparativo de la estructura ecológica de consorcios procaryotes asociados a biorreactores productores de hidrógeno y de digestión anaerobia. Bachelor degree thesis. Universidad Nacional Autónoma de México, México, p. 65.
Neubert, M.G., Caswell, H., 1997. Alternatives to resilience for measuring the responses of ecological systems to perturbations. Ecology 78 (3), 653–665. https://doi.org/10.2307/2266047.
Newman, M., 2018. Networks, Second ed. Oxford University Press, Oxford.
Odum, E.P., 1953. Fundamentals of Ecology. Saunders, Philadelphia.
Perfecto, I., Hajian-Forooshani, Z., White, A., Vandermeer, J., 2021. Ecological complexity and contingency: ants and lizards affect biological control of the coffee leaf miner in Puerto Rico. Agric. Ecosyst. Environ. 305, 107104 https://doi.org/10.1016/j.agee.2020.107104.
Perfecto, I., Vandermeer, J., 2015. Coffee agroecology: a New Approach to Understanding Agricultural biodiversity, Ecosystem Services and Sustainable Development. Routledge, London.
Piraveenan, M., Thedchanamoorthy, G., Uddin, S., Chung, K.S.K., 2013. Quantifying topological robustness of networks under sustained targeted attacks. Soc. Netw. Anal. Min. 3 (4), 939–952. https://doi.org/10.1007/s13278-013-0118-8.
Puche, E., Jordán, F., Rodrigo, M.A., Rojo, C., 2020. Non-trophic key players in aquatic ecosystems: a mesocosm experiment. Oikos 129 (11), 1714–1726. https://doi.org/10.1111/oik.07476.
Ramos, I., González, C.G., Urrutia, A.L., Van Cauwelaert, E.M., Benítez, M., 2018. Combined effect of matrix quality and spatial heterogeneity on biodiversity decline. Ecol. Complex. 36, 261–267. https://doi.org/10.1016/j.ecocom.2018.10.001.
Raghavan Unnithan, S.K., Kannan, B., Jathavedan, M., 2014. Betweenness Centrality in Some Classes of Graphs. Int. J. Comb. 2014, 1–12. https://doi.org/10.1155/2014/241723.
Roopnarine, P., 2010. Graphs, networks, extinction and paleocommunity food webs. Nat. Preced. 1. https://doi.org/10.1038/npre.2010.4433.1. -1.
RStudio Team, 2020. RStudio: Integrated Development For R. RStudio, PBC, Boston, MA. URL. http://www.rstudio.com/.
Saavedra, S., Medeiros, L.P., AlAdwani, M., 2020. Structural forecasting of species persistence under changing environments. Ecol. Lett. 23 (10), 1511–1521. https://doi.org/10.1111/ele.13582.
Saavedra, S., Rohr, R.P., Bascompte, J., Godoy, O., Kraft, N.J., Levine, J.M, 2017. A structural approach for understanding multispecies coexistence. Ecol. Monogr. 87 (3), 470–486. https://doi.org/10.1002/ecm.1263.
Sanchez, A., 2019. Defining higher-order interactions in synthetic ecology: lessons from physics and quantitative genetics. Cell Syst 9 (6), 519–520. https://doi.org/10.1016/j.cels.2019.11.009.
Scheffer, M., 1997. Ecology of Shallow Lakes. Springer Science & Business Media, Dordrecht. https://doi.org/10.1007/978-1-4020-3154-0.
Sharma, D., Surolia, A., 2013. Degree centrality. In: Dubitzky, W., Wolkenhauer, O., Cho, K.H., Yokota, H. (Eds.), Encyclopedia of Systems Biology. Springer, New York, p. 29. https://doi.org/10.1007/978-1-4419-9863-7_935.
Sheykhali, S., Fernández-Gracia, J., Traveset, A., Ziegler, M., Voolstra, C.R., Duarte, C. M., Eguíluz, V.M., 2020. Robustness to extinction and plasticity derived from mutualistic bipartite ecological networks. Sci. Rep. 10 (1), 1–12. https://doi.org/10.1038/s41598-020-66131-5.
Singh, P., Baruah, G., 2020. Higher order interactions and species coexistence. Theor. Ecol. 1–13. https://doi.org/10.1007/s12080-020-00481-8.
Vandermeer, J., Hajian-Forooshani, Z., Perfecto, I., 2018. The dynamics of the coffee rust disease: an epidemiological approach using network theory. Eur. J. Plant Pathol. 150 (4), 1001–1010. https://doi.org/10.1007/s10658-017-1339-x.
Vandermeer, J., Perfecto, I., 2006. A keystone mutualism drives pattern in a power function. Science 311 (5763), 1000–1002. https://doi.org/10.1126/science.1121432.
Vandermeer, J., Perfecto, I., 2019. Hysteresis and critical transitions in a coffee agroecosystem. PNAS 116 (30), 15074–15079. https://doi.org/10.1073/pnas.1902773116.
Vandermeer, J., Perfecto, I., Philpott, S., 2010. Ecological complexity and pest control in organic coffee production: uncovering an autonomous ecosystem service. Bioscience 60 (7), 527–537. https://doi.org/10.1525/bio.2010.60.7.8.
Vázquez, D.P., Melián, C.J., Williams, N.M., Blüthgen, N., Krasnov, B.R., Poulin, R., 2007. Species abundance and asymmetric interaction strength in ecological networks. Oikos 116 (7), 1120–1127. https://doi.org/10.1111/j.0030-1299.2007.15828.x.
Vázquez, D.P., Poulin, R., Krasnov, B.R., Shenbrot, G.I., 2005. Species abundance and the distribution of specialization in host–parasite interaction networks. J. Anim. Ecol. 74 (5), 946–955. https://doi.org/10.1111/j.1365-2656.2005.00992.x.
Watts, D.J., Strogatz, S.H., 1998. Collective dynamics of 'small-world' networks. Nature 393 (6684), 440–442. https://doi.org/10.1038/30918.
Werner, E.E., Peacor, S.D., 2003. A review of trait-mediated indirect interactions in ecological communities. Ecology 84 (5), 1083–1100. https://doi.org/10.1890/0012-9658(2003)084[1083:AROTII]2.0.CO;2.
Worthen, W.B., Moore, J.L., 1991. Higher-order interactions and indirect effects: a resolution using laboratory Drosophila communities. Am. Nat. 138 (5), 1092–1104. https://doi.org/10.1086/285271.
Wootton, J.T., 1993. Indirect effects and habitat use in an intertidal community: interaction chains and interaction modifications. Am. Nat. 141 (1), 71–89. https://doi.org/10.1086/285461.
Wright, J.S., 2002. Plant diversity in tropical forests: a review of mechanisms of species coexistence. Oecologia 130 (1), 1–14. https://doi.org/10.1007/s004420100809.
Yang, Y., Chen, J., Chen, X., Jiang, Q., Liu, Y., Xie, S., 2021. Cyanobacterial bloom induces structural and functional succession of microbial communities in eutrophic lake sediments. Environ. Pollut. 284, 117157 https://doi.org/10.1016/j.envpol.2021.117157.
Yoon, I., Williams, R.J., Levine, E., Yoon, S., Dunne, J.A., Martinez, N.D., 2004. Webs on the Web (WoW): 3D visualization of ecological networks on the WWW for collaborative research and education. In: Proceedings of the IS&T/SPIE Symposium on Electronic Imaging, Visualization and Data Analysis, 5295, pp. 124–132. https://doi.org/10.1117/12.526956.
Zamkovaya, T., Foster, J.S., de Crécy-Lagard, V., Conesa, A., 2021. A network approach to elucidate and prioritize microbial dark matter in microbial communities. ISME J 15 (1), 228–244. https://doi.org/10.1038/s41396-020-00777-x.

Further reading

Armbrecht, I., Perfecto, I., 2003. Litter ant's diversity and predation potential in two Mexican coffee matrices and forest fragments. Agric. Ecosyst. Environ. 97 (1–3), 107–115.
Avelino, J., Willocquet, L., Savary, S., 2004. Effects of crop management patterns on coffee rust epidemics. Plant Pathol 53 (5), 541–547. https://doi.org/10.1111/j.1365-3059.2004.01067.x.
Bess, H.A., 1958. The green scale, Coccus viridis (Green) (Homoptera: coccidae), and ants. Proceedings, Hawaiian Entomological Society 16 (3), 349–355.
Damon, A., 2000. A review of the biology and control of the coffee berry borer, Hypothenemus hampei (Coleoptera: scolytidae). Bull. Entomol. Res. 90 (6), 453–465. https://doi.org/10.1017/S0007485300000584.
De la Mora, A., Livingston, G., Philpott, S.M., 2008. Arboreal ant abundance and leaf miner damage in coffee agroecosystems in Mexico. Biotropica 40 (6), 742–746. https://doi.org/10.1111/j.1744-7429.2008.00444.x.
Fragoso, D.B., Guedes, R.N.C., Picanço, M.C., Zambolim, L., 2002. Insecticide use and organophosphate resistance in the coffee leaf miner Leucoptera coffeella (Lepidoptera: lyonetiidae). Bull. Entomol. Res. 92, 203–212. https://doi.org/10.1079/BER2002156.
Gonthier, D.J., Ennis, K.K., Philpott, S.M., Vandermeer, J., Perfecto, I., 2013. Ants defend coffee from berry borer colonization. BioControl 58 (6), 815–820. https://doi.org/10.1007/s10526-013-9541-z.
Hodge, M.A., 1999. The implications of intraguild predation for the role of spiders in biological control. Journal of Arachnology 351–362.
Hsieh, H.Y., Perfecto, I., 2012. Trait-mediated indirect effects of phorid flies on ants. Psyche (Camb. Mass.) 2012, 11. https://doi.org/10.1155/2012/380474.
Humphries, M.D., Gurney, K., 2008. Network 'small-world-ness': a quantitative method for determining canonical network equivalence. PLoS ONE 3 (4), e0002051. https://doi.org/10.1371/journal.pone.0002051.
Ibarra-Núñez, G., Garcia, J.A., López, J.A., Lachaud, J.P., 2001. Prey analysis in the diet of some ponerine ants (Hymenoptera: formicidae) and web-building spiders (Araneae) in coffee plantations in Chiapas. Mexico. Sociobiology 37 (3), 723–756.
Jackson, D., Vandermeer, J., Perfecto, I., 2009. Spatial and temporal dynamics of a fungal pathogen promote pattern formation in a tropical agroecosystem. Open Ecol. J. 2, 62–73. https://doi.org/10.2174/1874213000902010062.
Jha, S., Vandermeer, J.H., 2009. Contrasting bee foraging in response to resource scale and local habitat management. Oikos 118 (8), 1174–1180. https://doi.org/10.1111/j.1600-0706.2009.17523.x.
Jiménez-Soto, E., Cruz-Rodríguez, J.A., Vandermeer, J., Perfecto, I., 2013. Hypothenemus hampei (Coleoptera: curculionidae) and its interactions with Azteca instabilis and Pheidole synanthropica (Hymenoptera: formicidae) in a shade coffee agroecosystem. Environ. Entomol. 42 (5), 915–924. https://doi.org/10.1603/EN12202.
Johnson, M.D., Kellermann, J.L., Stercho, A.M., 2010. Pest reduction services by birds in shade and sun coffee in Jamaica. Anim. Conserv. 13 (2), 140–147. https://doi.org/10.1111/j.1469-1795.2009.00310.x.
Kalka, M.B., Smith, A.R., Kalko, E.K., 2008. Bats limit arthropods and herbivory in a tropical forest. Science 320 (5872), 71. https://doi.org/10.1126/science.1153352. -71.
Klein, A.M., Steffan–Dewenter, I., Tscharntke, T., 2003. Fruit set of highland coffee increases with the diversity of pollinating bees. Proc. R. Soc. Lond. B Biol. Sci. 270 (1518), 955–961. https://doi.org/10.1098/rspb.2002.2306.
Klein, A.M., Vaissiere, B.E., Cane, J.H., Steffan-Dewenter, I., Cunningham, S.A., Kremen, C., Tscharntke, T., 2007. Importance of pollinators in changing landscapes for world crops. Proc. R. Soc. Lond. B Biol. Sci. 274 (1608), 303–313. https://doi.org/10.1098/rspb.2006.3721.
Kremen, C., Williams, N.M., Thorp, R.W., 2002. Crop pollination from native bees at risk from agricultural intensification. Proc. Natl. Acad. Sci. 99 (26), 16812–16816. https://doi.org/10.1073/pnas.262413599.
Larsen, A., Philpott, S.M., 2010. Twig-nesting ants: the hidden predators of the coffee berry borer in Chiapas. Mexico. Biotropica 42 (3), 342–347. https://doi.org/10.1111/j.1744-7429.2009.00603.x.
Liere, H., Perfecto, I., 2008. Cheating on a mutualism: indirect benefits of ant attendance to a coccidophagous coccinellid. Environ. Entomol. 37 (1), 143–149. https://doi.org/10.1603/0046-225X(2008)37[143:COAMIB]2.0.CO;2.
Lomeli-Flores, J.R., Barrera, J.F., Bernal, J.S., 2009. Impact of natural enemies on coffee leafminer Leucoptera coffeella (Lepidoptera: lyonetiidae) population dynamics in Chiapas. Mexico. Biol. Control 51 (1), 51–60. https://doi.org/10.1016/j.biocontrol.2009.03.021.

Mathis, K.A., Philpott, S.M., Moreira, R.F., 2011. Parasite lost: chemical and visual cues used by Pseudacteon in search of Azteca instabilis. J. Insect Behav. 24 (3), 186–199. https://doi.org/10.1007/s10905-010-9247-3.

Mooney, K.A., Gruner, D.S., Barber, N.A., Van Bael, S.A., Philpott, S.M., Greenberg, R., 2010. Interactions among predators and the cascading effects of vertebrate insectivores on arthropod communities and plants. Proc. Natl. Acad. Sci. 107 (16), 7335–7340. https://doi.org/10.1073/pnas.1001934107.

Pardee, G.L., Philpott, S.M., 2011. Cascading indirect effects in a coffee agroecosystem: effects of parasitic phorid flies on ants and the coffee berry borer in a high-shade and low-shade habitat. Environ. Entomol. 40 (3), 581–588. https://doi.org/10.1603/EN11015.

Perfecto, I., Vandermeer, J., 2006. The effect of an ant-hemipteran mutualism on the coffee berry borer (Hypothenemus hampei) in southern Mexico. Agric. Ecosyst. Environ. 117 (2–3), 218–221. https://doi.org/10.1016/j.agee.2006.04.007.

Perfecto, I., Vandermeer, J.H., Bautista, G.L., Nunñez, G.I., Greenberg, R., Bichier, P., Langridge, S., 2004. Greater predation in shaded coffee farms: the role of resident neotropical birds. Ecology 85 (10), 2677–2681. https://doi.org/10.1890/03-3145.

Philpott, S.M., Greenberg, R., Bichier, P., Perfecto, I., 2004. Impacts of major predators on tropical agroforest arthropods: comparisons within and across taxa. Oecologia 140 (1), 140–149. https://doi.org/10.1007/s00442-004-1561-z.

Philpott, S.M., Pardee, G.L., Gonthier, D.J., 2012. Cryptic biodiversity effects: importance of functional redundancy revealed through addition of food web complexity. Ecology 93 (5), 992–1001. https://doi.org/10.1890/11-1431.1.

Philpott, S.M., 2005. Trait-mediated effects of parasitic phorid flies (Diptera: phoridae) on ant (Hymenoptera: formicidae) competition and resource access in coffee agroecosystems. Environ. Entomol. 34 (5), 1089–1094. https://doi.org/10.1093/ee/34.5.1089.

Schmitz, O.J., Sokol-Hessner, L., 2002. Linearity in the aggregate effects of multiple predators in a food web. Ecol. Lett. 5 (2), 168–172. https://doi.org/10.1046/j.1461-0248.2002.00311.x.

Schoener, T.W., Spiller, D.A., Losos, J.B., 2002. Predation on a common Anolis lizard: can the food-web effects of a devastating predator be reversed? Ecol. Monogr. 72 (3), 383–407. https://doi.org/10.1890/0012-9615(2002)072[0383:POACAL]2.0.CO;2.

Styrsky, J.D., Eubanks, M.D., 2007. Ecological consequences of interactions between ants and honeydew-producing insects. Proc. R. Soc. Lond. B Biol. Sci. 274 (1607), 151–164. https://doi.org/10.1098/rspb.2006.3701.

Telesford, Q.K., Joyce, K.E., Hayasaka, S., Burdette, J.H., Laurienti, P.J., 2011. The ubiquity of small-world networks. Brain Connect 1 (5), 367–375. https://doi.org/10.1089/brain.2011.0038.

Vandermeer, J., Perfecto, I., 2015. Coffee agroecology: a New Approach to Understanding Agricultural biodiversity, Ecosystem Services and Sustainable Development. Routledge.

Vandermeer, J., Perfecto, I., Nuñez, G.I., Phillpott, S., Ballinas, A.G., 2002. Ants (Azteca sp.) as potential biological control agents in shade coffee production in Chiapas. Mexico. Agroforestry Syst. 56 (3), 271–276. https://doi.org/10.1023/A:1021328820123.

Vandermeer, J., Perfecto, I., Philpott, S.M., 2008. Clusters of ant colonies and robust criticality in a tropical agroecosystem. Nature 451 (7177), 457. https://doi.org/10.1038/nature06477.

Vandermeer, J., Perfecto, I., Liere, H., 2009. Evidence for hyperparasitism of coffee rust (Hemileia vastatrix) by the entomogenous fungus, Lecanicillium lecanii, through a complex ecological web. Plant Pathol 58 (4), 636–641. https://doi.org/10.1111/j.1365-3059.2009.02067.x.

Williams-Guillén, K., Perfecto, I., Vandermeer, J., 2008. Bats limit insects in a neotropical agroforestry system. Science 320 (5872), 70. https://doi.org/10.1126/science.1152944. -70.

Young, G.R., 1982. Recent work on biological control in Papua New Guinea and some suggestions for the future. Int. J. Pest Manag. 28 (2), 107–114. https://doi.org/10.1080/09670878209370686.

Apéndice 3 - Dispersal and plant arrangement condition the timing and magnitude of coffee rust infection (Material Suplementario)

Supplementary material 1- Complementary figures and tables

Supplementary material 3- Estimation of parameters

https://doi.org/10.1016/j.ecolmodel.2022.110206

SUPPLEMENTARY MATERIAL 1. Complementary figures and tables from: DISPERSAL AND PLANT ARRANGEMENT CONDITION THE TIMING AND MAGNITUDE OF COFFEE RUST INFECTION

Emilio Mora Van Cauwelaert, Cecilia González González, Denis Boyer, Zachary Hajian Forooshani, John Vandermeer , Mariana Benítez

1. Equilibrium points

The equilibrium points of the model with m= 0 (no diffusion) are:

$$(S_{eq}, I_{eq}, X_{eq}) \in \{(1,0,0), (\frac{1}{R_0}, \frac{\rho}{\gamma}(1-\frac{1}{R_0}), \frac{\alpha}{\mu}I_{eq})\}$$

For R_0 defined as:

$$R_0 = \frac{\beta_2 + \frac{\beta_1 \alpha}{\mu}}{\gamma}$$

The value of R_0 determines the stability for both equilibria. When R_0 is less than 1, the first equilibrium (1,0,0) is stable and the second equilibrium ($1/R_0$, ρ/γ (1-$1/R_0$), α/μ I_{eq}) is unstable. After any initial perturbation, the system reaches the first equilibrium where there is no infection. When R_0 ≥ 1, the first equilibrium point becomes unstable and the system reaches the second equilibrium (now stable) point where S decreases with R_0, whereas I and X "invade", or increase with R_0 (see (Cunniffe and Gilligan, 2010) for the full linear analysis).

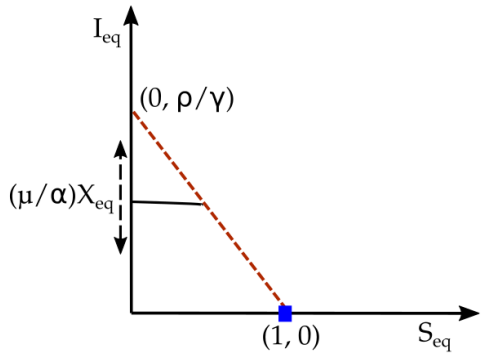

Fig. S1.1 Relationship between the equilibrium points of the model (S_{eq}, I_{eq}, X_{eq}) and the parameters. We represent I_{eq} in function of S_{eq} and represent the value of X_{eq} as a slider in the I_{eq} axis. The blue dot represents the first equilibrium point (stable when $R_0 < 1$) and the red dotted line represents the possible values of S_{eq} and I_{eq} in the second equilibrium point (stable when $R_0 \geq 1$).

2. *S*, *I* and *X* dynamics

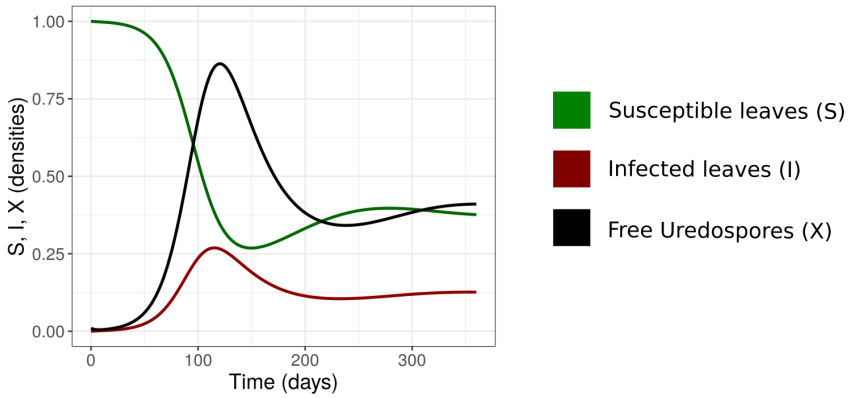

Fig. S1.2 Example of infection dynamics for susceptible, infected leaves and free uredospores. For this simulation, α=0.65, $\beta_1 = \beta_2$= 0.035, ρ= 0.011, μ= 0.2, γ=0.056 and I_0 = 0.01

3. MATI difference with I_{eq} for the single plant

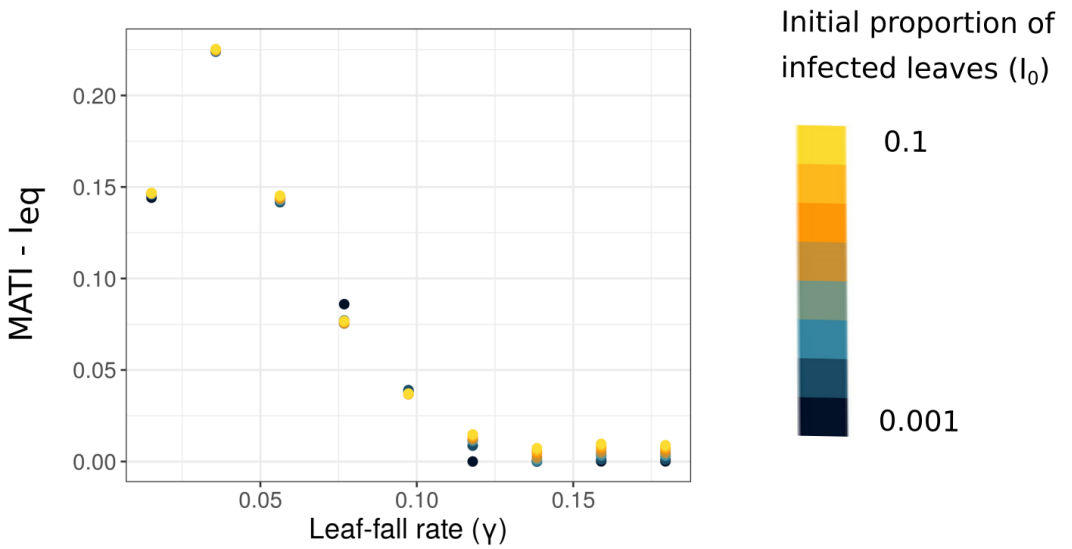

Fig. S1.3. Difference between MATI and I at equilibrium (Ieq) in isolated coffee plants as a function of the leaf-fall rate (γ), with different initial proportion of infected leaves (I_0).

The difference between MATI and the final amount of infected leaves in equilibrium (I_{eq}) shows the same dependence on γ (Fig. S1.3; see Fig. S1.1 for the influence of γ on equilibria and stability).

4. MATI dependence on distance-between-plant index <H>

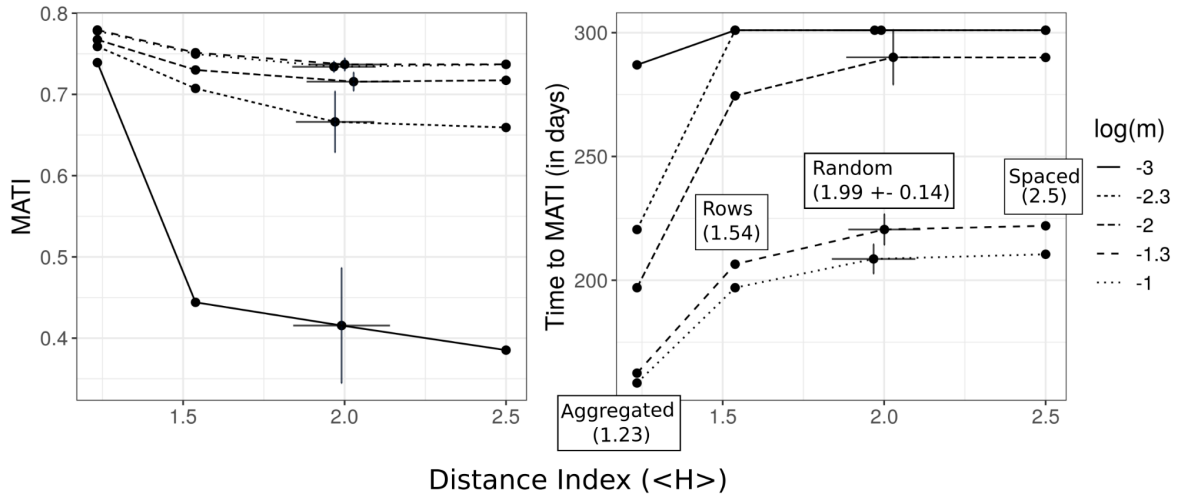

Fig. S1.4. MATI and time to MATI as a function of the distance-between-plant index <H>. Values of MATI and time to MATI corresponding to four values of <H>, with 2 levels of diffusion (high: 0.01 and low: 0.001) and one level of I_0 (0.001) (the figure for I_0 = 0.1 is very similar). For the random arrangement, each point represents a 30-simulation average, and the error bars the standard deviation both in the <H> and in MATI and time to MATI. The values of α, β_1, β_2, ρ and μ are shown in Table 1. We used γ=0.015.

5. Individual tree heterogeneity

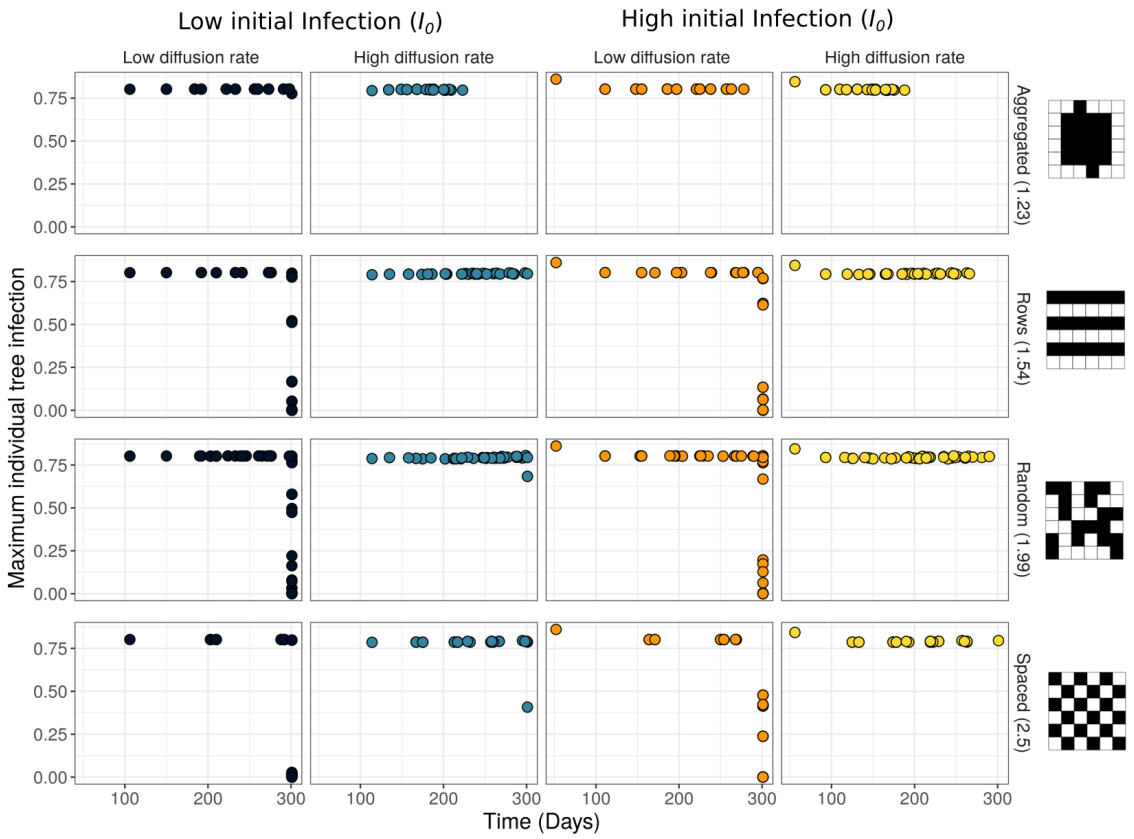

Fig. S1.5 Maximum individual tree infections and the time to reach it. This figure represents each tree's values for the different plant arrangements (aggregated, random, rows and spaced), two levels of diffusion (low=0.001 , high= 0.01) and two levels of I_0 (low= 0.001, high= 0.1). The values of α, β_1, β_2, ρ and μ are shown in Table 1. We used γ=0.015.

6. Time lags measurements from real time series and from simulations.

Table. S1. 1 Duration of the time lag (Time Lag, TL), the growth phase per se (Time Growth, TG) and the time to MATI (TL+ TG) measured in 5 different plots subject to coffee rust infections (Fig. 2). PP: Precipitation

Plot Letter in Fig.2	Day when PP> 50mm	Time Lag (TL)	Time Growth (TG)	Time to MATI (TL + TG)
B	67	24.5	104.5	129
C	114	80	105	185
C	465	145.5	180.5	326
F	105	81.5	120.5	202
G	104	134.5	132.5	267
I	896	27	68	95

Table. S1. 2 Duration of the time lag (Time Lag, TL), the growth phase per se (Time Growth, TG) and the time to MATI (TL+ TG) from simulations, for the different combinations of planting arrangements, diffusion rate (m) and initial proportion of infected leaves (I_0). For the random arrangement the values are the mean and standard deviation (+-) of 30 replicates.

Arrangement	m	*I0*	Time Lag	Time Growth	Time to MATI (TL + TG)
Aggregated (1.23)	0.001	0.001	99	188	287
		0.1	61	191	252
	0.005	0.001	78	143	220
		0.1	42	144	186
	0.01	0.001	73	124	197
		0.1	33	130	162
	0.05	0.001	69	94	162
		0.1	23	101	124
	0.1	0.001	69	89	158
		0.1	22	94	116
Rows (1.54)	0.001	0.001	150	150	300
		0.1	113	187	300
	0.005	0.001	94	206	300
		0.1	60	226	285
	0.01	0.001	84	190	274
		0.1	50	189	239
	0.05	0.001	83	123	206
		0.1	34	132	166
	0.1	0.001	88	109	197
		0.1	33	118	150
Random (1.99)	0.001	0.001	135 (+- 38)	166 (+- 38)	300 (+- 0)
		0.1	96 (+- 30)	205 (+- 30)	300 (+- 0)
	0.005	0.001	102 (+- 19)	199 (+- 19)	300 (+- 0)
		0.1	70 (+-20)	224 (+- 21)	294 (+- 10)
	0.01	0.001	86 (+- 15)	203 (+- 19)	290 (+- 11)
		0.1	56 (+- 17)	201 (+- 18)	257 (+- 12)
	0.05	0.001	83 (+- 8)	137 (+- 8)	221 (+- 16)
		0.1	34 (+- 7)	146 (+- 8)	179 (+- 5)
	0.1	0.001	88 (+- 6)	120 (+- 5)	209 (+- 6)
		0.1	32 (+- 5)	129 (+- 6)	161 (+- 5)
Spaced (2.5)	0.001	0.001	147	153	300
		0.1	108	192	300
	0.005	0.001	118	182	300
		0.1	78	216	294
	0.01	0.001	108	182	290
		0.1	67	185	252
	0.05	0.001	92	130	222
		0.1	44	135	179
	0.1	0.001	96	115	210
		0.1	38	123	161

7. Sensitivity analysis (size of the integration step and plant-level parameters variation)

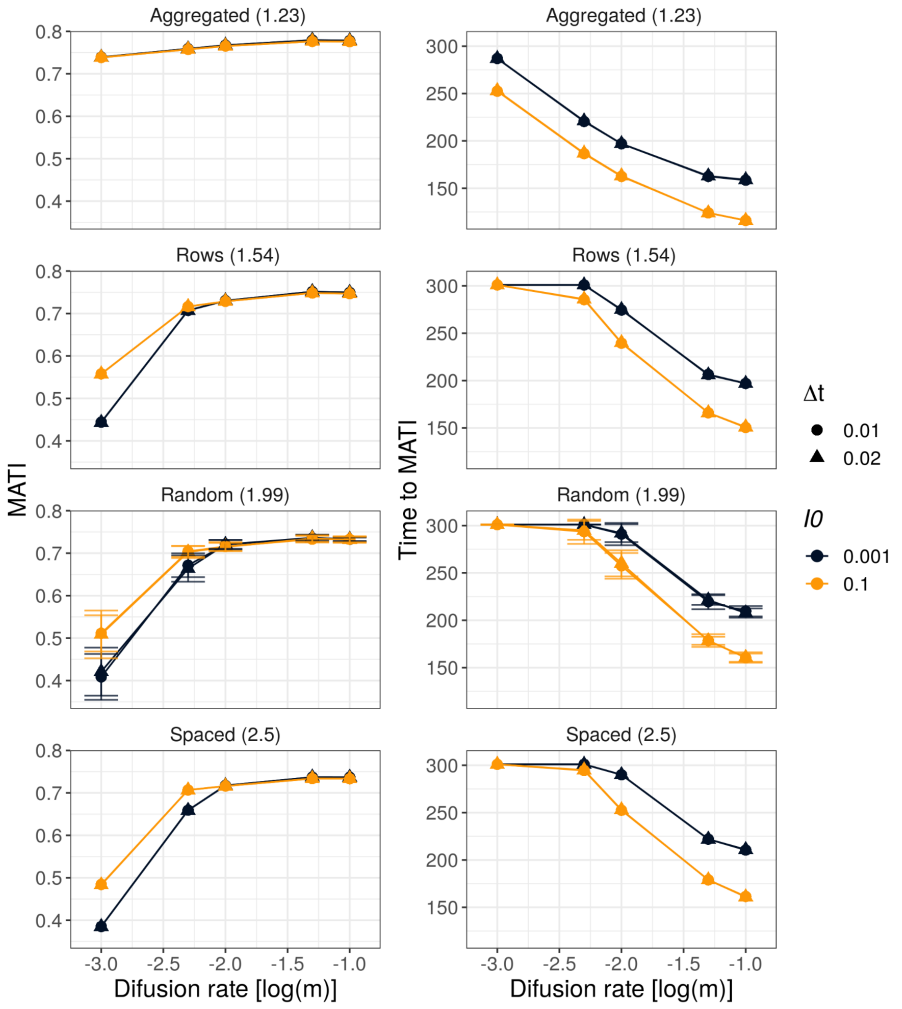

Fig. S1.6. Robustness of MATI and time to MATI results for two values of the integration step (Δt). Simulations of four different planting arrangements (aggregated, random, rows and spaced) with five levels of diffusion rate (*m* between 0.001 and 0.1, or log(m) between -3 and -1), two levels of I_0 (0.001 and 0.1, dark and orange lines respectively), and two values of Δt (0.01, 0.02). For the random arrangement, each point represents a 30-simulation average, and the error bars the standard deviation. The values of α, β_1, β_2, ρ and μ are shown in Table 1. We used γ=0.015.

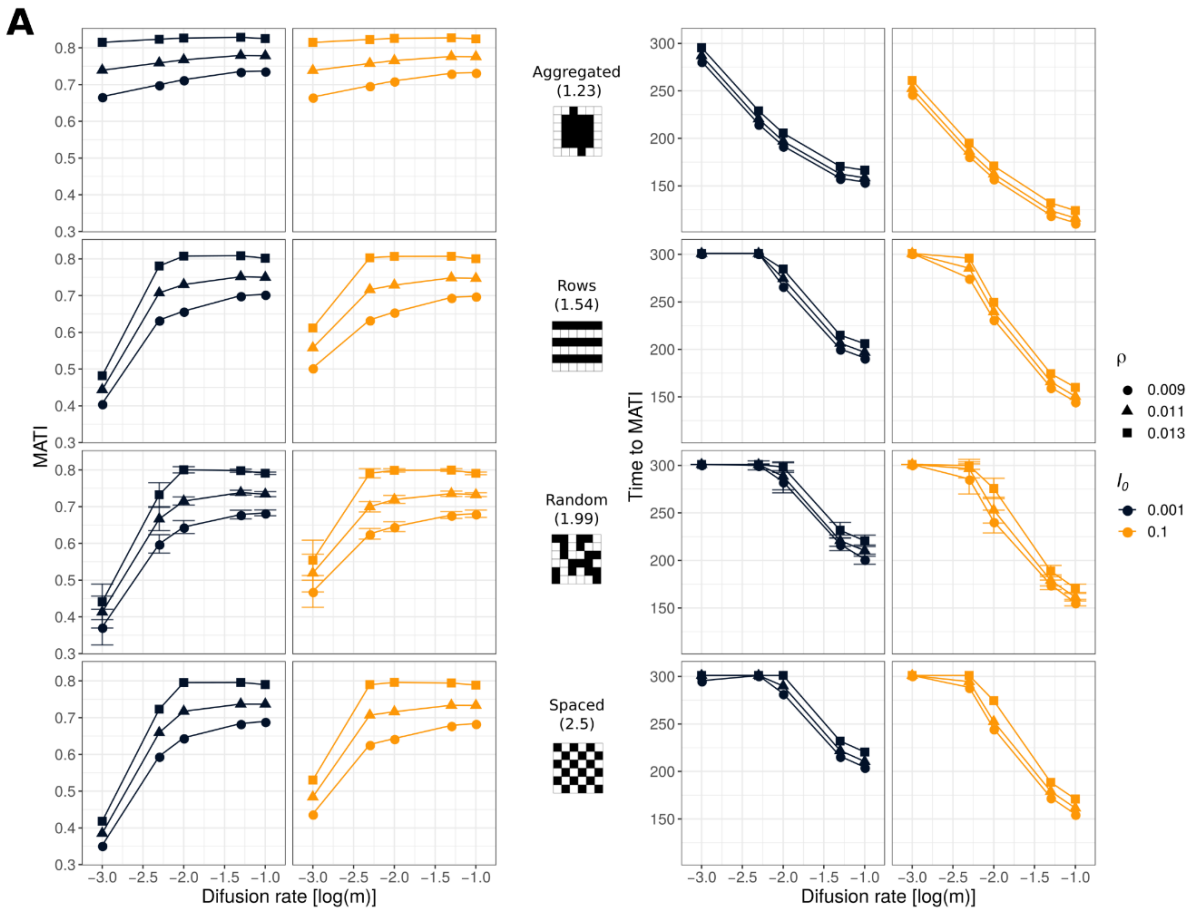
A
MATI
Time to MATI
Aggregated (1.23)
Rows (1.54)
Random (1.99)
Spaced (2.5)
Difusion rate [log(m)]
ρ
0.009
0.011
0.013
I_0
0.001
0.1

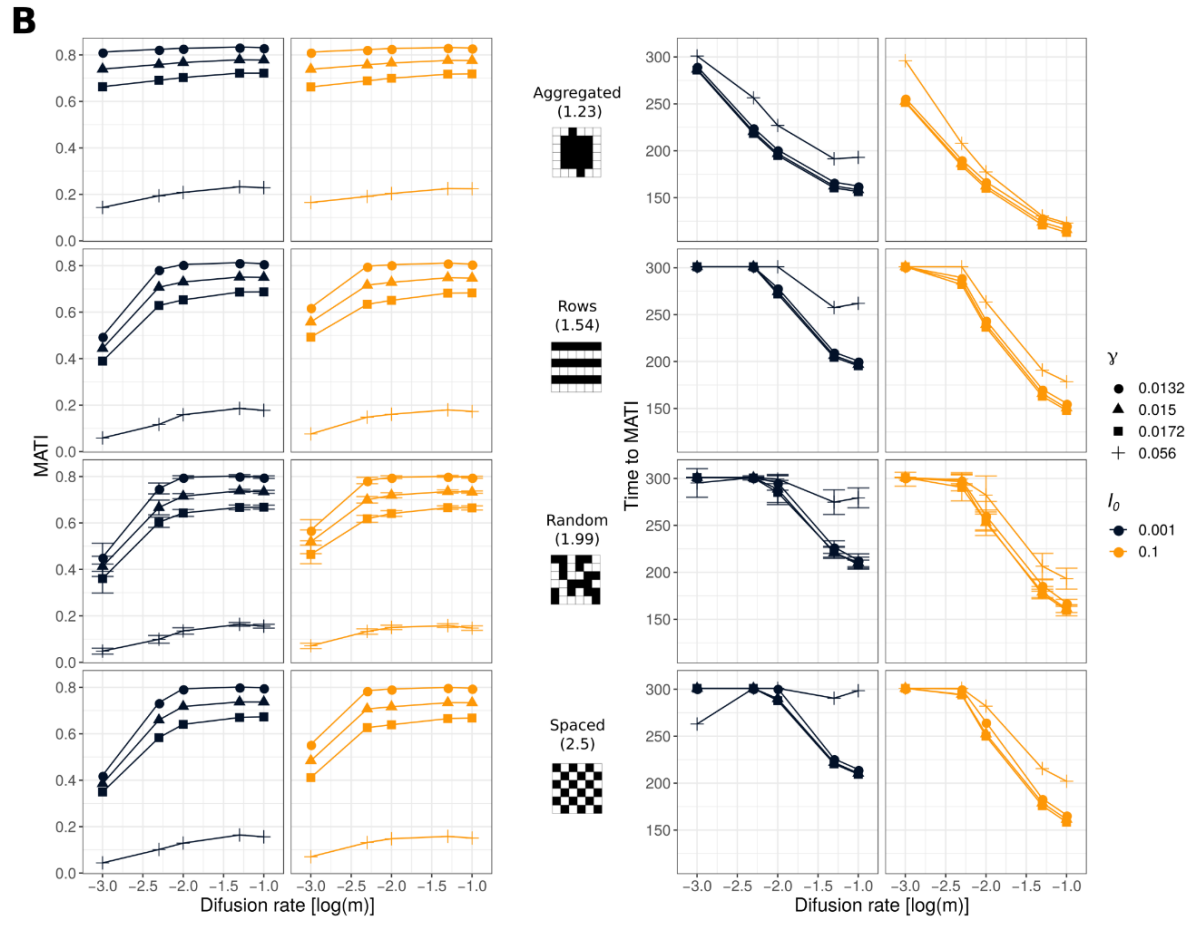
B
MATI
Time to MATI
Aggregated (1.23)
Rows (1.54)
Random (1.99)
Spaced (2.5)
Difusion rate [log(m)]
γ
0.0132
0.015
0.0172
0.056
I_0
0.001
0.1

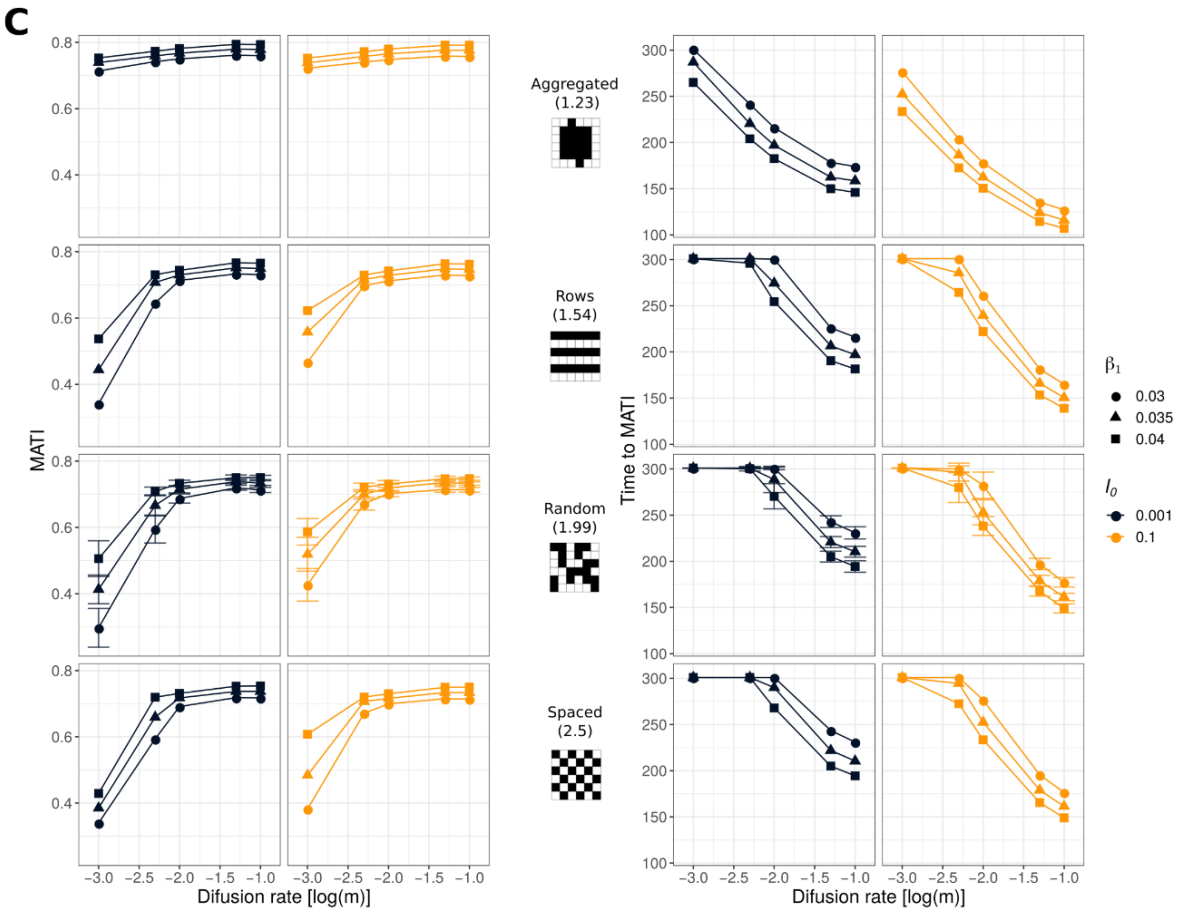
C
MATI
Time to MATI
Aggregated (1.23)
Rows (1.54)
Random (1.99)
Spaced (2.5)
Difusion rate [log(m)]
Difusion rate [log(m)]
β1
0.03
0.035
0.04
I0
0.001
0.1

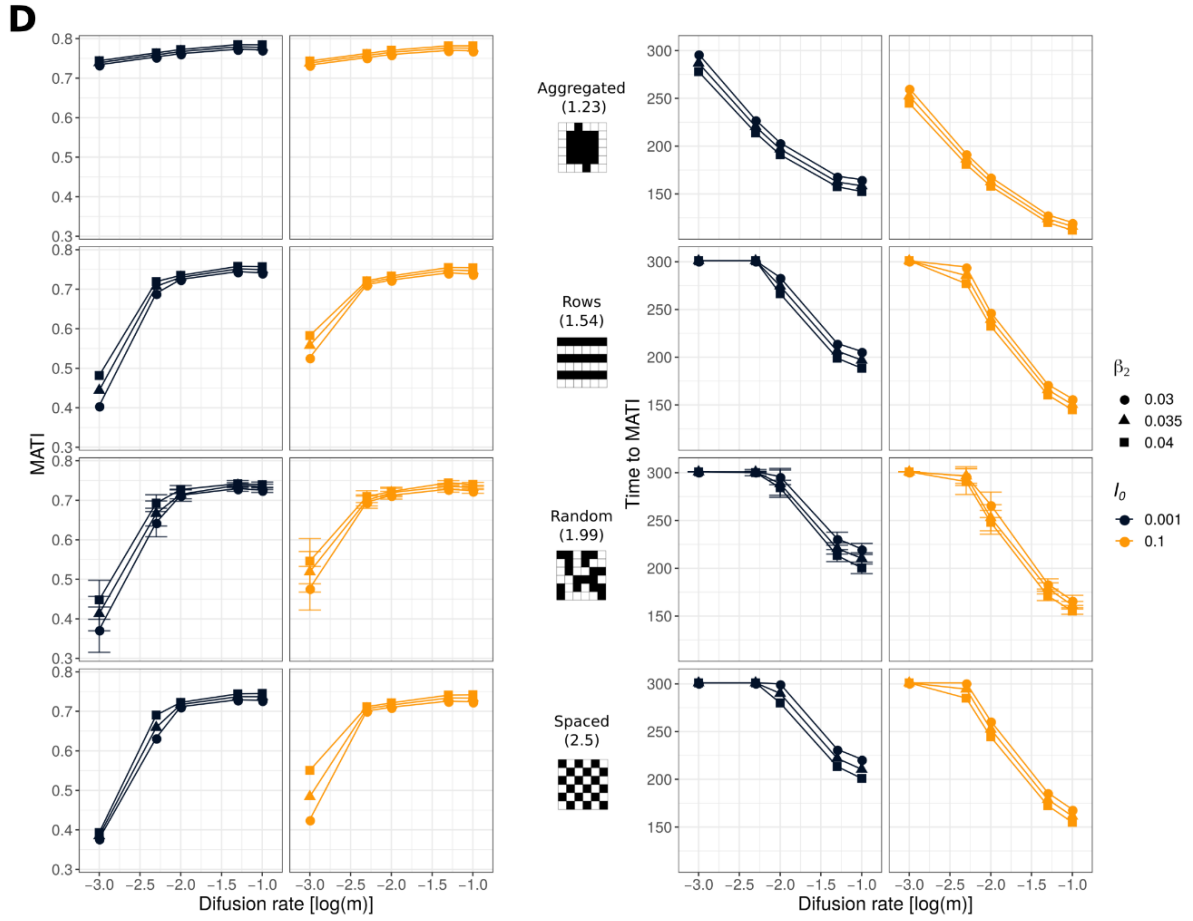
D
MATI
Time to MATI
Aggregated (1.23)
Rows (1.54)
Random (1.99)
Spaced (2.5)
Difusion rate [log(m)]
Difusion rate [log(m)]
β2
0.03
0.035
0.04
I0
0.001
0.1

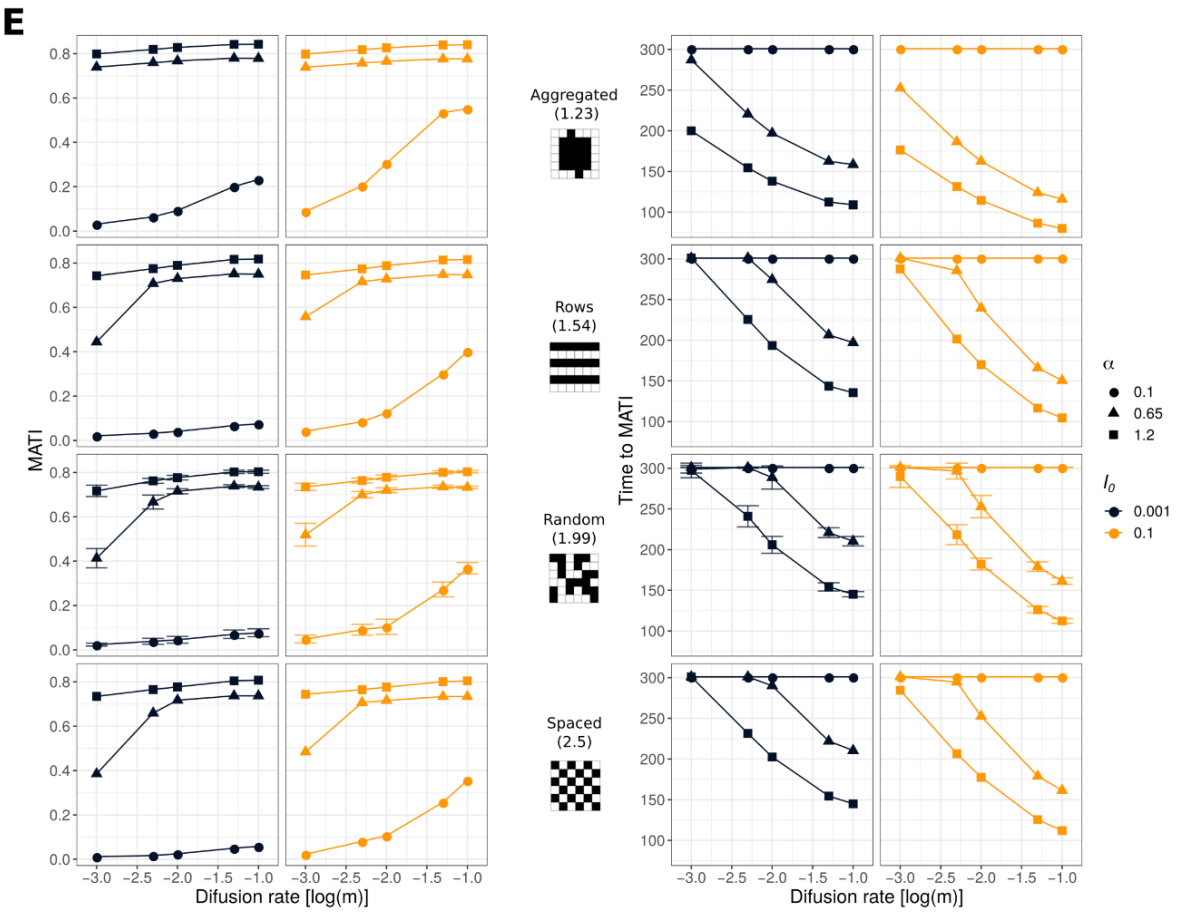
E
MATI
Time to MATI
Aggregated (1.23)
Rows (1.54)
Random (1.99)
Spaced (2.5)
Difusion rate [log(m)]
α
0.1
0.65
1.2
I_0
0.001
0.1

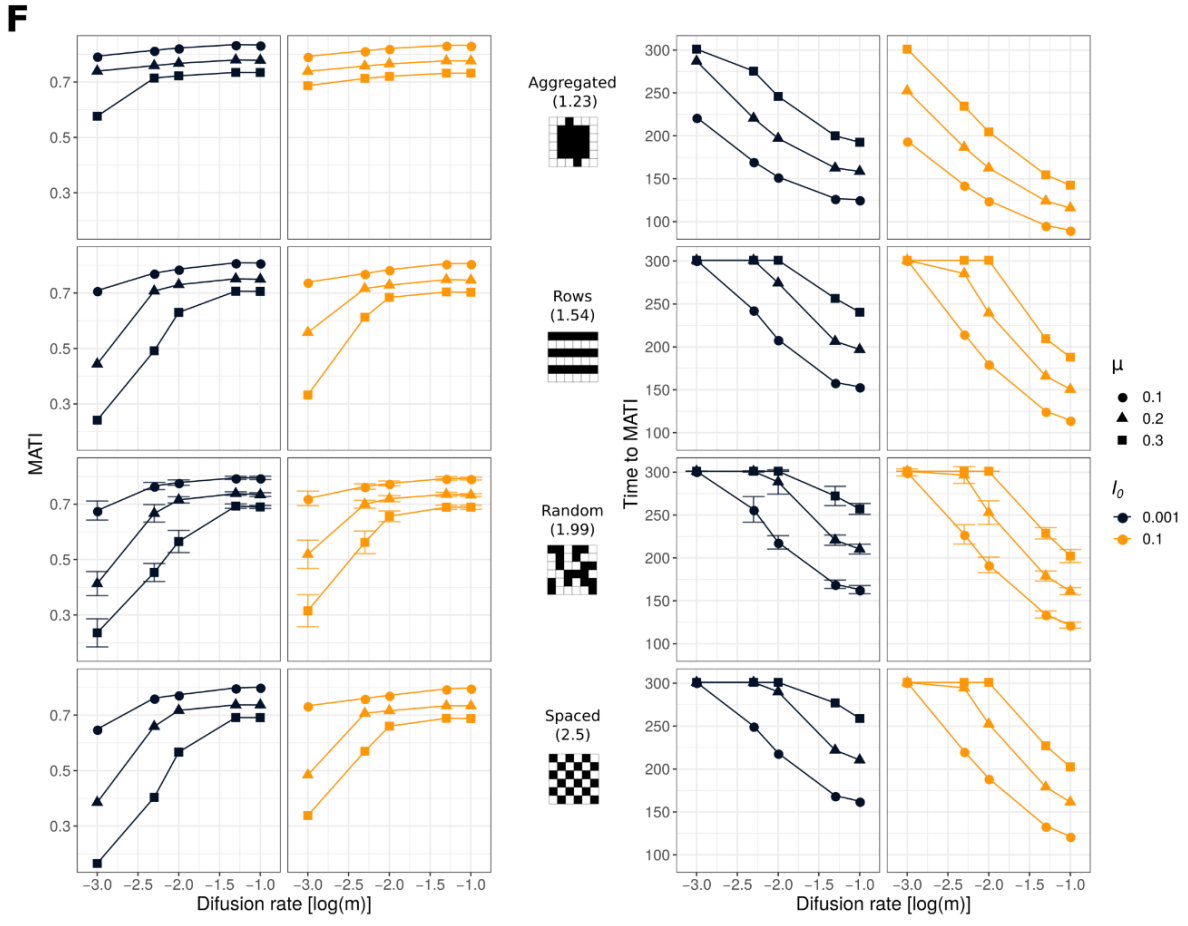
F
MATI
Time to MATI
Aggregated (1.23)
Rows (1.54)
Random (1.99)
Spaced (2.5)
Difusion rate [log(m)]
μ
0.1
0.2
0.3
I_0
0.001
0.1

Fig. S1.7. Robustness of MATI and time to MATI results for different values of the plant-level parameters. We represent the variation in the results of Fig. 4 (main manuscript) produced by changing one parameter at a time within its estimated range (A:ρ, B: γ , C: β_1, D: β_2, E: α, F: μ). For each scenario we represent the results with the used values of the parameters in the main manuscript (triangles) and with the lowest and highest values of the estimated range (circle and square). In the γ scenario we show the results with a higher value (γ= 0.056, cross point) that accounts for leaf-removal practices. The scenarios represent the four different planting arrangements (aggregated, random, rows and spaced) with five levels of diffusion rate (m between 0.001 and 0.1, or log(m) between -3 and -1) and two levels of I_0 (0.001 and 0.1, dark and orange lines respectively). For the random arrangement, each point represents a 30-simulation average, and the error bars the standard deviation.

Supplementary 3 - DISPERSAL AND PLANT ARRANGEMENT CONDITION THE TIMING AND MAGNITUDE OF COFFEE RUST INFECTION

E. Mora Van Cauwelaert C. González González D. Boyer J. Vandermeer
Z. Hajian-Forooshani M. Benítez

0. The model

The diagram for the local plant model is:

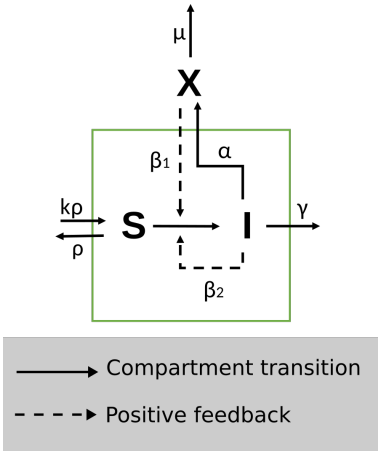

This model is then described by the following set of ODE. As we only focus on one plant, we removed the indices of the equation presented in the main text in order to simplify the notation.

$$\begin{aligned}\frac{dS}{dt} &= \rho(K-S) - \beta_1 X\frac{S}{K} - \beta_2 I\frac{S}{K}\\ \frac{dI}{dt} &= \beta_1 X\frac{S}{K} + \beta_2 I\frac{S}{K} - \gamma I\\ \frac{dX}{dt} &= \alpha I - \mu X\end{aligned} \tag{1}$$

where:

S: number of susceptible leaves in one coffee tree.

I: number of infected leaves with infective spores in one coffee tree.

X: amount of infective packages of spores *outside* the plant (see diagram). We call them packages since 15 to 30 spores are needed per cm2 per leaf to start an infection (Bock 1962).

$K = b/\rho$ is the carrying capacity (number of leaves per plant) where ρ is the inverse of the average time needed for a newly mature susceptible leaf to fall, and b is the number of leaves produced per unit of time (here [t]= days). We can also express b as $K\rho$ (see general diagram). Here we assume for simplicity that K = 1, so that ρ is equal to b. β_1 and β_2 are the rates of primary and secondary infection. $1/\beta_1$ is the time

Table 1: Estimated parameters range. The letters indicate the references. a-Rakocevic and Takeshi (2018), b- Mulinge and Griffiths, E., (1974), c- Firman and Wallis (1965) d- Leguizamón-Caycedo et al. (1998), e- Bock (1962), f-Rayner (1961), g-Gagliardi et al. (2020), h- Boudrot et al. (2016), i- Silva-Acuña et al. (1999) j- Deepak, K., et al. (2012), k- Nutman, et al. (1963).

Parameters	ρ	$\gamma = \rho + h_I$	$\beta_1\beta_2$	α	μ
Definition	Natural leaf growth and death rate	Infected leaves death rate	1st and 2d infection rate	Recruitment rate	Spore death rate
Units	t-1	t-1	nspore-1 t-1, nleaf-1. t-1	nspore nleaf-1. t-1	t-1
Range	[0.009-0.013]	pI= [0.0042]	[0.03-0.04]	[0.1-1.2]	[0.1-0.3]
Section	I, III	III	I	II	II
References	a, b	a, c	d, e	e, f, g, h, i	j, k

taken for one susceptible leaf in contact with one external package of infective spores to become an infected leaf with new infective spores. In this sense, this term includes spores that are surrounding the tree. $1/\beta_2$ is the time taken for one susceptible leaf, in contact with another infective leaf, to become an infected leaf with new infective spores[1]. Since one infected leaf has multiple spores, one leaf is sufficient to start an infection into another leaf. Besides, we are assuming that dispersion of spores from one leaf to another inside the tree is included in the β_2 term. α is the spore recruitment from infected leaves to the outside of the plant. γ is the infected leaf fall rate. This rate considers natural leaf fall and leaf fall due to the rust infection ($\gamma = \rho + h_I$). $1/\gamma$ is then the average time taken for an infected leaf to fall. Finally μ is the spore death rate.

Assumptions

The model is set up for the rainy season. This means that:

a) The spores are washed out from the top to the bottom of the plant (Bock 1962). So, spores from one leaf can be in contact with any other leaf in the plant. As the vector inside the plant is well mixed, we can assume that leaves are also "well mixed" (since β_2 includes this kind of infection).

b) Optimal conditions for rust development are always met.

I. In field measurements of parameters (direct estimation)

a) ρ measurement

In Rakocevic and Takeshi Matsunaga (2018) leaf life span and leaf expansion time were recorded in growing degree days (GDD). GDDs were calculated as $GDD = T_{mean} - T_b$, where T_{mean} is the mean air temperature calculated as the average of daily minimum and maximum air temperatures, and T_b is the base temperature for each species (Rakocevic and Takeshi Matsunaga 2018). The calculated T_b is 10.2 °C. Using Rakocevic supplementary material (2018) we estimated the relationship between GDD and a normal day in active season (The active season goes from oct-13 to abr-13 and from oct-14 to dic-14) (the warm-rainy season) and reduced season (remaining days, dry-cold season). We obtained the mean of GDD/day in active and reduced season in order to tranform the reported GDD for leaf growth parameters to days.

For Active season GDD/days = 13.7, for Reduced season, GDD/days = 9.25

In rust infection, fully expanded leaves are the most infected[2]. So we consider the adult life span of a leaf (S) from the moment when it is fully expanded to the moment when it falls. With this in mind, we

[1] Assuming $K = 1$, if this is not the case, $\beta_n = \beta_n^* K$ $(n \in 1, 2)$, where $1/\beta_n^*$ is the characteristic time

[2] With natural infection, young lesions have been observed on leaves of all ages except those still of juvenile (glossy) appearance. This appearance is lost on average in week 12.2 [85.4 days] of age (Rayner 1961). As the incubation period averages 5 weeks it is evident that leaves are rarely infected until fully expanded (Rayner 1961)

Table 2: Average GDD in active o reduced season. CFA refers to the climate classification, (see Rakocevic and Takeshi (2018) for full explanation)

Bar	Type	GDD.LifeSpan	GDD.LeafExpansion	GDD.AdultLife
Bar1	Act_Growth_CFA	1809.89	671.03	1138.85
Bar3	Red_Growth_CFA	1769.96	632.41	1137.55
Bar5	Act_Growth_CFA	2076.05	806.21	1269.84
Bar7	Red_Growth_CFA	1969.58	704.83	1264.75
Bar9	Act_Growth_CFA	1876.43	864.14	1012.29
Bar11	Red_Growth_CFA	2009.51	811.03	1198.47
Bar13	Act_Growth_CFA	2408.75	840.00	1568.75
Bar15	Red_Growth_CFA	2169.20	801.38	1367.82

Table 3: Mean life (F) range in GDD and real days

	Act_Growth_CFA	Red_Growth_CFA
meanGDD_Adult.Life	1247.43	1242.15
sdGDD_Adult.Life	238.63	98.58
MinDay_Adult.Life	73.64	123.63
MaxDay_Adult.Life	108.47	144.94

transformed the reported data for full life span (F), leaf expansion (E) and adult life span ($F - E$). This adult life time is then assumed to be $1/\rho$ (this measurement is more precise than considering expansion, because expansion depends a lot on the final size of the leaf). Our model simulates infection in climatic conditions with optimum precipitation and temperature values, so we only took the values for the "Active season" (warm and rainy). Specifically we only took Rakocevic's reported data for CFA Koppen-climate. This is a good proxy since during "Active Season" this climate is similar to the one present in Mexican coffee plantations in the rainy season (table 2 and 3). Specifically we took the {mean-sd, mean+sd} for GDD_Adult.Life (MinDay_Adult.Life and MaxDay_Adult.Life) and for each value, we transformed it to normal days (table 3).

In active season, the time taken for a fully expanded leaf S to fall is in $[74 - 108]$ days. So, $\rho \in [0.009, 0.013]$. (For reduced season (dry season) $\rho \in [0.007 - 0.008]$.)

b) Primary and secondary infection measurement (β_1, β_2)

The average time taken for a susceptible leaf in contact with an infective leaf or a infective package of spores, to become an infected leaf with new infective spores ranges from 26 to 35 days in average in conditions similar to the ones present in mexican coffee agroecosystems (Leguizamón-Caycedo, Orozco-Gallego, and Gómez-Gómez 1998). So in this case: $\beta_1, \beta_2 \in [0.03, 0.04]$.

II. Data-based estimation of parameters

a) Mortality rate of spores (μ)

If there is no new infection, we can say that the amount of infective spores in time follows the equation: $X(t) = X(0)e^{-\mu t}$ in our model. Deepak et al. (2012) reported that for rust RI variety only the 4% of original spores is viable after 15 days. In each day trial, spores were germinated for 16 hours. For rust RVIII, this

percentage increases to 23% (Deepak, Hanumantha, and Sreenath 2012). We can use this data to estimate the value of μ in our equation.

$$X(15) = 0.04X(0) = X(0)e^{-\mu(15)} \tag{2}$$

$$e^{-\mu(15)} = 0.04 \tag{3}$$

$$\mu = \frac{ln(0.04)}{-15} \tag{4}$$

$$\mu = 0.2 \tag{5}$$

And for RVIII

$$\mu = \frac{ln(0.23)}{-15} \tag{6}$$

$$\mu = 0.1 \tag{7}$$

In this case $\mu \in [0.1, 0.2]$

In another work by Nutman et al, (1963) spore viability is calculated at 22°C. They decrease in viability follows a power law (Nutman, Roberts, and Clarke 1963):

$$X(t) = X(0)(t+1)^{-0.809} \tag{8}$$

We generated a database with Nutman equation and fitted it to our exponential model for the first 5 days.

The μ that fitted the plot best is equal to 0.343 and is statistcally significant. We can say that $\mu \in [0.1, 0.3]$.[3] After 75 days, the viability remains at 20%. In this case $\mu = 0.02$. For models than consider spores travelling at high altitudes this might be relevant.

b) Recruitment rate of new spores (α)

α is the rate of recruitment of a new package of infective spores (to the external surrounding medium) from one infective leaf. If we only look at the production of new spores we have the equation:

$$\frac{dX}{dt} = \alpha I(t) \tag{9}$$

In this case, $[\alpha]$ = [spores/infected leaf/day]. We know from Rayner (1961)that one lesion produces around 300 thousand spores in a period of 3 to 5 months (Rayner 1961). This means that per day, one lesion produces around 2000 to 3000 spores (assuming constant production).

One rusted leaf has from 2 to 6 active lesions (amount of lesions that are constantly producing spores). (Firman and Wallis 1965)(Silva-Acuña et al. 1999). So, one infective leaf produces from 4000 to 18 000 spores per day.

[3] In both estimations, temperature is constant, but we know that this death rate decreases a lot with very low temperatures (4°C) (Capucho et al. 2005)

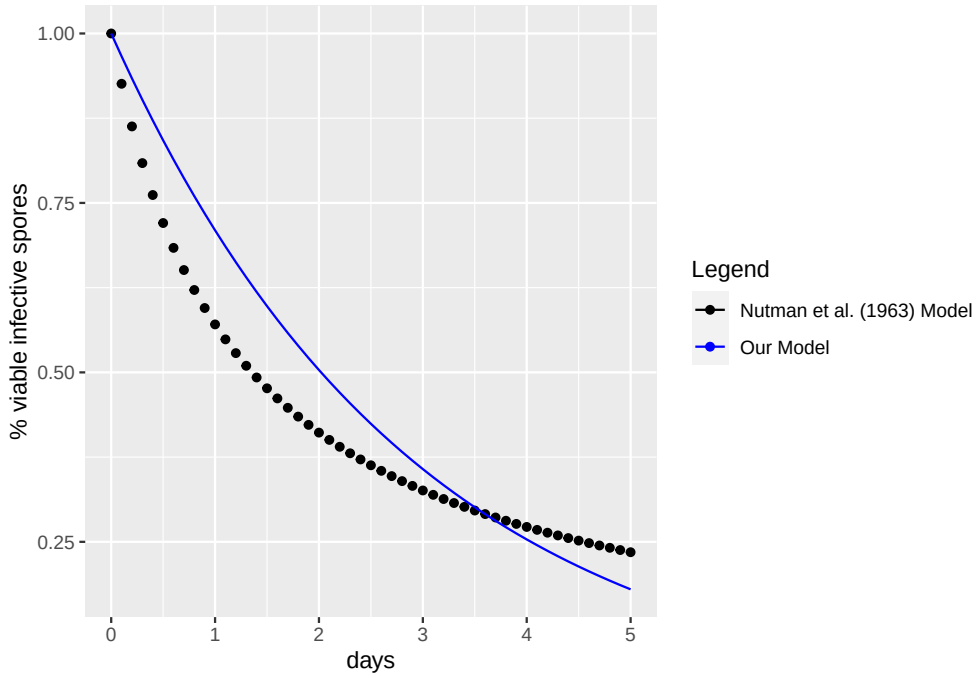

Figure 1: Viability of uredospores (Nutman, 1963) and our model fitting

According to Boudrot et al. (2016) and Gagliardi et al. (2020) there is a 1000-1 relationship between spores in the leaf and spores in the air (Boudrot et al. 2016) (Gagliardi et al. 2020) . As X represent specifically spores in the air surrounding the tree (that eventually fall down to the tree) we will use this relation.

Finally we know that, in order to be infective, the optimum quantity of spores (or package of spores) is between 15 to 30 spores (Bock, 1962). Taking all these factors into account we can conclude that one infected leaf releases from 0.1 to 1.2 infective packages of spores per day to the air. We will asume this same quantity falls back into the tree.

$\alpha \in [0.1, 1.2]$ spores/rusted leaf/day

III. Data based fitting-estimation

We used time-series data and few assumptions on the behaviour of some variables to extract the range of the missing parameters or to confirm the already reported ones. For this we extracted data using WebPlot-digitizer. We first used the data from Firman and Wallis (1965) on the fallen rusted and non rusted leaves to estimate ρ and γ (Firman and Wallis 1965). We then used Mulinge and Griffiths (1974) data set to have another estimation of ρ (Mulinge and Griffiths 1974).

a) Relationship between ρ and γ

With data from Firman and Wallis (1965) we first built a table (Table 4) with the total number of susceptible and infected leaves in a tree per month (roughly) from october 1961 to july 1963. The method was the following:

The paper reports the total number of fallen leaves per month (F) (Fig3. in the original paper) and the total amount of leaves in the tree both in october 61 and july 1963 (Table 8 in the original paper). The change in foliation during a specific interval (Δ) can be described with the following equation:

$$T_{(t+\Delta)} = T_{(t)} + [P_{(t+\Delta)} - P_{(t)}] - [F_{(t+\Delta)} - F_{(t)}] \tag{10}$$

where P is the new produced leaves, F, the fallen leaves and T, the total number of leaves in the tree. So, we can write:

$$[P_{(t+\Delta)} - P_{(t)}] = T_{(t+\Delta)} - T_{(t)} + [F_{(t+\Delta)} - F_{(t)}] \tag{11}$$

Firman and Wallis (1965) report that $T_{(jul63)} = 3613$, $T_{(oct61)} = 4000$ and that the total amount of fallen leaves during that period equals: $F_{(jul63)} - F_{(oct61)} = 7287$. This means that, according to equation 11, the production of leaves from october 61 to november 63 ($P_{(nov63)} - P_{(oct61)}$) equals 6900.

Now, if we assume that leaf production is constant during that time[4] (this time is 574 days) we can derive that the production of leaves per day equals: $6900/574 = 12.02$.

With this, we estimated the production of new leaves per month ($P_{t+d} - P_t$) and the total number of leaves in the tree (T_t) per month (Table 4). Finally, we calculated, among those total leaves (T_t), the total quantity of susceptible (St) and infected leaves (It) per recorded time using Fig 1 values in (Firman and Wallis 1965)] that report the proportion of infected leaves (Prop(It)) per month (Table 4).

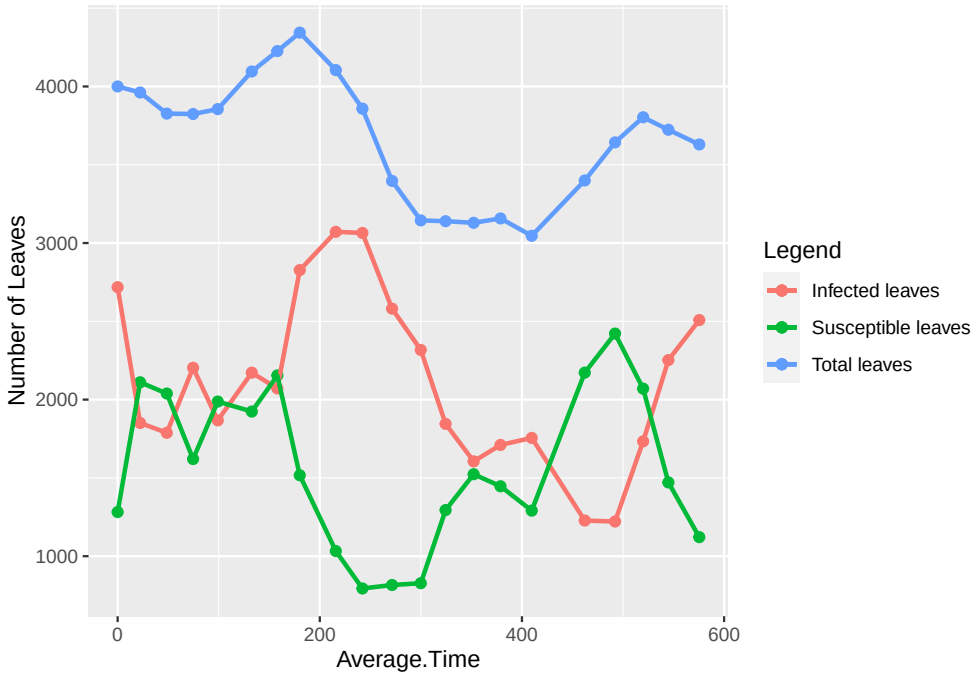

Figure 2: Proportion of Infected, Susceptible and Total Leaves. Data from: (Firman and Wallis, 1965)

[4]This makes sense since, with no infection, $\frac{dS}{dt} = b - hS = h(\frac{b}{h} - S) = \rho(K - S)$ which is the monomolecular model

Table 4: Proportion of rusted and non-rusted fallen leaves per time. Ft+d-Ft: Difference in fallen leaves, Ft: total fallen leaves, Prop(It): proportion of tree-level rust infection, Pt+d-Pt: produced leaves per recorded time, Tt: total leaves in the tree, It: number of infected leaves, St= number of susceptible leaves

Date	Ft+d-Ft	Ft	Prop(It)	Average Time	Pt+d-Pt	Tt	It	St
Oct61	NA	NA	67.95	0.00	NA	4000.00	2718.03	1281.97
Nov61	305.94	305.94	46.72	22.25	267.44	3961.50	1850.86	2110.63
Dec61	452.32	758.26	46.72	48.66	317.43	3826.61	1787.84	2038.77
Ene62	314.89	1073.16	57.62	74.63	312.23	3823.95	2203.47	1620.48
Feb62	262.22	1335.38	48.44	99.06	293.61	3855.34	1867.63	1987.71
Mar62	164.27	1499.65	53.03	132.72	404.57	4095.64	2172.03	1923.61
Apr62	173.76	1673.41	49.02	158.01	303.93	4225.81	2071.34	2154.47
May62	148.57	1821.98	65.08	180.19	266.63	4343.87	2827.08	1516.80
Jun62	668.01	2489.99	74.84	215.85	428.68	4104.55	3071.68	1032.87
Jul62	562.89	3052.88	79.43	242.18	316.51	3858.17	3064.40	793.77
Aug62	813.71	3866.60	75.98	271.50	352.32	3396.78	2580.99	815.78
Sep62	594.11	4460.71	73.69	299.93	341.82	3144.48	2317.12	827.36
Oct62	299.81	4760.52	58.77	324.45	294.75	3139.42	1845.05	1294.37
Nov62	344.10	5104.63	51.31	352.23	333.85	3129.17	1605.62	1523.55
Dec62	291.30	5395.92	54.18	378.79	319.28	3157.15	1710.56	1446.60
Ene63	482.26	5878.18	57.62	409.69	371.40	3046.29	1755.36	1290.93
Mar63	277.08	6155.26	36.11	462.13	630.33	3399.55	1227.46	2172.09
Apr63	117.06	6272.32	33.52	492.11	360.38	3642.86	1221.26	2421.61
May63	173.79	6446.11	45.57	519.91	334.08	3803.15	1733.24	2069.91
Jun63	379.93	6826.05	60.49	544.88	300.23	3723.45	2252.38	1471.07
Jul63	461.45	7287.50	69.10	575.46	367.51	3629.51	2507.93	1121.58

Secondly, we used this table to estimate ρ and γ. Firman and Wallis (1965) state that from May 1962 to September 1962, 87.6% of fallen leaves were rust-infected and the rest were without rust. This means that for the total amount of 2787 fallen leaves[5] in this period, 2441 were rust infected (R_I) and 346 were free of infection (R_S). We know that the amount of fallen susceptible leaves follows the next equation:

$\frac{dR_S}{dt} = \rho S$

This means that we can aproximate the value of ρ by:

$$R_S(t) = \rho \int_0^t S$$

We estimated the Area under the Curve (AUC) of S from May 1962 to September 1962 and calculated the corresponding ρ. This gives $\rho = 0.00300$

Then, we used the same procedure to estimate γ, using AUC of I(t) and the value of fallen leaves in may62-sep62. According to the next equation:

$$R_i(t) = \gamma \int_0^t I$$

We have $\gamma = 0.0072$. So, for this system $\gamma = \rho + 0.0042$.

b) Comparison of the estimated ρ value with data fitting

If we assume no infection, our model for the change of S becomes:

$$\frac{dS}{dt} = \rho(K - S) \tag{12}$$

whose solution is:

$$S(t) = K - e^{-\rho t}(K - S_0). \tag{13}$$

This model of growth (monomolecular growth) depends on the value of ρ (Fig.3). Interestingly, this explicit equation enables us to estimate ρ value using a non infected data set of leaf number, if we know the value of K and S in time, or if S/K is reported.

In Mulinge and Griffiths (1974), the value of S/K and I/K is reported (Fig.4). We do not have the amount of fallen leaves, so from this time series we consider a time interval where I/K is close to 0 (we assume that X/K is also near to zero). That is, between day 290 and day 370 which might correspond to the dry season.

From eq (12) one obtains:

$$S(t)/K = s(t) = 1 - (1 - s(0))e^{-\rho t} \tag{14}$$

$$ln(\frac{1 - s(t)}{1 - s(0)}) = -\rho t \tag{15}$$

and adjust a linear model to estimate ρ (Fig.5). (The assumptions of homoscedasticity and normality of residuals are respected). We got $\rho = 0.008$ with a $R^2 = 0.99$. This value for ρ is within the range estimated for non-rain season in section I ($\rho \in [0.007, 0.008]$). We will not use this result to estimate the range of ρsince our model is set for the rainy season, but it validates the direct method to estimate ρ range presented in section I.

[5]It does not correpond exactly to what Firman reported (2616 total fallen leaves). But this difference arises from rounding and from assuming constant production of leaves. The difference is not significant.

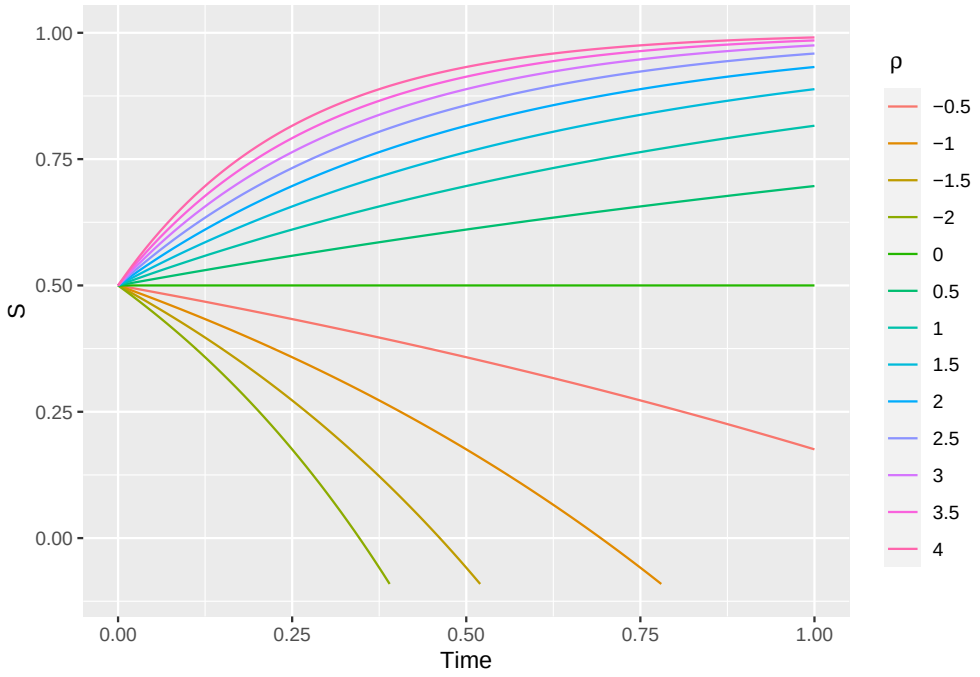

Figure 3: Time evolution of S, with ρ varying from -2 to 4. S_0= 0.5, $K = 1$.

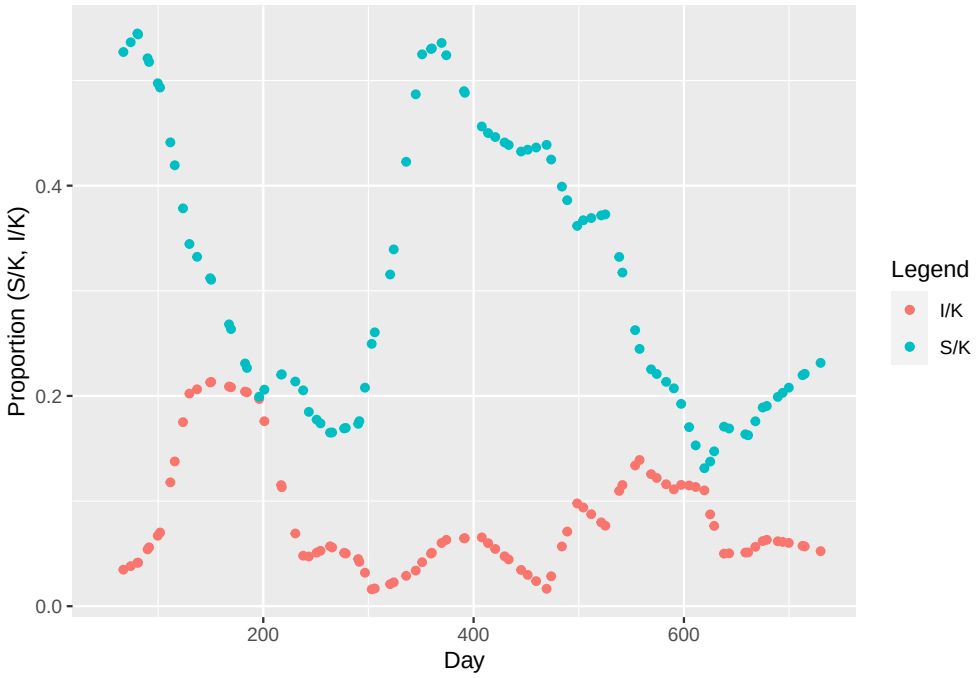

Figure 4: Proportion of infected and susceptible leaves in two epidemic years (Mulinge and Griffiths, 1974). S:Susceptible leaves, I:Infected Leaves, $K = 20$

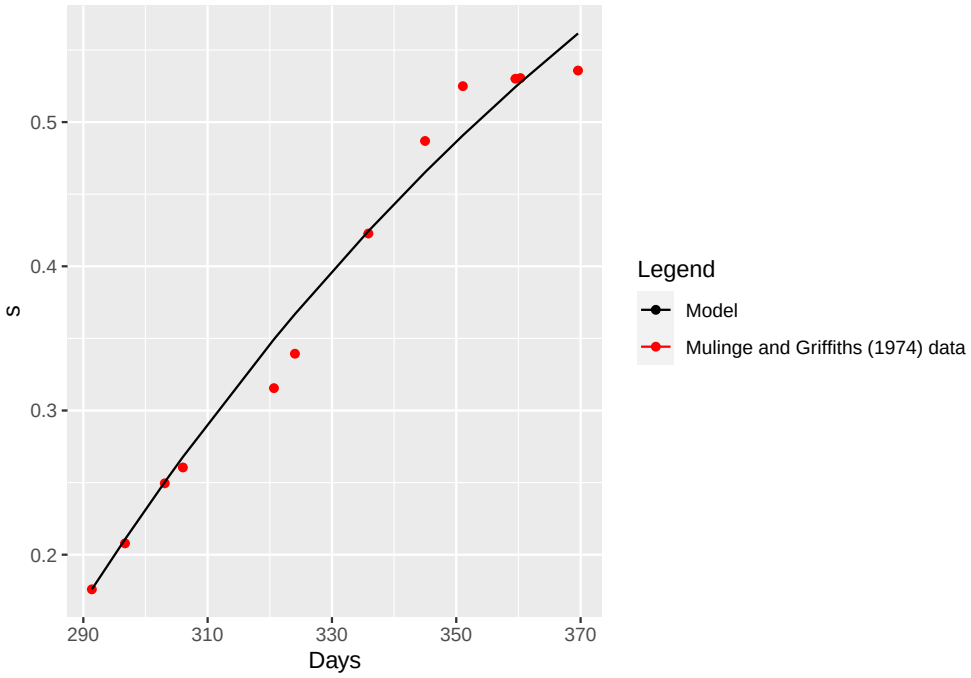

Figure 5: Linear fitting to Mulinge and Griffiths Data (1974).

References

Bock, K.R. 1962. "Dispersal of uredospores of Hemileia vastatrix under field conditions." *Transactions of the British Mycological Society* 45 (1). British Mycological Society: 63–74. https://doi.org/10.1016/s0007-1536(62)80035-7.

Boudrot, Audrey, Jimmy Pico, Isabelle Merle, Eduardo Granados, Sergio Vílchez, Philippe Tixier, Elías De Melo Virginio Filho, et al. 2016. "Shade effects on the dispersal of airborne Hemileia vastatrix uredospores." *Phytopathology* 106 (6): 527–80. https://doi.org/10.1094/PHYTO-02-15-0058-R.

Capucho, A. S., A.F. de Souza, E. M. Zambolim, E. T. Caixeta, R.J.N. Rufino, J. C. Barbosa, S. M. Alvarenga, and Laércio Zambolim. 2005. "Viabilidade de uredosporos da ferrugem do cafeeiro (Hemileia vastatrix Berk . et Br .) sob diferentes métodos de preservacao in vitro." *Embrapa Café-Artigo Em Anais de Congresso (ALICE). Simposio de Pesquisa Dos Cafés Do Brasil*, no. May: 0–3.

Deepak, K., B.T. Hanumantha, and H.L. Sreenath. 2012. "Viability of Coffee Leaf Rust (Hemileia vastatrix) Urediniospores Stored at Different Temperatures." *Journal of Biotechnology & Biomaterials* 02 (05): 2–4. https://doi.org/10.4172/2155-952x.1000143.

Firman, I. D., and J. A.N. Wallis. 1965. "Low-volume spraying to control coffee leaf rust in Kenya." *Annals of Applied Biology* 55 (1): 123–37. https://doi.org/10.1111/j.1744-7348.1965.tb07875.x.

Gagliardi, Stephanie, Jacques Avelino, Leïla Bagny Beilhe, and Marney E. Isaac. 2020. "Contribution of shade trees to wind dynamics and pathogen dispersal on the edge of coffee agroforestry systems: A functional traits approach." *Crop Protection* 130 (December 2019). Elsevier Ltd: 105071. https://doi.org/10.1016/j.cropro.2019.105071.

Leguizamón-Caycedo, J.E., L. Orozco-Gallego, and L. Gómez-Gómez. 1998. "Períodos de incubación (pi) y de latencia (pl) de la roya del cafeto en la zona cafetera central de colombia." *Cenicafé* 49 (56): 325–39.

Mulinge, S. K., and E. Griffiths. 1974. "Effects of fungicides on leaf rust, berry disease, foliation and yield of coffee." *Transactions of the British Mycological Society* 62 (3). British Mycological Society: 495–507.

https://doi.org/10.1016/s0007-1536(74)80061-6.

Nutman, F.J., F.M. Roberts, and R.T. Clarke. 1963. "Studies on the biology of Hemileia vastatrix Berk. & Br." *Transactions of the British Mycological Society* 46 (1). British Mycological Society: 27–44. https://doi.org/10.1016/s0007-1536(63)80005-4.

Rakocevic, Miroslava, and Fabio Takeshi Matsunaga. 2018. "Variations in leaf growth parameters within the tree structure of adult Coffea arabica in relation to seasonal growth, water availability and air carbon dioxide concentration." *Annals of Botany* 122 (1): 117–31. https://doi.org/10.1093/aob/mcy042.

Rayner, R. W. 1961. "Spore liberation and dispersal of coffee rust Hemileia vastatrix B. et Br." *Nature* 191 (4789): 725. https://doi.org/10.1038/191725a0.

Silva-Acuña, R., L. A. Maffia, L. Zambolim, and R. D. Berger. 1999. "Incidence-severity relationships in the pathosystem Coffea arabica-Hemileia vastatrix." *Plant Disease* 83 (2): 186–88. https://doi.org/10.1094/PDIS.1999.83.2.186.

Apéndice 4 - Harvesting trajectories in large-scale coffee plantations: ecological and management drivers and implications (Material Suplementario)

Emilio Mora Van Cauwelaert, Denis Boyer, Estelí Jimenez Soto, Cecillia González González and Mariana Benítez

Supplementary material- State-Space Model analysis with HMM

Supplementary Material 1. HMM analysis from: Harvesting trajectories in large-scale coffee plantations: ecological and managment drivers and implications

Mora Van Cauwelaert et al., 2023

0. Introduction to State-space models with HMM

State space models coupled with hidden Markov models (HMMs) are models in which the distribution that generates an observation Z_t depends on the state S_t of an underlying and unobserved Markov process (Fig.1) (Zucchini et al., 2016). In this sense, the observations Z_t can be retrieved from one to multiple distributions related to the number of states. In the context of animal movement, the state S_t is interpreted as a proxy for the behavioral state of the animal (e.g. foraging, exploring; (Michelot et al., 2016)). The observations Zt are bivariate time series ($Zt = (l_t, \phi_t)$) where l_t is the step length (the Euclidean distance) and ϕ_t the turning angle, between two succesive locations (Zucchini et al., 2016). Biologically speaking, these models try to include the process where the movement of agents (e.g. short or large steps) depends on its behavior (Patterson et al., 2008). With these models, we can define the different originary distributions and then decode the most likely sequence of states along the trajectory of an agent, its average time within a state, and the number of switches between states.

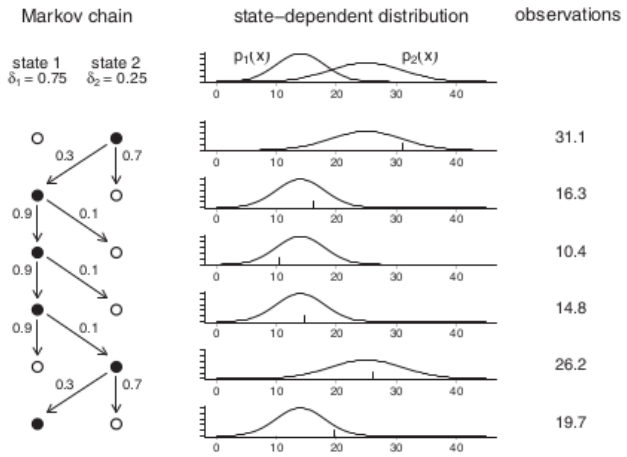

Figure 1: Process generating the observations in a two-state HMM. The chain followed the path 2, 1, 1, 1, 2, 1, as indicated on the left. The corresponding state-dependent distributions are shown in the middle. The observations are generated from the corresponding active distributions. Taken from (Zucchini, 2016)

Here we used the *movehmm* library (Michelot et al., 2019) to i) fit the most likely distributions to the harvester movement data in each plantation, ii) decode and compare the sequence of states in the two plantations (Ecological and Conventional) with the Viterbi algorithm. To see the full results and visualizations please refer to main text.

1. Preparation of data and algorithm

1.1. Preparation of data

We loaded *ggplot2*, *dplyr*, *tidyverse* and *movehmm* libraries. We then loaded the data of the trajectories and did some punctual modifications to it. We had in total 12 trajectories, with (x, y) coordinates (see Fig. 2).

We took these time irregular trajectories (where each point represents one different tree, but where the time between two trees is variable) and treated them as regular trajectories. This aimed to analyze the change in the movement of the workers during a day, generated by the underlying pattern of trees or by the differences in the fruit charge and ripening synchronicity. We convert this database into a *movehmm* object where the step distance l_t and the relative angle ϕ_t between the (x, y) coordinates is calculated. Now, for the following analysis, we only took the step distance and treated each plantation separately. We decided to exclude the angles because they didn't have a biological meaning for irregular trajectories.

1.2. Fitting algoritm

The algorithm of the *movehmm* library uses:

a) a predefined number of states. Here we will use one and two.

b) a defined family of distributions. Here we will try to fit two different exponential families (*gamma* and *weibull*).

c) prior parameters for each of the distributions, for each state.

d) The observations (step-lengths) (the data of harvesters)

With these inputs, the algorithm extracts the most likely two-state and one-state distributions with their respective parameters (within the predefined family of distributions) from the data. During the fitting process, the algorithm uses the maximum-log likelihood and the *forward algorithm* (a recursive algorithm starting with the prior distributions; (Zucchini et al., 2016)). We ran a loop across 1000 prior parameters within the range shown in Table 1 to fit the data to two different families (*weibull* and *gamma*) and to avoid local maximal likelihoods (Michelot et al., 2019). For the *gamma* distribution, the minimum and maximum values of each prior parameter range were chosen to encompass the full distribution (including values below and over the mean). For the *weibull* distribution, the maximum shape considered the left-skew shape and the scale was chosen to include the 120m long steps (Table 1). Many of these combinations of prior parameters converged to the same final distributions.

Table 1: Minimun and maximum values of the prior parameters for each distribution

value	gamma.mean	gamma.sd	weibull.shape	weibull.scale
min	0.1	0.1	0.1	0.1
max	10.0	10.0	2.7	15.0

1.3. Outputs

We first ran the model for each plantation (Organic and Conventional) assuming two-state distributions.The output is stored in /output/dataFrameAnalysis/.

We then ran the model for each plantation (Organic and Conventional) assuming one-state distributions. The output is stored in /output/dataFrameAnalysis/

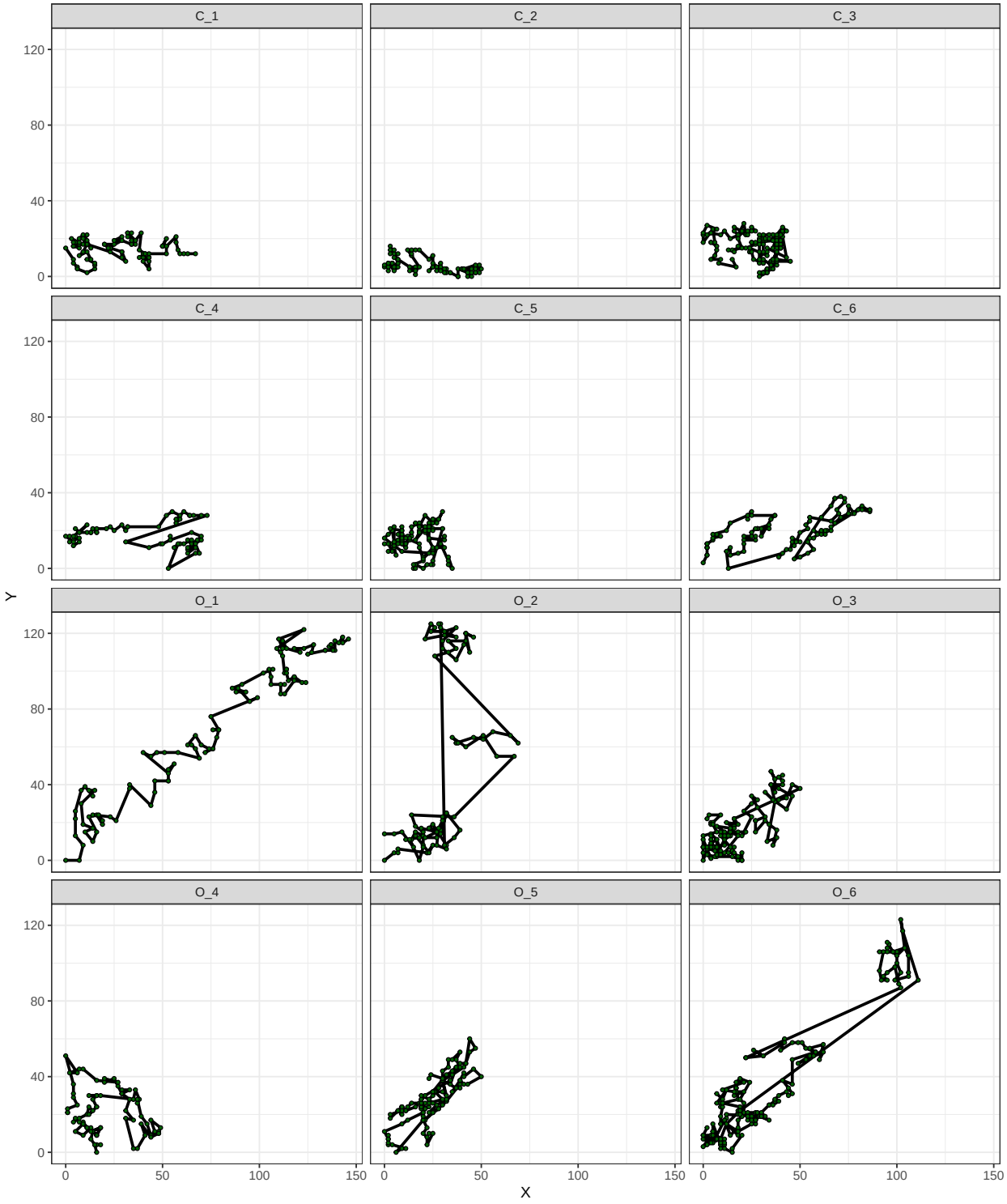

Figure 2: Trajectories of harvesters for both plantations (O: organic, C: conventional). Each green dot represent a tree

2. Results

2.1 Two-state and one-state fitting

Some combinations resulted in distributions with zero variance. We decided to remove those cases as they did not make any biological sense. We also removed states with means higher than the ranges (this does not change the results as they had maximal AIC that would be removed anyways). We then plotted the AIC without these outliers (Fig.3). Almost all the combinations of prior parameters converge to two models with equivalent AIC for both distributions (Fig. 3). In this sense, the parameters of the models are robust to the initial prior parameters chosen. Two-state gamma distributions had the minimal AIC. The minimal AIC for each family and number of states are represented in Table 2 and stored in: output/dataFramesGenerated/

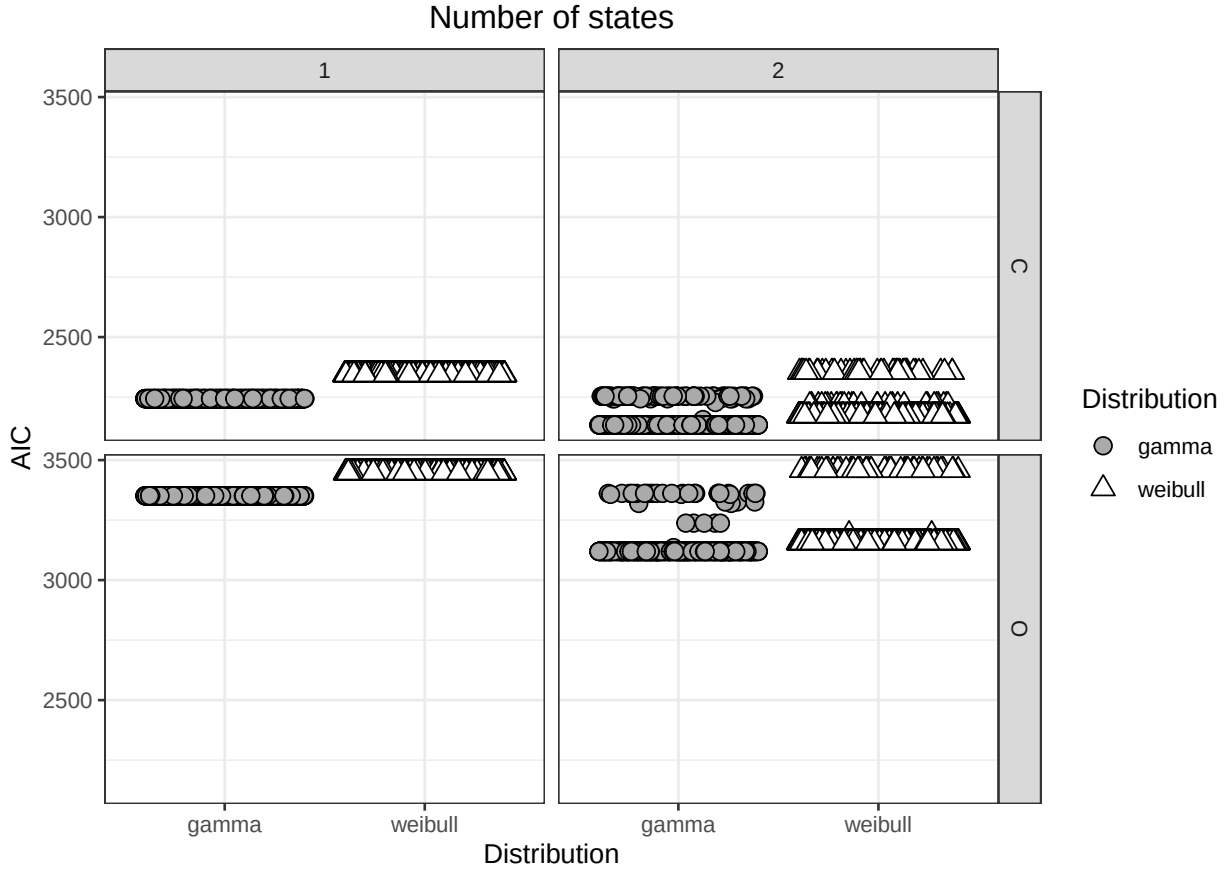

Figure 3: Minimun AIC per combination of prior parameters for two different distributions, for 1 and 2 states, for each of the plantations. O:Organic, C: Conventional

Table 2: Best models for each of the distributions. We added the prior parameters, the min negative likelihood, AIC criteria and the final parameters. pr:prior, st1: state 1, p1: parameter 1 (shape for weibull and mean for gamma), p2: parameter 2 (scale for weibull and sd for gamma).

model	prior_par0_st1	prior_par1_st1	minNegLike	AIC_model	st1_par0	st1_par1	farm	prior_par0_st2	prior_par1_st2	st2_par0	st2_par1	states
weibull	2.26	9.99	1169.82	2343.64	1.47	4.66	C	NA	NA	NA	NA	1
gamma	7.79	7.35	1119.84	2243.68	4.17	2.47	C	NA	NA	NA	NA	1
weibull	1.08	2.57	1721.75	3447.51	1.16	6.35	O	NA	NA	NA	NA	1
gamma	3.77	9.08	1673.67	3351.34	5.94	4.29	O	NA	NA	NA	NA	1
weibull	0.14	13.68	1079.15	2172.30	1.46	10.12	C	1.39	7.67	2.42	3.87	2
gamma	8.01	6.10	1059.92	2133.84	3.47	1.56	C	8.49	8.06	10.03	6.41	2
weibull	1.44	9.92	1571.22	3156.44	1.96	5.47	O	0.86	13.83	0.97	21.25	2
gamma	7.89	4.90	1552.71	3119.43	5.01	2.80	O	0.48	8.46	32.95	30.91	2

2.2 Sequence of states for each plantation (two states gamma distribution)

In the following analysis we only used the two-states gamma distribution as it had the lower AIC. For each plantation we assigned each step to "state 1" or "state 2" according to the Viterbi algorithm. The output tables used for the plotting the results are exported to data/

With the Viterbi algorithm, the package *movehmm* decodes the most likely sequence of states (assuming a markov chain) and the transitions matrix between hidden states. This takes into account the conditional probabilities between the observations and hidden states $P(Z_t|S_t)$) (Zucchini et al., 2016) (Fig. 4 and 5). In this sense, *movehmm* can estimate the state with the highest probability for each step but this might not be the same as the state in the most probable sequence returned by the Viterbi algorithm (Fig. 4 and 5, second and third row vs first row). This is because the Viterbi algorithm performs "global decoding", whereas the state probabilities are "local decoding" (Zucchini et al., 2016). In the main text we plot the result of the Viterbi algoritm for each of the algoritms.

```
## Decoding states sequence... DONE
## Computing states probabilities... DONE
```

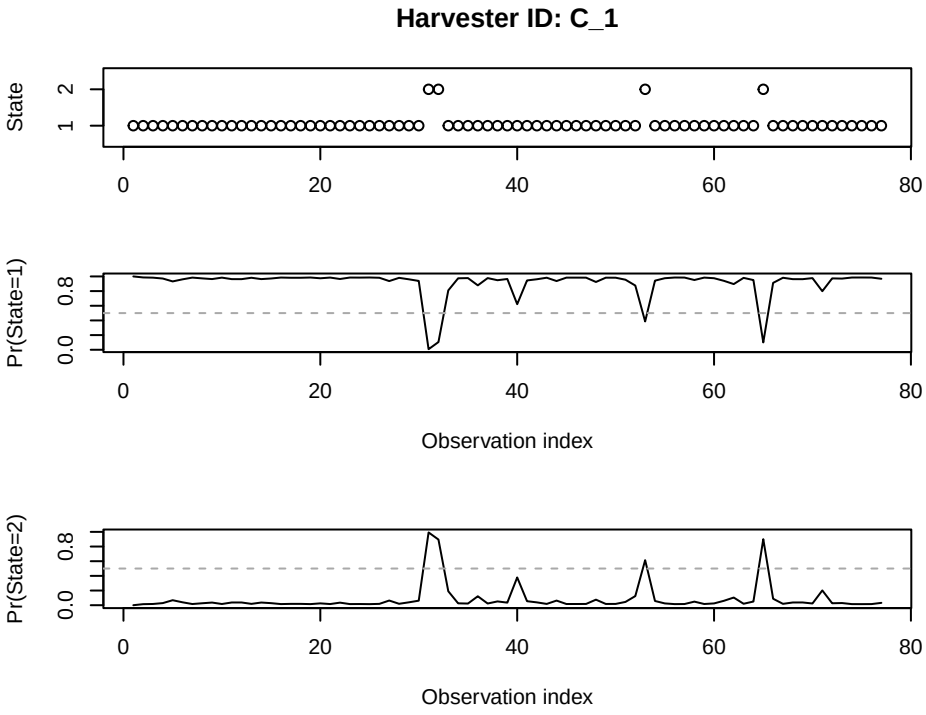

Figure 4: State probabilities for each step of harvester C_1 trajectory and result of the Viterbi algorithm

```
## Decoding states sequence... DONE
## Computing states probabilities... DONE
```

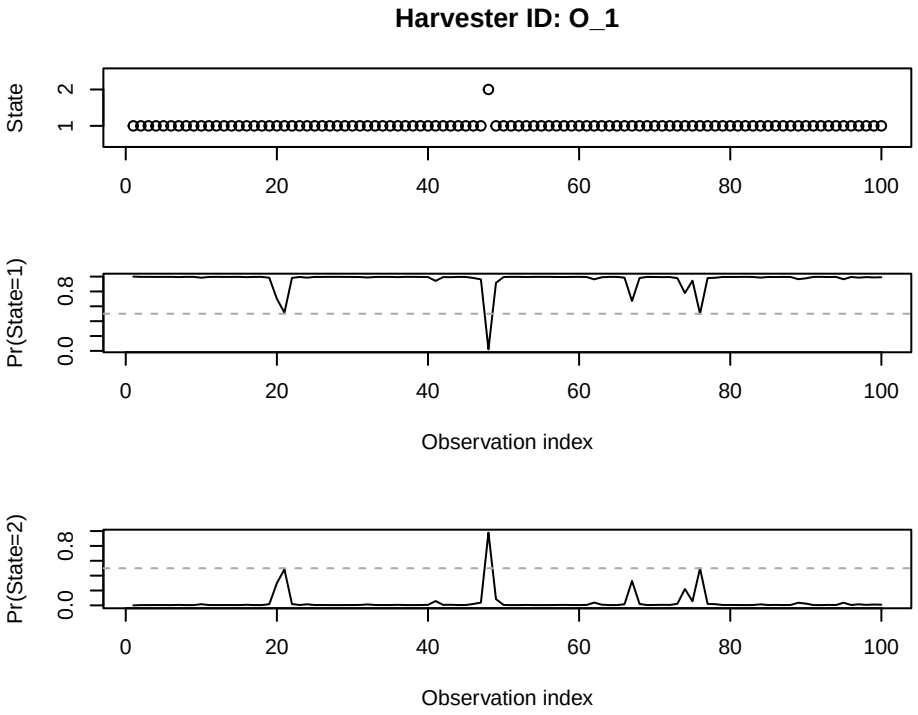

Figure 5: State probabilities for each step of harvester O_1 trajectory and result of the Viterbi algorithm

4. References

Michelot, T., Langrock, R., Patterson, T.A., 2019. moveHMM: An r package for the analysis of animal movement data. ArXiv Preprint 1–24.

Michelot, T., Langrock, R., Patterson, T.A., 2016. moveHMM: An r package for the statistical modelling of animal movement data using hidden markov models. Methods in Ecology and Evolution 7, 1308–1315.

Patterson, T.A., Thomas, L., Wilcox, C., Ovaskainen, O., Matthiopoulos, J., 2008. State–space models of individual animal movement. Trends in ecology & evolution 23, 87–94.

Zucchini, W., MacDonald, I.L., Langrock, R., 2016. Hidden markov models for time series: An introduction using r. Chapman; Hall/CRC Press.

Apéndice 5 - Interplay between harvesting, planting density and ripening time affects coffee leaf rust dispersal andinfection (Material Suplementario)

Emilio Mora Van Cauwelaert, Kevin Li, Zachary Hajian-Forooshan, John Vandermeer and Mariana Benítez

Supplementary material 1- Supplementary figures and tables

Supplementary figures from: Interplay between harvesting, planting density and ripening time affects coffee leaf rust dispersal and infection

Emilio Mora Van Cauwelaert[a, b, *], Kevin Li[c], Zachary Hajian-Forooshani[d], John Vandermeer[e]

and Mariana Benítez[a, *]

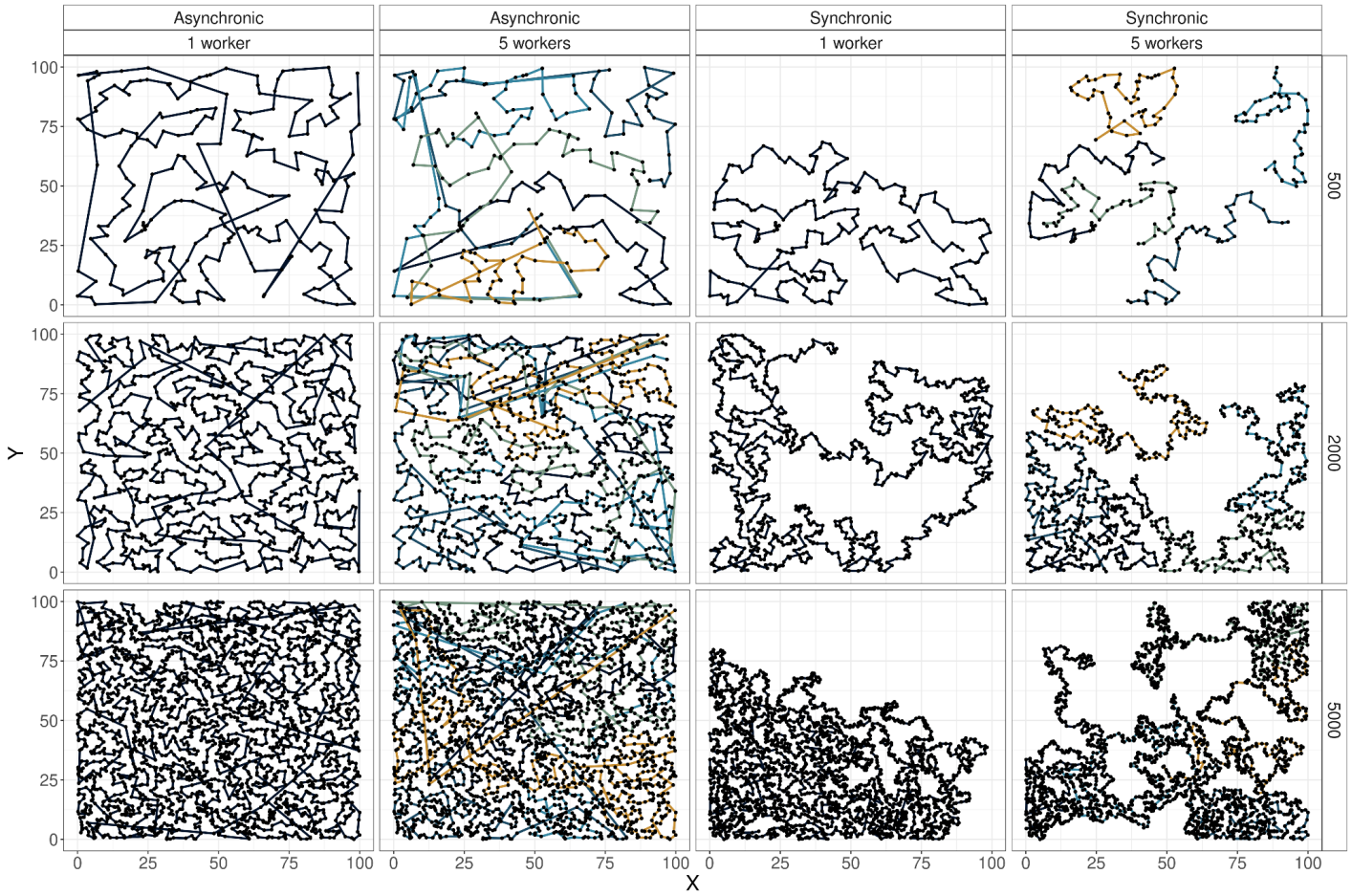

Figure S1. 1. Simulated trajectories under two scenarios of coffee ripening, two quantities of workers and three planting densities. The columns represent the four combinations of ripening scenarios and number of workers, and each row represents one planting density (plants/ha). Colors correspond to each of the workers for w = 5. In all scenarios, the simulations were run until half of the plants were harvested (N/2). The trajectories of N= 1000 and N= 3000 were qualitatively the same and are not shown.

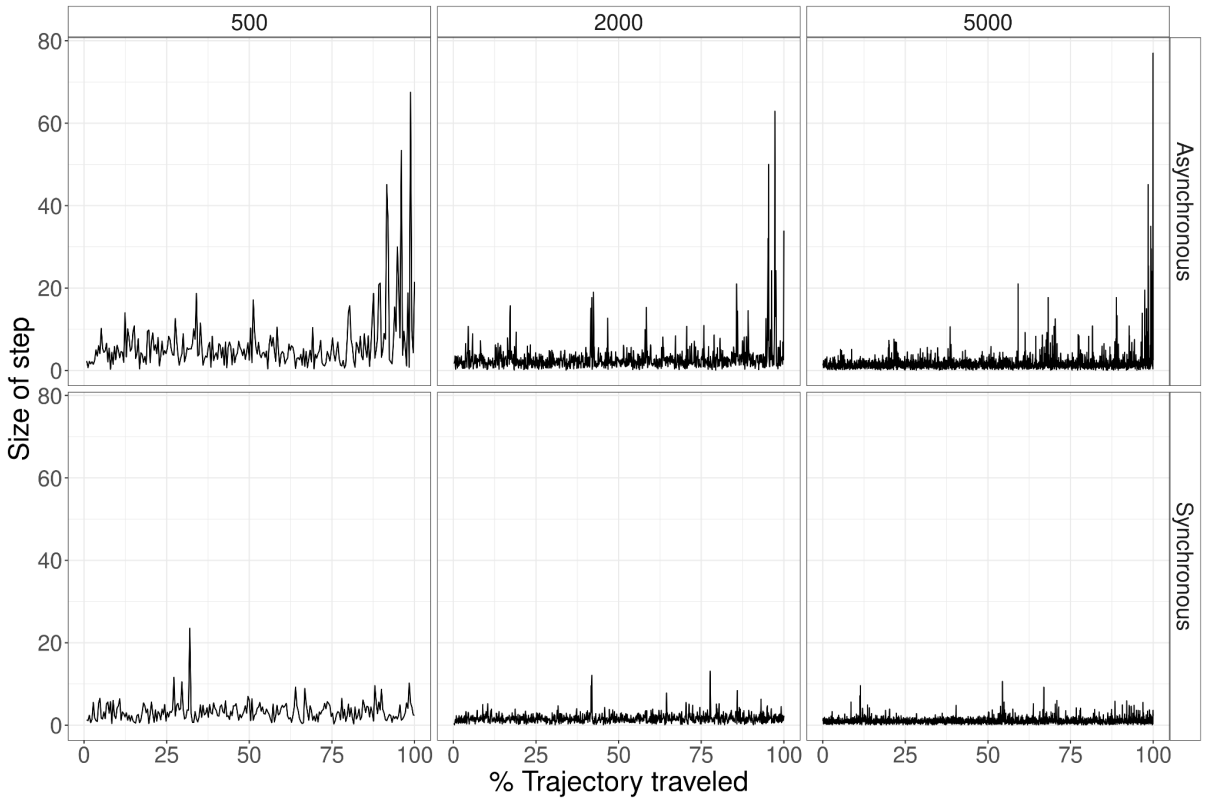

Figure S1. 2. Size of steps (in m) in relation to the percentage of the trajectory traveled, under two scenarios of coffee ripening and three planting densities. The % of trajectory traveled represents the number of current visited trees normalized by the maximum number of visited trees per scenario. The columns represent the three planting density (plants/ha) and each row the coffee ripening scenario. In all scenarios, the simulations were run until half of the plants were harvested (N/2). The dynamics of N= 1000 and N= 3000 and w = 5, were qualitatively the same and are not shown.

Table S1.1. Central tendency values of the distribution of steps for five different plating densities and two scenarios of coffee ripening. The mean distance, mode and median are in meters.

Density (plants/ha)	Coffee maturation	Mean distance	Mode	Median
500	A	22.1	3.7	17.0
	S	9.6	2.7	8.4
1000	A	22.8	2.4	17.3
	S	8.9	1.8	8.1
2000	A	22.6	1.7	17.7
	S	7.5	1.3	7.0
3000	A	21.4	1.8	17.0
	S	7.8	1.1	7.0
5000	A	22.3	1.0	17.5
	S	6.5	0.7	6.0

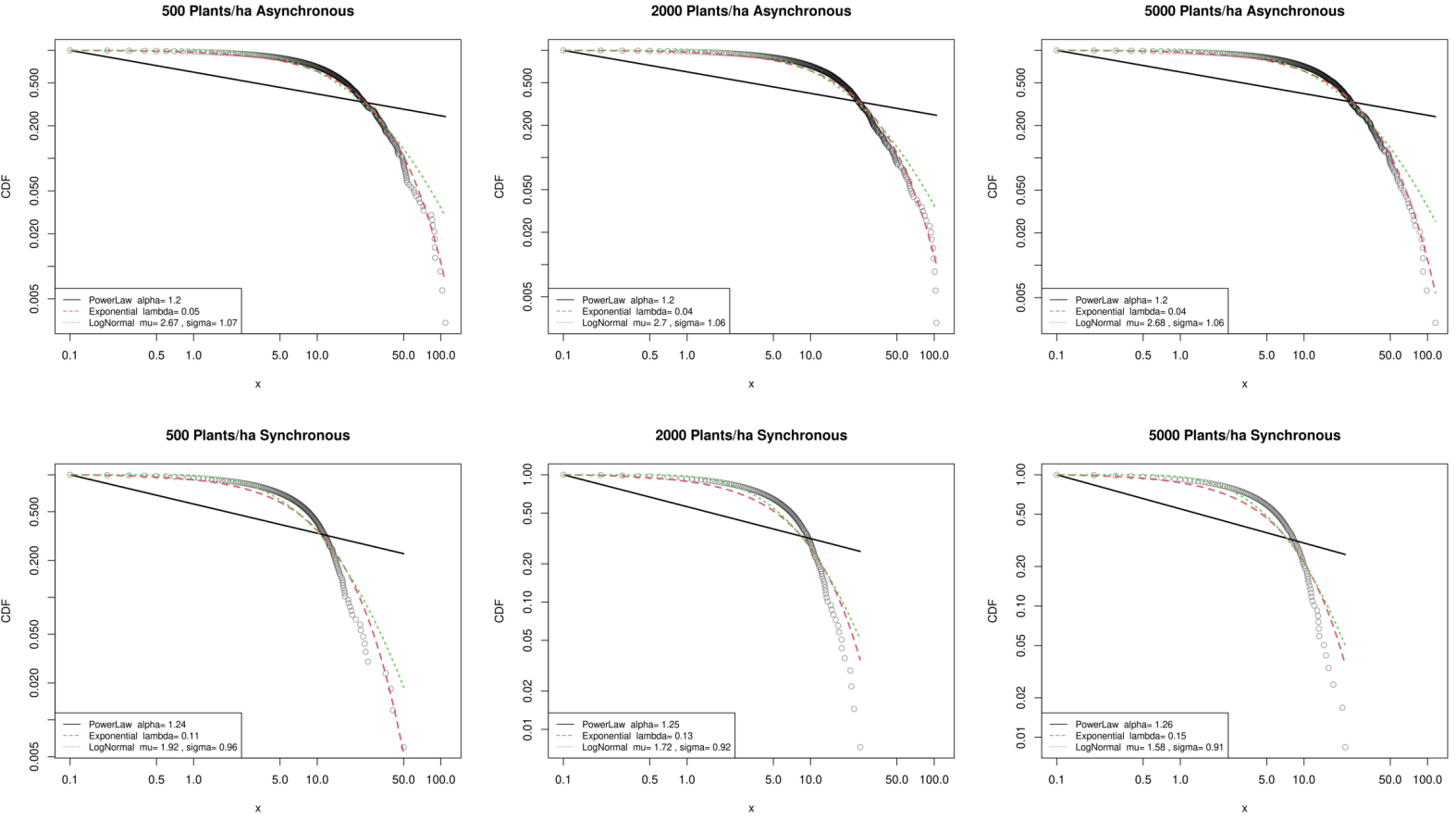

Figure S1. 3. Cumulative distribution function and fitting of three models for the distribution of steps under two harvesting scenarios and three planting densities. The real data for each scenario is presented with empty circles, and the three models are presented as lines (power law: black continuous, exponential: red dotted, lognormal: green dotted line). The characteristic parameters are presented in the small box of each plot.

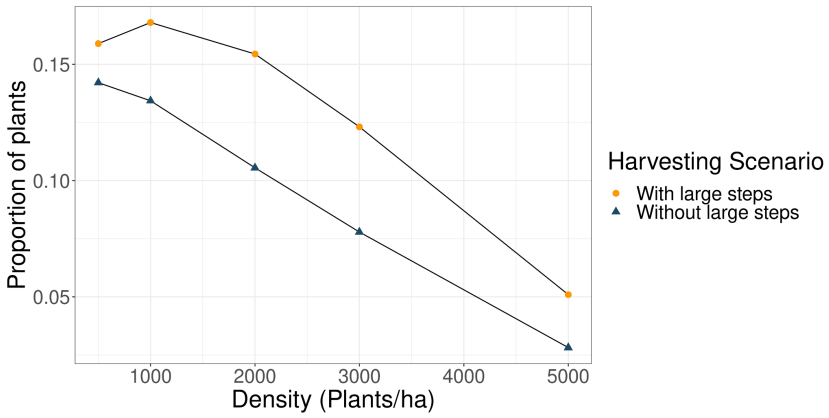

Fig. S1.4 Proportion of newly infected plants during harvesting under two types of trajectories and five planting densities. Orange circles: with large steps, blue triangles: without large steps. Each point represents an average of 30 repetitions.


2
COFFEE
Coffea arabica
Fig 1
3
Fig 1. Coffee tree.
2. Coffee flower opened artificially.
3. Lower half of shell containing the fruit.